The University of Nottingham

UNITED KINGDOM · CHINA · MALAYSIA

Numerical Analysis of Ground Improvement using Column-Like Elements

A thesis submitted for the degree of

Doctor of Philosophy in Civil Engineering

at The University of Nottingham

by

Wisam Al-Ani

(4066797)

September 2020

Nottingham Centre for Geomechanics (NCG)

Department of Civil Engineering

Faculty of Engineering

Abstract

The issue of constructing foundations and embankments over highly compressible soft soils is of great importance for geotechnical engineers due to their undesirable characteristics such as excessive settlement and low bearing capacity. A number of techniques including column-like elements, such as settlement-reducing 'piles' and vibro stone columns, are available for improving strength of weak soils. These techniques are mainly used to reduce the applied pressure on soft soils without altering the soil structure significantly.

Several piled-embankment design procedures (i.e. Hewlett and Randolph, 1988 and the German method (EBGEO), 2004) currently used by industry appear to yield significant difference in predicting the load transfer mechanism within the embankment material due to lack of modelling various aspects of the embankment geometry, soil properties, and load transfer mechanism with the embankment material.

The use of column-like elements, for improving both the settlement performance and bearing capacity of foundations constructed over soft soils is well rehearsed for large groups of columns support an infinitely wide load area such as embankments and slabs where all columns are equally restrained on all sides; but little is understood for lightly loaded low-rise structures supported by pad foundations constructed on stone columns, particularly when a crust layer is available at the top of the soft soil.

A two-dimensional Finite Element analysis (FEA) in conjunction with a hardening soil model was used in this research to investigate the load transfer mechanism within embankment fill using Zaeske's model (Zaeske, 2001). A frictional design method which depends to a large extent on the coefficient of lateral earth pressure (K) was used to investigate the load transfer mechanism. It is shown in this research that using the friction method in conjunction with a plane of equal settlement method can be very useful tool to investigate the load transfer mechanism within embankment material. It is also shown in this study that BS 8006 (2010) revealed unrealistic results when analysing Zaeske (2001) model test.

This research includes the first comprehensive three-dimensional FEA modelling of the presence of a stiff crust layer overlying soft soil for lightly loaded structures supported by stone columns. The soft soils at Bothkennar site, Scotland, were modelled in this research. The modelling of the Bothkennar field trials has shown that both drained and undrained analyses agree very well in predicting a long-term settlement. The presence of a stiff crust has a significant influence on the deformational mode of the stone columns which is not normally captured by laboratory tests. It was found that the lateral bulging is constrained by the crust at the upper part of the column. It has been demonstrated in this research that the use of geogrid encasement around the column improves the column bearing capacity and their stress-displacement behaviour beyond an average applied pressure of 70 kPa. The greater the length of encasement used, the more the total and differential settlement are reduced. The encasement of the top metre of the column reduces the lateral bulging considerably. However, the lateral bulging can also reduce significantly by extending the encasement below the maximum lateral bulging zone (around 2 times the diameter of the column). It was found that the most common design method (Priebe, 1995) underestimates the settlement of the stone columns; this is attributed to the fact that Priebe (1995) method does not consider the presence of a stiff crust layer, also it does not take account the disturbance of the sensitive soft clay during the installation of the stone columns which will contribute to the increase of footing settlement during the field trials.

Finally, a simplified design method derived by Satibi (2009) has been modified to estimate the relative settlement reduction ratio (RSR) of small and large groups of stone columns with the knowledge of the foundation applied pressure, column diameter, column spacing, and the column installation effects. It appears that the effectiveness (RSR) of the stone columns lies in the range 0.6-0.95 and (0.35-0.6) times the soil layer thickness for small and large groups, respectively. The RSR ratio predicted by the FEA agrees quite well with the analytical model when the soft layer thickness over critical column length ratio is in the range of 2 to 5.

Acknowledgment

I would like to express my thanks and gratitude to my supervisor Dr Dariusz Wanatowski, who devoted so much time and effort to support this research. I am extremely grateful for his guidance, patience and his insight and constructive comments throughout these years. My gratitude also extends to Mr Andrew Dawson for his contribution and support. Many thanks to my colleague Dr. Saad Raoof for his support and encouragement.

I would like to present my profound thanks to the University of Nottingham for their generous financial support provided to this research project. I would also like to acknowledge Balfour Beatty Ground Engineering for awarding the study leave. I am especially grateful to Dr Colin Serridge for his highly practical advice and support on the stone column analysis and also extend my gratitude to Tony Suckling for his support.

Dedications

This research is dedicated to both the memory of my late father Abdulsattar Al-Ani and my mother and also to my wife and children Layanne and Adam for their love and patience, and to my wonderful brothers and sister for their tireless support, and encouragement throughout this research.

Table of Content

Abstract ..... **iii**

Acknowledgment ..... **v**

List of Tables xii
List of Figures xiv
List of abbreviations xxiv
List of Notations xxiv

Chapter 1: INTRODUCTION **1**

1.1 Background 1

1.2 Research aims and objectives 4

1.3 Methodology 5

1.4 Outline of thesis 6

Chapter 2: LITERATURE REVIEW **8**

2.1 Introduction 8

2.2 Classification of soft soil 9

2.3 Soil primary compression 10

2.4 Soil improvement and stabilisation techniques 12

2.4.1 Piled-embankment system advantages 13

2.4.2 Stone column advantages 16

2.5 Previous investigations on piled-embankment system behaviour 17

2.5.1 Arching in a piled-embankment system 18

2.5.1.1 Terzaghi (1943) *22*
2.5.1.2 Guido et al. (1987) *24*
2.5.1.3 Hewlett and Randolph (1988) *25*
2.5.1.4 German method EBGEO (2004) *27*
2.5.1.5 British Standard - BS 8006 (2010) *30*
2.5.1.6 Other mechanisms *34*
2.5.2 Summary of arching in a piled-embankment 36
2.6 Vibro stone column construction and design methods. 39
2.6.1 Construction methods 40
2.6.2 Previous investigations of stone column behaviour 43
2.6.2.1 Laboratory modelling *44*
2.6.2.2 Field trials *46*
2.6.2.3 Other design methods *48*
2.6.2.3.1 Stone column bearing capacity 49
2.6.2.3.2 Settlement 51
2.6.3 Summary of stone column behaviour 56
2.7 Encased stone column (ESC) 57
2.7.1 Experimental, numerical, and analytical studies 59
2.7.1.1 Experimental Studies *60*
2.7.1.2 Numerical and analytical studies *61*
2.8 Background for numerical analysis 62
2.8.1 Numerical modelling approaches 64
2.8.2 Numerical analysis of piled-embankment 66
2.8.2.1 Efficacy *67*
2.8.2.2 Soil arching ratio or stress reduction ratio *67*
2.8.2.3 Stress concentration ratio *67*
2.8.2.4 Other definitions *68*
2.8.3 Numerical studies of stone columns 68
2.8.3.1 Modelling of column installation effects *72*

2.8.3.1.1 Increased coefficient of lateral pressure 72
2.8.3.1.2 Cylindrical Cavity Expansion..... 73
2.8.3.2 Modelling of soft soil long-term behaviour.....77

2.9 Summary 78

Chapter 3: NUMERICAL MODELLING OF PILED-EMBANKMENTS 82

3.1 Introduction.....82

3.2 PLAXIS program 87

3.2.1 Description of PLAXIS constitutive models 88

3.2.1.1 Mohr-Coulomb (MC) failure parameters 89
3.2.1.2 Basic parameters for soil stiffness 90

3.2.2 Interface Element.....91

3.2.3 Geometry 93

3.2.4 Mesh generation 94

3.2.5 Initial conditions.....94

3.3 Details of FEA.....94

3.4 Finite Element analysis 98

3.5 Summary of the numerical analysis development and validation 101

3.6 Midpoint of lateral earth pressure coefficient 102

3.7 Results..... 103

3.8 Summary 121

Chapter 4: NUMERICAL MODELLING OF STONE COLUMNS 125

4.1 Introduction..... 125

4.2 Field trials design 127

4.3 Bothkennar Numerical Analysis 131

4.4 Hardening Soil model parameters 132

4.4.1 Bothkennar Hardening Soil model verification 134

4.5 Reinforcement material parameters 137

4.6 Preliminary checks to assess the influence of distance to boundary 138

4.7 FEA and modelling issues 141

4.8 Summary of the numerical analysis development and validation 142

4.9 Influence of column spacing (trial Footing 1 and 2) L/d= 7.5..... 143

4.9.1 Vertical settlement 143

4.9.2 Lateral bulging 147

4.9.3 Influence of geogrid encasement 151

4.10 Influence of stone column length (trial Footings 3, 4, and 5): .. 153

4.10.1 Vertical settlement 153

4.10.2 Lateral Bulging 158

4.10.3 Influence of geogrid encasement 161

4.10.4 Influence of encasement depth 163

4.11 Effect of crust 175

4.11.1 Vertical settlement 175

4.11.2 Lateral Bulging 177

4.11.3 Influence of geogrid encasement 178

4.12 Investigation of footing shape 178

4.12.1 Vertical settlement 179

4.12.2 Lateral Bulging 180
4.12.3 Influence of geogrid encasement 181
4.13 Review of Priebe (1995) method 182
4.14 Influence of column diameter and strength 185
4.15 Influence of reinforcement stiffness 186
4.16 Summary of results 187
Chapter 5: SIMPLIFIED ANALYTICAL MODEL FOR STONE COLUMNS 191
5.1 Introduction 191
5.2 Analytical model derivations 194
5.3 Settlement improvement analysis 197
5.3.1 Settlement improvement of single and strip footings 214
5.4 Definition of compression and punching ratios 218
5.4.1 Deformational behaviour 220
5.4.1.1 Soft soil layer thickness 220
5.4.1.2 Influence of the coefficient of lateral soil pressure 226
5.5 Summary of the results 227
Chapter 6: CONCLUSIONS 230
6.1 Introduction 230
6.2 Piled-embankments 231
6.3 Stone columns 233

6.3.1 Settlement 233
6.3.2 Bulging 234
6.3.3 Encasement 235
6.3.4 Crust effect 237
6.4 Simplified design method 238
6.5 Recommendations for future research 240
REFERENCES 242
Appendix A: 254
Appendix B: 266
Appendix C: 268
Conference Papers 268

List of Tables

Table 2.1 Summary of partial factors (DIN-1054 Revision 4). 28

Table 2.2 Summary of BS8006 partial factors. 31

Table 2.3 Arching coefficient for basal reinforced piled-embankments (British Standard BS8006, 2010). 32

Table 2.4 Key missing parameters from design methods. 38

Table 2.5 Pros and cons of different design methods. 39

Table 3.1 Soil parameters for Hardening Soil model. 98

Table 3.2 Normalised K_o/K_p with relevant angle of internal friction. 103

Table 4.1 Summary of Bothkennar trial footing arrangements. 130

Table 4.2 Summary of loading increments applied to trial footings at Bothkennar. 130

Table 4.3 Bothkennar field trials soil parameters (McCabe and Killeen, 2010). 133

Table 4.4 Measured (Serridge, 2013) vs PLAXIS 3D vertical settlement prediction in drained and undrained condition for the field trials at Bothkennar site. 136

Table 4.5 Properties of the geogrid materials. 138

Table 4.6 Influence of the side boundary distance upon footing settlement. ...141

Table 4.7 Influence of the lower boundary distance upon footing settlement. .141

Table 4.8 Estimated post treatment settlements of trial footings under first load increment. 184

Table 4.9 Estimated post treatment settlements of trial footings under second load increment. 184

Table 5.1 Material parameters for models. 198

Table 5.2 Analytical model predicted critical column length $L_{critical}$ and L/d ratio. 198

List of Figures

Figure 2.1 Empirical equations after Kempfert and Gebreselassie (2006) to estimate K_0 from (a) plasticity index I_p, (b) liquid limit WL and (c) effective angle of friction φ' (Scherzinger, 1991). 11

Figure 2.2 Overview of the soil improvement and stabilisation techniques (Kempfert and Gebreselassie, 2006). 13

Figure 2.3 Main four elements influencing (reinforced) piled-embankment system. 14

Figure 2.4 Load transfer mechanism of reinforced piled-embankment (Han and Gabr, 2002). 19

Figure 2.5 Piled-embankment showing potential arching mechanisms, and notation for geometry and settlement (δ) used in this thesis (Zhuang, 2009).....22

Figure 2.6 Forces acting on an elemental strip, after (Ranjan and Rao, 2007) ..23

Figure 2.7 Guido's experimental set-up (geogrid-reinforced sand in a confined, rigid box).....24

Figure 2.8 The mechanism of load spreading from the pile caps through an embankment (shown in 2D after Zhuang (2009)). 25

Figure 2.9 Section through a piled-embankment (Hewlett and Randolph, 1988). 27

Figure 2.10 Geometry of arching and equilibrium stresses (Kempfert, 2003; Zaeske, 2001).....27

Figure 2.11 Load distribution on the geotextile for rectangular pile layout (Kempfert et al., 2004). 30

Figure 2.12 Piled-embankment parameters after BS8006 (2010). 32

Figure 2.13 Geometry of assumed log spiral shaped yield zone (Naughton, 2007). 35

Figure 2.14 Influence of angle of friction on the critical height of the embankment (Naughton, 2007). 35

Figure 2.15 Comparison of design methods (a) stress reduction ratio; (b) geosynthetic tension; (c) pile efficacy (Ariyarathne and Liyanapathirana, 2015). 37

Figure 2.16 (a) dry top-feed stone column installation sequence. (b) dry top-feed stone column installation in the field (Serridge, 2013). 41

Figure 2.17 (a) dry bottom-feed stone column installation sequence. (b) dry bottom-feed stone column installation in the field (Serridge, 2013).....42

Figure 2.18 (a) wet top-feed vibro stone column installation sequence. (b) wet top-feed stone column installation in the field (Serridge, 2013). 43

Figure 2.19 Deformation of 38mm diameter laboratory model column for 25mm displacement with limit of 1% radial strain in clay shown (after Hughes and Withers, 1974). 46

Figure 2.20 (a) to (c) Comparison of large scale field loading test results on untreated soft clay, soft clay reinforced with stone columns and soft clay reinforced with sand columns, after (Greenwood, 1970). 47

Figure 2.21 Allowable working load for stone column(s), after Thorburn (1975). 50

Figure 2.22 Settlement design curves and design philosophy for composite ground (soft soil reinforced with stone columns) after Priebe (1976). 52

Figure 2.23 Consideration of (a) column compressibility (b) determination of depth factor, after Priebe (1995). 54

Figure 2.24 Limit value of depth factor, after Priebe (1995). 55

Figure 2.25 Settlement of small foundations (a) single pad footings. (b) strip footings, after Priebe (1995). 56

Figure 2.26 Encased Stone column (ESC) installation method (a) the displacement method and (b) the replacement method (Kempfert and Gebreselassie, 2006).....59

Figure 2.27 (a) load versus settlement of composite bed with various encasements and (b) variation of modular ratios with settlement (Malarvizhi and Ilamparuthi, 2004). 61

Figure 2.28 Variation of (a) excess pore pressure (pwp) and (b) total radial stress with normalised radial distance for different lateral expansions (McCabe et al., 2008). 75

Figure 3.1 Finite Element model mesh and boundary conditions (Zhuang, 2009). 85

Figure 3.2 Pile capping ratio for reinforced and unreinforced piled-embankment after Han and Gabr (2002).....87

Figure 3.3 Dilatancy Angle: (a) results from standard drained triaxial test; (b) Elasto-plastic model (Vermeer and Brinkgreve, 2008). 90

Figure 3.4 Hardening Soil model stiffness moduli (a) $E_{50\ ref}$ and $E_{ur\ ref}$ for drained triaxial test results; (b) $E_{oed\ ref}$ in oedometer test results (Brinkgreve et al., 2018).....91

Figure 3.5 Influence of interface reduction factor upon the embankment surface settlement performance. 92

Figure 3.6 Zaeske (2001) model test dimensions and configuration: (a) plan view of piles; (b) section view. 95

Figure 3.7 Sand particle size distribution used by Zaeske (2001). 97

Figure 3.8 Axisymmetric model mesh used for the calculations. 99

Figure 3.9 Validation of soil parameters for Zaeske (2001) model test: applied load vs pile load. 99

Figure 3.10 Validation of soil parameters for Zaeske (2001) model test: Applied load vs geogrid tensile force.....100

Figure 3.11 Profiles of normalised earth pressure coefficient (K/K_p) on a vertical profile at the midpoint between piles.....109

Figure 3.12 The fill angle of internal friction variation with (a) soft soil surface settlement and (b) pile load. 111

Figure 3.13 Developed arching in embankment in terms of principle stresses after applying 104 kPa external load (a) h=0.7 m (b) h = 1 m (c) h = 1.3 m. 112

Figure 3.14 Stress concentration ratio: (a) influence of the height of embankment; (b) influence of geogrid. 114

Figure 3.15 Calculated and measured efficacy. 115

Figure 3.16 Efficacy for reinforced and unreinforced embankment.....116

Figure 3.17 Vertical settlements shading after applying 104 kPa external load. 117

Figure 3.18 Vertical embankment settlement vs external applied load. 118

Figure 3.19 Total shear strain contours: (a) unreinforced model; (b) reinforced model. 119

Figure 3.20 Plasticity points (Mohr-Coulomb failure zone). 121

Figure 4.1 Key soil properties for Bothkennar soft clay (Nash et al., 1992a). ..127

Figure 4.2 Bothkennar field trials (Serridge, 2013).....131

Figure 4.3 Validation of soil profile and parameters. 135

Figure 4.4 Measurement locations beneath footing.....139

Figure 4.5 Load-displacement behaviour (a) Footing 1 and (b) Footing2. 145

Figure 4.6 Influence of column spacing on the footing and ground vertical displacement in drained conditions- Footing 1 and Footing 2. 147

Figure 4.7 Triaxial test analogy 149

Figure 4.8 Influence of applied load on lateral bulging of the stone column for Footing 1 and 2- drained conditions. 150

Figure 4.9 Vertical stress ratio at column base level for Footing 1 and Footing 2- Drained conditions. 151

Figure 4.10 Load-displacement behaviour for OSC and ESC-Footing 1 and Footing 2. 152

Figure 4.11 Load-displacement behaviour (a) Footing 3, (b) Footing 4 and Footing 5. 154

Figure 4.12 Column bulging of Footings 3, 4 and 5 at applied load= 190kPa. .155

Figure 4.13 Influence of column length on the footing and ground vertical displacement in drained conditions- Footing 3. 156

Figure 4.14 Influence of column length on the footing and ground vertical displacement in (a) drained and (b) undrained conditions- Footing 4...157

Figure 4.15 Influence of column length on the footing and ground vertical displacement in drained conditions - Footing 5. 157

Figure 4.16 Lateral bulging (Ux) with depth observed in drained conditions- Footing 3. 158

Figure 4.17 Lateral bulging with depth observed in (a) drained and (b) undrained conditions- Footing 4.....159

Figure 4.18 Lateral bulging (Ux) with depth observed in drained conditions- Footing 5. 160

Figure 4.19 Effective vertical stress transfer to the column base in drained condition- Footing 3. 161

Figure 4.20 Load-displacement behaviour for OSC and ESC-Footing 3, 4 and 5. 162

Figure 4.21 Influence of encasement depth upon vertical settlement in (a) drained and (b) undrained conditions.....164

Figure 4.22 Lateral bulging (a) in x-direction, and (b) in y-direction with depth observed in drained conditions- h/d= 1.33.....165

Figure 4.23 Settlement at the ground surface for (i) ordinary and (ii) reinforced stone columns with h/d=1.33 in (a) drained and (b) undrained conditions. 166

Figure 4.24 Vertical stress distribution (h/d=1.33): (a) 1st load cycle; (b) 2nd Load cycle. 167

Figure 4.25 Lateral bulging in (a) x-direction, and (b) y-direction with depth observed in drained conditions- h/d= 2.67.....168

Figure 4.26 Settlement at the ground surface for an encasement of h/d= 2.67- drained and undrained conditions. 169

Figure 4.27 Lateral bulging (a) in x-direction, and (b) in y-direction with depth observed in drained conditions- h/d= 7.6. 170

Figure 4.28 Settlement at the ground surface for an encasement of h/d= 7.6- drained and undrained conditions. 172

Figure 4.29 Influence of encasement depth on the hoop tension forces (h/d = 1.3)- drained conditions. 173

Figure 4.30 Influence of encasement depth on the hoop tension forces (h/d = 2.67)- drained conditions.....174

Figure 4.31 Influence of encasement depth on the hoop tension forces (h/d = 7.6)- drained conditions. 174

Figure 4.32 Load-displacement behaviour for pad footing 4 and footing 6. 176

Figure 4.33 Influence of footing shape on the footing and ground vertical displacement in drained conditions- Footing 6. 176

Figure 4.34 Lateral bulging (Ux) with depth observed in drained conditions- footing 6. 177

Figure 4.35 Load-displacement behaviour for OSC and ESC-Footing 6. 178

Figure 4.36 Load-displacement behaviour for pad footing 7.....179

Figure 4.37 Influence of footing shape on the footing and ground vertical displacement in drained conditions- Footing 7 180

Figure 4.38 Lateral bulging (Ux) with depth observed in drained conditions- Footing 7. 180

Figure 4.39 Lateral bulging (Uy) with depth observed in drained conditions- Footing 7. 181

Figure 4.40 Load-displacement behaviour for OSC and ESC-Footing 7. 182

Figure 4.41 Influence of column diameter upon footing settlement- drained conditions. 185

Figure 4.42 Influence of column strength upon footing settlement- drained conditions. 186

Figure 4.43 Influence of geogrid encasement on Load-displacement behaviour for OSC and ESC. 187

Figure 5.1 Settlement analysis of one cell of an infinite grid of floating stone columns (a) vertical cross section (b) vertical effective force equilibrium of element A. 193

Figure 5.2 FE mesh and geometry. 200

Figure 5.3 Variation of RSR with column length for (i) RF= 0.42 and (ii) RF= 0.5 for soft soil thickness of H= 10 m and column spacing of s= 1.0 m. 202

Figure 5.4 Variation of RSR with column length for (i) RF=0.42 and (ii) RF= 0.5 for soft soil thickness of H= 10 m and column spacing of s= 1.2 m. 203

Figure 5.5 Variation of RSR with column length for (i) RF= 0.42 and (ii) RF= 0.5 for soft soil thickness of H= 10 m and column spacing of s=1.5 m. 204

Figure 5.6 Variation of RSR with column length for (i) RF= 0.42 and (ii) RF= 0.5 for soft soil thickness of H= 14.5 m and column spacing of s= 1.0 m. .205

Figure 5.7 Variation of RSR with column length for (i) RF= 0.42 and (ii) RF= 0.5 for soft soil thickness of H= 14.5 m and column spacing of s= 1.2 m. .206

Figure 5.8 Variation of RSR with column length for (i) RF= 0.42 and (ii) RF= 0.5 for soft soil thickness of H= 14.5 m and column spacing of s=1.5 m. ..207

Figure 5.9 Distribution of plastic points within a cross-section of (a) A/A_c= 3.5, (b) A/A_c=5.1, (c) A/A_c=8.0, and (d) A/A_c= 14.1 for column length of 6 m. 208

Figure 5.10 Variation of RSR with column length for (i) RF= 0.42 and (ii) RF= 0.5 for soft soil thickness of H= 20 m and column spacing of s=1.0 m. 209

Figure 5.11 Variation of RSR with column length for (i) RF= 0.42 and (ii) RF= 0.5 for soft soil thickness of H= 20 m and column spacing of s=1.2 m. 210

Figure 5.12 Variation of RSR with column length for (i) RF= 0.42 and (ii) RF= 0.5 for soft soil thickness of H= 20 m and column spacing of s= 1.5 m. 211

Figure 5.13 Variation of RSR with critical column length to the soil thickness ($l_{critical}/H$) for (i) RF= 0.42 and (ii) RF= 0.5 at applied pressure= 50 kPa. 213

Figure 5.14 Simplified analytical model program used to predict the settlement of strip/spread footings 215

Figure 5.15 Column configurations to examine RSR of single footings. 216

Figure 5.16 Variation of RSR with critical column length to the soil thickness ($l_{critical}/H$) for (i) Single footing and (ii) 2x2 group. 217

Figure 5.17 Variation of RSR with critical column length to the soil thickness ($l_{critical}$/H) for (i) 3x3 group and (ii) 2-column footing. 218

Figure 5.18 Displacements of footing, at column toe, and soil surrounding base of columns. 220

Figure 5.19 Variation of (a) punching and (b) compression ratios for lateral coefficient (i) RF= 0.42, and (ii) RF= 0.5 with column length for unit cell model. 221

Figure 5.20 Vertical displacement for q= 50 kPa with column length L= 2m and L= 7m (A/A_c= 3.53).....223

Figure 5.21 Variation of (a) punching and (b) compression ratios for lateral coefficient (i) RF= 0.42, and (ii) RF= 0.5 with column length for unit cell model. 223

Figure 5.22 Variation of (a) punching and (b) compression ratios for lateral coefficient (i) RF= 0.42, and (ii) RF= 0.5 with column length for unit cell model 225

Figure 5.23 Block failure with different area ratio (L= 6 m and q= 50 kPa). ...226

Figure A.1 Vertical settlement prediction using Priebe (1995) method- Footing 1. 255

Figure A.2 Vertical settlement prediction using Priebe (1995) method- Footing 2. 256

Figure A.3 Vertical settlement prediction using Priebe (1995) method- Footing 3. 257

Figure A.4 Vertical settlement prediction using Priebe (1995) method- Footing 4. 258

Figure A.5 Vertical settlement prediction using Priebe (1995) method- Footing 5. 259

Figure A.6 Vertical settlement prediction using Priebe (1995) method- Footing 6. 260

Figure A.7 Vertical settlement prediction using Priebe (1995) method- Footing 7. 261

Figure A.8 Mean vertical stress (σ_z) at a depth Z beneath a rectangular area (L x B) loaded to a uniform bearing pressure of P_0, after Boussinesq (1885). 262

Figure A.9 Influence values (I) based on L/B = 1, for various soil layer thickness (H), after Ueshita and Meyerhoff (1968). 263

Figure A.10 Depth of influence, after Burland and Burbridge (1985). 265

Figure B.1 Simplified analytical model program used to predict the RSR. 267

List of abbreviations

ESC	Encased Stone Column
FEA	Finite Element Analysis
FEM	Finite Element Method
HS	Hardening Soil
MC	Mohr- Coulomb
OSC	Ordinary Stone Column
RSR	Relative Settlement Reduction
SS	Soft Soil

List of Notations

A_f	Area of foundation
A/A_c	Area ratio
B	Half width of strip (Hewlett and Randolph, 1988)
c_c, c_s	Compression and swelling indices, respectively.
c_c	Arching coefficient (BS8006, 2010)
c_u	Undrained shear strength
D_f	Depth of foundation
E	Efficacy
E_s	Young's modulus (soil)
E_{50}	Secant Young's modulus at 50% deviatoric stress
E_{oed}	Tangent stiffness for primary oedometer loading
E_{ur}	Young's modulus for unload-reload
F_k	Vertical load on geotextile

H	Soft soil layer thickness
H_c	Arching critical length
I	Stone column length
I_c	Consistency index
I_p	Displacement influence factor
J	Axial geogrid stiffness at 2% elongation
K_o	Coefficient of lateral earth pressure at rest
K_s	Final coefficient of horizontal soil pressure
L	Column length
LL	Liquid limit
L_w	Geotextile length
$Nc, N\gamma, Nq$	Bearing capacity factors
$P, \acute{P}$	Mean principal total and effective stress, respectively
P_b	Average vertical pressure above geosynthetic reinforcement
P_c	Yield stress in the steel rebar
P_{ref}	Reference pressure (Hardening Soil model)
PL	Plasticity limit
R	Radius of circular cell (unit cell)
RF	Lateral stress reduction factor
R_{inter}	Interface strength reduction factor
RSR	Relative settlement reduction
S, S_o	Soft soil settlement with and without treatment, respectively
S_{col}	Displacement corresponding to the cracking load
s_d	Displacement corresponding to ultimate load in the bond test
S_l	Settlement of soft soil below the stone column base level
T_{rp}	Geotextile tensile load
$U_{footing}$	Footing settlement at surface
U_{soil}	Vertical settlement of soil at column base level

W_T	Distributed tensile load in the geotextile
W	Footing width
a	Pile cap size
b_{ref}	Geotextile width
c	Cohesion
d	Column diameter
e_0	Initial voids ratio
F_d	Depth factor
h	Embankment height
h_g	Arching height
l_{crit}	Critical column length
m	Power for stress dependency (Hardening Soil model)
m_v	Modulus of volume change
n	Stress concentration ratio
n_0, n_1, n_2	Settlement improvement factors
q	Deviatoric stress
r	Radius of the stone column
s	Column spacing
u	Pore water pressure
u_z	Vertical displacement
u_x, u_y	Lateral displacement in x and y directions
v_b, v_c, v_d	Shape factors
w	Water content
z	Vertical distance upwards from the base of the embankment
γ	Bulk unit weight
δ	Average angle of friction between column and soil

δ_v	Footing vertical settlement
ε	Strain in the Geotextile
κ	Slope of unload/reload line on plot of v versus ln($\acute{P}$)
λ	Slope of isotropic normal compression line on plot of v versus ln($\acute{P}$)
μ	Pore water pressure
ν	Poisson's ratio
ρ	Soil arching ratio
$\sigma, \acute{\sigma}$	Total and effective normal stress, respectively
σ_c	Vertical stress on pile cap
σ_s	Vertical stress on subsoil
σ_{ro}	Free-field lateral effective stress
$\sigma_{zo,k}$	Subsoil vertical stress
τ	Unit shaft friction of column
φ	Angle of internal friction
ψ	Angle of Dilatancy
ΔS_0	Soft soil settlement over the column shaft

CHAPTER 1

INTRODUCTION

1.1 Background

Soft soils cannot sustain external loads without exhibiting large deformations. Several solutions are available to improve the strength and mechanical characteristics of soils such as ground improvement and stabilisation methods. Ground improvement and stabilisation is a broad field which may include a variety of techniques such as soil consolidation, soil replacement and column-like elements. This research, however, limits itself to ground stabilisation methods using column-like elements. Piled-embankments and vibro stone columns provide a possible solution for the construction of roads, railways and foundations over soft soils. The fundamental principle of the piled-embankment and vibro stone columns techniques is to relieve the stress on the weak soils without a major change in that soil's structure. The installation of both large displacement piles and stone columns will displace soft and loose soils laterally altering in-situ soil properties such as the lateral stress in the soil. Therefore, any change to the initial stress state may be attributed to the lateral soil displacement as a result of installation.

The vibro stone columns can be installed using various methods in a regular grid in low bearing capacity or high compressibility soils. A component material of columns is stiffer than the surrounding soft soil. Therefore, they attract a significant portion of applied load at ground level. The loads taken by the soil thus can be reduced as a result of ground improvement to a level where the foundation settlement and bearing capacity becomes satisfactory and in line with the structure specified performance. Embankments and foundations constructed on piles and stone columns have advantages over conventional forms of ground improvement (i.e. preloading and surcharging) as they are relatively rapid to construct and do not require extended time periods that other ground improvement techniques demand (Liu et al., 2007).

Piled-embankments are used in construction of railways and highways on weak soils because the majority of the load will be carried by the piles rather than the soft soil leading to a significant reduction of the total and differential settlement compared with traditional soft soil improvement methods (Han et al., 2014). If a load is applied on top of the piled-embankment system, a differential settlement tends to occur between piles and the surrounding soft soils which will cause the granular embankment material above the relatively rigid piles to settle less than the material above the soft soil. Shear stresses will be developed within the embankment as a result of the differential settlement of the underlying weak soil leading to vertical stress redistribution from the embankment over the weak soil to the top of the piles (arching). The settlement performance of the piled-embankment system relies upon the ability of the embankment material to arch between two adjacent piles.

While the bearing capacity of the piles has been well investigated by many researchers, a dearth of information exists regarding the effect of using soil lateral

pressure as an illustration for embankment arching phenomena. The most common design methods used in the UK (i.e. the 'Guido' method, 1987; Hewlett and Randolph, 1988; BS 8006, 2010) can estimate quite variable stresses acting on top of the soft soil ignoring completely the soft soil properties. Little work has been carried out to investigate the arching action using the profile of normalised earth pressure coefficient (K/K_p) on a vertical profile at the midpoint between piles after the application of embankment surcharge (Zhuang, 2009). Previous works have not comprehensively modelled the material of the piles and the surrounding soils. Piles were modelled as a rigid support and the soft soil is simulated as a vertical stress applied at the bottom boundary of the model. Zhuang (2009) presented the profile of normalised earth pressure coefficient (K/K_p) on a vertical profile at the midpoint between piles method claiming that this method gives a good illustration of arching behaviour. The research reported in this thesis used the frictional method presented by Zhuang (2009) in combination with the plane of equal settlement method to describe the development of arching within the embankment fill material in an attempt to address the lack of knowledge and understanding of embankment arching.

The use of stone columns as a ground improvement technique has been successfully implemented around the world. Foundation design in soft soils is usually governed by settlement performance criteria rather than bearing capacity due to their compressibility. The majority of studies are related to the bearing capacity of large groups of stone columns (Black, 2006; McCabe et al., 2009; McCabe and Killeen, 2016). The lack of information regarding the settlement of stone columns used to support a narrow shallow foundation for lightly loaded low-rise structures was identified by McCabe and Killeen (2010) and Serridge (2013). It is difficult due to scale effects associated with the laboratory tests to draw

definite conclusions with regard to the settlement and deformational behaviour of stone columns (McCabe and Killeen, 2016), and also the influence of lateral bulging and stone column reinforcement on the settlement performance at working stress levels.

1.2 Research aims and objectives

The aim of this research is to build upon previous studies and use commercial software to predict the effect of installing column-like elements (precast concrete piles and stone columns) upon granular embankment arching and pad foundation behaviour. Mechanically, the modus operandi of precast piles and stone columns differ significantly, the former operates largely by carrying stress down to a more substantial stratum better able to carry the load whilst the latter tend to improve the upper weak soil. Yet both seek to address the same problem and can be analysed with similar tools. To achieve the above aim, an in-depth investigation was carried out by building a numerical model based on the Finite Element method. The numerical analyses were verified against well-established case studies as presented by Zaeske (2001) and Serridge (2001). The specific objectives of the study reported herein have been to:

i. Examine the development of embankment arching after the application of embankment surcharge using the profile of normalised earth pressure coefficient (K/K_p) on a vertical profile at the midpoint between piles method combined with the plane of equal settlement method.
ii. Investigate the effect of shallow crust layer upon the behaviour of the stone columns beneath pad footings for lightly loaded structures.
iii. Investigate the settlement performance of ordinary and encased stone columns surrounded by soft soil in short and long-term conditions.

iv. Combine a simplified analytical design method derived by Satibi (2009) with the Priebe (1995) method to calculate the relative settlement reduction ratio associated with small groups of "floating" stone columns (i.e. columns not penetrating the full-depth of the weak soil).

1.3 Methodology

A series of two (2D) and three-dimensional (3D) Finite Element analyses are presented to investigate arching of piled-embankments and the settlement performance of small groups of stone columns beneath pad footings. PLAXIS is a Finite Element program which is specifically developed to perform geotechnical analysis and is adopted for this thesis (Killeen, 2012). An advanced constitutive model is used to simulate soil stress- strain behaviour of soil and stone columns. The soil profile adopted for piled-embankment analysis is that of the well characterised test model described by Zaeske (2001) and Kempfert et al. (2004). A soil profile and set of material parameters is used for the well-characterised Bothkennar test site to develop a better understanding of the behaviour of small groups of stone columns. The adopted soil profile and material properties are validated against published data by Jardine et al. (1995) and field trials of Serridge (2001). The analysis is extended to perform a parametric study to investigate the influence of key parameters. The effect of column spacing, length, foundation depth and dimension and the presence of a stiff crust play a key role in the settlement performance of stone columns. Furthermore, a simplified analytical model has been used to investigate the improvement of footing settlement due to the installation of stone columns.

1.4 Outline of thesis

A detailed description of the piled-embankment and the stone columns are provided in Chapter 2. A comprehensive review of the piled-embankments standards and available design methods is presented. Furthermore, a comprehensive review of the previous investigations of the stone columns such as laboratory modelling, field trials, analytical models, and numerical analysis is presented. Numerical analysis of arching effect and reinforcement materials tension (geogrids) developed in the piled-embankments are also reviewed. Column installation effect modelling in FEA is also discussed. The material model (Hardening Soil model) used in the FEA is discussed. Finally, the drained and undrained analysis (long-term behaviour) of the soft soil in PLAXIS program is discussed.

The accuracy of PLAXIS 2D to capture the load-settlement, geogrid tension force and pile loads is assessed in Chapter 3. The adopted soil profile and material parameters are described by Zaeske (2001) and Kempfert et al. (2004). Zaeske's model test is simulated with PLAXIS 2D and the predicted pile loads, geogrid tension force, and efficacy are validated with Zaeske (2001) measurements. The results from the piled-embankment analysis of this thesis regarding the influence of the normalised earth pressure coefficient upon characterising the arching effect, the developed tension in the geogrid reinforcement, and the influence of the key design parameters are presented and interpreted in Chapter 3.

A series of field tests installed in the Bothkennar site by Serridge (2013) are simulated and the predicted settlement are compared with the measured settlement on site. A well characterised Bothkennar soil profile and soil parameters are taken from a thorough investigation conducted by McCabe et al. (2009) which

also validated against Jardine et al. (1995) field trials. The Bothkennar field trials are simulated by PLAXIS 3D and the results of this thesis regarding the settlement performance, ground settlement profile at ground level, lateral bulging and the influence of encasement and their depths upon the settlement performance are presented and interpreted in Chapter 4.

A simplified analytical design method to estimate the improvement of footing settlement as a result of stone column installation for a group of stone columns is presented in Chapter 5. The analytical model is further developed to evaluate the effectiveness of stone columns to support pad and strip footings. The results of the analytical design method are compared with 2D Finite Element analysis. The influence of soft soil thickness, lateral earth pressure coefficient, column effective length upon settlement reduction ratio is discussed. The mode of deformation for a specific column length is presented and interpreted, accordingly.

Finally, the conclusions and the recommended future works are presented in Chapter 6. A better understanding of the piled-embankment arching and of the behaviour of lightly loaded narrow footings supported by small groups of stone columns installed using the dry bottom- feed technique is gained, and the findings can be used by the industry to relate with the existing design methods and standards.

CHAPTER 2

LITERATURE REVIEW

2.1 Introduction

The design and construction of foundations over soft compressible soils is a real challenge for the industry and geotechnical engineers due to the insufficient shear strength and high compressibility of the soft soils. A variety of techniques are available to overcome the difficulties associated with excessive settlement and low bearing capacity of the soft soils. Column-like elements such as piles and vibro stone columns are considered to be the most known (column-like elements) ground improvement techniques used to enhance the bearing capacity and settlement performance of the foundations constructed over soils with undesirable characteristics (Kempfert and Gebreselassie, 2006). Deep foundations such as piles as a technique have been used in civil engineering construction industry for a very long time. In Britain, examples of pile foundations can be dated back to the Romans who used piles in bridge works (Tomlinson, 2015). However, stone columns as an improvement technique were developed from the vibro compaction technique in mid 1930's (Serridge 2013). The vibro stone column technique was developed in 1956 to allow the treatment of the cohesive fine-grained soils using the vibratory action of the vibroflot (the principal piece of equipment used to install the stone columns). Piles can be installed to different lengths (depending on technique) and their main function is to transfer the loads to a deeper bearing

layer. Stone columns can be installed up to 15 m and can replace up to 35% of the soft soil (McKelvey et al., 2004). Vibro concrete columns and stone columns encased with geotextile developed by Van Impe and Silence (1986) are hybrid vibro techniques. In soft clays, bulging is the most common mode of failure due to insufficient lateral confining pressure provided by the surrounding soil. Therefore, it is more convenient to use encased stone columns in very soft soils to enhance the column bearing capacity and settlement performance because of the lateral support provided by the geotextile casing (Han and Gabr, 2002).

2.2 Classification of soft soil

Soft soil layers may extend to a depth of more than 30 m in the UK and elsewhere (Kempfert and Gebreselassie, 2006). In the UK, many cities and towns are located at river crossings for ancient strategic reasons, near estuaries, deltas or lakes. New roads and railway alignments frequently pass over soft soils or loose sands. Therefore, it is important to describe and classify soft soils to identify their characteristics among the wide variety of soil types to be understood by the geotechnical engineers and researchers. Soft soil (very soft to soft consistency) is normally defined as a normally consolidated fine grained soil (Bjerrum, 1973). Consistency of soils is determined from hand tests and can be used alongside other parameters to classify fine grained soils. Consistency has no quantitative connotation. Soil may be classified as soft clay if the following criteria have been fulfilled (Gaba et al., 2017):

- very soft to soft consistency with a consistency index;

$$\boldsymbol{I_c = \frac{LL - w}{LL - PL} < 0.5} \qquad (2.1)$$

where LL is the liquid limit, w is the water content, and PL is the plastic limit.

- the undrained shear strength $C_u \leq 40$ kPa (where laboratory or field tests of strength are available);

- Finger easily pushed in by up to 10 mm. Moulds with light finger pressure (BS5930, 2015).

The nature and properties of the soil such as sensitivity to vibration (soil sensitivity is defined here as the ratio between the undisturbed shear strength at failure and the remoulded shear strength in the field vane shear test) must also be carefully investigated. Some applications, such as the vibro stone column technique, are not recommended in very sensitive soils with a sensitivity greater than 5 due to the dramatic reduction in the soil shear strength if the soil is disturbed by the installation of the columns (Serridge, 2013).

The study of soil behaviour may be approached by measuring index properties, compression properties, strength properties, and deformation properties. The study of soil behaviour is out of the scope of this research topic and can be found in various resources (Lambe and Whitman, 1979; Terzaghi et al., 1996).

2.3 Soil primary compression

The ratio of the lateral effective stress to the vertical effective stress is known as the coefficient of lateral earth pressure K, and is given by:

$$\boldsymbol{K = \frac{\sigma'_h}{\sigma'_v}} \qquad (2.2)$$

$$\boldsymbol{\sigma'_v = \sigma_v - u} \ \textit{and} \ \boldsymbol{\sigma'_h = \sigma_h - u} \qquad (2.3)$$

where $\boldsymbol{\sigma'_h}$ and $\boldsymbol{\sigma'_v}$ represent the effective lateral and vertical stresses respectively, u is the pore water pressure, and σ_h and σ_v represent the lateral and vertical total stresses respectively. The soil stress increases during the sedimentation process

of a normally consolidated soil (Lambe and Whitman, 1979). Where there has been no lateral deformation, the value of K is then known as the 'at rest' value and is given the symbol K_o.

K_o can be determined either from laboratory tests carried out on an undisturbed sample or from field tests. However, in the absence of tests or for simplicity K_o can be estimated from the well-known empirical formula (Jaky, 1948):

$$K_o = 1 - \sin \emptyset' \qquad (2.4)$$

where φ' is the soil effective angle of internal friction. However, there are also other empirical equations to estimate K_o, particularly in soft soils. Jaky's formula which is widely accepted among engineers and researchers underestimates the K_o value for soft soils. In order to find out the right approach to calculate K_o, measured K_o values from Scherzinger (1991) and published work by Alphan (1967), Lee and Jin (1979) and Sherif and Koch (1970) were compared with Jaky's formula (Figure 2.1) for lacustrine soft clays.

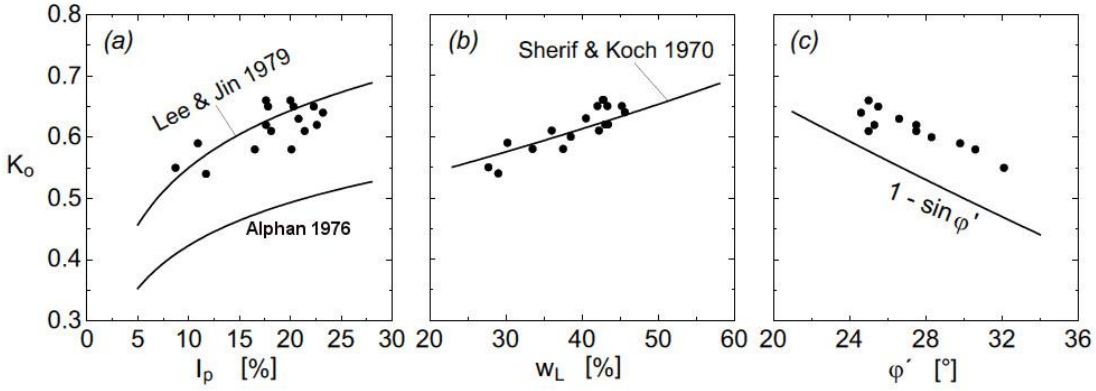


Figure 2.1 Empirical equations after Kempfert and Gebreselassie (2006) to estimate K_0 from (a) plasticity index I_p, (b) liquid limit WL and (c) effective angle of friction φ'(Scherzinger, 1991).

The K_o values obtained from Jaky's formula lies outside the range of K_o values measured by Scherzinger (1991). Hence, the K_o values calculated based on Scherzinger's (1991) work are adapted in the subsequent piled-embankment numerical analysis (see Figure 2.1). The effective angle of friction of the soft soil was used to determine the coefficient of lateral pressure at rest (K_o).

2.4 Soil improvement and stabilisation techniques

There are several foundation solutions available to overcome the undesirable characteristics of the soft soils. These solutions could be classified as follows: (1) change the embankment material by using lightweight materials, (2) improve the ground by the use of preloading, surcharging, stone columns, (3) acceleration of consolidation process such as vertical drainage, (4) technique to use structural support such as piles, (5) technique to use reinforced embankment fill (Magnan, 1994).

Each solution has its own advantages and disadvantages. Ground improvement and stabilisation methods are used to control the undesirable characteristics of the soft soils like excessive settlement, differential settlement and global instability of the foundations. Figure 2.2 illustrates and categorises the different methods and techniques available.

The benefits associated with each technique are out of the scope of this research. This research is limited to soil stabilisation methods using column-like elements such as stone columns and piled-embankment techniques. The main advantage of the latter technique is to reduce the applied stress on the weak soils without significant alteration in the soil structure, while stone columns can combine the action of piles with the improvement of weak soil. Therefore, it is important to

highlight the benefits associated with the use of each soil stabilisation method discussed in this thesis.

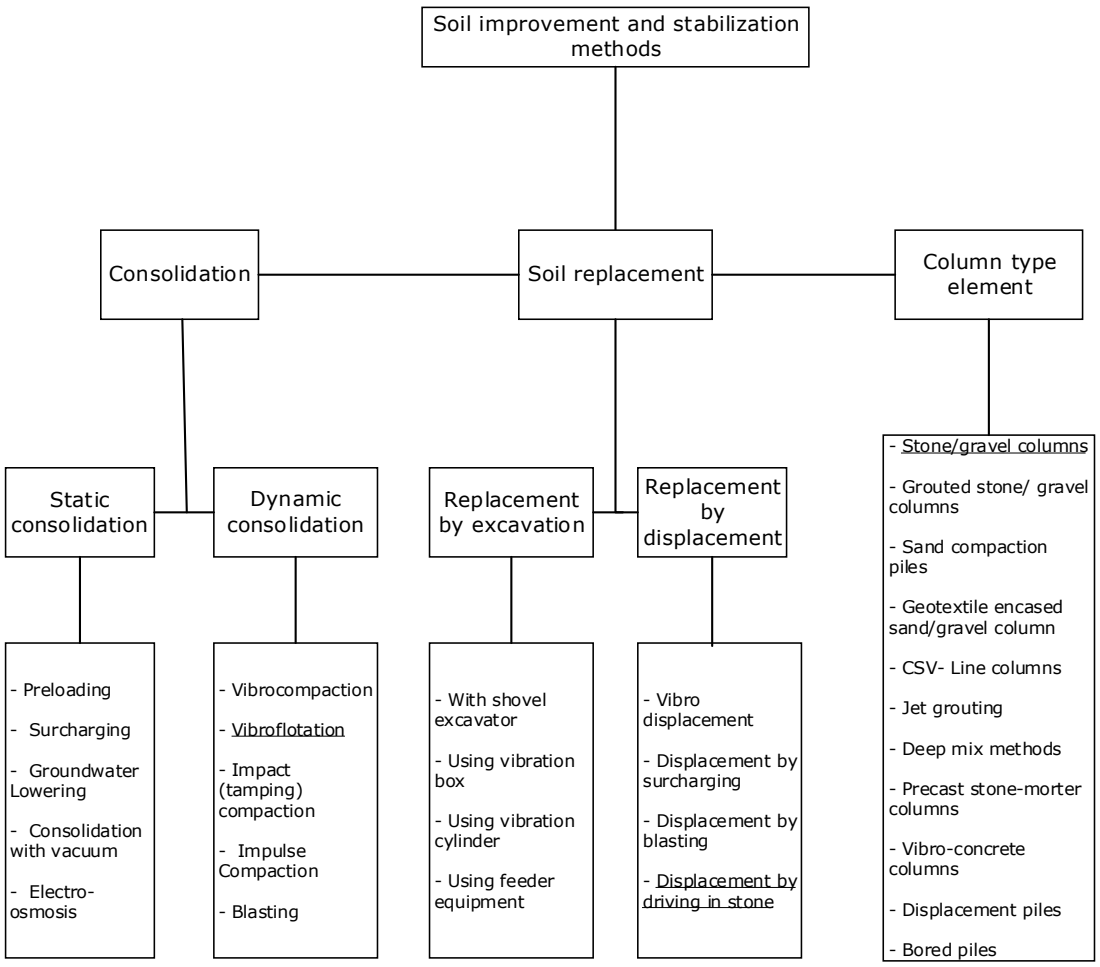


Figure 2.2 Overview of the soil improvement and stabilisation techniques (Kempfert and Gebreselassie, 2006).

Underlined text indicates aspects of the stone column technique as discussed further in this thesis.

2.4.1 Piled-embankment system advantages

There are many advantages associated with the use of the piled-embankment system and they are as follows (Liu et al., 2007):

- various geotechnical techniques can be addressed using a pile supported embankment method;

- rapid to construct and do not require extended time periods that many conventional forms of ground improvement demand;

- reduce total and differential settlement significantly.

Figure 2.3 shows several factors that are related to the settlement of the improved ground. Therefore, it is important to elucidate the mechanism of the settlement of improved ground with friction or end bearing piles.

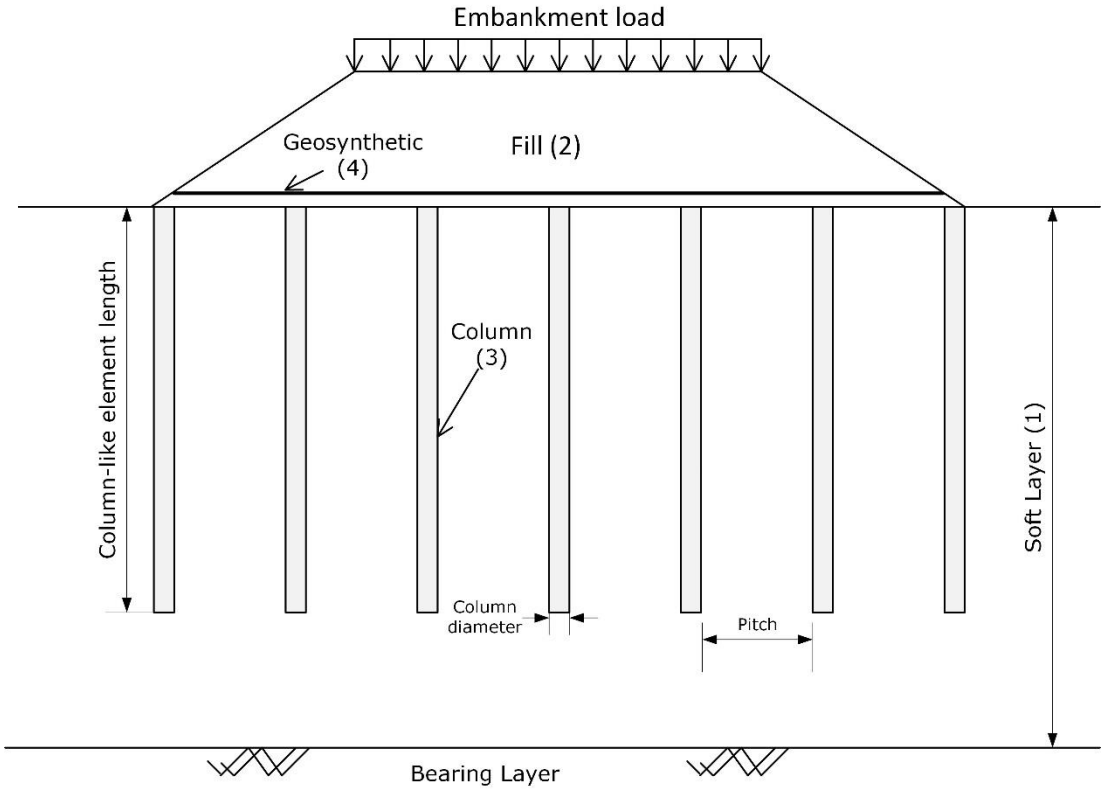


Figure 2.3 Main four elements influencing (reinforced) piled-embankment system.

The piled-embankment technique is one of the most common options when constructing roads and railways over soft soil because it is an economic and effective solution in comparison to other techniques (Ishikura et al., 2006). The piled-embankment technique enables the efficient construction of roads or high embankments on soft ground with a deep soil layer.

Ground improvement methods using column-like elements have been used since the 1960's in road and railway embankments (Kempfert and Gebreselassie, 2006). The basic principle of a reinforced embankment on rigid piles is to relieve the load on the soft soils and to transfer applied loads to a competent layer to avoid aforementioned problems in soft soils. Piled-embankments have been used with or without geosynthetic reinforcement at the base of the embankment (called conventional and reinforced piled embankments, respectively). The pile-embankment system is a complex system where four materials including soft soil, embankment fill, column-like element and geosynthetic (if reinforced) mainly influencing the settlement performance and the load transfer mechanism within the embankment fill.

Since column-like elements used to support the embankments are typically constructed with larger column diameters, therefore, this solution negates the need for a column cap (Han and Gabr, 2002). The arrangement of column-like elements and embankment geometry are very important for load transfer mechanism from the embankment to the columns, reinforcement, and soft soils. A closer column spacing, and/or larger column caps are required for the conventional piled-embankments compared with reinforced piled-embankments. A minimum embankment height is very important to ensure a sufficient load transfer mechanism within the embankment fill. It was found that the load transfer

mechanism within the embankment fill would not be improved if the embankment height is increased beyond the optimum height (Han and Gabr, 2002).

Furthermore, the tensile stiffness of the geosynthetic reinforcement plays an important role in the load transfer mechanism as explained in Section 2.5.1. The theoretical solutions such as BS8006 (2010) and Hewlett and Randolph (1988) ignore the influence of the tensile stiffness of the geosynthetic reinforcement. Due to the complexity of the problem, a numerical analysis is carried out and the outcomes are presented in Chapter 3 showing fundamental aspects of the behaviour of the piled-embankment over soft soils.

2.4.2 Stone column advantages

Historically, using deep foundations such as piles are considered as the first option when building over soft soil. Piles are normally extended to a competent stratum to resist applied loads. However, in very deep soft soils, floating piles can be considered as an option if the settlement performance is in line with the project specification. Long piles installed in soft soils are not cost effective and not considered a sustainable solution. Therefore, geotechnical engineers have been looking for more efficient methods to increase the soft soil strength and to reduce the cost associated with the long pile option.

A stone column technique has been used as an effective method to improve the mechanical properties and the state of stresses of soft soils (Najjar et al., 2010). In practice, vibrated stone columns are frequently used to treat weak soils due to the following reasons (Babu et al., 2013):

a) accelerating the consolidation of soft soil due to shortened drainage path;

b) improving load carrying capacity (as the increase in lateral stress caused by stone insertion provides consolidation that leads to soil strengthening) and;

c) reducing settlement due to the improved soil-structure system stiffness by introducing stiffer granular material.

The behaviour of the soft soil and stone is simulated using Finite Element method; a detailed analysis of the results is provided in Chapters 4 and 5 showing fundamental aspects of the behaviour of small and large group of stone columns installed in soft soils.

2.5 Previous investigations on piled-embankment system behaviour

Piled-embankments have been used to improve the soft soil beneath infrastructures such as railways and highways. Embankments can often be built to the desired elevation in stages, with side slopes being governed by the fill material and not the underlying soil (O'Riordan et al., 1994). Embankments are normally constructed to raise highway or railway level in flooding areas, minimise disposal of surplus materials excavated elsewhere, and to provide a satisfactory vertical alignment.

The minimum height of the embankment is determined from various codes and standards such as British Standard BS8006 (2010) and German EBGEO recommendations (Johnson, 2012). It is possible to construct roads and railways more quickly with acceptable settlement performance, which gives relatively low life cycle costs. Furthermore, underground services adjacent to the embankment can be built safely without being affected by the soil lateral movements.

Geosynthetics are often used to reinforce piled-embankments constructed over soft soils. The benefits of using geosynthetic layers are to reduce the pile cap sizes and to eliminate the use of raking piles (Reid and Buchanan, 1984). There are many types of geosynthetic materials that provide uniaxial, biaxial, or triaxial tension (load transfer in all directions) with the tensile strength varying between 20 to 1100 kN/m.

2.5.1 Arching in a piled-embankment system

The main concept of the piled-embankment system is that the embankment fill between two adjacent piles has a tendency to settle due to the presence of soft soil supporting the embankment. Shear resistance developed in the fill above the pile heads will restrain the movement of the embankment fill reducing the pressure on the reinforcement and soft soils but increasing the loads applied on top of the piles as indicated in Figure 2.4. The mechanism of the above load transfer was called the "arching effect" by various authors (i.e. Terzaghi (1943) and McNulty (1965)). Although the concept of arching has been recognised and acknowledged for many years, it remains not well understood. One of the main objectives of this research is to advance the state of understanding of arching in this context.

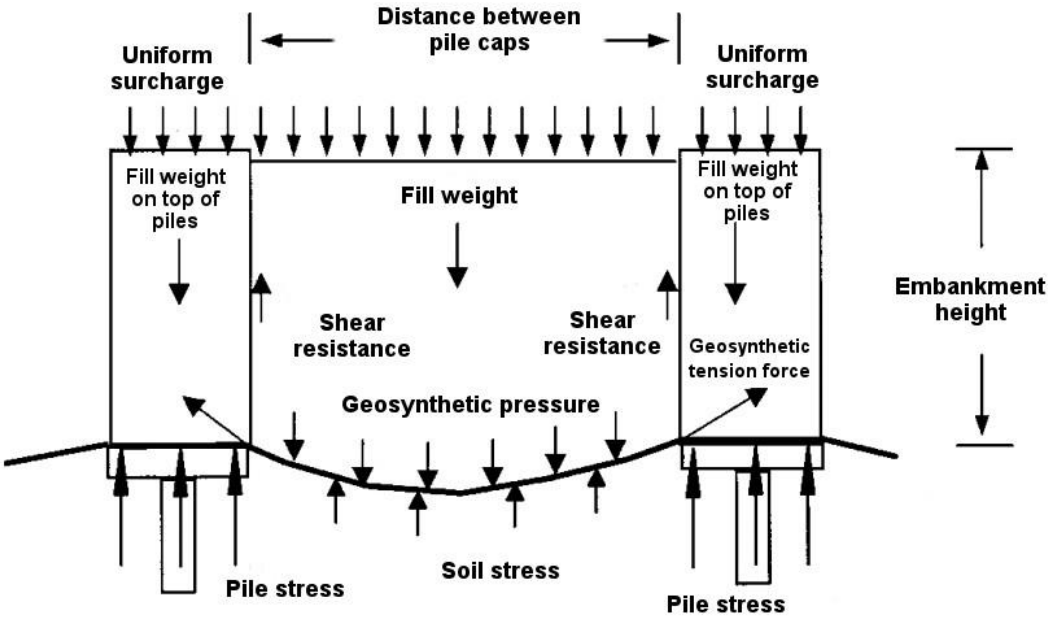


Figure 2.4 Load transfer mechanism of reinforced piled-embankment (Han and Gabr, 2002).

Geometry, load transfer mechanism and embankment stability are the main factors to consider in the piled-embankment design. Embankment stability can be checked using common slope stability methods such as the limit equilibrium method. Embankment stability and geometry are well defined; however, uncertainties lie with the load transfer mechanism through soil arching. Therefore, any improvement in design of the piled-embankment system should address the embankment fill arching and how to measure this aspect of the design.

Arching action has been recognised by many published standards and papers. As stated by Handy (1987), arching is defined as the transfer of stress from a yielding part of soil mass to adjoining less-yielding or restrained parts of a soil mass. The lack of a standard piled-embankment design has led to the development of many design theories and methods (Love and Milligan, 2003; Van Eekelen et al., 2003).

Additionally, soil-structure interaction is complex and the precise mechanism by which load transfers occur remains unknown.

Current design procedures such as BS 8006 and German method EBGEO 2004 Section 6.9 give a significant difference in the design results. Most of the design standards and procedures generally assume that the pile toe is founded on a rigid layer (Poulos, 2007; Satibi et al., 2009). Therefore, further studies are required to analyse embankments behaviour constructed on floating piles, although some studies on floating piled-embankments exist.

Construction of embankments over soft soils imposes a significant load over a wide area. Therefore, geotechnical engineers face big challenges during the design and construction over soft soils due to the soil compressibility. These challenges include potential bearing failure, intolerable settlement, large lateral pressure and movement, global or local instability and soil arching (Han and Gabr, 2002). The use of geotextile reinforcement enhances the arching effect (load transfer mechanism) by effectively transferring the loads from the subsoil to the pile head. Most of the embankment load is transferred to the pile head due to the embankment material arching. The remaining portion of the load is carried by both the soft soil and the geogrid at the top of the soil. The geogrid has very small resistance to bending and therefore will deflect and stretch accordingly (see Figure 2.4). The vertical component of the developed tensile force in the geogrid because of stretching in the geogrid will in turn transfer the load to the pile head which leads to a significant reduction in the subsoil pressure. The mechanism of transferring the load from the geogrid to the pile head is known as the membrane effect (Han and Collin, 2005).

One of the main benefits associated with the use of an embankment supported by piles is reducing the total and differential settlement significantly. In order to ensure efficient load transfer mechanism occur through soil arching from applied surcharge and embankment weight to the piles, the piles need to have large pile caps. Therefore, the influence of the pile cap is investigated in Chapter 3.

It is good practice in industry to use up to three layers of geogrids, although the current design procedures specified in the British Standard BS8006 (2010) and German code EBGEO (2004) are based on one layer of reinforcement. Numerical analyses performed by various researchers agree that one layer of strong geogrid layer is sufficient for stability purposes (Satibi et al., 2009). The main objective behind using more than one layer is to increase safety factor against uncertainties in the strength of the material and possible construction problems such as any damage that might occur during geosynthetic layers' installation.

In 1943, Terzaghi was one of the first researchers to define the soil arching in his text "Theoretical Soil Mechanics". He described the arching effects based on his experiment from which came the 'trap-door' theory. Although arching effect has been acknowledged for decades, arching still needs to be investigated due to various design uncertainties (i.e. the shape of the arch and different approximations and assumptions used to calculate pile and geosynthetic loads). As shown in Figure 2.4, Terzaghi (1943) initially proposed vertical shear planes at either side of a 'trapdoor'. Hewlett and Randolph (1988) derived a theoretical solution based on observations from experimental tests of arching in a granular soil attempting to investigate arching in coarse-grained soils. A semi-circular arch was proposed for the piled-embankments as shown in Figure 2.5.

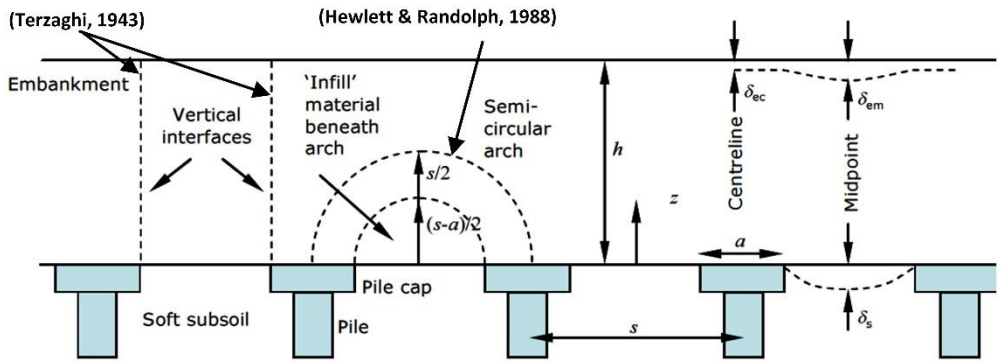


Figure 2.5 Piled-embankment showing potential arching mechanisms, and notation for geometry and settlement (δ) used in this thesis (Zhuang, 2009).

One of the main research objectives was to perform a numerical analysis for the piles installed in a grid pattern into soft soil and investigate the piled-embankment behaviour. The most commonly used theoretical models of embankment arching, often assumes a plane strain condition and this is described in the subsequent sections.

2.5.1.1 Terzaghi (1943)

Terzaghi (1943) argued that a gradual settlement of a soil strip below an embankment fill will cause the fill layer to settle accordingly. The settlement is resisted by the shear resistance alongside the vertical plane between the moving and stationary embankment fill (Figure 2.6). The total pressure on the moving soil is reduced and, consequently, leads to an increase in the load of the adjacent stationary soils (in terms of force).

Several authors extended Terzaghi's theory and his description of the load transfer mechanism in the piled-embankment system to derive expressions for the earth pressure coefficient, stress reduction ratio and stress distribution in the piled-embankment system (Handy, 1985; Mckelvey, 1994; Potts and Zdravkovic, 2008;

Russell et al., 2003). The vertical stress (σ_v) determined by Terzaghi (1943) was extended by Mckelvey (1994) as follows:

$$\sigma_v = \frac{\gamma B}{K \tan \emptyset} \left(1 - e^{-K \tan \emptyset \frac{Z}{B}}\right) + q\, e^{-K \tan \emptyset \frac{Z}{B}} \qquad (2.5)$$

where q is the applied embankment load (kN/m^2), γ is the unit weight of the soil (kN/m^3), 2B is the width of the strip (m), φ is the fill angle of internal friction (degree), and z is the thickness of the soil overlying the element (m).

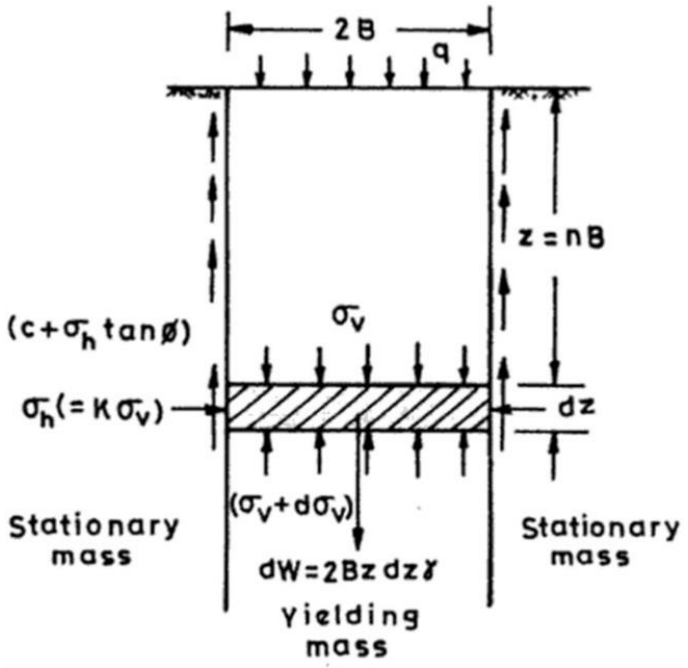


Figure 2.6 Forces acting on an elemental strip, after (Ranjan and Rao, 2007)

A drawback to Terzaghi's method is that the coefficient of earth pressure (K) is unknown also the K value is variable along the sliding surface. Therefore, several equations for the earth pressure coefficient were derived by other researchers (Handy, 1985; Potts and Zdravkovic, 2008; Russell et al., 2003). The coefficient of earth pressure (K) on the sliding surface can approach the passive coefficient of lateral earth pressure. However, a value of K=0.5 was suggested by Russell et al. (2003) claiming that the magnitude of the fill movement and the lack of lateral

support to a failing soil mass will reduce the K value on the yielding surface. This somewhat contradicts Zhuang (2009) findings, since the numerical analyses results show that a K value larger than the passive coefficient of lateral earth pressure on the yield surface. Although the idea underlying the frictional models (i.e. K profile on the yield surface) can be extremely important to determine the embankment critical Height and to address the lack of knowledge and understanding of the development of arching within the embankment fill, there is a little if any research data available for the application of frictional models to determine the critical height of the embankments due to arching. The research reported in this thesis is therefore concerned with evaluating the embankment critical height using the method of normalised earth pressure coefficient (K/K_p) on a vertical profile at the midpoint between piles (see Section 3.7).

2.5.1.2 Guido et al. (1987)

The Guido et al. (1987) method is different from other methods of modelling embankment arching, as it is based on empirical evidence from model tests carried out with geogrid-reinforced granular soil beneath a footing confined in a rigid box (Figure 2.7).

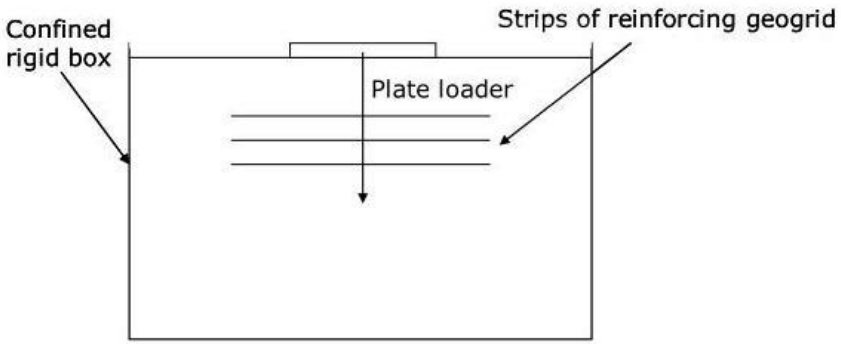


Figure 2.7 Guido's experimental set-up (geogrid-reinforced sand in a confined, rigid box).

Guido et al. (1987) observed that the inclusion of stiff biaxial geogrid within a granular fill improved the strength (or otherwise angle of friction) for the composite soil/geogrid material (Slocombe and Bell, 1998). It was concluded by Guido et al. (1987) that the angle of load spread through a granular fill reinforced with geogrid would be at an angle of 45 degrees (Figure 2.8).

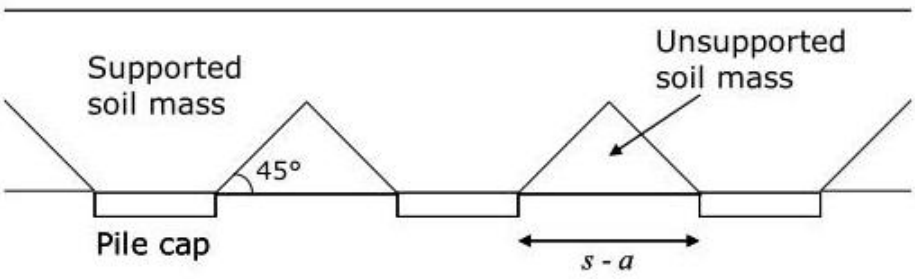


Figure 2.8 The mechanism of load spreading from the pile caps through an embankment (shown in 2D after Zhuang (2009)).

For the 2D condition, the stress acting on the subsoil (σ_s) is:

$$\sigma_S = \frac{\gamma (S-a)}{4} \qquad (2.6)$$

For the 3D condition, the equation is modified to:

$$\sigma_S = \frac{\gamma (S-a)}{3\sqrt{2}} \qquad (2.7)$$

where, a is the size of the pile cap (m), s is the pile spacing c/c (m), and γ is the unit weight of the embankment fill (kN/m^3). The height of the embankment has no effect on the pressure acting on subsoil as indicated by equation (2.6) and (2.7). Moreover, there is no consideration of the angle of friction of the fill.

2.5.1.3 Hewlett and Randolph (1988)

The proportion of load transferred to the piles and the foundation soil due to arching was investigated by Hewlett and Randolph (1988). A series of model tests

were carried out on a granular embankment overlying a rectangular grid of piles. Following experimental tests, it was observed that the majority of the embankment loads were transferred to the pile caps due to arching. It was also observed that the load applied on top of the foundation soil was predominantly due the weight of the material beneath the arches (Figure 2.9).

Hewlett and Randolph (1988) derived theoretical solutions based on the assumption of the semi-spherical arches in the embankment granular material. The method assumes that the infill pressure on the top of the foundation soil is uniform. It is worth noting that no reinforcement is incorporated in their model tests. The vertical stress acting on top of the foundation soil, σ_S, is:

$$\boldsymbol{\sigma_S} = \boldsymbol{\sigma_i} + \gamma\,(s-a)/2 \qquad (2.8)$$

where σ_i is the vertical stress acting immediately beneath the lower crown of the semi-circular arch. Low et al. (1994) improved the vertical stress calculation method derived by Hewlett and Randolph (1988) by incorporating the reinforcement (geosynthetic) layer contribution and also by considering a non-uniform vertical stress acting on the foundation soils. The improved vertical stress acting on the soft soil is given by:

$$\boldsymbol{\sigma_S} = \boldsymbol{\gamma}\frac{(s-a)(K_p-1)}{2(K_p-2)}\left(\frac{s-a}{s}\right)^{K_p-1}\left[\boldsymbol{\gamma H} - \frac{\gamma\, s}{2}\left(1+\frac{1}{K_p-2}\right)\right] \qquad (2.9)$$

where K_p is the passive earth pressure.

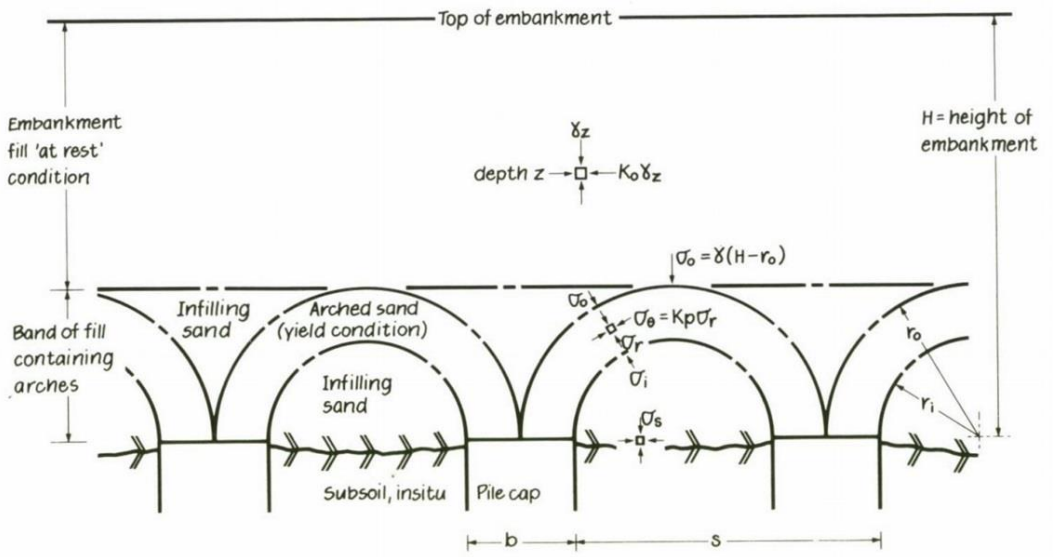


Figure 2.9 Section through a piled-embankment (Hewlett and Randolph, 1988).

2.5.1.4 German method EBGEO (2004)

The German method EBGEO (2004), Section 9.6, is based on a 3D arching model proposed by Kempfert et al. (1997), which is similar to the Hewlett and Randolph (1988) approach. However, following Figure 2.10 and by equilibrium of dome shaped arches of varying size in the 'infill' material beneath a hemisphere; the average vertical pressure acting on the soft soil can be calculated.

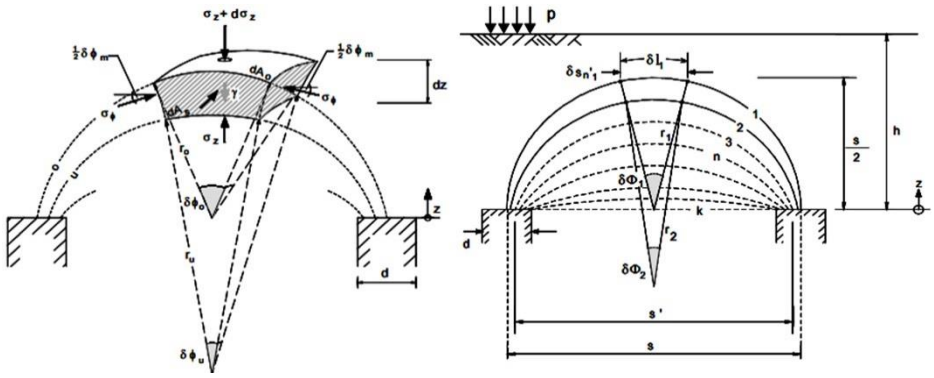


Figure 2.10 Geometry of arching and equilibrium stresses (Kempfert, 2003; Zaeske, 2001).

The German method is not only dependent on the parameters in British Standard BS8006 (2010), but also on the fill angle of friction and modulus of subgrade reaction *k* of the soft soil. The German method adopts partial factors like the design requirement of BS8006 (2010). However, more partial factors in the German method are used for the load and resistance properties of the embankments, piles and reinforcement as shown in Table 2.1.

Table 2.1 Summary of partial factors (DIN-1054 Revision 4).

Load factors		Load conditions[a]		
GZ 1B: Limit condition for construction failure		**LF 1**	**LF 2**	**LF 3**
Influence of dead load	γ_G	1.35	1.20	1.10
Influence of live load	γ_Q	1.50	1.30	1.10
GZ 1C: Limit condition for lost of overall stability				
Influence of dead load	γ_G	1.00	1.00	1.00
Influence of live load	γ_Q	1.50	1.30	1.10
Resistance factors				
GZ 1B: Limit condition for construction failure				
Pile resistance from pile loading tests	γ_{Pc}	1.20	1.20	1.20
Geotextile tensile resistance	γ_M	1.15	1.15	1.15
GZ 1C: Limit condition for lost of overall stability				
To be applied to tan φ'	γ_φ	1.25	1.15	1.10
To be applied to cohesion c'	γ_c	1.25	1.15	1.10
Geotextile pull-out resistance	γ_B	1.40	1.30	1.20

[a] LF 1 : end of construction. LF 2 : during construction, LF 3 : special cases, e.g. earthquake

3D soil elements are considered and the equilibrium of the forces about the radial direction is used to calculate the vertical stress $\sigma'_{zo,k}$ applied on the founding soil:

$$\sigma'_{zo,k} = \lambda_1^{\chi}\left(\gamma_k + \frac{q_k}{h}\right)\left(h\left(\lambda_1 + h_g^2\,\lambda_2\right)^{-\chi} + h_g\left(\left(\lambda_1 + \frac{h_g^2\,\lambda_2}{4}\right) - \left(\lambda_1 + h_g^2\,\lambda_2\right)^{-\chi}\right)\right) \qquad (2.10)$$

where

$$\chi = \frac{d.(K_P - 1)}{\lambda_2 .S};\ \lambda_1 = \frac{1}{8}.(s_d - d)^2;\ \lambda_2 = \frac{S_d^2 + 2.d.S_d - d^2}{2.S_d^2};\ K_P = \tan^2(45^o + \frac{\phi}{2}) \qquad (2.11)$$

and

$$h_g = {}^{S_d}/_{2}\ for\ h \geq {}^{S_d}/_{2};\ h_g = h\ for\ h < {}^{S_d}/_{2} \qquad (2.12)$$

where h_g is the arching height (m), d is the pile diameter (m), h is the embankment height (m), q is the embankment applied load (kPa), γ is the fill unit weight (kN/m^3), and s_d is the diagonal spacing (m).

The vertical stress acting on the top of the subsoil $\boldsymbol{\sigma'_{z0,k}}$ is used to calculate the vertical load F_K on the geotextile. The subscript k denotes the characteristic value of the stress. The geotextile vertical force and load distribution for rectangular pile layout are shown in Figure 2.11.

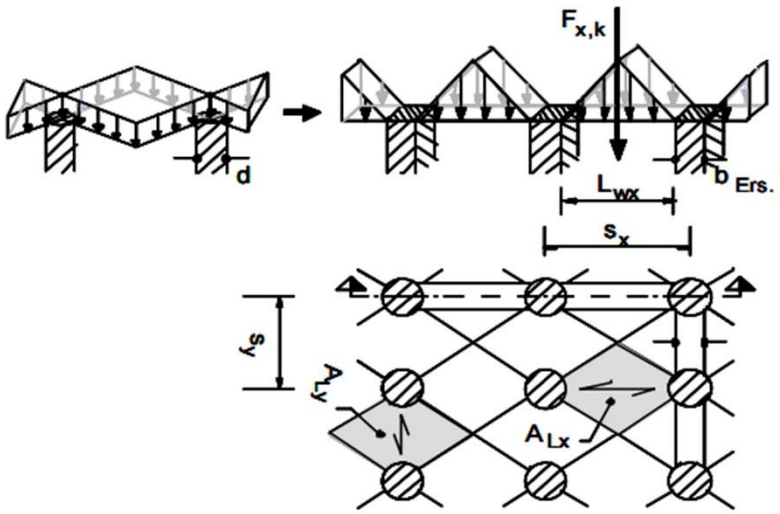
The vertical force F_K is acting on a strip geotextile (placed at the base of the embankment) with a width b_{ers} and a length of L_W as shown in Figure 2.11 for a rectangular grid:

$$\boldsymbol{F_x = A_{Lx} . \sigma'_{z0}} \;\; ; \; \boldsymbol{F_y = A_{Ly} . \sigma'_{z0}}$$

where

$$\boldsymbol{A_{Lx} = 0.5 . (S_x . S_y) - \frac{d^2}{2} . arctan\left[\frac{S_y}{S_x}\right] . \frac{\pi}{180}} \; ; \; \boldsymbol{A_{Ly} = 0.5 . (S_x . S_y) - \frac{d^2}{2} . arctan\left[\frac{S_x}{S_y}\right] . \frac{\pi}{180}} \qquad (2.13)$$

where S_x and S_y are the spacing between column-like elements in x and y directions (m), respectively.



$$A_{Lx} = \frac{1}{2} \cdot (s_x \cdot s_y) - \frac{d^2}{2} \cdot \text{atn}\left[\frac{s_y}{s_x}\right] \cdot \frac{\pi}{180} \qquad F_{x,k} = A_{Lx} \cdot \sigma_{zo,k}$$

$$A_{Ly} = \frac{1}{2} \cdot (s_x \cdot s_y) - \frac{d^2}{2} \cdot \text{atn}\left[\frac{s_x}{s_y}\right] \cdot \frac{\pi}{180} \qquad F_{y,k} = A_{Ly} \cdot \sigma_{zo,k}$$

Figure 2.11 Load distribution on the geotextile for rectangular pile layout (Kempfert et al., 2004).

The vertical and horizontal stress distribution with depth in the reinforced piled-embankments is neither described nor explained by any of the available design methods, including the German method. Van Eekelen et al. (2013) presented a series of field tests, claiming that the German method tends to under-predict arching of the embankment fill due to the assumption of the pressure distribution on top of the reinforcement.

2.5.1.5 British Standard - BS 8006 (2010)

BS 8006 (2010) adopted two methods for strengthened/reinforced soils and other fills: (1) based on the empirical relationship developed by Jones et al. (1990b) which is based on the 2D pipeline theory according to Marston and Anderson (1913) formula for positive projecting conduits, and (2) the method based on the

arching theory which is proposed by Hewlett and Randolph (1988). A further development to BS 8006 (2010) has been proposed by Van Eekelen et al. (2011) to account for the 3D configuration of the piles.

Jones et al. (1990b) developed an empirical relationship to design piled-embankment systems. Partial factors should be applied to the load, embankment material, piles and geotextiles to assure safe design. The list of partial factors listed by BS8006 (2010) is summarised in Table 2.2.

Table 2.2 Summary of BS8006 partial factors.

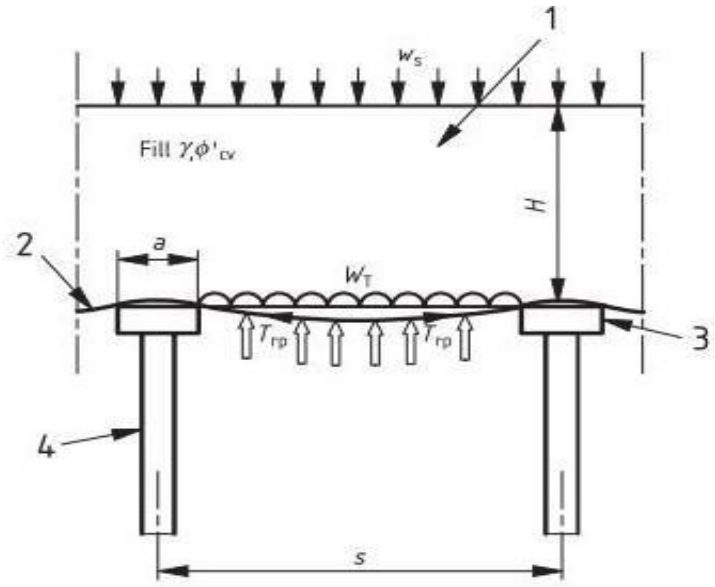
	Partial factors	Ultimate limit state	Serviceability limit state
Load factors	Soil unit mass, e.g. embankment fill	f_{fs} = 1.3	f_{fs} = 1.0
	External dead loads, e.g. line or point loads	f_f = 1.2	f_f = 1.0
	External live loads, e.g. traffic loading	f_q = 1.3	f_q = 1.0
Soil material factors	To be applied to tan ϕ'_{cv}	f_{ms} = 1.0	f_{ms} = 1.0
	To be applied to c'	f_{ms} = 1.6	f_{ms} = 1.0
	To be applied to c_u	f_{ms} = 1.0	f_{ms} = 1.0
Reinforcement material factor	To be applied to the reinforcement base strength	The value of f_m should be consistent with the type of reinforcement to be used and the design life over which the reinforcement is required (see **5.3.3** and Annex A)	
Soil/reinforcement interaction factors	Sliding across surface of reinforcement	f_s = 1.3	f_s = 1.0
	Pull-out resistance of reinforcement	f_p = 1.3	f_p = 1.0

Jones et al. (1990b) developed an empirical formula to derive the ratio of average vertical stress acting on the pile caps to the average vertical stress acting across the base of the embankment due to soil arching (Figure 2.12):

$$\frac{P'_c}{\sigma'_v} = \left[\frac{C_c\, a}{H}\right]^2 \quad where\ \sigma'_v = f_{fs}\gamma_{emb}H + f_q\, q \qquad (2.14)$$

where P'_c is arched vertical stress on top of the pile cap (kPa), σ'_v is average vertical stress on top of the founding soil (kPa), C_c is arching coefficient, a is the width of the pile caps (m), H is embankment height (m), and q is embankment external

surcharge (kPa). British Standard BS8006 (2010) suggests that C_c can be taken from Table 2.3.



Key

1	Embankment	3	Pile cap
2	Reinforcement	4	Pile

Figure 2.12 Piled-embankment parameters after BS8006 (2010).

The arching coefficients in Table 2.3 are appropriate for 3-dimensional analysis of the reinforced piled-embankment. The term $\frac{C_c\, a}{H}$ has been squared to account for the 3-dimensional effect in the piled-embankment.

Table 2.3 Arching coefficient for basal reinforced piled-embankments (British Standard BS8006, 2010).

Pile arrangement	Arching coefficient
End-bearing piles (unyielding) [A)]	$C_c = 1.95H/a - 0.18$
Friction and other piles (normal) [A)]	$C_c = 1.5H/a - 0.07$

[A)] See *A Guide to design loadings for buried rigid pipes [102].*

BS 8006 stated that the external applied load and embankment weight will not be transferred to the pile caps. Applied loads should be resisted solely by basal (geotextile) reinforcement on the top of pile caps. The vertical equilibrium is not satisfied in BS8006 when calculating the line load applied on top of the geosynthetic layer. BS8006 made this choice to overpredict the geosynthetic stresses and to guarantee sufficient safety leading to a stronger design outcome. However, this may yield unrealistic results for some piled-embankment problems (Ariyarathne and Liyanapathirana, 2015).

Two different arching conditions are defined in BS 8006 (2010) to calculate the tensile load in the geotextile: (i) the partial arching condition, and (ii) the full arching condition.

For partial arching,

$$W_T = \frac{s\,(f_{fs}\,\gamma H + f_q q)}{s^2 - a^2}\,[s^2 - a^2\,(P_c'/\,\sigma_v')\ \text{for}\ \textbf{0.7 (s-a) ≤ H ≤ 1.4 (s-a)} \qquad (2.15)$$

For full arching,

$$W_T = \frac{1.4\,s\,f_{fs}\,\gamma\,(s-a)}{s^2 - a^2}\,[s^2 - a^2\,(P_c'/\,\sigma_v')\ \text{for}\ \textbf{H > 1.4 (s-a)} \qquad (2.16)$$

The distributed tensile load W_T carried by the geotextile in Equation 2.16 considers a full arch developing at embankment height (H) > 1.4 (s-a). Hence, the external embankment load has no effect on distributed load carried by the reinforcement between adjacent pile caps. On the other hand, the external applied load on the top of the embankment has an impact on geotextile tensile load if the embankment height is less than 1.4 (s-a), following Equation 2.15.

Tensile load T_{rp} generated in the geotextile resulting from distributed load W_T can be taken as:

$$T_{rp} = \left(W_T \cdot (s-a)/2a\right) \cdot \sqrt{1 + (1/6\,\varepsilon)} \qquad (2.17)$$

where ε is the strain in the reinforcement. Soft soil support to the reinforcement is totally ignored in Equation 2.16. The calculated tensile load in the geotextile due to the vertical load and arching is dependent on the geometry of the system and embankment. The angle of friction has an influence only on the tensile force due to "spreading" near edges of the embankment. There is no dependence on other fill properties such as fill strength on the geotextile strength is considered.

2.5.1.6 Other mechanisms

Carlsson (1987) considered a wedge of soil with an internal angle at the apex of the wedge equal to 30 degrees. This method is called the Swedish method and is only valid for a 2D model (i.e. a plane strain condition). Carlsson's method adopts a critical height approach where the critical height is equal to 1.87 (s-a) in 2D. In order to account for the 3D effect, the average height would be 1.87/ 3 (s-a) = 0.62 (s-a) and hence σ_s/ γ (s-a) =0.62.

Naughton (2007) proposed a new method to calculate the magnitude of arching, which is based on the critical height of arching (Figure 2.13). It is assumed that the extent of yielding in the embankment material is defined by a log spiral shaped shear plane in the embankment fill from the edge of the pile caps in order to calculate the arching critical height (H_c).

$$H_c = C\,(s-a) \qquad (2.18)$$

where

$$C = 0.5\, e^{\frac{\pi}{2}\tan\varphi} \qquad (2.19)$$

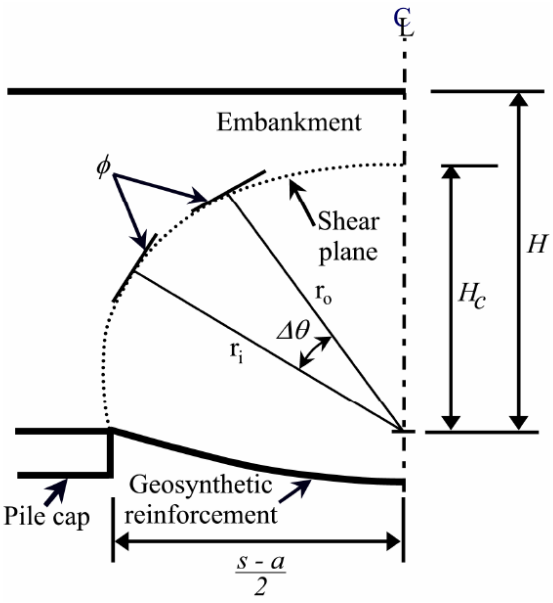


Figure 2.13 Geometry of assumed log spiral shaped yield zone (Naughton, 2007).

According to Naughton (2007), the effect of friction angle on the critical height of arching is significant, as demonstrated in Figure 2.14, where the critical height is proportional to the angle of friction.

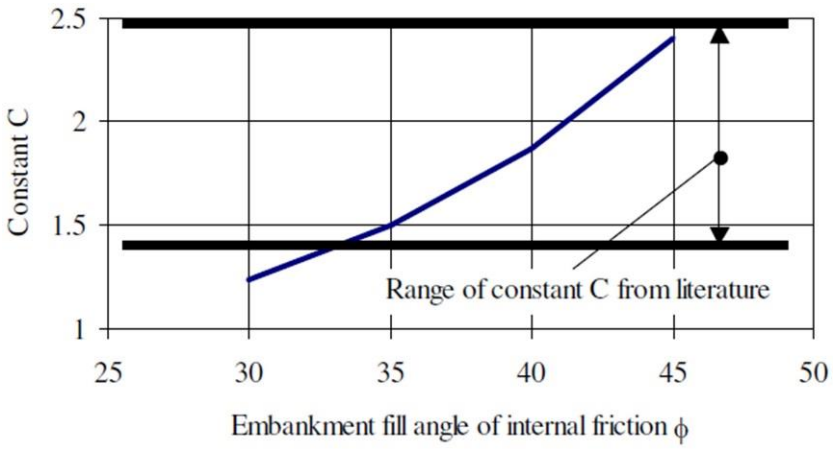


Figure 2.14 Influence of angle of friction on the critical height of the embankment (Naughton, 2007).

According to Naughton (2007), the height of the yielding zone is related to the subsoil stress as per equation 2.19:

$$\sigma_s = \gamma H_c = \gamma.C\,(s-a) \qquad (2.20)$$

and hence

$$\sigma_s / \gamma\,(s-a) = C \qquad (2.21)$$

The Dutch method (van Eekelen and Brugman, 2016) was first introduced in 2009 and revised in 2016. This method adopts major parts of the German EBGEO (2004). The EBGEO method has been modified to suit the design of a flat terrain-shallow embankments (Van Eekelen et al., 2010). The main difference from the German method is that a different set of load and resistance factors was adopted in the Dutch guidelines.

2.5.2 Summary of arching in a piled-embankment

A review of the embankment arching considered in the main design methods was presented in the previous sections. The arching of the piled-embankment system is recognised as the main mechanism for transferring the loads from the embankment to the piles. However, the shape of arching is not well understood and a review of the main design methods reveals inconsistency within each method in quantifying the arching effect. Ariyarathne and Liyanapathirana (2015) studied the stress reduction ratio (defined as the ratio of the average vertical stress carried by the reinforcement to the average vertical stress due the embankment fill), the geosynthetic tensile force, and the pile efficacy (defined as the proportion of embankment load carried by the pile) to demonstrate the inconsistency of the available design methods as shown in Figure 2.15. It is clear from Figure 2.15 that various design methods yield significantly different results when predicting stress reduction ratio, geosynthetic tensile force, and pile efficacy.

Terzaghi (1943) oversimplified arching by assuming the failure on a vertical plane. A semi-circular arching is assumed by Hewlett and Randolph (1988) the which is also assumed by the British Standard BS8006 (2010) with the introduction of the concept of partial and full arching. According to the British Standard BS8006 (2010), embankment height, h, and pile spacing, s, can be used to define arching. Meanwhile, the arching is formed with an internal angle of 45° from horizontal as demonstrated by Guido et al. (1987) method.

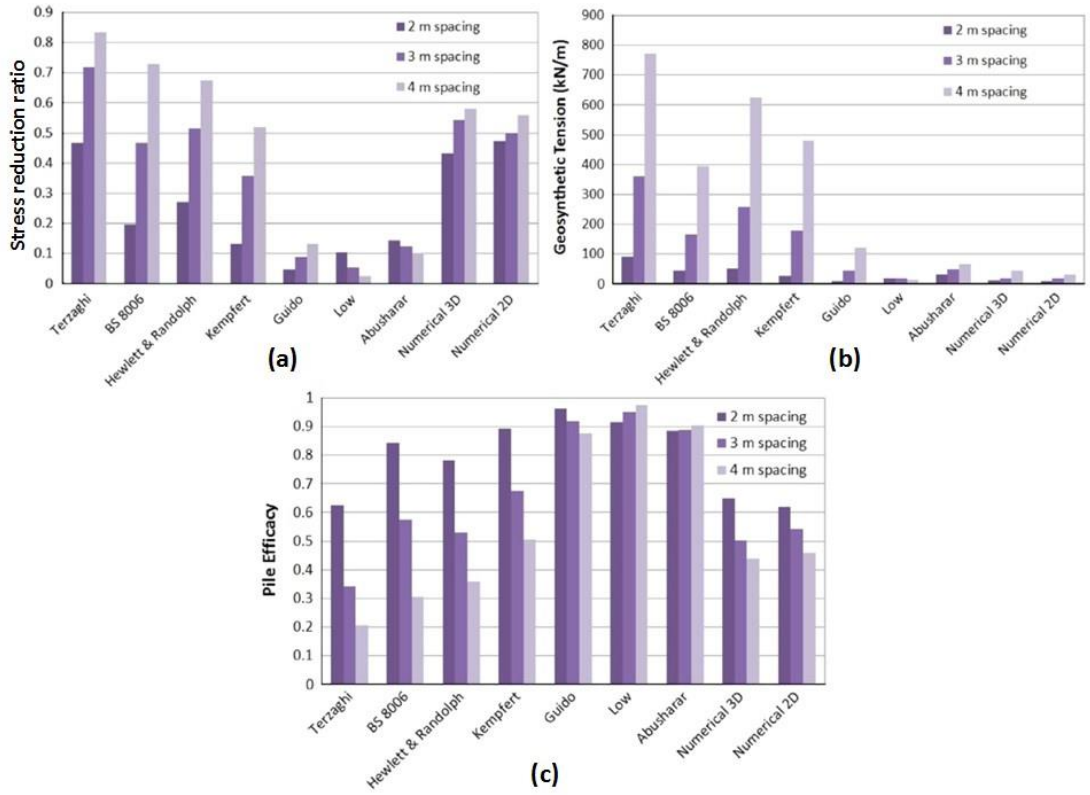


Figure 2.15 Comparison of design methods (a) stress reduction ratio; (b) geosynthetic tension; (c) pile efficacy (Ariyarathne and Liyanapathirana, 2015).

Finally, the German standard assumed a domed arch spanning between the pile caps. Furthermore, the adaptation of different assumptions to derive the equations of load transfer from the embankment to the piles by arching influences the level of accuracy of each method in predicting the arching effect. Also, some key

parameters such as the angle of internal friction of the embankment fill, the soft soil contribution, and the elastic modulus of the piles are not considered in these methods as outlined in Table 2.4.

Table 2.4 Key missing parameters from design methods.

Design method	Missing parameters			
	Subsoil	**Embankment Fill**	**Geosynthetic**	**Piles**
Terzaghi (1943)	X*	Construction rate	X*	Elastic modulus
Guido et al. (1987)	X*	Friction angle, construction rate	Stiffness	Elastic modulus
Hewlett and Randolph (1988)	X*	Construction rate	X*	Elastic modulus
German standard (2004)	X**	Construction rate	Stiffness	Elastic modulus
BS 8006 (2010)	X*	Friction angle, construction rate	Stiffness	Elastic modulus

*Subsoil support/ geosynthetic reinforcement are not considered in the analysis.

** Only considered for reinforced piled-embankment.

The principle advantages and disadvantages of each design method are summarised in Table 2.5. The influence of these missing parameters can be considered if a Finite Element model is developed with appropriate material parameters and element sizes. It is deemed reasonable to assume that a validated FEA can be used to simulate the embankment material arching and to investigate the system settlement performance.

Although many researchers have investigated these design methods, a universal method is not yet available (Ariyarathne and Liyanapathirana, 2015; Van Eekelen et al., 2013; Zhuang, 2009). While the arching of embankment material is well recognised as a load transfer mechanism, there exists a dearth of information regarding the application of frictional models to determine the critical height of the embankments due to arching. This research is therefore concerned with evaluating

the embankment critical height using the method of normalised earth pressure coefficient (K/K_p) on a vertical profile at the midpoint between piles.

Table 2.5 Pros and cons of different design methods.

Design method	Advantages	Disadvantages
Terzaghi (1943)	- simple arching mechanism by assuming the failure on a vertical plane. - simple to use but generally gives a conservative design result.	- coefficient of earth pressure (K) is unknown. - the K value is variable along the sliding surface.
Guido et al. (1987)	- a multi-layer biaxial geogrid is used within the granular platform to improve the strength of granular material. - consider the effect of lateral spreading of the embankment.	- the height of the embankment has no effect on the pressure acting on subsoil. - no consideration of the angle of friction of the fill.
Hewlett and Randolph (1988)	- a non-uniform vertical stress acting on the foundation soils is considered in this method.	- assumes that the infill pressure on the top of the foundation soil is uniform. - no reinforcement is incorporated in their model tests.
German standard (2004)	- good for preliminary design but not for detailed design due to simplifications adopted in the procedure. - for the safety of design, certain partial factors for the load and resistance are applied during construction stage, after construction and in special cases (e.g. earthquakes).	- the vertical and horizontal stress distribution with depth in the reinforced piled-embankments is neither described nor explained. - tends to under-predict arching of the embankment fill due to the assumption of the pressure distribution on top of the reinforcement.
BS 8006 (2010)	- most widely used method and very conservative. - partial factors are applied to the load and resistance for safe design.	- the external applied load and embankment weight will not be transferred to the pile caps. - the external embankment load has no effect on distributed load carried by the reinforcement between adjacent pile caps. - the external applied load on the top of the embankment has an impact on geotextile tensile load if the embankment height is less than 1.4 (s-a).

2.6 Vibro stone column construction and design methods.

The composite nature of the ground, reinforced with stone columns, results in a load sharing mechanism between the column material and surrounding weak soil. Therefore, it is important to highlight that both the stone column material and

surrounding soil play an important role in the composite ground performance. This section provides a comprehensive review of the available construction and design methods.

2.6.1 Construction methods

Several terms are used to describe vibro stone column construction techniques such as vibrocompaction, vibroreplacement, and vibrodisplacement which necessitate addressing the terminology of various techniques in a consistent manner (Serridge, 2013). One of the best attempts can be found in the Building Research Establishment (BRE) – Specifying vibro stone columns (Watts, 2000). Two main fundamental principles are used to describe the terminology of stone column installation, the method of supplying the stone and jetting medium. This specification used the terms top/bottom feed to describe stone delivery or supply and wet/dry to describe the jetting medium. Three main terms are used for this purpose:

- Dry top-feed
- Dry bottom-feed
- Wet top-feed

The dry top technique can be used for all types of soil given that the bore remains stable during construction (Figure 2.16). There should be no ground water within the treatment depth range. This technique is typically employed for soils with undrained shear strength in the range 30-60 kPa (Greenwood and Kirsch, 1984).

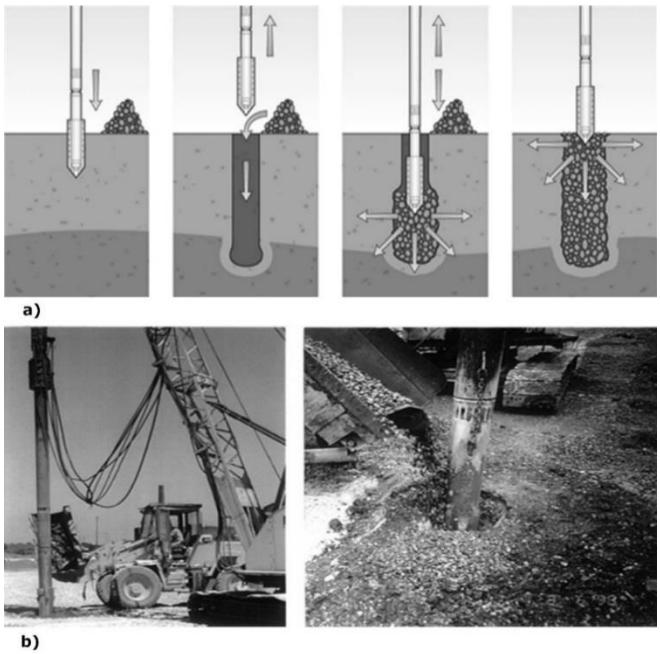


Figure 2.16 (a) dry top-feed stone column installation sequence. (b) dry top-feed stone column installation in the field (Serridge, 2013).

In a weak cohesive soil with high water table the dry bottom-feed technique is considered an appropriate method to construct the stone column. This technique is typically recommended for soils with undrained shear strength in the range 15-30 kPa where bore stability cannot be guaranteed using the conventional dry top-feed technique (Figure 2.17).

The main difference from the dry top technique is the vibroflot has a stone feed pipe attached allowing the introduction of stone aggregate to the tip of the vibroflot (Serridge, 2013). The construction process being similar to the dry top feed method where the vibroflot is lifted sufficiently to allow further charges of stones, which are then compacted by the vibration of the vibroflot until a full length of column formed to the ground level.

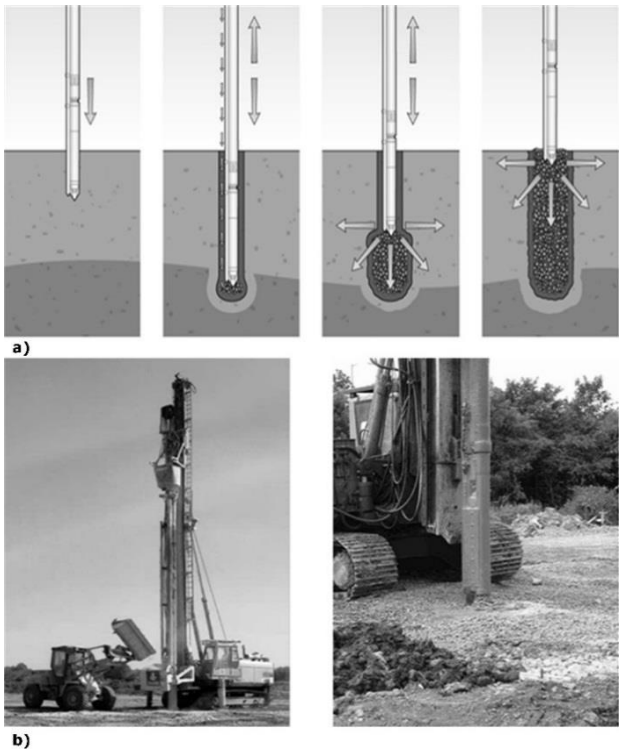


Figure 2.17 (a) dry bottom-feed stone column installation sequence. (b) dry bottom-feed stone column installation in the field (Serridge, 2013).

Following discussions with specialist ground improvement contractors (Balfour Beatty Ground Engineering and Vibro Menard), the range of stone column diameter is typically 500-600 mm and 600-800 mm for dry top and bottom feeding, respectively.

The wet top-feed technique is used historically in saturated fine-grained soils. This technique has replaced the dry bottom-feed technique on environmental grounds (Serridge, 2001). The main reason for such environmental constraints with the wet technique is that the soil is totally removed (washed out) from the bore whereas in the dry technique the soil is displaced to the sides of the bore (Figure 2.18).

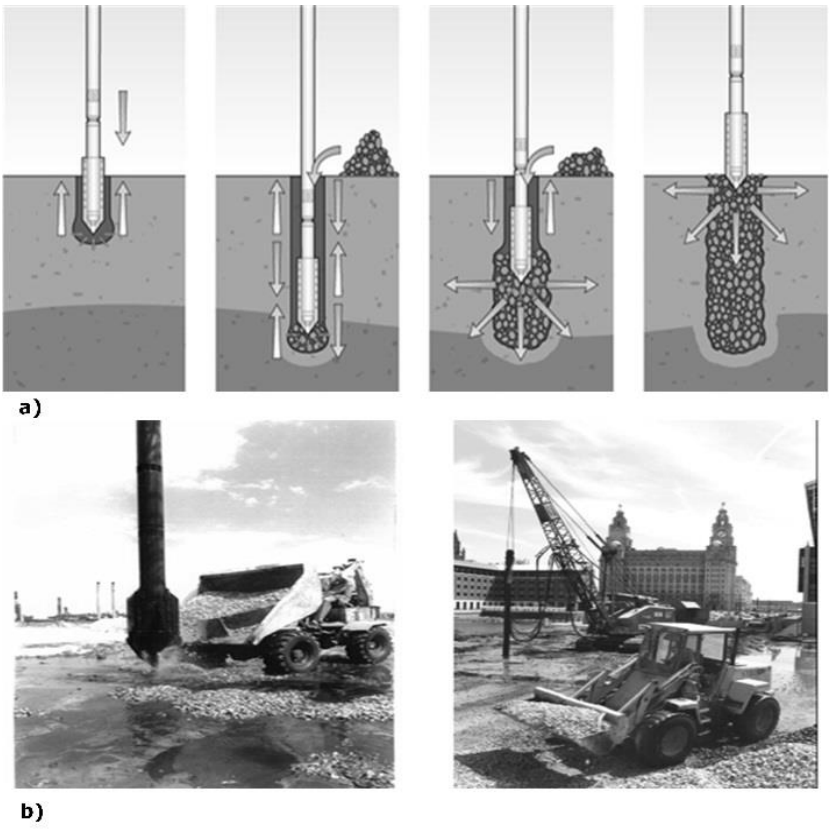


Figure 2.18 (a) wet top-feed vibro stone column installation sequence. (b) wet top-feed stone column installation in the field (Serridge, 2013).

Therefore, it is very important to take the necessary environmental precautions if soils removed from contaminated sites and the arisings should not be used as a backfill material without treatment. It is perhaps important to recognise that the wet technique is still sometimes used in very soft silty sensitive soils with undrained shear strength less than 15-20 kPa. In the wet technique, since the soil is removed or flushed out, a larger stone column can typically be built within the range of 750-1100 mm diameter based on discussions with specialist contractors.

2.6.2 Previous investigations of stone column behaviour

The stone column concept was first used in France in the 1930's (Serridge, 2013). Since then, the stone column-soil interaction has been investigated and

approached by many researchers to consolidate the current design methods and improve understanding to facilitate more economic design. These investigations comprised laboratory modelling, field trials, numerical modelling and empirical methods. Previous research mainly focused on the calculation and evaluation of the stone column bearing capacity and the settlement reduction due to the column installation (Babu et al., 2013).

2.6.2.1 Laboratory modelling

The main objectives of laboratory modelling are to simulate the field conditions and validate theoretical models. There are many problems associated with laboratory modelling and they are as follows:

Soils used in modelling (fine grained) are either remoulded or consolidated from a slurry which implies that specialised apparatus is necessary for testing (Burland, 1969; Hughes and Withers, 1974). The removal of the existing consolidation stresses causes swelling, therefore, the soil becomes over consolidated and the history of the soil is unknown which in turn creates problems.

Rigorously speaking, all geometrical dimensions and material properties of any model should be reduced by appropriate scale factors to be equivalent with the (field) prototype (Hu, 1995). However, it is impossible that any physical model can be identical in terms of all parameters that govern the field response.

It is very useful to use geotechnical centrifuge modelling due to the possibility of maintaining the prototype stress levels (Schofield, 1980). However, the use of centrifuge modelling is expensive and not always available in the research establishments. The laboratory analyses appear to focus on studying of isolated stone columns and those which investigate the group behaviour of stone columns,

even though most of the design procedures appear to have been derived from a single column analysis. It is worth noting, that the natural soils are not fully represented due to reconstitution of the soil during the preparation of the model (Castro et al., 2013). However, geotechnical centrifuge modelling has yielded very important research database where it has been utilised.

One of the greatest advances in knowledge of the stone column behaviour in soft soils comes from the laboratory tests on columns of Leighton Buzzard sand in Kaolin clay by Hughes and Withers (1974), which influenced much of the subsequent research . These tests provided most influential data to enable ground engineering practitioners and researchers to better understand stone column carrying capacity. The ultimate capacity of a stone column is governed primarily by the soil lateral confining pressure against bulging and the extent of stone column vertical movement. Hughes and Withers (1974) revealed that the mode of failure for a single stone column in soft clay is prominent in the upper part of the column where the depth of bulging was observed to be around 4 times the column diameter. Hughes and Withers (1974) used an X-Ray technique (and lead shot markers) to monitor the isolated columns deformation and the surrounding clay (Figure 2.19). It is important to note that the authors have adopted Gibson and Anderson (1961) elasto-plastic theory for cavity expansion because it represents the measured column behaviour very well. They proposed that the ultimate vertical effective stress (σ'_v) carried by a stone column as it bulges could be predicted by:

$$\boldsymbol{\sigma'_v = \left(\frac{1+sin\varphi'_s}{1-sin\varphi'_s}\right)(\sigma_{ro} + 4c_u - u)} \qquad (2.22)$$

where φ'_s is the stone angle of friction (degree), σ_{ro} is the total in-situ lateral stress (kPa), c_u is the undrained shear strength of the soil (kPa), and u is the pore water

pressure (kPa). This equation is widely used in today's practice due to its simplicity providing a catalyst for subsequent research programs.

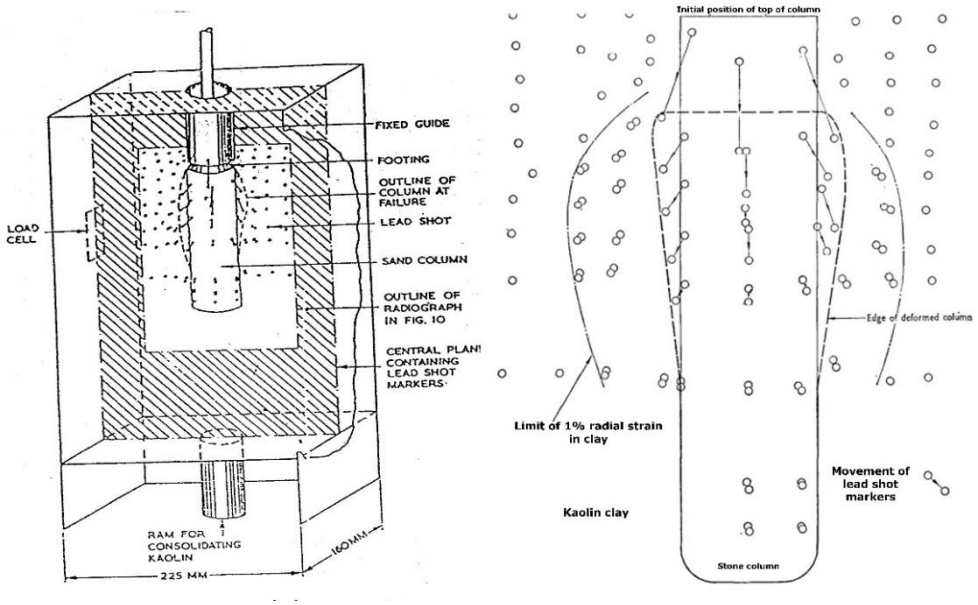


Figure 2.19 Deformation of 38mm diameter laboratory model column for 25mm displacement with limit of 1% radial strain in clay shown (after Hughes and Withers, 1974).

A series of laboratory tests was carried out by Sivakumar et al. (2007) with a visual examination of the stone column behaviour during the application of the loads. It was observed that a trade-off exists between the short columns (possibly column length to diameter ratio ≤ 6) which give adequate bearing capacity and the longer columns to satisfy the settlement performance criteria. It was also observed in these tests that a column under circular and strip footings can fail in different modes such as bulging, punching, shear and bending.

2.6.2.2 Field trials

Greenwood (1970) described full scale field trials undertaken at Bramerhaven (UK). Vibro stone columns and sand columns were constructed in order to find out

which material provides better performance. The field trials shown in Figure 2.20 highlighted the importance of using gravel in lieu of sand as a column material due to its effect on the column rigidity (stiffness).

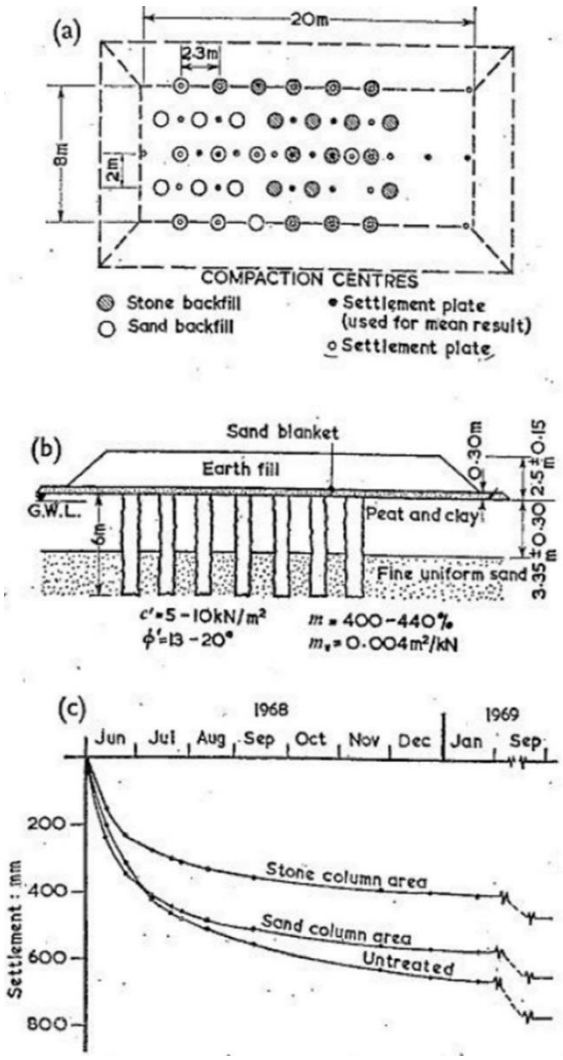


Figure 2.20 (a) to (c) Comparison of large scale field loading test results on untreated soft clay, soft clay reinforced with stone columns and soft clay reinforced with sand columns, after (Greenwood, 1970).

Field trials were undertaken by Hughes et al. (1976) to confirm the theory proposed by Hughes and Withers (1974) from their laboratory tests discussed in

Section 2.6.2.1. The measured load-settlement behaviour in the field was consistent with the laboratory test results.

(Goughnour and Bayuk, 1979b) carried out field trials on a group of stone columns in Hampton, Virginia (US), the recorded stress concentration ratios (defined as the column stress over the surrounding soft soil stress) were between 2.6 to 3.0 on top of the stone column. Greenwood (1970) and Bergado and Lam (1987) reported the results of field trials in Bangkok (Thailand) and the UK, both trials clearly conformed the Hughes and Withers (1974) and Hughes et al. (1976) hypothesis.

2.6.2.3 Other design methods

There are several design methods (i.e. empirical, semi-empirical, analytical and numerical) available to carry out a stone column design (Bouassida et al., 2009). Based on the discussions with the specialists in the ground improvement industry, reviewing available published information and available case studies, the author has been able to limit the design of stone column into two main specific areas, which are the stone column bearing capacity and settlement performance. Most of the design approaches are based on the unit cell idealisation. A one-dimensional unit cell which consists of one column surrounded by soils has often been used when analysing stone columns for simplification (Han, 2015).

The use of empirical or semi-empirical methods to design vibro stone columns typically require an experience in the stone column technique and they tend to be conservative. There is an element of uncertainty with these design methods when used to model complex structures or ground conditions. Therefore, numerical computation can provide answers and additional insight into these problems. This is addressed in Section 2.8 of this thesis.

2.6.2.3.1 Stone column bearing capacity

A relationship between allowable single column load and undrained shear strength for soft soil was proposed by Thorburn and MacVicar (1968) using an empirical approach. Vesic (1972) used cylindrical cavity expansion theory to determine the column bearing capacity. Further development of the Thorburn and MacVicar (1968) work was carried out by Thorburn (1975) to predict the single column allowable stress from the weak soil undrained shear strength, as shown in Figure 2.21. The stone column will attract a greater proportion of loads (Pc) than the surrounding soil (Ps) because the installed stone columns are generally an order of magnitude stiffer than the surrounding soils. Baumann and Bauer (1974) defined the column and surrounding soils loads as follows:

$$\frac{P_c}{P_s} = \frac{1 + 2\left(\frac{E_s}{E_c}\right).K_s\,.\,ln\left(\frac{a}{r_o}\right)}{2\left(\frac{E_s}{E_c}\right)K_c\,.\,ln\left(\frac{a}{r_o}\right)} \qquad (2.23)$$

and

$$P_o.A_o = P_c\,A_c + P_s\,A_s \qquad (2.24)$$

where P_o is imposed load from foundation (kPa); P_c is the stone column stress (kPa); P_s is the soil stress; E_c is the modulus of deformation of column (kPa); E_s is the modulus of deformation of soil (kPa); K_c is the column earth pressure coefficient; K_s is the soil earth pressure coefficient; A_s is the cross-sectional area of treated soil (m^2); A_c is the cross-sectional area of stone column (m^2); r_o is the radius of the stone column; a = $\sqrt{\left(\frac{A_o}{\pi}\right)}$.

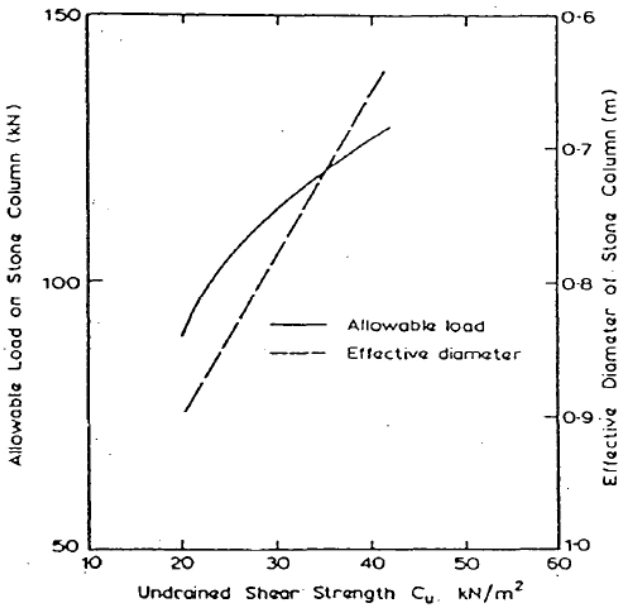


Figure 2.21 Allowable working load for stone column(s), after Thorburn (1975).

A good engineering judgement recommended by Barksdale and Bachus (1983) is recommended to estimate single column bearing capacity. Their approach is summarised in the following basic formula:

$$q_{ult} = c_u N_c \qquad (2.25)$$

where q_{ult} is the ultimate bearing capacity of the stone column (kPa), c_u is the undrained shear strength for the soil (kPa), and N_c is stone column bearing capacity factor which is related to the compressibility of the surrounding soil. N_c is usually ranging between 18-22 (where higher N_c values should be used for stiffer soils).

Stone column bearing capacity is also calculated based upon German DIN standards by Priebe (1991). Design charts developed subsequently by Priebe (1995) to calculate the stone column load in an infinite grid. Area replacement ratio (defined as the ratio of the stone column area to the tributary area of soil

per column in a large grid) and the stone column angle of friction were used to calculate the stone column load.

2.6.2.3.2 Settlement

One of the main elements of the stone column design is the settlement of the composite ground. Generally, an improved ground is assumed as an infinitely wide loaded area reinforced with stone columns having a constant diameter and spacing across the treated area. One of earliest attempts to assess the preliminary settlement was carried out by Poulos and Mattes (1969), where they presented an analytical solution to calculate the settlement as follows:

$$S_{col} = [P/(E_s.I)].I_p \qquad (2.26)$$

where S_{col} is the settlement of the stone column (m), P is the total applied load (kN), E_s is the Young modulus of the cohesive soil (kPa), I is the length of the stone column (m), and I_p is the displacement influence factor.

During the past four decades, many research works for calculating the column settlement have been reported in the literature. The most common methods include: Greenwood's method (Greenwood, 1970), Priebe's method (Priebe, 1976), an equilibrium method (Aboshi et al., 1979), a granular wall method (Van Impe and DeBeer, 1983), and a predictive method (Balaam and Booker, 1985). All these approaches are based on the unit cell idealisation. From the discussions with ground improvement specialists and also from the literature, the approaches proposed by Priebe (1976) and Baumann and Bauer (1974) are the most common.

Settlement analysis approaches typically assume that a stone column in an infinitely large group interacts with the surrounding soil and both the soil and the column are modelled as a unit cell. The area ratio (A/A_c) defined as the ratio of

the unit cell area to the stone column area is a measure of the proportion of the soil replaced by the column (Figure 2.22), where A represents the frequency of stone column per unit area of the foundation and A_c is the section area of the stone column.

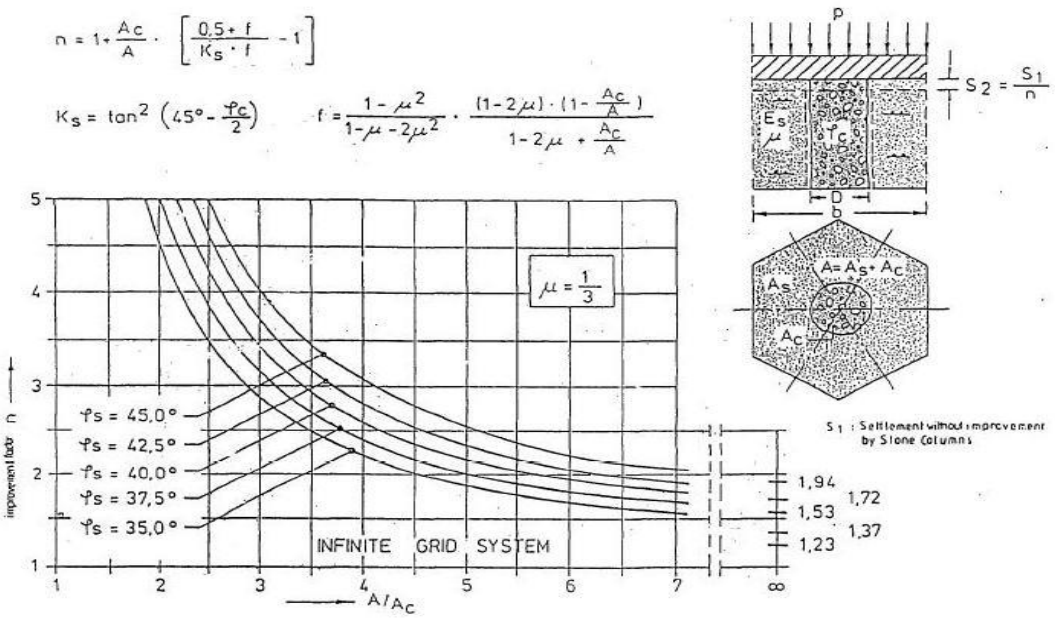


Figure 2.22 Settlement design curves and design philosophy for composite ground (soft soil reinforced with stone columns) after Priebe (1976).

It appears that all of the previous studies were investigating stone columns constructed in weak soils without considering other cases where soft soils are overlain by relatively stiff layers of either granular or cohesive nature similar to soil profiles at Bothkennar in Scotland and at Kinnegar in Belfast. The presence of a stiff crust at shallow depths and its influence on the deformational mode of the stone columns is not normally captured by laboratory tests or any other design method. Therefore, this aspect will be addressed in Section 4.9.2, 4.10.4, and 4.11 of this thesis.

Priebe's method (1976)

Priebe (1976) proposed a method to estimate the stone columns settlement based on a unit cell concept. Essentially, the Priebe's method is based upon elasticity theory and the earth pressure theory by Rankine. Also, the method assumed that the foundation is resting on an infinite grid of stone columns. The state of the final settlement in most cases is expressed as the basic improvement factor (the ratio of the settlement for untreated footing to a treated footing). The basic improvement factor is derived as a function of the total area of stone column to the original area of non-reinforced soil (A_c/A) , soil Poisson's ratio (μ_s) and the stone angle of internal friction (φ_c) (Figure 2.22). The derived basic improvement factor assumed that the column base is founded in a rigid layer ignoring the column material compressibility and the effect of overburden.

Further improvements were made by Priebe (1995) by considering the effects of column material compressibility and the overburden (Figure 2.23 and Figure 2.24). The ratio of the (oedometric) moduli of column and initial soil (D_c/D_s) in Figure 2.23 is used to calculate a reduced improvement factor (n1) due to the column compressibility. A depth factor (f_d = ratio between the initial stress difference at the surface of the reinforced soil and stress difference at a given depth) is introduced in Figure 2.24 to calculate the increase in the improvement factor from n1 to n2 = f_d. n1.

It is perhaps also worthy to note that the Priebe design method does not take account the disturbance of the sensitive soft clay during the installation of the stone columns which may contribute to the increase of the footing or slab settlement, also it does not consider the presence of stiff soils at shallow depth

and their impacts on the calculated settlement. This is addressed in Section 4.13 of this thesis.

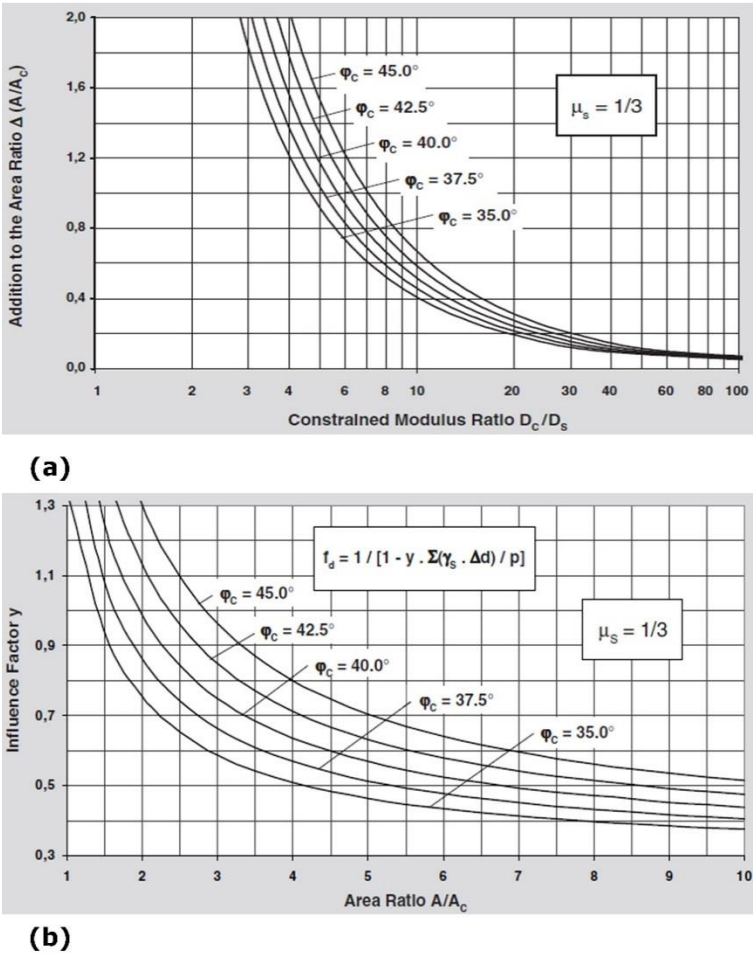


Figure 2.23 Consideration of (a) column compressibility (b) determination of depth factor, after Priebe (1995).

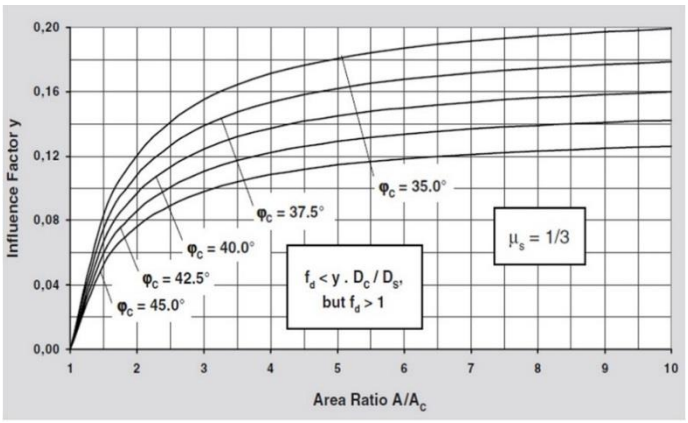


Figure 2.24 Limit value of depth factor, after Priebe (1995).

Also, Priebe (1995) developed additional design charts to predict settlements of single and strip footing supported by a limited number of stone columns. The design chart in Figure 2.25 was based on the total settlement of a large number of stone columns constructed to support an unlimited area (s). The design charts in Figure 2.23 and Figure 2.24 were used to investigate the effectiveness of stone columns in Chapter 4. The analytical model in Chapter 5 used the design chart in Figure 2.25 to calculate the reduction in the settlement of isolated pad and strip footings supported by a finite number of stone columns.

Baumann and Bauer method (1974)

Based on their field observations, Baumann and Bauer (1974) indicated that stone columns could accelerate the rate of consolidation of soft clay. The rate of consolidation is increased following the stone column installation due to the following mechanisms. Firstly, permeability of stone column material is higher than the surrounding soil so that excess pore water pressure is dissipated faster, and secondly, the column stiffness is higher than the soft soil stiffness which in turn reduces stresses in the soft soil body; therefore, a significant reduction in the generated pore water pressure.

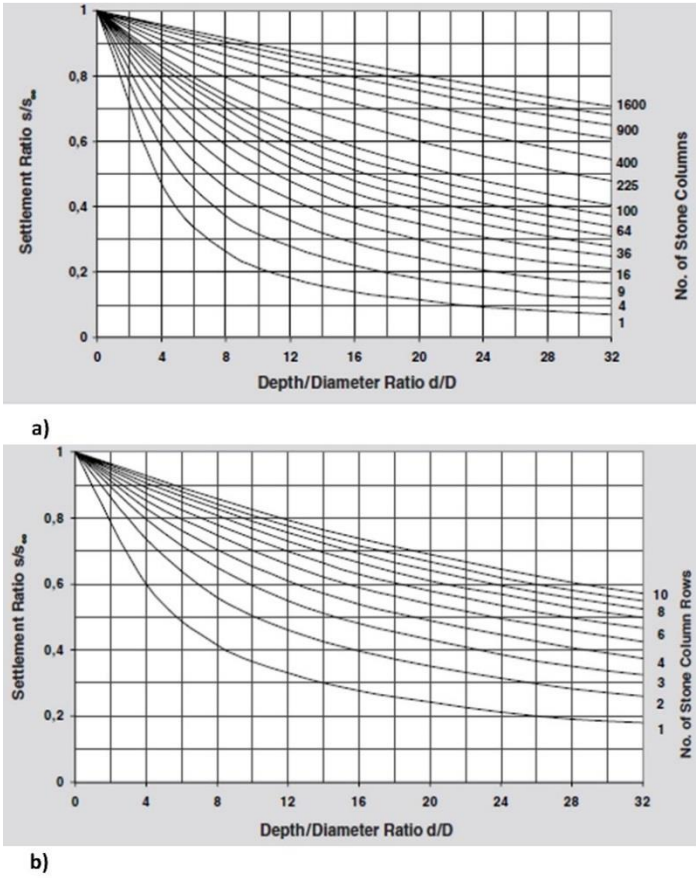


Figure 2.25 Settlement of small foundations (a) single pad footings. (b) strip footings, after Priebe (1995).

Baumann and Bauer (1974) considered that the total settlement is comprised of two components: immediate settlement where no volume change in the soil was assumed and consolidation settlement where Terzaghi's one-dimensional consolidation theory is adopted.

2.6.3 Summary of stone column behaviour

A review of the previous investigations of stone columns and design methods was presented in the previous sections. Most experience in the settlement performance of stone columns has been with widespread loads (large groups) which is well understood. It was found that the mode of failure in soft clay is prominent at

shallow depths with bulging observed to be around 4 times the diameter below the existing ground level. Field experience indicates that the column bearing capacity and settlement performance are the main two design criteria which should be checked prior to the installation of stone columns. Most of these design methods are based on the unit cell idealisation.

It appears that all previous investigations presented in previous sections conducted using a uniform weak soil without considering the impact of using crust layer at shallow depths on the column behaviour. The settlement performance of small groups of stone columns is predicted using Priebe (1995) design charts. The state of final settlement in Priebe (1975) method is derived as a function of the treated area, Poisson's ratio and the stone angle of friction. However, Priebe method and other design methods are not considering the influence of sensitive clay disturbance during stone column installation.

2.7 Encased stone column (ESC)

Ground improvement using the vibro stone column technique is considered to be very suitable and a favourable technique to improve soft soils worldwide due to its performance, simplicity of the construction (program), low costs and durability. The stone column performance can be improved by encasing it with a suitable geosynthetic material. An encased stone column can be used to prevent excessive bulging at shallow depths and prevent the stone from penetrating into the surrounding soft soil (Malarvizhi and Ilamparuthi, 2004).

In addition, the encased column enhances the load carrying capacity and reduces the column's settlement compared with an ordinary stone column. Moreover, the encased stone column can be used in very soft soils like peat or sludge with a very low undrained shear strength c_u = 2 kPa (Kempfert, 2003). The undrained shear

strength is considered as a means to express surrounding soil lateral constraint. In very soft soils, the conventional stone column may not mobilise a sufficient load capacity due to the low lateral restraint. If the soil is not capable of providing enough lateral constraint this will cause a large lateral deformation at the upper part of the column and therefore, excessive settlement which may lead to failure by bulging.

Van Impe and DeBeer (1983) were probably the first to discover that the column could be encased by a geotextile. There are two common methods to install the encased stone columns as explained in the subsequent sections.

Displacement Method:

The displacement method is most commonly used in very soft soils (i.e. Cu < 15 kPa). In this method, a closed ended steel tube is driven into the soft ground to the design length. Upon reaching the required depth, the geosynthetic cylindrical casing inserted into the steel tube. A granular and non-cohesive material such as gravel and sand is introduced from the surface into the geosynthetic casing. After that, the tip of the steel tube opens and the steel tube is then completely withdrawn under vibration (Figure 2.26a).

Replacement Method:

The replacement method is preferred to be used adjacent to sensitive structures where vibration effect should be minimised to avoid future claims (Figure 2.26b). An open steel shaft (casing) is installed deep into soft soil resting on a bearing layer. Soil within the casing is removed using auger boring technique.



Figure 2.26 Encased Stone column (ESC) installation method (a) the displacement method and (b) the replacement method (Kempfert and Gebreselassie, 2006).

A geosynthetic casing is inserted inside the steel tube and then filled with a granular and non-cohesive material. Steel casing is withdrawn from ground under vibration and circumferential tensile forces will be generated in the geosynthetic casing due to column expansion under imposed loads. The replacement method is suitable for soils with relatively higher penetrating resistance.

2.7.1 Experimental, numerical, and analytical studies

Several researchers (Kempfert, 2003; Murugesan and Rajagopal, 2009) have proved that the high stiffness encasement materials used as a confinement around the column material has significantly reduced lateral column bulging as well as improving the bearing capacity of the whole system and significantly reduced the settlement of the foundation (e.g. Kempfert (2003); Malarvizhi and Ilamparuthi (2006); Murugesan and Rajagopal (2009)). The radial support provided by the encasement is due to the ring tension forces developed in the geosynthetic material.

2.7.1.1 Experimental Studies

The effectiveness of the encased granular columns was assessed by using various tests such as triaxial test, uniaxial test, and load test using cylindrical tank (Elsawy, 2010; Kempfert, 2003; Murugesan and Rajagopal, 2009). The major conclusions drawn from these studies are as follows:

i. Load carrying capacity is increased by using encased stone columns irrespective of the column being either end bearing in a strong layer or floating, as illustrated in Figure 2.27a (Malarvizhi and Ilamparuthi, 2004). The settlement of untreated soils (c), soils treated with stone column (sc), and soils treated with encased stone columns (net) is presented in Figure 2.27 (where net1, net2, and net3 refers to a geogrid stiffness of 45 kN/m, 125 kN/m and 148 kN/m, respectively)

ii. The ratio of load sharing between the soft clay and column (Modular ratio) increases with settlement, as shown in Figure 2.27b (Malarvizhi and Ilamparuthi, 2004).

iii. As the stiffness of the geogrid increases, the ultimate load capacity of reinforced stone column increases accordingly (Elsawy, 2010).

iv. The improvement in the stone column settlement increases with reducing the encased column diameter (Murugesan and Rajagopal, 2008). The reason was attributed to the larger lateral stresses mobilised in the smaller diameter columns compared to the larger diameter columns (improvement of overall column stiffness).

v. Load-settlement performance of the stone column generally shows an excessive settlement at ultimate load (punching) unlike the encased stone column where the settlement behaviour tends to be linear (Murugesan and Rajagopal, 2009).

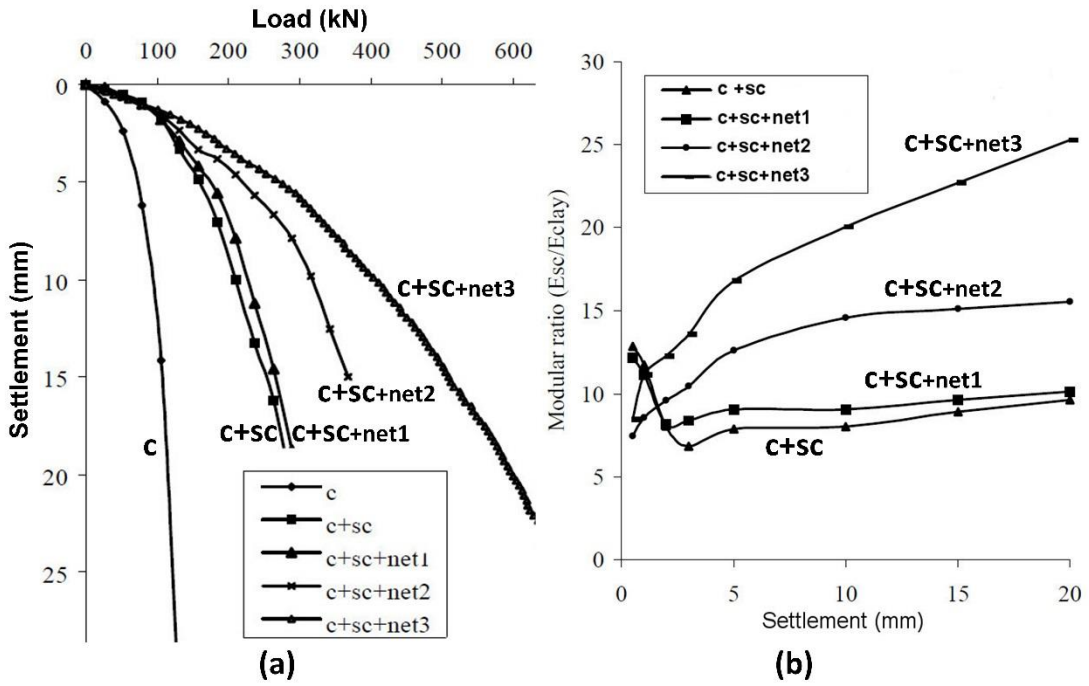


Figure 2.27 (a) load versus settlement of composite bed with various encasements and (b) variation of modular ratios with settlement (Malarvizhi and Ilamparuthi, 2004).

2.7.1.2 Numerical and analytical studies

FEA has been used to simulate a geogrid encased column in experimental conditions. The following conclusions drawn from these studies:

i. The encased column load carrying capacity improvement is attributed mainly to the hoop stress generated in the geogrid. The stiffer the geogrid, the higher the hoop stress is generated, and consequently the encased column capacity is increased (Malarvizhi and Ilamparuthi, 2006).

ii. The hoop tension stress is significant at a depth of twice the diameter of the stone column (Murugesan and Rajagopal, 2006).

iii. The load carrying capacity improvement is attributed to the improvement of the stone column material strength (friction angle and stiffness). However, it is found that using a stiffer geogrid is more efficient for better performance (Khabbazian et al., 2009).

iv. The settlement of the encased stone column was examined by Lo et al. (2010). The computed settlement was relatively insensitive to the material stiffness of the column.

v. Load carrying capacity is insensitive to the elastic modulus of the ESC (Keyhosropur et al., 2011).

vi. The ESC effectiveness increased when the stone of the column compressed well. Furthermore, if the ratio of the column length to the column diameter (l/d) increases, the reduction of the settlement increases up to l/d = 7.5 compared to l/d = 10 for ordinary stone columns (Malarvizhi and Ilamparuthi, 2007).

2.8 Background for numerical analysis

The design of various ground improvement techniques in soft soil is typically based on empirical or semi-empirical methods, as demonstrated in the previous sections of this Chapter. It is perhaps also worthy to note that available design approaches typically require an experience in the relevant technique and that they tend to be conservative. The recent experimental studies on column-like elements have concentrated mainly on field tests and physical models in the laboratory (Black 2006, Serridge, 2012, Almeida, et al. 2019). The use of numerical analyses in the study of column-like element behaviour has also been of interest, due to its simplicity and ability to model complex structures and ground conditions. Therefore, numerical computation can provide answers and additional insight into these problems. The research reported in this thesis is therefore concerned with compare the results of laboratory and field tests with numerical and analytical methods to analyse and determine the behaviour of column-like elements in subsequent chapters.

As a result, a significant contribution in developing an understanding of column-like elements deformation behaviour and load transfer mechanisms has been demonstrated by various researchers (e.g. Killeen (2012), and Ariyarathne and Liyanapathirana (2015)). In the past few decades, a significant development of computers (software and hardware) has led to the use of the numerical modelling in the soil and rock mechanics problems including foundations, excavations, embankments, and ground improvement. Numerical analysis using Finite Element modelling (FEM) has become increasingly popular and powerful in geotechnical engineering applications and research.

There are many types of software available in the market specially written to solve geotechnical problems using FEM codes. It is vital to choose suitable constitutive relationship to model the behaviour of soils. Various constitutive models from simple elastic model to mathematically complex non-linear elasto-plastic models have been developed. Therefore, any particular geotechnical problem must be associated with a relevant soil model that addresses the constitutive relation between the stress and relative strain of the soil. In soft soils, there are limitations, advantages and disadvantages for developed soil models in relation to model soil behaviour in geotechnical problems.

Soil strength and deformation parameters have a great influence on the outcome of analysis for a particular soil model. The selection of geotechnical and structural parameters should be based on derived values from the laboratory and field tests, complemented by well-established experience.

Pile foundations in very deep soft layer may not be feasible and economical. A pile/column-like element supported embankment is commonly used in the current practice. By making use of advanced knowledge in soft soil engineering, available

in the field of geotechnical engineering, it is possible to reach a technically safe and economically justifiable solution. This research is expected to contribute significantly in this regard.

2.8.1 Numerical modelling approaches

Many researchers have proposed numerical approaches to predict the column-like elements bearing capacity and settlement (e.g. Han and Gabr (2002); Killeen (2012); Castro et al. (2013); Fayed et al. (2017)). The author has been able to briefly summarise the development of the column-like elements numerical analysis in respect of modelling approaches as follows:

1. Many of the historic Finite Element methods were developed in the 1970's using the unit cell approach where only the column and surrounding soil were modelled axisymmetrically (Balaam and Brown, 1977). In order to simplify the column-soil interaction and the settlement behaviour of the substructure, unit cell concept neglects the variable boundary conditions of different unit cells. Unit cell concept relies on many assumptions which may not apply to all possible conditions. Generally, unit cell approach is considered an appropriate approach to model an infinite grid of columns used to support a wide loaded area (such as used to support embankments).

2. The homogenisation Finite Element approach developed on the back of unit cell approach. Homogenisation technique models column-like elements and soil as homogeneous soil with improved properties to simulate ground improvement after installation of columns (Schweiger and Pande, 1986). The main advantage of homogenisation approach over the unit cell concept is the lack of restriction for boundary conditions. However, it is very difficult

to model a specific value of the excess water pressure between adjacent columns. Additionally, whilst the average degree of consolidation and the settlement rate may be modelled using the homogenisation technique, a proper calibration of the parameters of the equivalent homogeneous soils should be carried out to guarantee a correct capturing of the settlement rate (Castro, 2017a).

3. Plane strain modelling when plane strain condition is available such as long loading areas, which is commonly used to model the column-like elements beneath embankments (Bergado and Long, 1994; Van Impe and DeBeer, 1983).

4. Axisymmetry technique, in which a 3D column-like element cell is transformed into a circular cell with the area of the column and soil remain the same (Han and Gabr, 2002; Mitchell and Huber, 1985).

5. Full 3D model, where a complex numerical model is necessary due to the complexity of the problem and no other modelling can accurately represent the problem in hand. However, 3D modelling requires high computing effort and is much easier to perform other modelling techniques where possible (McCabe and Killeen, 2010). Furthermore, there exists a dearth of information regarding the long-term settlement using undrained analysis (stone columns in particular) due to the computational time consumed during calculations.

One needs to make sure, though, whatever modelling technique used is the right approach to provide a good representation of the site geometry, soil and structure properties, and loads.

2.8.2 Numerical analysis of piled-embankment

Load transfer mechanism (soil arching) is currently assessed by conservative analytical methods (Jones et al., 1990a; Russell et al., 2003). There are two main reasons for such conservatism. Firstly, researchers use simplified analytical procedures which rely on empirical relations to quantify the soil arching across the adjacent pile caps and secondly, these simplified procedures do not consider existing soft soil support underlying geosynthetic reinforcement. Therefore, numerical analysis such as FEM is one of the best methods to analyse such complex soil structure interaction. Soft soil's strength attribution to the whole system resistance can be modelled by using the FEM. Many researchers have used several relations to investigate arching effect, system settlement and geosynthetic tension. The following relations and their definitions mostly used in the piled-embankment numerical analysis are often referred to in the subsequent Chapter 3.

In the past few decades, numerical analysis using Finite Element modelling (FEM) has become increasingly popular as a tool used to design the piled-embankment system (Ariyarathne and Liyanapathirana, 2015; Van Eekelen et al., 2013; Zhuang, 2009). FEM is capable of modelling the whole geometry and loading conditions however challenges still exists (e.g. proper verifications, boundary conditions and selecting an appropriate soil model). Therefore, a combination of laboratory and field tests, complemented by well-established experience should be used to derive and calibrate the geotechnical and structural parameters of the program and to verify the results of the FEA.

2.8.2.1 Efficacy

The proportion of the embankment weight and external load carried by the pile caps can be referred to as the efficacy, E, of the pile support. The definition of the efficacy can be expressed as (Hewlett and Randolph, 1988):

$$E = \frac{P}{s^2\,(\gamma H + q)} \qquad (2.27)$$

where P is the total force carried by the pile caps (kN), γ is embankment unit weight (kN/m^3), H is embankment height (m), s is pile spacing (m), and q is the embankment external surcharge (kPa).

2.8.2.2 Soil arching ratio or stress reduction ratio

The term 'soil arching ratio' or 'stress reduction ratio' is the term used by McNulty (1965) and Kempton et al. (1998) to quantify the soil arching. It is defined as follows:

$$\rho = P_b/(\gamma H + q) \qquad (2.28)$$

where ρ is soil arching ratio or stress reduction ratio, where:

ρ=0 indicates full soil arching

ρ=1 indicates no soil arching

P_b is the average vertical pressure above geosynthetics (kPa).

2.8.2.3 Stress concentration ratio

Han and Akins (2002) used a stress index called 'stress concentration ratio' (n) to determine the load transfer portion into the pile caps where n can be expressed as follows:

$$n = \sigma_c / \sigma_s \quad (2.29)$$

where σ_c is the vertical stress on the top of the piles (kPa), and σ_s is the vertical stress on the surrounding soil (kPa).

2.8.2.4 Other definitions

Total settlement and differential settlement were used extensively to evaluate the effectiveness of the proposed column-like elements solution. Settlement is usually measured at the column head and between the centre of the column and at the middle of the column spacing at the same level. Zhuang (2009) used the ground reaction curve (GRC) proposed by Iglesia et al. (1999) and the profile of normalised earth pressure coefficient (K/K_p) on a vertical profile at the midpoint between piles to consider the arching of the material above the piles. However, piles were modelled as a rigid support and the soft soil is simulated as a vertical stress applied at the bottom boundary of the model. Zhuang (2009) claims that the profile of normalised earth pressure coefficient (K/K_p) on a vertical profile at the midpoint between piles gives a good 'indication' of arching behaviour. The method of normalised earth pressure coefficient (K/K_p) appear to have provided a satisfactory basis for understanding the changes in the vertical and horizontal stresses within the embankment fill material so will be used in this thesis.

2.8.3 Numerical studies of stone columns

The most common numerical methods are the Finite Difference method, the Finite Element method, the Boundary Element method and the Discrete Element method. The Discrete Element method is not used frequently in the geotechnical engineering analysis because of the time and computing capacity required to analyse all but the simplest problems (Al Ammari and Clarke, 2016; Chen et al.,

2011). The Boundary Element method (BEM) is used to provide a solution to problems of similar nature to the boundary integral equations, therefore BEM is considered as an obvious answer to the dominant partial differential equation. The Boundary Element method cannot provide an accurate solution to non-linear problems as compared with other numerical methods (Katsikadelis and Nerantzaki, 1999).

Numerical analysis methods are appropriate to provide solutions for problems generally with a minimum variation in the results (Fang et al., 2002; Marfurt, 1984). However, the preference of one numerical method over the other is debatable and depends very much on the definition of the referenced process. The choice of the most suitable method depends on the nature of the problem and the advantages/disadvantages of every method (Zienkiewicz et al., 1977).

The use of the Finite Difference method can be very difficult when modelling complex geometries in multiple dimensions (Peiró and Sherwin, 2005). Consequently, Peiró and Sherwin (2005) argue that there are difficulties associated with the Finite Difference method which utilizes a topological square network of lines to build the discretisation of partial differential equations. Therefore, other numerical methods, such as the Finite Element method have been developed to overcome these difficulties (Al Ammari and Clarke, 2016).

Numerical analysis using the FEM to investigate the influence of stone column installation upon the settlement performance is largely based on a large array of stone columns supporting wide area of loadings such as embankments. Balaam and Brown (1977) undertook a numerical analysis of large groups of stone columns to investigate the influence of key design parameters such as column spacing, length and stiffness on the settlement performance using the unit cell concept

assuming that the load applied on both the soil and the column is uniform (simulation of an embankment and large raft). The long-term settlement (drained and undrained conditions) is predicted using the FEA. The undrained analysis carried out by Balaam and Brown (1977) revealed a very small amount of settlement, therefore, undrained analysis was neglected. The main findings are as follows:

- The stone column diameter and penetration into the soft clay were found to have a significant impact on the settlement.
- The modular ratio (the ratio of modulus of the column to the soil) was considered of less importance on the settlement performance.

Barksdale and Bachus (1983) conducted 2D FEA using the unit cell concept to predict the primary consolidation settlement. The installation effect of stone column was considered by increasing the coefficient of lateral pressure (K_o= 0.75). The coefficient of lateral pressure value adopted in the analysis is lower than the Priebe (1995), who recommended a value of K_o= 1.0 and higher than K_o = 1 – sin (φ') (Jaky, 1948). A series of design curves was presented as a result of the analysis to predict the average primary consolidation settlement.

Elshazly et al. (2008) carried out 2D axisymmetric approximation based on the unit cell concept. The authors developed a modification factor to find a relationship between the settlement of a group of stone columns supporting a wide spread load and the settlement of finite groups of stone columns (small group of columns). The incorporation of the installation effects is considered by increasing the K_o of the surrounding soils up to 1.5. The main findings of this study were the stress distribution beneath the pad footing and widespread loaded area and the loss of confinement experienced by the column at the edge of the pad footing. Firstly, the

vertical stress was negligible below a depth of 2W (W= foundation width) for a pad footing.

In contrast to the pad footing stress distribution, the vertical stress beneath a wide area loading is extended to full depth and, therefore, associated with higher settlement compared with the pad footing settlement. The second observation was related to the loss of the lateral confinement of the edge columns beneath pad footings compared with a full lateral confinement provided to the columns installed within infinite grid of columns due to the installation of adjacent columns.

The homogenisation method was developed to evaluate the influence of the stone column installation beneath a flexible and rigid raft foundations using FEA (Schweiger and Pande, 1986). FEA was carried out under drained condition where improved clay properties were assigned to the treated soil beneath the raft. The homogenisation approach was developed further by Lee and Pande (1998), where both the soil and column materials were assumed to behave elasto-plastically. A good relationship in predicting the ultimate loads was found to exist between the numerical analysis and experimental data conducted by Hu (1995). A marked difference was observed in predicting the initial stiffness using the homogenisation approach, which tends to over-predict the ground composite stiffness.

It is worthy to note that Lee and Pande (1998) found that the vertical stresses beneath the footing were higher at the edge of the footing. Therefore, it was suggested to use shorter columns under the centre of the footing and longer columns towards the edges of the footing. The optimisation of column length appears to have a positive impact on the foundation load carrying capacity and provides cost savings as suggested by the authors. It is important to recognise that field trials are necessary to validate such hypotheses.

Killeen (2012) carried out a series of three-dimensional FEA to investigate the settlement behaviour of small groups of stone columns supporting rigid square pad footings. The influence of key design parameters upon the deformation behaviour was also investigated by predicting the normalised punching at the base of the column and the axial strain along the column shaft. The author suggests that the settlement performance improves beyond L/d = 10 (where L is the column length and d is the column diameter) and relates the improvement with the area ratio. Another interesting observation from the FEA is that the columns toward the periphery perform better than the short columns closer to the centre. It is worth noting that increasing the number of columns, for a given area ratio, leads to enhanced settlement performance due to the full confinement around the column perimeter.

2.8.3.1 Modelling of column installation effects

A vibrating poker is normally used to form stone columns. The vibrating poker displaces soils laterally and imparts horizontal vibrations. Driven pile installation also alters in-situ soil properties such as the lateral stress in the soil. Therefore, any change to the initial stress state may be attributed to the lateral soil displacement as a result of installation (Greenwood, 1970). A number of methods are used to simulate the column installation effect.

2.8.3.1.1 Increased coefficient of lateral pressure

Increasing the coefficient of soil lateral earth pressure at rest (K_o) is considered as one of the simplest techniques to account for the installation effects of the driven columns such as large displacement piles and stone columns. The soil properties adopted are determined after installing the column and therefore incorporate soil property changes due to installation. Mitchell and Huber (1985)

and Elshazly et al. (2006) attribute any discrepancy in the load settlement curve to the change of stress due to installation. They have used an axisymmetric FEA assuming a full confidence in the soil parameters and have adjusted K_o until the calculated load- settlement curve matched the measured settlement behaviour. The back calculated lateral pressure values for various researchers ranged from 0.7 to 1.5 depending on the corresponding area ratio and adopted columns grid.

The effect of increasing coefficient of the lateral pressure upon the column deformational behaviour supporting 3m footing at Bothkennar site was investigated by Killeen (2012). It was concluded that increasing K_o has a minor influence upon the mode of column deformation, which is consistent with Kirsch (2006), where a group of stone columns was analysed using FEA. It was observed that increasing K_o enhances columns' performance but do not influence the deformational behaviour of the column.

2.8.3.1.2 Cylindrical Cavity Expansion

The application of the cylindrical cavity expansion theory in conjunction with FEA was used to approximate post-installation K values due to the lateral expansion imposed during column-like element installation. The cavity expansion process must be controlled either by displacement or stress. A suitable pseudo displacement should be used to perform a displacement control cavity expansion. On the other hand, imposing a radial pressure on the cavity wall is considered appropriate to simulate the stress control method (Henke and Grabe, 2006; Lancellota, 1995).

A series of small scale laboratory experiments conducted by various researchers (Debats et al., 2003; Guetif et al., 2007) show that the driven column-like element installation effect can be predicted using cylindrical cavity expansion theory.

Debats et al. (2003) and Guetif et al. (2007) have investigated this approach numerically in 2D axisymmetric FEA to simulate the stone column installation. If a stone column is installed into the ground quickly, it is reasonable to consider an undrained condition to simulate the loading process. A numerical analysis by Randolph et al. (1979a) simulated the installation effects associated with column-like elements installation using the undrained cylindrical expansion of a dummy material which was assigned a nominal stiffness and later converted into concrete. The soil was modelled using the Mohr-Coulomb (MC) model. In order to replicate the actual installation condition, it would be necessary to expand the cylindrical cavity from zero radius to double the radius to model the installation process sufficiently. However, there are two important shortcomings of the total stress analysis. First of all, the pore water pressure generated during shear is ignored. The second limitation of the MC model instability in linking the soil strength with the change in the current effective stress state (Yu, 2013).

Based on field measurements carried out by Kirsch (2006), it was found that due to the column installation effect, the horizontal stress and stiffness increased within a zone of (2-5)d from the centre line of columns (d is the column diameter). Therefore, Kirsch (2006) applied the cavity expansion to model the column installation effect and increase the soil stiffness in the enhanced zone. However, using this process is offset by the effect of remoulding and dynamic excitation within the treated zone.

McCabe et al. (2008) conducted a numerical analysis using PLAXIS 3D to assess the program ability to simulate column installation effect using the cylindrical cavity expansion theory (Figure 2.28). It is evident in Figure 2.28 that PLAXIS 3D is currently incapable of simulating stone column installation using cavity expansion theory because of the level of scatter in the excess pore water pressure

and radial stress prediction when compared with the published data developed by Gibson and Anderson (1961) and Randolph et al. (1979b).

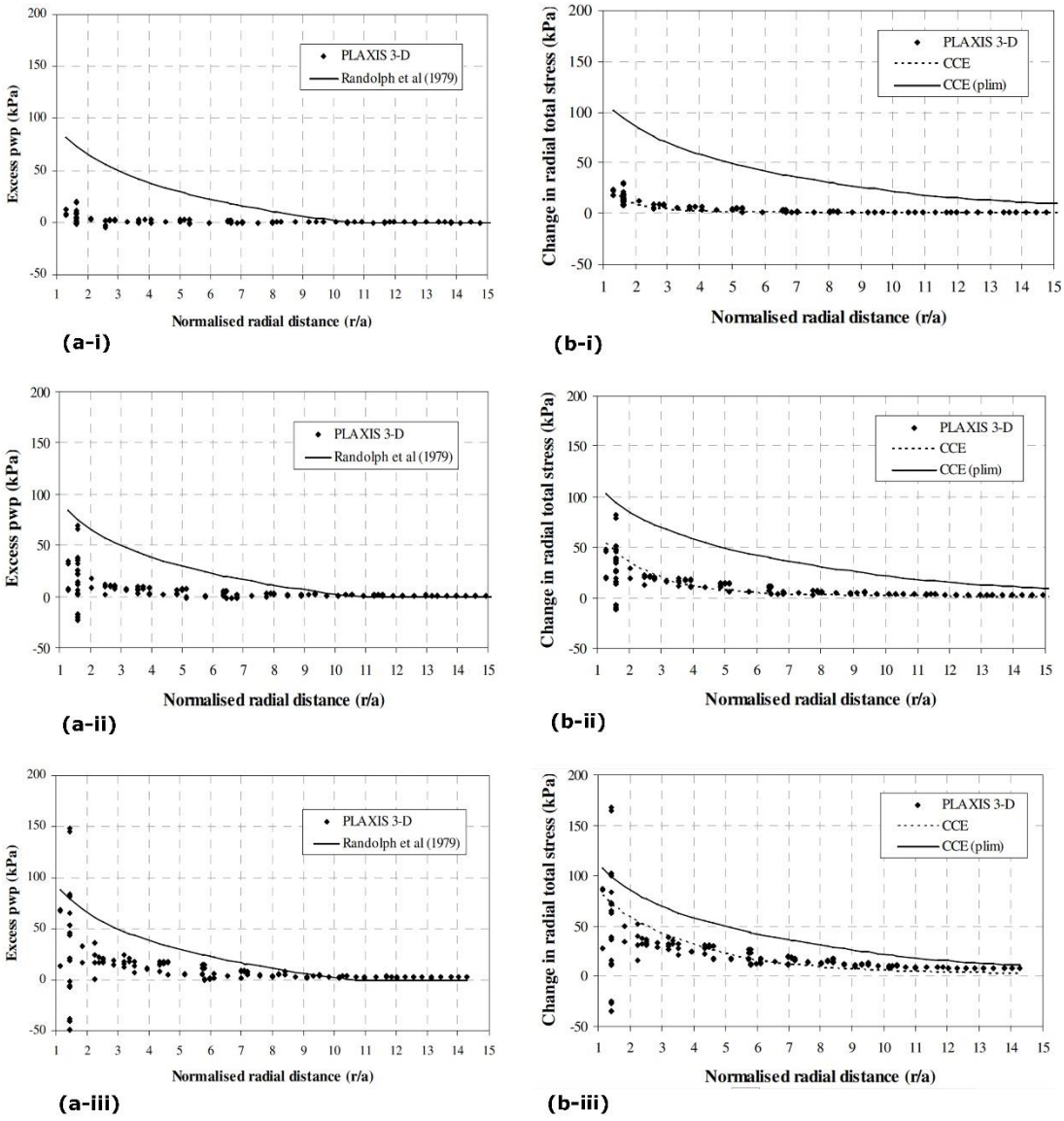


Figure 2.28 Variation of (a) excess pore pressure (pwp) and (b) total radial stress with normalised radial distance for different lateral expansions (McCabe et al., 2008).

It is clear that the extent of the scatter between PLAXIS analysis and published data precludes cavity expansion (displacement control method) option for simulating the installation effects of stone columns. Therefore, the stress control

method is used in Chapter 5 to simulate the installation effect of stone columns installed in soft founding soils.

The increase of radial soil stress adjacent to the column-like element as a result of pile installation can be modelled by increasing the value of the coefficient of lateral earth pressure (Castro, 2017b; Killeen, 2012) as commonly expressed below:

$$\boldsymbol{K} = \frac{\sigma_h'}{\sigma_v'} \qquad (2.30)$$

The coefficient of lateral earth pressure K=1 has been used in Chapter 5 to model the increase in the lateral stress rather than the coefficient of lateral earth pressure at rest K_o (Lancellotta, 2014). The stress control method can be applied in the FEA as follows:

- Set in situ soil conditions (K_o condition) to calculate initial stresses.
- Create a cavity of similar size to the pile along the centerline and consequently apply radial stress ($\sigma_h = \mathrm{K} \times \sigma_v$) to the cavity wall and also apply a vertical pressure at the base of the cavity, σ_v (= γ x L), where γ is the density of the removed soil in kN/m^3, and L is the column length. The applied radial stress increases linearly with depth according to equation 2.30.
- Assign stone material to the cavity zone and consequently remove the applied stresses on the cavity wall and the base of the column.

Summary of column installation effects

The effect of column installation is that the horizontal stress and stiffness of the surrounding soil will increase accordingly. A number of methods is available to simulate the column installation process as summarised below:

1. Increase the coefficient of lateral pressure K_0 from 0.75 to 1.5 (this methodology is used in Chapter 4 to model the installation effect of stone columns).
2. Cylindrical cavity expansion to column using a dummy material and convert property to concrete/gravel after expansion or use the stress control method.
3. Apply the cylindrical cavity expansion and increase soft clay stiffness across an enhancement zone.

The results of McCabe et al. (2008) suggest that PLAXIS 3D is incapable of using cavity expansion theory (displacement control method) to simulate the column installation appropriately. Therefore, an approximate technique is used in this research (see Section 2.3) by increasing the coefficient of lateral pressure (K_o) as recommended by researchers (Kirsch, 2006; McCabe et al., 2008).

2.8.3.2 Modelling of soft soil long-term behaviour

The modelling of long-term behaviour of fine-grained soils in PLAXIS 3D can be applied by two methods:

(i) Drained analysis
(ii) Undrained analysis accompanied with consolidation stage.

The use of method (ii) is time consuming but it is more accurate than method (i) in simulating the real behaviour of the material. The initial settlement is determined during the application of the load and long settlement can be

computed at consolidation stage. Total or effective strength parameters can be used in PLAXIS 3D to define the soil strength. However, it is not possible to measure the increase in soil strength during the consolidation stage by using total strength parameters. Method (i) on the other hand does not separate the settlement between the undrained response initially occurring during the application of the load and the following primary consolidation stage. The consistency of the two methods is compared in Chapter 4 for the Bothkennar field trials (Serridge, 2013).

2.9 Summary

Column-like elements, such as driven piles and vibro stone columns, are used across the world to enhance the soft soil bearing capacity and settlement performance. Several researchers in the last few decades discussed the column-like elements' mechanism in various ground improvement studies. Piled-embankments and vibro stone columns provide possible solutions to construct roads, embankments and foundations over soft soils without excessive settlement. The main fundamental principle of the piled-embankment and vibro stone columns techniques is to relive the stress on the weak soils without a major change in the soil structure.

Embankment arching is considered as the main mechanism of load transfer from the embankment to the pile head. However, the shape of arching is not well understood, and until now engineers and researchers are not fully confident regarding which method provides the best solution. Therefore, it is necessary to model the piled-embankment considering the influence of subsoil using a simple method to evaluate the impact of arching on the load transfer mechanism. Furthermore, the adaptation of different assumptions to derive the column-like

element and soft soils stresses influences the level of accuracy of each design method in predicting the arching effect. Also, some key parameters such as the angle of internal friction of the embankment fill and the soft soil contribution are not considered in these design methods. The use of the frictional methods (i.e. Zhuang, 2009) to describe the development of arching within the embankment fill is not fully explored by researchers.

Foundations constructed on soft soils undergo large settlement under applied loads, therefore, the foundation settlement is considered as one of the main criteria used in the column-like elements design. There is a dearth of information available regarding the settlement performance for lightly loaded low-rise structures supported by pad foundations. Design methods typically use various assumptions and simplifications, such as a unit cell concept, which is considered appropriate to model the settlement performance of an infinite grid of column-like elements such as slabs and embankments constructed over a large group of columns. Therefore, a unit cell approach is used only to simulate the piled-embankment case in the following chapter because embankments are normally constructed over a wide area.

Stone column settlement performance and bearing capacity are the main two design criteria necessary to check with every column design. It has been found that the mode of failure in soft clay is prominent at shallow depths with bulging observed to be around 4 times the diameter below the existing ground level (Bergado and Lam, 1987; Goughnour and Bayuk, 1979a; Greenwood, 1970; Hughes and Withers, 1974). The lack of information regarding the settlement performance of a small group of stone columns was identified by Killeen (2012), who conducted a drained numerical analysis to study the settlement performance of small groups of stone columns supporting rigid square pad footings. However,

the settlement during the application of the load was not assessed and the influence of lateral bulging and stone column reinforcement on settlement performance were not investigated during the study.

Serridge (2013) identified the lack of information regarding the settlement performance of pad footings relevant to light weight low rise structures supported by stone columns. Therefore, it is necessary to model the stone columns beneath the pad footings at discrete locations, rather than modelling the stone columns using the approximation of unit cell concept, homogenisation technique, or a plane strain approach.

On the basis of this review, this thesis performs:

a) a two-dimensional FEA using PLAXIS 2D to investigate the piled-embankment system behaviour. The influence of the key design parameters, such as embankment height, fill strength, external surcharge, reinforcement stiffness and coefficient of lateral earth pressure upon the embankment material arching will be investigated. An important purpose is to achieve (see Section 2.1) one of the main aims of this thesis is to examine the impact of embankment material arching on piled-embankment behaviour by using a simple method. This is the subject of Chapter 3.

b) predicts the settlement performance of the pad footings at the Bothkennar site by using a three-dimensional FEA. The influence of a shallow crust layer on stone column behaviour will be investigated in Chapter 4. The numerical analyses will be used to determine the influence of the column lateral bulging, column length, area ratio, the depth of the footing, the shape of the footing, the number of columns and the effect of encasing the stone column with geogrids upon the settlement performance of pad footings

supported by stone columns. From this, a simple analytical model of stone column behaviour is developed in Chapter 5.

CHAPTER 3

NUMERICAL MODELLING OF PILED-EMBANKMENTS

3.1 Introduction

The main focus of this chapter is to develop a better understanding of the arching mechanism in the embankment, loads transferring to underlying piles, and tension forces developed in the geogrids installed at the base of the embankment. Results from axisymmetric FEA are presented in this chapter. The adopted soil profile and the material properties are taken from the well-characterised Zaeske (2001) model test, which is also described in Kempfert (2006). The FEA results are validated with Zaeske (2001) model test.

The preference of one numerical method over the other is debatable and depends very much on the definition of the referenced process. FEM was developed to overcome the difficulties associated with other numerical methods such as the Finite Difference method, the Boundary Element method and the Discrete Element method as described in Section 2.8.3 (Al Ammari and Clarke, 2016). The FEM has become the most used numerical method due to its capability of modelling heterogeneous materials and because the flexible requirements of FEM in using the unstructured and irregular meshes that can solve the complex geometry problems. FEM is an appropriate method to model inelastic and nonlinear soil and

rock behaviour where various soil models have been developed by the academia and the industry to simulate the material hardening and softening behaviour. All of these reasons position the FEM as the mostly used numerical method in soil and rock mechanics (Nikolić et al., 2016). Therefore, FEM was selected by the researcher to carry out the analyses in this study, however, there are some challenges still exist such as the verification of the results and the selection of an appropriate soil model.

There are many FEM packages are available in the market, however PLAXIS software has been specifically developed to analyse the geotechnical Engineering problems. Other softwares such as Abacus and ANSYS were designed for multi purposes analyses including the geotechnical engineering problems where all the features of solving these problems required further programming e.g. to generate pore water pressure then scripting in FORTRAN language is required. Therefore, PLAXIS software is chosen because it is reliable and time effective compared to other softwares. PLAXIS package capability of simulating a wide range of complex geotechnical problems and soils behaviour is well recognised in research and industry and hence the selection of PLAXIS package is therefore proposed and undertaken in the subsequent sections to analyse the column-like elements problems (see Section 3.2). The researcher has conducted a sensitivity analyses by comparing the results with experimental and field tests in the subsequent chapters to validate the results of PLAXIS model.

A series of FEA were conducted using PLAXIS 2D to evaluate the influence of the following parameters upon the embankment arching and the settlement performance:

- The presence of geogrid at the base of the embankment

- Geogrid stiffness
- Applied load
- Embankment height
- Granular embankment strength
- Capping ratio

In this research, the lateral earth pressure coefficient K normalised by the passive earth pressure coefficient K_p (K_p = (1+sin φ)/ (1-sin φ)) plotted on a vertical profile at the mid-point between piles is presented in a form which can be compared with the semi-circular arching of piled-embankments proposed by Hewlett and Randolph (1988) in Figure 2.5. The approach of using the earth pressure coefficient as a tool to analyse the arching developed in the embankment was proposed by Zhuang et al. (2010).

This approach was originally proposed based on 2D plane strain and 3D models. Piles were modelled as a rigid support and the soft soil is simulated as a vertical stress applied at the bottom boundary of the model as shown in Figure 3.1.

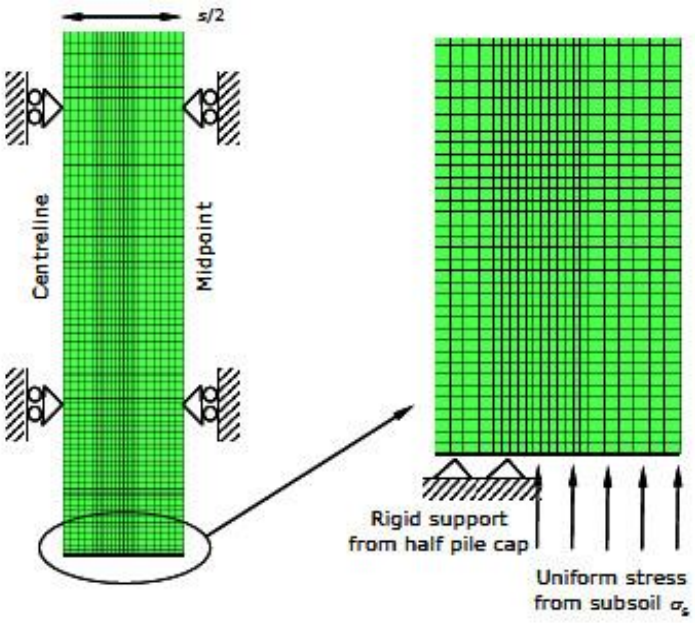


Figure 3.1 Finite Element model mesh and boundary conditions (Zhuang, 2009).

Zhuang (2009) assumed that the embankment material is a granular material. A linear elastic-perfectly plastic model (Mohr-Coulomb constitutive relation) was used to simulate the granular material behaviour. In the current research, the piles and soft soils are modelled using a linear elastic and Hardening Soil (HS) model, respectively. Also, arching is compared with the theory to evaluate the potential sensitivity of the key design parameters upon the embankment arching.

The design of the piled-embankment on soft soils is usually governed by the settlement performance rather than the bearing capacity of the piles, due to the high compressibility of the soft soils. However, there are several simplified methods available to calculate loads acting on the top of the pile and tension force developed in the geosynthetic reinforcement due to the embankment and external applied loads such as those in the British Standard BS8006 (2010), and German method EBGEO (2004).

In addition to these methods, there are various research studies investigating the soil arching and the embankment settlement which can be seen in the literature (Guido et al., 1987; Hewlett and Randolph, 1988; Mckelvey, 1994; Terzaghi, 1943). These methods produce dramatically different results, and until now engineers and researchers are not fully confident regarding which method provides the best answer. In this research, axisymmetric FEA provides an alternative approach for determining the arching effect that develops in the embankment and relevant stresses acting on the geosynthetic reinforcement.

It is very important to construct a pile cap to ensure efficient load transfer mechanism through soil arching from applied surcharge and embankment weight to the piles. The capping ratio of the piled-embankment system will be used to study the influence of the pile cap on arching. The ratio of the pile cap area to the cross-section area of one cell is defined as the capping ratio of the piled-embankment system (i.e. the proportion of native soil area replaced by the pile cap). From reference to work conducted by Han and Gabr (2002) and discussions with a ground improvement contractor, 5% to 25% capping ratios have been used for reinforced piled-embankments with geotextile at the base of the embankment. Han and Gabr (2002) have summarised applied capping ratios for reinforced piled-embankment in Figure 3.2. The suggested capping ratio by Rathmayer (1975) is shown in the same Figure 3.2.

It can be seen in Figure 3.2 that the required capping ratio percentage for conventional piles supported by embankments as suggested by Rathmayer (1975) is higher than geosynthetic-reinforced piles proposed by Han and Gabr (2002). The range of capping ratio for piled-embankment system reinforced by geogrid at the base of the embankment is between 10% and 20% of the capping ratio. The

influence of capping ratio upon arching is evaluated in a subsequent parametric study.

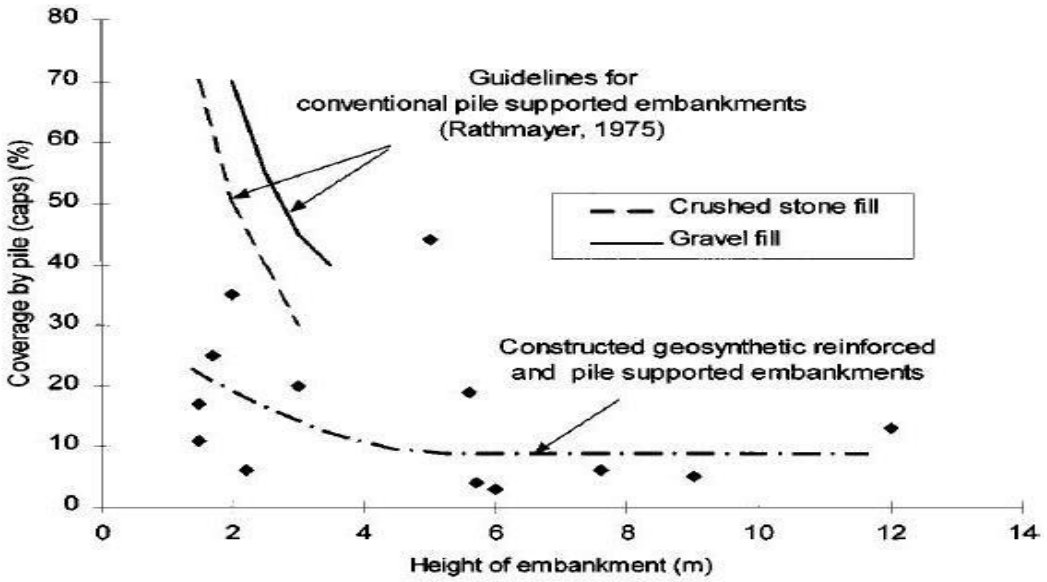


Figure 3.2 Pile capping ratio for reinforced and unreinforced piled-embankment after Han and Gabr (2002).

3.2 PLAXIS program

The FEA is a computational tool used to calculate stresses and strains distribution, deformations and forces throughout the structures and soil geometry. It is worthy to note that the Finite Element results should be validated against field works or laboratory tests. Several constitutive models are available in PLAXIS which enable PLAXIS users to simulate the linear and nonlinear behaviour, elastic and elasto-plastic behaviour, shear hardening and compression hardening, time dependent behaviour, and stress dependent stiffness of soils (Brinkgreve et al., 2018).

PLAXIS is a powerful tool to investigate the extent of the influence of key design parameters on the performance of column-like elements. It is worth noting that several options are available in the program to perform staged constructions with

drained, undrained, and consolidation analyses. The FEA can be generated by drawing the geometry and assigning properties to the soils and structures. Furthermore, loads and boundary conditions must be specified based on convenient drawing procedures.

PLAXIS performance and accuracy have been tested by carrying out analyses of problems with known theoretical solutions, as described in Chapter 2 to 6 of the PLAXIS manual (Brinkgreve et al., 2018). Also, various back-analysis calculations of many full-scale structures using PLAXIS has been carried out to check program accuracy and performance. There are various projects published on PLAXIS website (http://www.plaxis.nl) and many others published in PLAXIS bulletins. Direct support from a large network of researchers accompanied by training support from PLAXIS and industry to the author provided reassurance and confidence in the selection of PLAXIS to model column-like elements in soft soils. Therefore, the researcher chooses PLAXIS to carry out the numerical analysis in this study.

3.2.1 Description of PLAXIS constitutive models

Various constitutive models can be used in the FEA code PLAXIS, from simple linear elasticity to advanced elasto-plastic cap soil models. The details of each model can be found in PLAXIS user's manual (Brinkgreve et al., 2018). Soil is a complex material, therefore, the selection of the soil models and the relevant material parameters are very important to provide a qualitative description of the material behaviour and to quantify this behaviour (Brinkgreve, 2005). The Hardening Soil (HS) model as implemented in PLAXIS has been used as a reference model for the soft soil and granular embankment material as HS model formulation incorporates two hardening mechanisms. The shear mechanism deals with the

plastic straining which is dominated by shearing (observed in granular soils and overconsolidated clays). The other mechanism is the volumetric hardening which is governed by the compression plastic strains, HS model is also suitable for modelling soft soils as demonstrated by various researchers (Black, 2006; Kirsch, 2006; McCabe and Killeen, 2016; Satibi et al., 2009)). The soil behaviour is highly non-linear, therefore, the HS model is preferable to model the soil behaviour where both the strength and stiffness highly depending on the stress and strain level.

The HS model requires a total of 9 soil parameters, which generally can be obtained from triaxial compression and one-dimensional consolidation tests. These parameters are as follows:

3.2.1.1 Mohr-Coulomb (MC) failure parameters

The MC model idealises the soil behaviour as a linear elastic- perfectly plastic material where Young's modulus (E) and Poisson's ratio (υ) are used to model the elastic behaviour of the soil. The MC failure criterion is used to define the soil failure and can be defined by two parameters, the friction angle (Φ') and, cohesion (c'). However, the angle of dilation (Ψ') is an additional parameter required to capture the plastic strains due to shearing. The dilatancy angle is a constant of the MC model, which defines the plastic volumetric strain. The dilatancy angle can be obtained from volumetric strain versus axial strain plot in conventional triaxial test as shown in Figure 3.3.

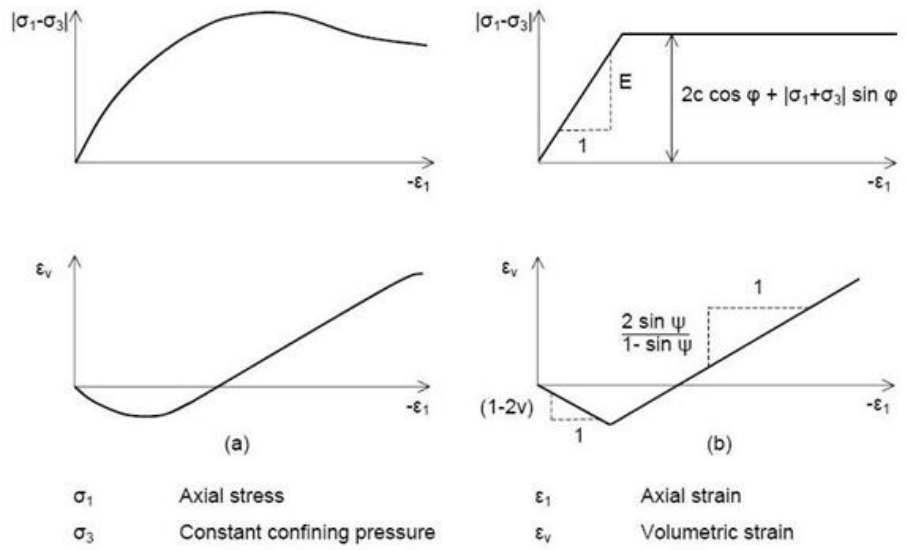


Figure 3.3 Dilatancy Angle: (a) results from standard drained triaxial test; (b) Elasto-plastic model (Vermeer and Brinkgreve, 2008).

3.2.1.2 Basic parameters for soil stiffness

The HS model idealises the soil as an elasto-plastic model, where generated irreversible strains as a result of deviatoric and compression loadings can be captured using this model. The HS model uses a hyperbolic model derived by Duncan and Chang (1970) to model the soil stress strain behaviour. Three stiffness moduli are used in the HS model to define the hyperbolic relationship between deviatoric stress and the vertical strain for a primary loading as shown in Figure 3.4.

The 3D stiffness parameters required for HS model to take account for the stress path dependency of the soil are as follows: (i) E_{50}, a secant modulus at 50% strength, (ii) E_{oed}, tangent stiffness for primary oedometer loading. Hence, E_{Oed}^{ref} is a tangent stiffness at a vertical stress of $\sigma = \sigma_{ref}$ and (iii) E_{ur}, unloading/reloading stiffness. The soil stiffness tends to increase with increasing confining pressure as

per equation (3.1). The HS model captured the stress dependency of soil stiffness by the following power law (Brinkgreve et al., 2018):

$$\frac{E}{E_{ref}} = \left(\frac{\sigma}{\sigma_{ref}}\right)^{m} \qquad (3.1)$$

where E_{ref} is the reference stiffness at reference confining stress (σ_{ref}) calculated either from oedometer or triaxial tests. The PLAXIS manual recommends using a stress dependency parameter, m, of 0.5 to 1.0 for sands and soft soils, respectively, which can be determined from one-dimensional stiffness test data (Brinkgreve et al., 2018). E_{50} and E_{ur} are read directly from the stress- strain curves by drawing a tangent through the corresponding points Figure 3.4.

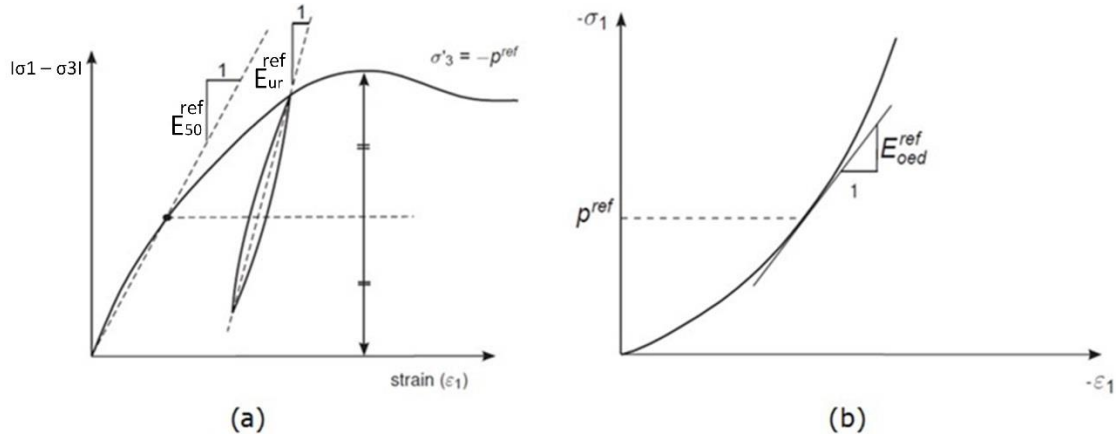


Figure 3.4 Hardening Soil model stiffness moduli (a) E_{50}^{ref} and E_{ur}^{ref} for drained triaxial test results; (b) E_{oed}^{ref} in oedometer test results (Brinkgreve et al., 2018).

3.2.2 Interface Element

The friction between the column-like elements and the surrounding soil should be included in the numerical analysis. An interface element is normally used to simulate the interaction between rough and smooth surfaces such as column-like element and the surrounding soils. The interface element is modelled in PLAXIS as elasto-plastic, where elastic and plastic behaviour is distinguished by following

Coulomb's criterion. The strength reduction factor R_{inter} is used to model the loss of strength at the interface between the column-like element and adjacent soils, which relates the soil strength to the interface strength as shown in equations 3.2 and 3.3.

$$c_i = R_{inter} \times c_{soil} \quad (3.2)$$

$$Tan\ \varphi_i = R_{inter} \times Tan\ \varphi_{soil} \quad (3.3)$$

where c_i and φ_i = cohesion and friction angle of the interface element

c_{soil} and φ_{soil} = cohesion and friction angle of the adjacent soil

The influence of interface element upon the settlement performance of Zaeske (2001) model test (test model details in the following Section 3.3) is presented in Figure 3.5. Three different interface reduction factors, R_{inter}= 0.35, 0.7, and 1.0 are used to investigate the impact of interface element on the piled-embankment analysis in the following sections.

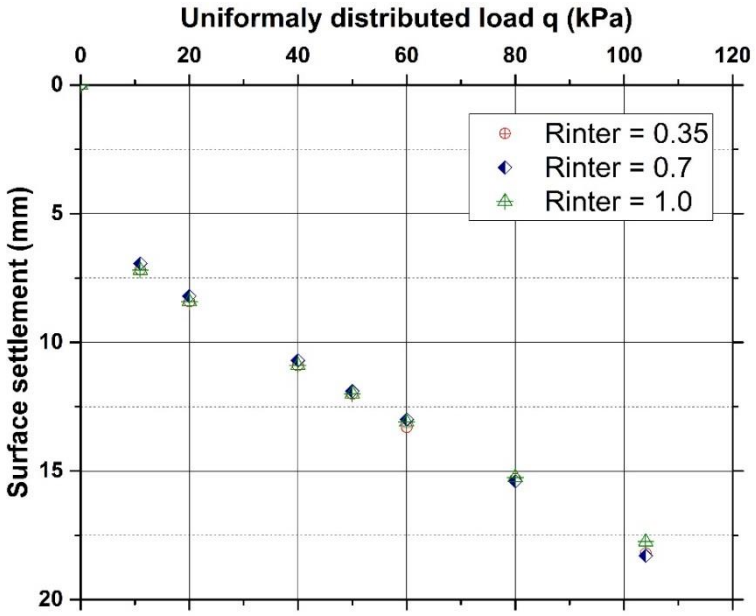


Figure 3.5 Influence of interface reduction factor upon the embankment surface settlement performance.

It can be seen in Figure 3.5 that a similar variation of the embankment surface settlement under applied load was observed. The influence of the interface reduction factor is minimal; therefore, it was deemed appropriate to model the model test in the subsequent FEA using R_{inter}= 0.7.

3.2.3 Geometry

There are many geometrical idealisations that can be found in the literature, as mentioned in Section 2.8.1. Although the embankment section could be considered approximately as a plane strain problem, the presence of columns poses difficulties for the 2D modelling (Gäb et al., 2010). The FEA with a plane strain geometry leads to calculation instability (Satibi et al., 2009). The piled-embankment system can be modelled using two-dimensional FEA, however, the piles are modelled as a wall with some modification in the pile stiffness. The modification of the pile stiffness will influence the relative stiffness between the piles and the soils and subsequently will affect the accuracy of the analysis. Therefore, for the piled-embankment analysis, a 2D axisymmetrical geometry has been used for the piled-embankment.

In the axisymmetric case the 3D cell of the piled-embankment is transformed into a circular cell with the area of the pile and the soil kept the same. The standard fixities are assigned to the boundary conditions, which is available in PLAXIS 2D. No load reduction percentage on the boundary been reported on the test model by Zaeske 2001. Therefore, a reduction factor of 0.7 is used to calibrate the model and to verify analysis results in the subsequent Section 3.4 (see Figure 3.9 and Figure 3.10) .

3.2.4 Mesh generation

PLAXIS uses unstructured mesh, which is generated automatically with options for global and local mesh refinement. There are five choices of mesh density in PLAXIS. Mesh density varies from very coarse mesh to very fine mesh. Mesh is refined around the upper part of column and the surrounding soil where high stresses and strains are expected.

The level of sophistication of the soil model constitutive relation and the number and type of the elements used in the domain discretisation have a significant impact on the FEA accuracy. In this study, the mesh is refined to a fine mesh around the pile and the geogrid to increase the level of accuracy.

3.2.5 Initial conditions

Once the geometry of the model has been created and the Finite Element mesh has been generated, the initial stresses must be specified. PLAXIS provides an option to generate the initial conditions during input using K_o procedure or calculation of initial stresses by weight loading using gravity loading. K_o procedure is used in this study (as recommended by the PLAXIS manual) to calculate the initial soil stresses because all the geometry including the ground surface, soil layers and ground water table are horizontal.

3.3 Details of FEA

A very useful set of laboratory model tests were performed at the University of Kassel in Germany. As described by Zaeske (2001) and Kempfert et al. (2004), a group of four piles (length = 40 cm) was placed in a square grid in a 40 cm thickness of soft soil, above which a reinforced and unreinforced sand fill was

placed as shown in Figure 3.6. A square pile section (16 cm x 16 cm) was placed at a 50cm grid, which corresponds to a capping ratio of 10%. A uniform pressure was applied on the top of the sand (embankment).

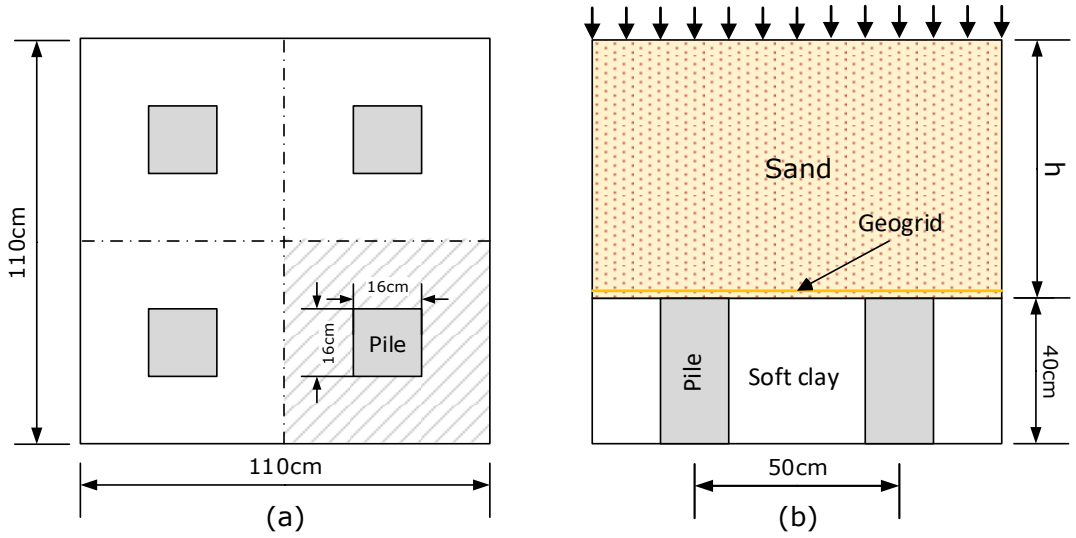


Figure 3.6 Zaeske (2001) model test dimensions and configuration: (a) plan view of piles; (b) section view.

In this research, the Zaeske (2001) model test is modelled using PLAXIS 2D to investigate the development of arching in the embankment material. The pile-soil unit was modelled using a unit cell concept to simplify the analysis which simulates a flexible loading such as an embankment. A maximum surcharge of 104 kPa (i.e. the maximum applied load in Zaeske's model test) is applied on top of the sand.

The coefficient of compression (C_c) and coefficient of swelling (C_s) of the soft soil were derived from the one-dimensional oedometer data presented by Zaeske (2001) and they are equal to 2.48 and 0.5, respectively, which is also described in Kempfert (2006). Soil tends to exhibit an increase in the stiffness with increasing confining pressure. Therefore, the one-dimensional stiffness

parameters were converted by PLAXIS into 3D parameters to capture the stress dependency of the soil stiffness by the HS model.

The strength characteristics of the soft soil were investigated by Zaeske (2001) and the critical state friction angle of 24° and an effective cohesion of 8.5 kPa were determined from his laboratory tests. The unloading-reloading Poisson's ratio of 0.2 has been assumed for both soft clay and sand (PLAXIS default value). The initial values of unloading/reloading Poisson's ratio vary between 0.1 and 0.2 for soils and rocks following experimental measurements taken from local strain gauges, therefore a characteristic value of 0.2 can be adopted for most types of soils (Obrzud and Truty, 2018). For loading of normally consolidated materials, the unloading-reloading Poisson's ratio play a minor role, but it becomes important in unloading problems (Brinkgreve et al., 2018). There is no unloading-reloading in the case study analysed in Chapter 3 (Zaeske model) therefore PLAXIS default value of 0.2 is adopted in the current analysis. The sand has a saturated unit weight of 18 kN/m^3 and a constrained modulus of 28 MN/m^2. While no effective cohesion was observed in the tests, a nominal value of 0.1 kPa was adopted for the sand to ensure a numerical stability in all of the subsequent FEA. An effective friction angle of 38° and a dilation angle of 11° were also determined by Zaeske (2001).

Nowadays, it is a common practice to install a geosynthetic reinforcement (geogrid) either on the top of the soft clay or above piles where loads need to be transferred into a deep bearing layer. In this research, a geogrid is laid on the top of the piles and modelled as a linear elastic material with axial stiffness, J, of 1000 kN/m. The main function of the geogrids at an embankment base is to resist embankment load and the outward spreading force. The in-situ coefficient of lateral earth pressure of the soft clay K_0 = 0.65 (corresponding to an angle of

friction φ = 24^0) is used in this study following the recommendation made by Scherzinger (1991) as shown previously in Figure 2.1.

In separate experiments, sand was placed on top of the piles to represent embankment in two thicknesses: 35 cm and 70 cm. A dearth of information is available for 35cm experiment, therefore, 70 cm test is chosen to verify the numerical analysis. A poorly graded sand with d_{50}= 0.35 mm (see Figure 3.7) is used in Zaeske's model tests. Concrete piles are modelled as a linear elastic non-porous material in the numerical analysis with the modulus of elasticity E=26 GPa. All simulations are performed with the Finite Element code PLAXIS 2D.

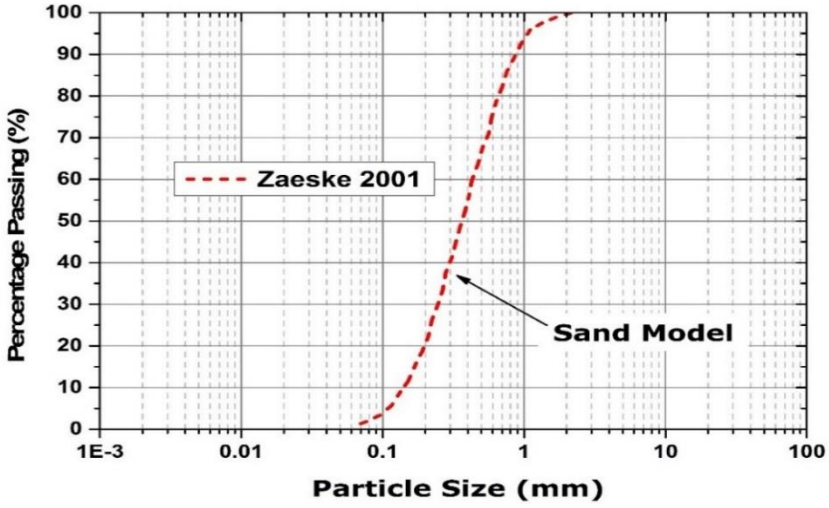


Figure 3.7 Sand particle size distribution used by Zaeske (2001).

The sand and soft clay properties used in the soil model described by Zaeske (2001) and Kempfert (2006) are presented in Table 3.1. Soil parameters adopted in this analysis were derived from a series of tests such as one-dimensional oedometer and direct shear tests. The system has been simulated as the axisymmetric unit cell in PLAXIS 2D. Half of the geometry is selected to reflect the effect of symmetry.

Table 3.1 Soil parameters for Hardening Soil model.

Properties	Unit	Sand	Soft clay
Φ'	[°]	38.0	24.00
C'	[kPa]	0.1	8.50
ψ	[°]	11.0	0.00
γ	[kN/m^3]	18.0	17.70
E_{50}^{ref}	[MPa]	23.0	1.70
E_{oed}^{ref}	[MPa]	28.0	0.85
E_{ur}^{ref}	[MPa]	112.0	12.75
ν_{ur}	[-]	0.2	0.20
m	[-]	0.5	1.00
R_{inter}	[-]	1.0	0.70

The nodes on the lateral boundaries were restrained in the x-direction only but the nodes on the bottom boundary were restrained in both x and y-directions. The finite element mesh was generated automatically with six-node elements for axisymmetric model.

3.4 Finite Element analysis

A well-documented set of laboratory model tests as performed by Zaeske (2001) is simulated using PLAXIS 2D in order to substantiate the use of parameters in Table 3.1. Firstly, the initial stresses were generated under Ko conditions. Then, a pile sector was activated to represent pile installation (wish in place). The embankment fill was then added to simulate the embankment construction on the top of the piles. If embankment was reinforced with a geotextile placed at the top of the piles, it was applied simultaneously with the embankment construction. Finally, the external load was placed on to top of the embankment. The finite element mesh generated by PLAXIS is shown in Figure 3.8.

The influence of applying an external load on piled-embankment system is shown in Figure 3.9.

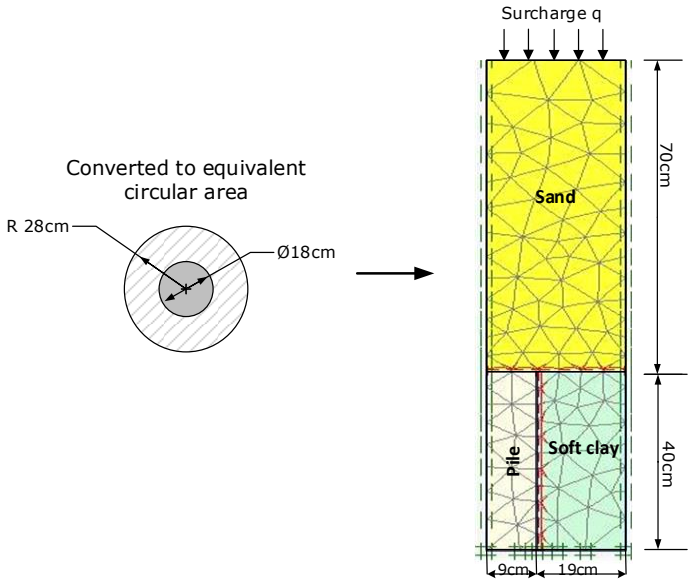


Figure 3.8 Axisymmetric model mesh used for the calculations.

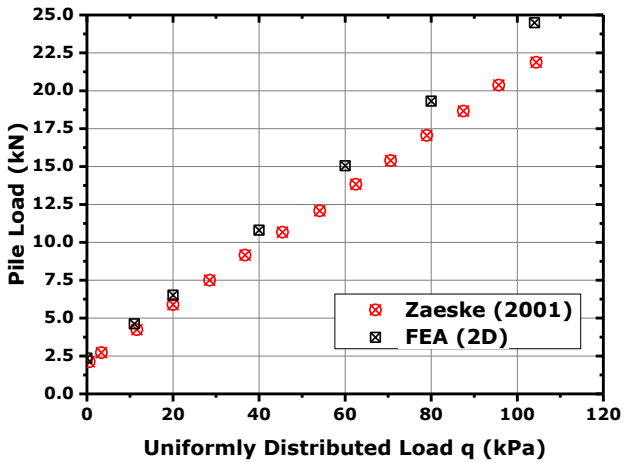


Figure 3.9 Validation of soil parameters for Zaeske (2001) model test: applied load vs pile load.

It is observed that piles carried a significant portion of the load in comparison to the soft soil; for example, the total applied load on one-unit cell at 40 kPa is 12.96 kN (Load= (The density of the sand x height of the sand layer + 40 kPa) x unit

cell area), therefore 85% (11/12.96 kN) of the unit cell load is transferred to the pile head. The pile load prediction from the FEA and Zaeske (2001) model test agrees quite well. The calculated pile loads confirm that the embankment material is arching, hence the larger proportion of the embankment load is transferred to the piles.

The influence of a geotextile reinforcement at the base of the embankment is shown in Figure 3.10, where the geogrid tensile force developed at various applied embankment loads predicted by the FEA and of the model test recorded by Zaeske (2001) are compared near the pile face. In the reference case (Zaeske, 2001), the tensile force in the geogrid is calculated at 4.5 cm from the pile face.

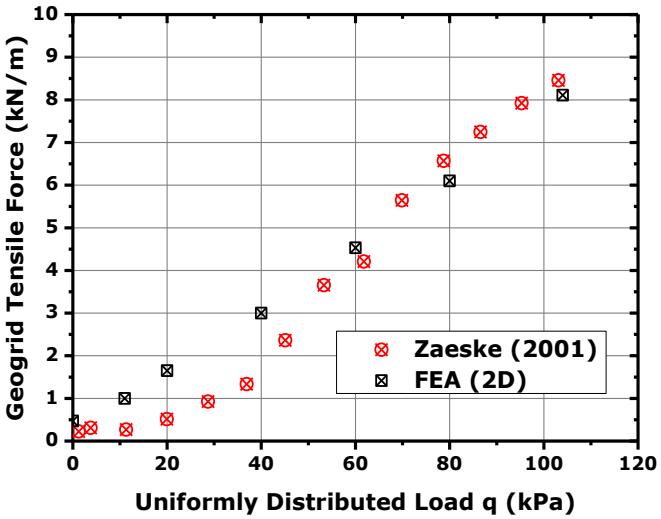


Figure 3.10 Validation of soil parameters for Zaeske (2001) model test: Applied load vs geogrid tensile force.

Therefore, the tensile force is predicted at the same distance to allow an appropriate comparison between the FEA and the reference case.

It is clear that both the pile loads and the geogrid tensile force due to applied embankment loads are in good agreement with Zaeske (2001) model test, affirming the selection of the adopted soil profile and material parameters.

3.5 Summary of the numerical analysis development and validation

A combination of laboratory tests and modelling experience were used in the current analysis to derive and calibrate the geotechnical and structural parameters of the model and to verify the results of the FEA in the subsequent analyses. PLAXIS software package was selected to carry out the FEM analyses in Chapter 3 and 4 because PLAXIS performance and accuracy have been tested by academia, industry and software developers (see Section 3.2). The Hardening Soil (HS) model as implemented in PLAXIS has been used as a reference model for the soft soil and granular embankment material. The soil behaviour is highly non-linear, therefore, the HS model is preferable to model the soil behaviour where both the strength and stiffness highly depending on the stress and strain level.

A very useful set of laboratory model tests performed at the University of Kassel in Germany by Zaeske (2001) is modelled using PLAXIS 2D to investigate the development of arching in the embankment material. Two-dimensional axisymmetrical geometry has been used to study the piled-embankment behaviour. Two-dimensional axisymmetrical geometry is approximating the model geometry therefore it is vital to validate the FEM against field works or laboratory tests. A soil profile and set of material parameters were developed from a series of tests such as one-dimensional oedometer and direct shear tests as described by Zaeske (2001) and Kempfert et al. (2004). The adopted soil profile and choice

of material parameters were validated by simulating the Zaeske (2001) laboratory test.

No load reduction percentage on the boundary been reported on the test model by Zaeske 2001. Therefore, a sensitivity analysis was carried out to investigate the influence of the interface reduction factor on the embankment surface settlement under applied load. The influence of the interface reduction factor is minimal. It is worth mentioning that Zaeske model and subsequent analyses in Chapter 3 are ignoring the effect of lateral thrust at the side of the embankment on the load transfer mechanism through arching, settlement behaviour, and geogrid strength requirements.

It is also worth noting that the case study in Chapter 3 was modelled using 2D-dimensional unit cell concept to simplify the analysis, however, the ability of the PLAXIS 2D-dimensional axisymmetrical model to capture the pile loads and the geogrid tensile forces was assessed and compared with Zaeske (2001) model test, affirming the selection of the adopted soil profile and material parameters.

3.6 Midpoint of lateral earth pressure coefficient

In this research, the K profile has been normalised by the passive lateral earth pressure K_p (taking the standard Rankine value and ignoring the small cohesive element of strength $K_p = (1+\sin \varphi)/ (1-\sin \varphi)$) plotted upward from the base of the embankment normalised by the pile spacing (s). This approach will provide a direct answer if the soil is in a plastic state by comparing K value with K_p and also allow the comparison with Hewlett and Randolph (1988) method as summarised in Figure 2.5. The lateral earth pressure at rest, represented as K_o, and passive lateral earth pressure K_p corresponding to the angle of friction values used in this research are listed in Table 3.2. The lateral earth pressure at rest (or in-situ

horizontal pressure) for the granular embankment material is calculated using the following expression (Jaky, 1948):

$$K_0 = 1\text{-}\sin \Phi \qquad (3.4)$$

Table 3.2 Normalised K_o/K_p with relevant angle of internal friction.

Internal angle of friction (Φ)	K_o	K_p	K_o/K_p
30^0	0.5	3	0.17
35^0	0.43	3.7	0.12
40^0	0.36	4.6	0.08
44^0	0.31	5.6	0.06
45^0	0.29	5.8	0.05

3.7 Results

Zaeske (2001) model test, shown in Figure 3.6, is revisited to evaluate the influence of the key parameters variation upon the normalised K value (K/K_p profile). Figure 3.11 shows the profiles plotted with vertical distance (z) upwards from the base of the embankment normalised by the pile spacing (s). The profile as plotted extends to the top of the embankment, values of 0.5 (s - a) (where (a) is the pile cap size as shown in Figure 2.5) and 0.5 s are highlighted on the z/s axis. The influence of the external applied load on the top of sand layer (embankment) and the embankment material strength (angle of the internal friction) upon embankment arching are shown in Figure 3.11 (a to c).

It can be seen from Figure 3.11 (a) that $K = K_o$ at $(z/s) > 1.1$, and thus the embankment above this point has not been affected by the formation of arching. The load is transferred laterally to a stiffer embankment element (embankment fill above pile which settles much less relative to the subsiding soil body above soft soil) within a distance (see Figure 3.13, a distance of approximately 0.5 m) above

the embankment base level. Lateral load transfer to the stiffer element will cease once the embankment fill has settled equally at a horizontal plane. Therefore, above this horizontal plane the soil will not be disturbed by arching (see Figure 3.13).

The embankment height was varied from 0.7 m to 1.3 m in Figure 3.11, for embankment where h/s = 1.25, the value for K is observed to increase gradually with depth commencing at z/s = 1.1 up to a maximum at z/s lower than 0.2. The increase may be attributed to the increase in arching with depth. The coefficient of lateral pressure (K) starts to decrease due to the stress redistribution as a result of the embankment fill arching.

In the case of the larger surcharge (85 kPa) the value of K exceeds K_p value just under z ≈ 0.5 (s - a). A slight increase in the K/K_p ratio is associated with increasing the external load applied on top of the embankment within the infill material zone. Compared with a semi-circular arch in Figure 2.5, the upper limit of the effect of arching in Hewlett and Randolph (1988) is about 2.0 times higher than the arching effect indicated in Figure 3.11 (c), but the passive limit is only reached (q= 85 kPa) below the inner radius of the arch, where the infill material is evidently in a plastic state. The value of K_p indicated in Figure 3.11, taking the standard Rankine value neglects the small cohesion intercept, and thus can be exceeded, particularly when stress is small (e.g. near the surface of the embankment or immediately above the subsoil).

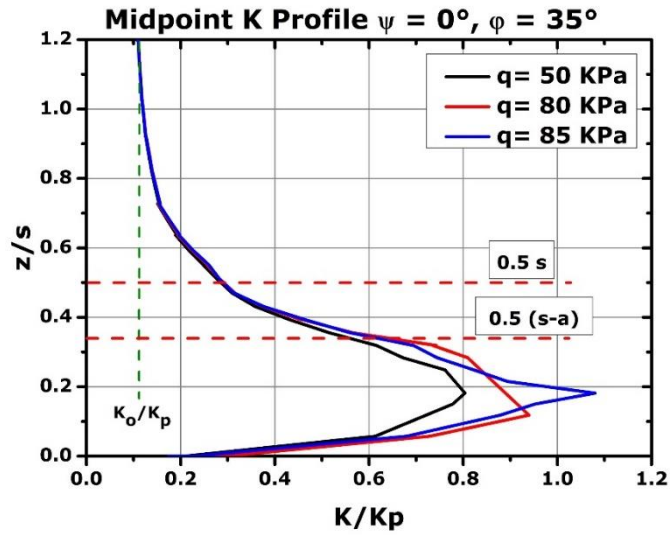
The influence of changing embankment height upon embankment arching is examined in Figure 3.11 (a to g), it can be seen for h/s =1.25 (h= 0.7 m) that K = K_o at (z/s) ≈ 1.1, and thus has not been modified by the formation of the arch. The midpoint K/K_p profile for the higher embankments h = 1.0 m (h/s = 1.79) and

h =1.3 m (h/s = 2.3) shows similar trends to the lower embankment h = 0.7 m (h/s = 1.25). It can also be seen that increasing the embankment height to h/s = 1.79 and h/s = 2.3 suggests that the embankment fill is not disturbed by the arching effect at (z/s) between ≈ 1.0 to 0.95, respectively. Therefore, comparing the results with a semi-circular arch in Figure 2.5, the upper limit of the arching is about 1.8 to 2.0 times higher for h/s = 1.25 to 2.3.

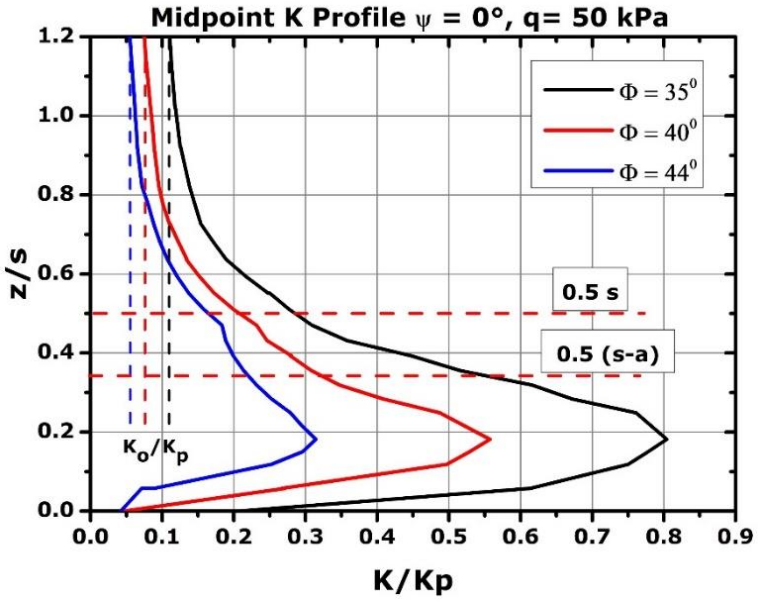
It is evident in this research that the method of Midpoint K profile is predicting a higher arching level compared with the predictions of Hewlett and Randolph (1988) as shown in Figure 3.11. According to Figure 3.11, the normalised value of K/K_p starts to increase due soil arching at a height about z/s= 1.0 above the pile head and then starts to decrease at a height about z/s= 0.2 above the pile head. This shows that the outer line of the arch is at a height of z= 0.5 m (for s= 0.5 m) and the inner line of the arch is at a height of z= 0.1 m (for s= 0.5 m) above the pile head midway between the piles. Therefore, the thickness of the arch midway between the piles is about 0.4 m. However, Hewlett and Randolph (1988) design method assumes that the thickness of the arch midway between the piles is about 0.09 m, which is half of the equivalent pile diameter. It is clear in this study that the thickness of the arch midway between the piles and the level of arching (crown) calculated by Hewlett and Randolph (1988) method, in this instance, is not accurate which is consistent with the findings of Ariyarathne and Liyanapathirana (2015).

It would appear that at least in this research, the higher embankment is modified by arching at relatively lower level than the lower embankment, as shown in Figure 3.11. Moreover, it appears that K is slightly lower for the higher embankment than the lower embankments which indicates that the tendency is arching failure at the

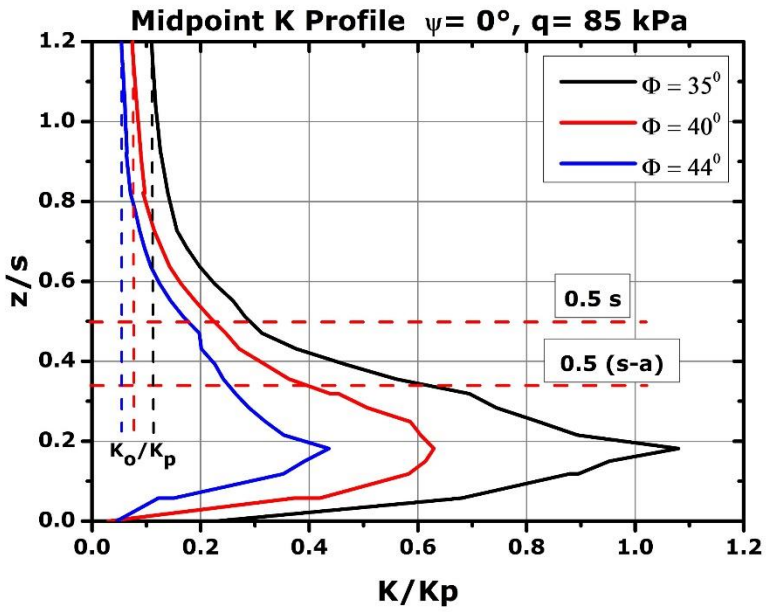
pile cap level rather than at the crown for higher embankments (Hewlett and Randolph, 1988).



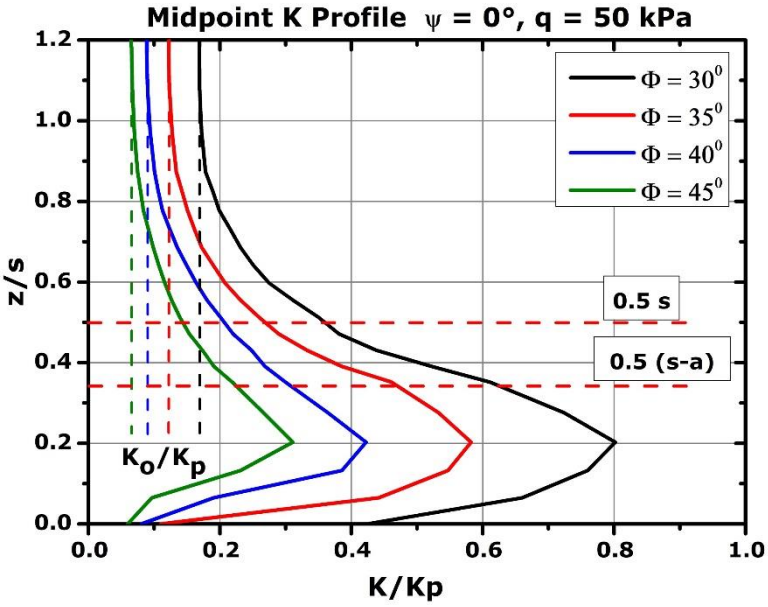
(a) h/s =1.25, Ψ=0° and Φ= 35°



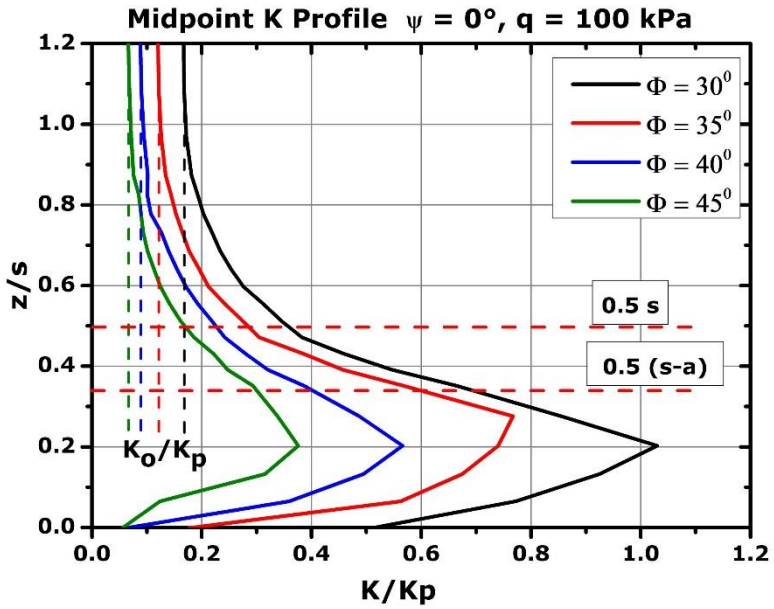
(b) h/s= 1.25, Ψ=0° and q= 50 kPa



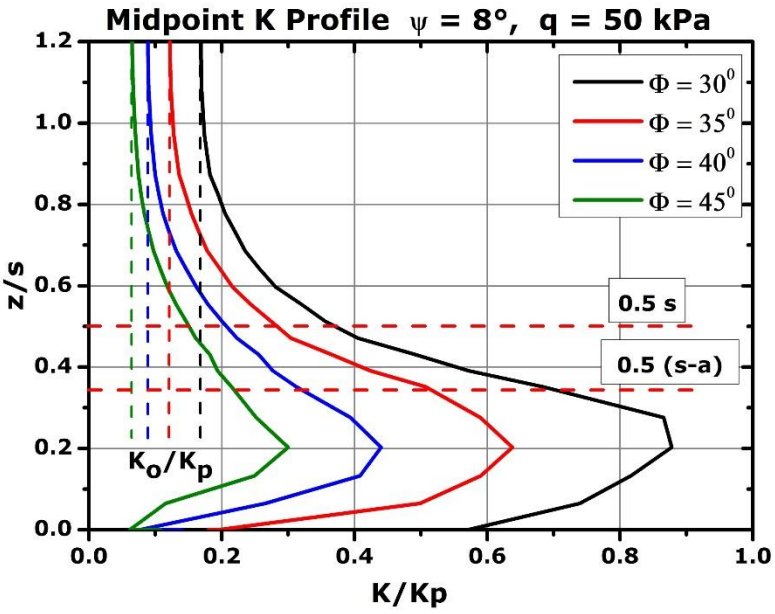
(c) h/s = 1.25, Ψ=0° and q=85 kPa



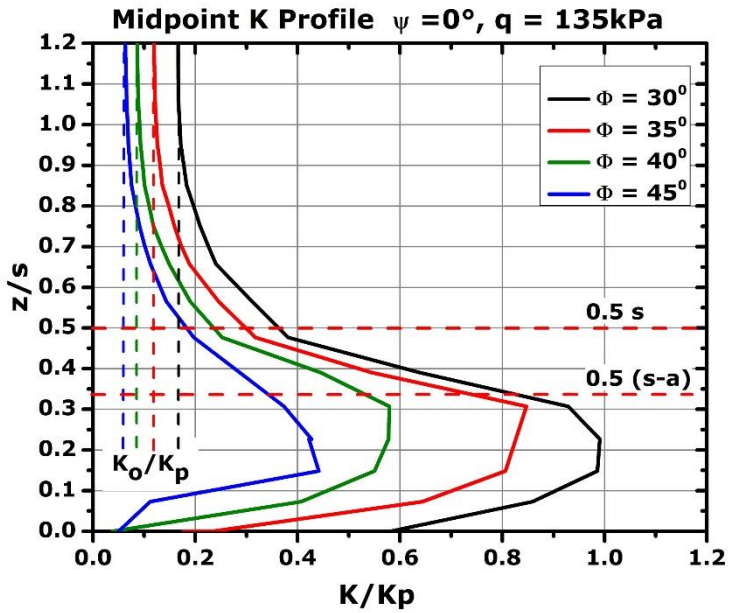
(d) h/s = 1.79, Ψ=0° and q= 50 kPa



(e) h/s = 1.79, Ψ=0° and q= 100 kPa



(f) h/s = 1.79, Ψ=8° and q= 50 kPa



(g) h/s = 2.3, Ψ=0° and q= 135 kPa

Figure 3.11 Profiles of normalised earth pressure coefficient (K/K_p) on a vertical profile at the midpoint between piles.

Since for a granular embankment the effective cohesion can be assumed zero, the evaluation in this research is focused on the variation of φ' and ψ to investigate the influence of shear parameters. In order to assess the influence of φ', all other parameters are kept constant – with the exception of the dilation angle ψ, taken as 0° and 8° to evaluate its influence on the piled-embankment system behaviour.

The effective angle of internal friction φ' of the embankment soil has an influence on the subsoil (soft soil) surface settlement, as illustrated in Figure 3.12 (a). The higher the angle of friction, the less predicted subsoil surface settlement is obtained. Figure 3.12 (b) shows that pile loads have a proportional relationship with the fill angle of internal friction (see Figure 3.9). Therefore, φ' has significant influence on embankment soil arching.

Figure 3.11 (b to g) shows the effect of increasing the angle of internal friction upon K/K_p ratio for various embankment heights and applied external loads. The

higher φ' leads to a lower lateral earth pressure K at the same height compared to lower φ'. The influence of ψ on subsoil surface settlement is less significant than that of φ', as shown in Figure 3.12 (a). However, a similar trend of increasing φ' is observed when ψ increases, where a lower dilatation ψ angle leads to a larger subsoil surface settlement. It can be observed in Figure 3.11 (b and d) and Figure 3.12 that the higher φ' results in better load distribution (arching) in the embankment which might be characterised by the lower subsoil settlement and K/K_p ratio.

As presented in Figure 3.11 (e and f), the higher the ψ, the higher lateral earth pressure coefficient K value below z= 0.5 (s - a), particularly for the embankment materials with lower angle of internal friction φ'. A possible explanation was put forward by Taylor (1948), where the soil strength improvement is associated with the increase in the dilatancy angle on the basis of a remarkable phenomenon of an increase in the volume observed when granular materials are sheared under applied load (Bolton, 1986).

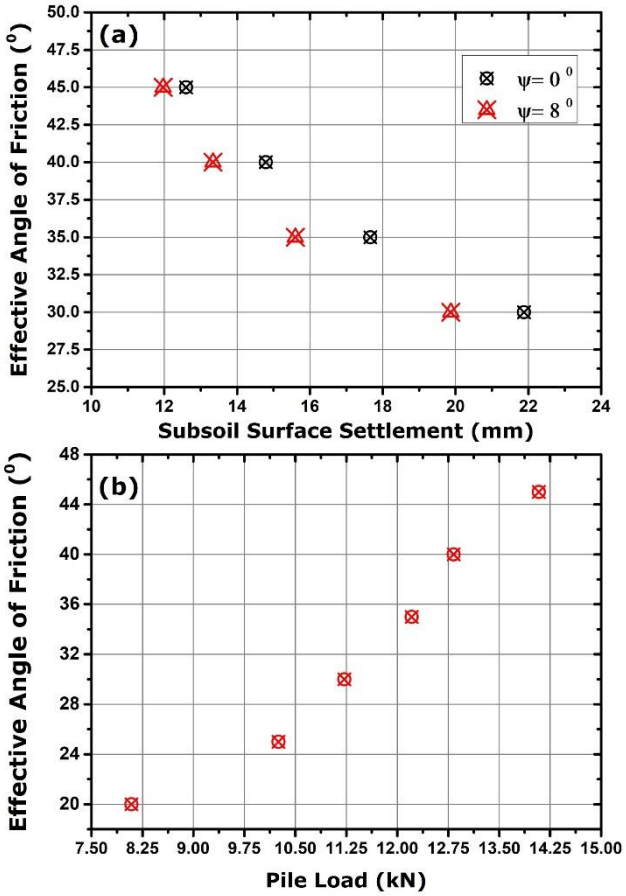


Figure 3.12 The fill angle of internal friction variation with (a) soft soil surface settlement and (b) pile load.

To examine the influence of external applied load upon the piled-embankment behaviour, the surcharge has been increased from 85 kPa to 135 kPa in Figure 3.11 (c, e and h). If the embankment surcharge was increased beyond these surcharges, the FEA would stop due to soil failure (i.e. collapse). Therefore, it appears that in this particular case, the higher embankment, the more load the system can resist. This is reflecting the fact that the increase in the embankment height will improve the load transfer mechanism to the piles and the surrounding soils, accordingly. Figure 3.11 (a) demonstrates the influence of external embankment surcharge on the piled-embankment system. Increasing the applied

load (q) from 50 kPa to 85 kPa promotes the tendency to mobilise K_p where the increase in applied load leads to an increase in the K value at the same level.

The material parameters outlined in Table 3.1 are used to calculate the principal stress distribution with depth due to developing of arching in the embankment as shown in Figure 3.13.

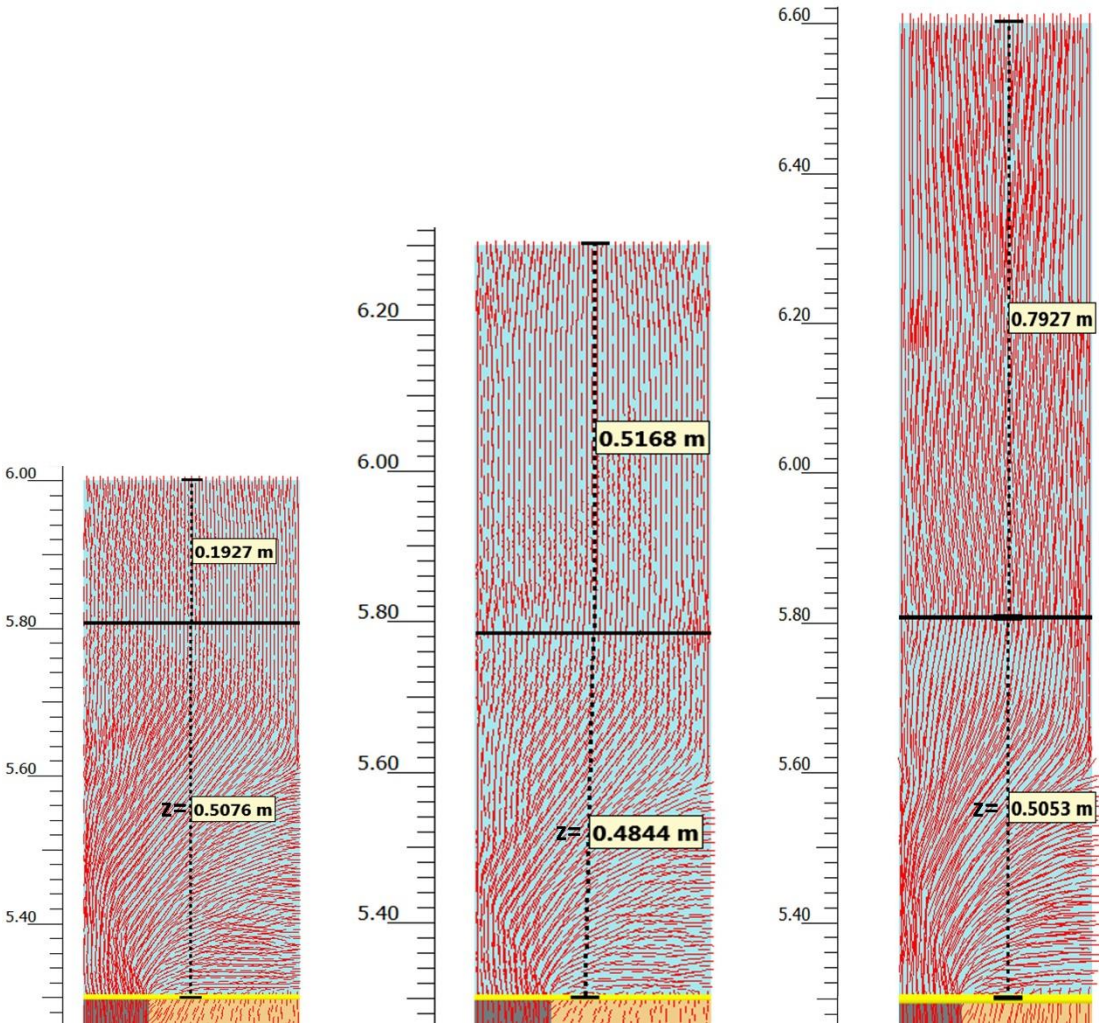


Figure 3.13 Developed arching in embankment in terms of principle stresses after applying 104 kPa external load (a) h=0.7 m (b) h = 1 m (c) h = 1.3 m.

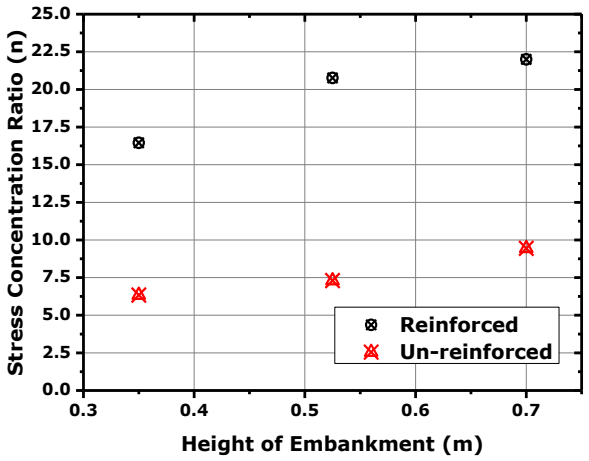
It can be seen that the orientation of the principal stresses forming a catenary shape from the embankment body toward the pile head. The developing of arching

from z≈ 0.5 m (z= distance from the embankment base) is in agreement with the previous findings of the midpoint of lateral earth pressure coefficient in Figure 3.11, where K value is not disturbed by arching ($K=K_0$) at z/s ≈ 0.95 to 1.1 (s=0.5 m).

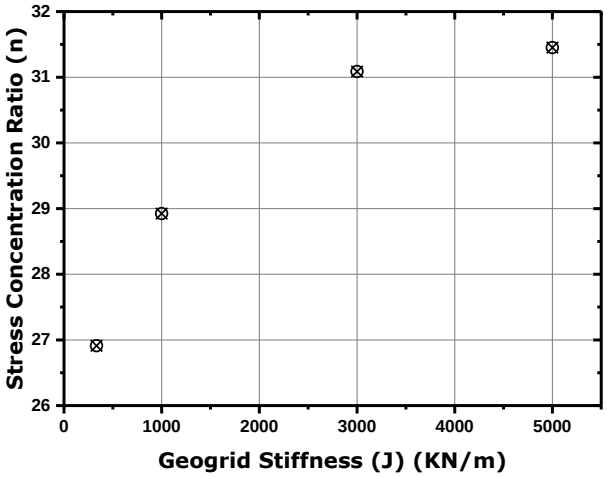
The stress concentration ratio (n) can be identified as the ratio between the vertical effective stress in the pile and the surrounding soft soil (see Section 2.8.2.3). The stress concentration ratio is used to measure the effectiveness of the pile in improving the soft soil and the embankment settlement. The stress concentration ratio is measured at the top of the pile. The stress of the soil surrounding the head of the pile is determined by averaging the soil stress within a zone surrounding each pile head. The higher the stress concentration ratio, the more stress is transferred onto the piles.

The influence of the embankment height upon the concentration ratio is shown in Figure 3.14 (a). The height of the embankment has a significant impact on the stress concentration ratio. The concentration ratio is increased with an increase of the embankment height. The stress transferred onto the piles is higher with reinforced case than that with unreinforced case. These results are in good agreement with the findings of Han and Gabr (2002) in addition to the findings of Han (1999) and Han and Wayne (2000) analysing the field data. The inclusion of geosynthetic into the piled-embankment system enhances the stress transferring from the soil to the piles. The main function of the geogrid is reducing the subsoil settlement and therefore the differential settlement by transferring the stresses from the subsoil to the pile head due to the interlocking action between the geogrid and the embankment fill.

The influence of the tensile stiffness of the geogrid upon the stress concentration ratio is investigated by varying the geogrid stiffness over a wide range, while all other parameters are kept constant. As shown in Figure 3.14 (b), the stress concentration ratio increases with the increase of the geogrid tensile stiffness and then the increase in the stress concentration ratio remains relatively small with increasing the stiffness, for example, increasing the geogrid stiffness from 3000 kN/m to 5000 kN/m will only increase the stress concentration ratio by 0.3.



(a)



(b)

Figure 3.14 Stress concentration ratio: (a) influence of the height of embankment; (b) influence of geogrid.

These results are in good agreement with the findings of Han and Gabr (2002) who indicates an approximate geogrid value of 4000 kN/m where the stress concentration ratio approaches a constant value. The increase of the stress concentration ratio with the stiffness of the geosynthetic is attributed to the geogrid by promoting the stress transfer from the soft soil to the pile head.

The amount of load transfer to the pile head can be quantified by using the efficacy parameter as described in Section 2.8.2.1. The calculated efficacy from the FEA and Zaeske (2001) model test is presented in Figure 3.15. It is evident that a good agreement exists between the calculated and the measured efficacy. As illustrated in Figure 3.15, the higher the applied external surcharge, the higher the pile load or the higher efficacy.

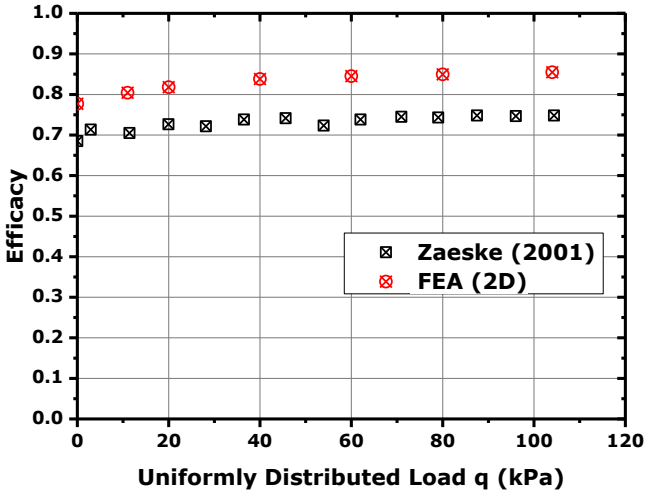


Figure 3.15 Calculated and measured efficacy.

It was again found that the geogrid was capable of increasing pile loads in comparison with the conventional pile-supported embankment as presented in Figure 3.16, which may be attributed to the fact that the geotextile reinforcement can stabilise the arching effect by so-called a membrane effect. Hence, the subsoil stress and settlement reduced accordingly. Therefore, the embankment

settlement is considerably reduced by introducing piles and geogrids at the base of the embankment.

Shear stresses will be generated due to the differential settlement of the embankment fill above the pile cap and at the midpoint between adjacent pile caps which will extend upward into the embankment. These shear forces would terminate at some horizontal plane above the base of the embankment (plane of equal settlements) if the embankment is sufficiently high.

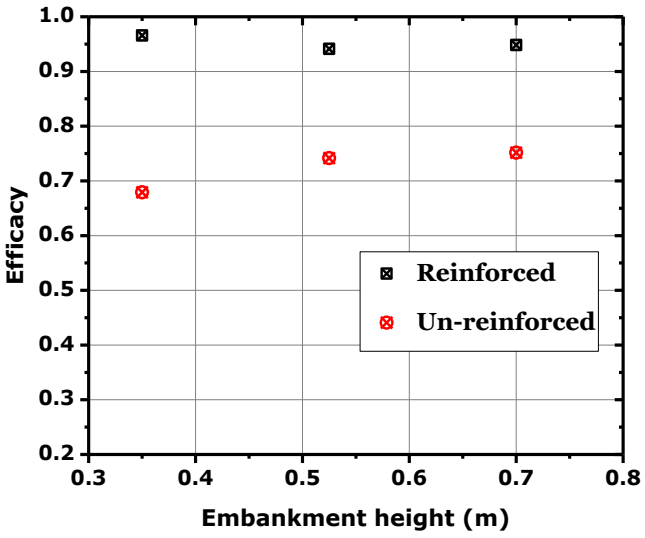


Figure 3.16 Efficacy for reinforced and unreinforced embankment.

Naughton (2007) has proposed a plane of equal settlement which can be used to determine the soil arching height. A horizontal plane of equal settlement can be found at z≈ 0.48 m from the base of the embankment as shown in Figure 3.17 (using soil properties in Table 3.1 and external surcharge of 104 kPa) . It was shown in Figure 3.11 and Figure 3.13 that K/K_p profile method and the profile of principle stresses from FEA that the embankment was modified by arching at z= 0.5 m to 0.56 m from the base of the embankment. It is evident from the results

of FEA that both methods of the plane of equal settlement and K/K_p profile at mid-point can characterize arching and can indicate the starting level of arching.

Soil arching height found by either a plane of equal settlement method or by the K/K_p midpoint profile method can be considered as the minimum embankment height required in order to develop a full arching in the embankment fill material. For instance, British Standard BS8006 (2010) states a minimum embankment height of 1.4 (s - a) for a full soil arching (a=0 no pile cap in Zaeske (2001) model test).

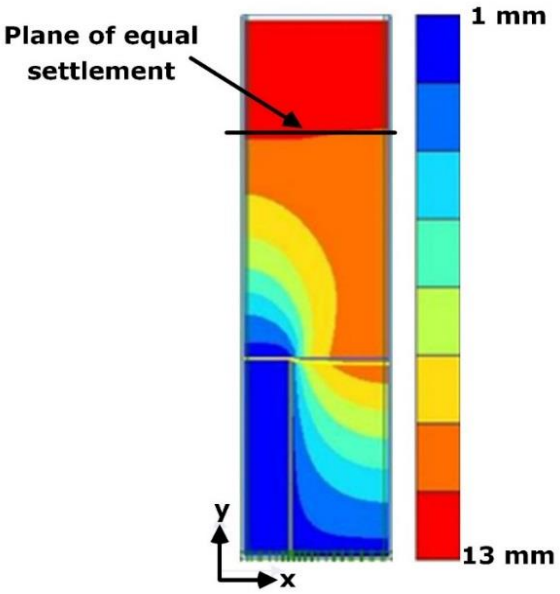


Figure 3.17 Vertical settlements shading after applying 104 kPa external load.

Meanwhile, German method (EBGEO, 2004) specified a minimum embankment height of 0.7 s. It appears that the British Standards BS8006 method is more accurate than the German method in this particular case (Full arching condition). It is worth mentioning that the British Standard BS8006 method is in good agreement with both the minimum embankment height case of z/s= 0.95 - 1.1 (minimum embankment height z= 0.475 to 0.55 m; s=0.5 m) presented in Figure

3.11 and the z= 0.5m case shown in Figure 3.13 and Figure 3.17. It appears that a partial arching condition was achieved in the current case rather than a full arching condition following the German method recommended minimum height of embankment which is not economical.

Figure 3.18 shows the predicted embankment surface settlement for both the reinforced and unreinforced piled-embankments. It is shown that the use of reinforcement will improve the embankment performance generating less settlement than the conventional piled-embankment at the same applied load. Both the reinforced and unreinforced piled-embankment systems have been analysed to study the influence of changing the pile capping ratio and compare the results with Han and Gabr (2002) findings shown in Figure 3.19.

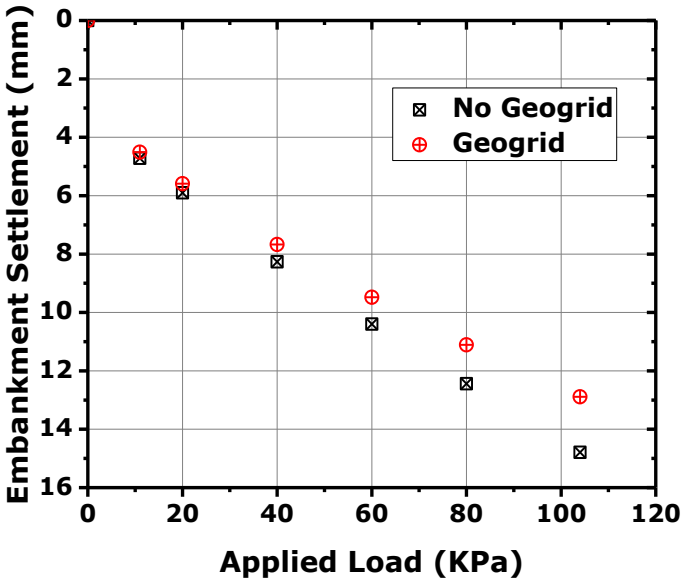


Figure 3.18 Vertical embankment settlement vs external applied load.

The possibility of the embankment punching is verified by analysing the distribution of total shear strain around the pile. In this study, the distribution of the shear strain around the pile and the cap is investigated to have a better understanding of the interaction between the soil and the pile.

Finite Element analyses were performed to evaluate the influence of capping ratio upon the arching and the mode of failure (punching) by changing the capping ratio, which corresponded to a capping ratio ranging from 0% to 20%. A load of 50 kPa was applied on top of the embankment and the total shear strain contours are illustrated in Figure 3.19 against the capping ratio percentage.

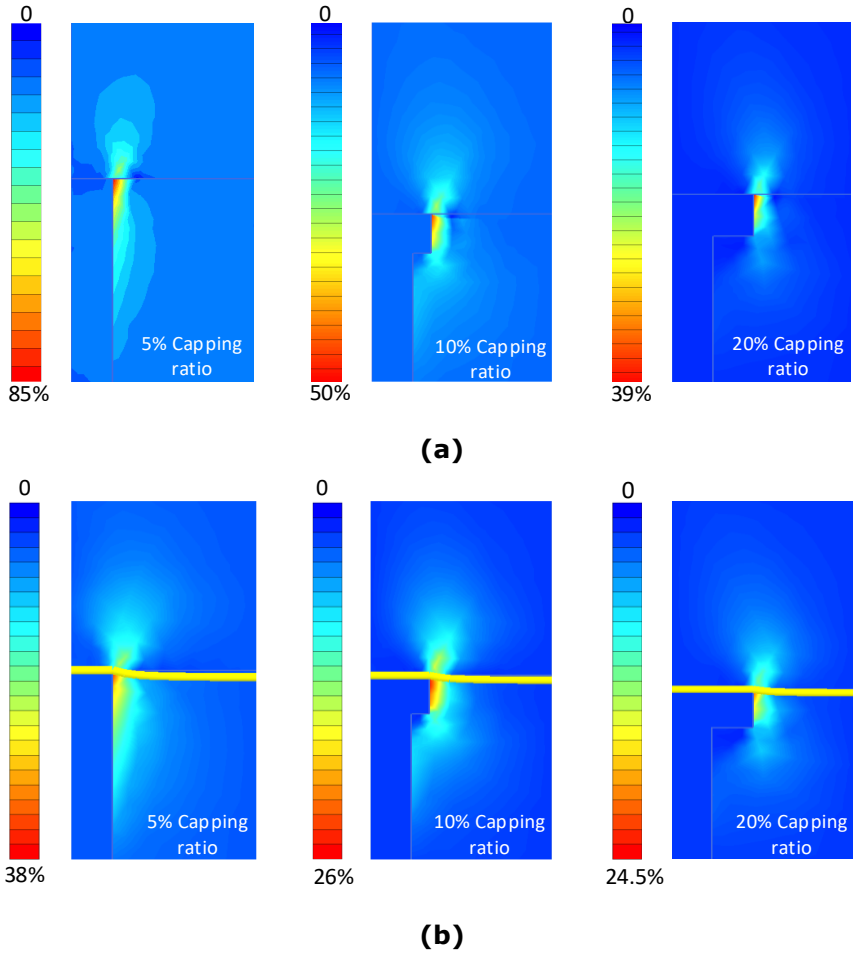


Figure 3.19 Total shear strain contours: (a) unreinforced model; (b) reinforced model.

It can be seen in Figure 3.19 that the majority of shear strain is developed in the upper part at lower capping ratio. This means that punching occurred at the upper part of the piles rather than at the lower part. As demonstrated in Figure 3.19 (a), when a small pile cap is utilized for unreinforced piled-embankment, piles tend to

have a punching failure rather than developing arching in the embankment fill. The tendency of punching reduces with increasing the pile capping ratio. Although all calculations do not show any failure, the tendency for pile punching into the embankment is clearly shown when there is no cap placed on top of the pile head. In addition, the tendency of pile punching through embankment material reduces significantly by introducing a strong layer of reinforcement at the bottom of the embankment.

It can be seen from Figure 3.19 (b) that using a one layer of geotextile will improve the piled-embankment system safety against punching. On the other hand, it is clearly shown from Figure 3.19 that if the capping ratio lies in the range between 10% - 20%, it is sufficient to prevent pile penetration into the embankment. Therefore, it is clearly shown in this research that the minimum capping ratio of 20% is considered the best option if no strong geotextile is used. However, if the embankment is constructed without reinforcement, the risk of collapse of soil arching is larger. Therefore, a one layer of reinforcement should be considered in piled-embankment design to avoid severe damage to the pile embankment load transfer mechanism (arching).

The zone of plasticity points on top of the pile represents the stress points that reached Mohr-Coulomb failure condition as are shown in Figure 3.20.

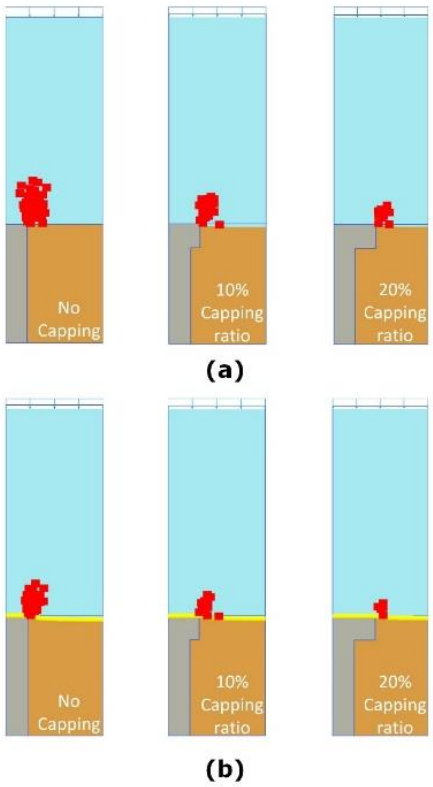


Figure 3.20 Plasticity points (Mohr-Coulomb failure zone).

The reduction in plastic points on top of the cap confirms the theory of punching. The numerical analysis agrees favourably with the findings of Han and Gabr (2002) that a capping ratio of 10% to 25% is necessary to assure a stable piled-embankment behaviour.

3.8 Summary

A parametric FEA study was carried out in PLAXIS 2D to examine the influence of several key design parameters upon the behaviour of a granular embankment supported by piles installed in soft soils. The following conclusions may be drawn:

- There is no evidence of arching above z/s ≈ 1.1 for h/s = 1.25 embankment, z/s ≈ 1.0 for h/s = 1.79 and above z/s ≈ 0.95 for h/s = 2.3 embankment based on the profile of normalised earth pressure coefficient

(K/K_p) on a vertical profile at the midpoint between piles. Therefore, the embankment height is one of the key parameters when assessing the embankment soil arching.

- The K value increases with increasing depth reaching K_p below $z \approx 0.5$ (s - a). Comparing this with a semi-circular arch proposed by Hewlett and Randolph (1988), the upper limit of arching is about 1.8 to 2.0 times higher for h/s = 1.25 to 2.3.
- The passive limit was reached for embankment with lower strength below the inner radius of the arch, where the infill material is evidently in a plastic state.
- It was observed that arching developed at relatively lower level for high embankments compared to lower embankments.
- The normalised earth pressure coefficient (K/K_p) on a vertical profile at the midpoint between piles is in agreement with the British Standards BS8006 method in predicting the minimum embankment height required to mobilise a full embankment arching.
- The higher the effective angle of internal friction φ' results in better load distribution (arching) in the embankment. It is observed that a lower soft soil settlement below the embankment is accompanied by a lower K/K_p ratio if the strength of the embankment increases (for example increasing the effective angle of friction).
- The higher φ' also leads to a lower K value at the same height.
- The influence of the angle of dilatation ψ on subsoil surface settlement is less significant compared to that of φ'. However, similar trend of increasing

φ' is observed when ψ increases. The higher subsoil surface settlement is obtained for reduced ψ angle.

- The earth pressure coefficient K normalised by the passive earth pressure coefficient K_p plotted on a vertical profile at the midpoint between can be a very useful tool to study the embankment material arching. Furthermore, the K/K_p method can be used to perform a sensitivity analysis and to measure the effect of a number of key design variables on the arching when analysing piled-embankment system.

- It appears that the British Standards BS8006 method is more accurate than the German method when analysing Zaeske's (2001) model. The British Standards BS8006 method was in good agreement with both the profiles of the normalised earth pressure coefficient (K/K_p) method and the plane of equal settlement method.

- It is evident from the results of the FEA that both, the plane of equal settlement and the K/K_p profile at mid-point methods can characterise the embankment arching and can also indicate the starting level of arching. Therefore, a minimum embankment height can be determined using both the plane of equal settlement and the K/K_p profile at mid-point methods.

- The increase in the stress concentration ratio was very small when increasing the geogrid tensile stiffness from 3000 kN/m to 5000 kN/m. Similarly, Han and Gabr (2002) indicated that the stress concentration ratio approaches a constant value at an approximate geogrid stiffness value of 4000 kN/m.

- The numerical analysis agrees favourably with the findings of Han and Gabr (2002) that a capping ratio of 10% to 25% is necessary to assure a stable

piled-embankment behaviour. This agreement was confirmed by studying the shear strain around the pile and pile cap and also by investigating the zone of plasticity points on top of the pile.

CHAPTER 4

NUMERICAL MODELLING OF STONE COLUMNS

4.1 Introduction

The main focus of this thesis is to study the behaviour of lightly loaded narrow footings supported by small groups of stone columns installed using the dry bottom feed technique. Most experience in this context has been with wet top feed technique. The dry bottom feed technique has largely superseded the stone columns installed by the wet top feed technique on environmental grounds (Serridge, 2001). Soft soils are typically characterized by low strength and high compressibility, therefore the settlement performance of the stone columns is the governing factor in the design rather than column capacity. This research is therefore principally concerned with the footing behaviour by evaluating the settlement performance of floating stone columns installed with a dry bottom-feed method in a deep soft clay, together with the influence of the following key design parameters:

- Stone column spacing (s)
- Stone column length (L)
- Founding depth and crust influence
- Footing shape
- Drained and undrained behaviour

- Stone column diameter (d)
- The use of encasement (geogrid).
- The effect of geogrid stiffness
- The influence of encasement depth upon stone column deformation.

The field trials at the former Bothkennar soft clay research site in Scotland (Serridge, 2013) was used as the basis of this study as it is well-characterised geotechnically (Institution of Civil Engineers, 1992) and is representative of many soft soil profiles locally and internationally for which the stone column is considered of great interest to the industry on cost and environmental grounds. The Bothkennar site is located between Edinburgh and Glasgow on former intertidal mudflats on the southern bank of the Forth Estuary and adjacent to the Kincardine Bridge. The aforementioned site selected for the trials was a place of extensive soft soil research including in situ testing, soil sampling techniques (undisturbed), and also shallow and deep foundations full-scale performance on untreated soft clay together with widespread load on vibro stone columns (Hight et al., 1992; Jardine et al., 1995; Serridge, 2001). The soft soil in this site was devoid of any peat layers. The soil profile associated with the current study consists of 1.2 m of crust underlain by a deep deposit of soft clay. The soft clay strength is relatively small compared to the overlying crust layer. The soft clay becomes soft to firm with depth. Key soil properties for Bothkennar soft clay are given in Figure 4.1.

Very soft clays at shallow depths may not provide adequate confinement to stone columns. In some applications, the use of geotextile is considered an appropriate remedy for the lack of strength (Al-Refeai, 1992). Therefore, the settlement performance of encased stone columns is also of importance in such soils. The influence of encasement is investigated by analysing the settlement performance of stone columns encased with different types of geogrid and geogrid/nonwoven geotextile composite materials.

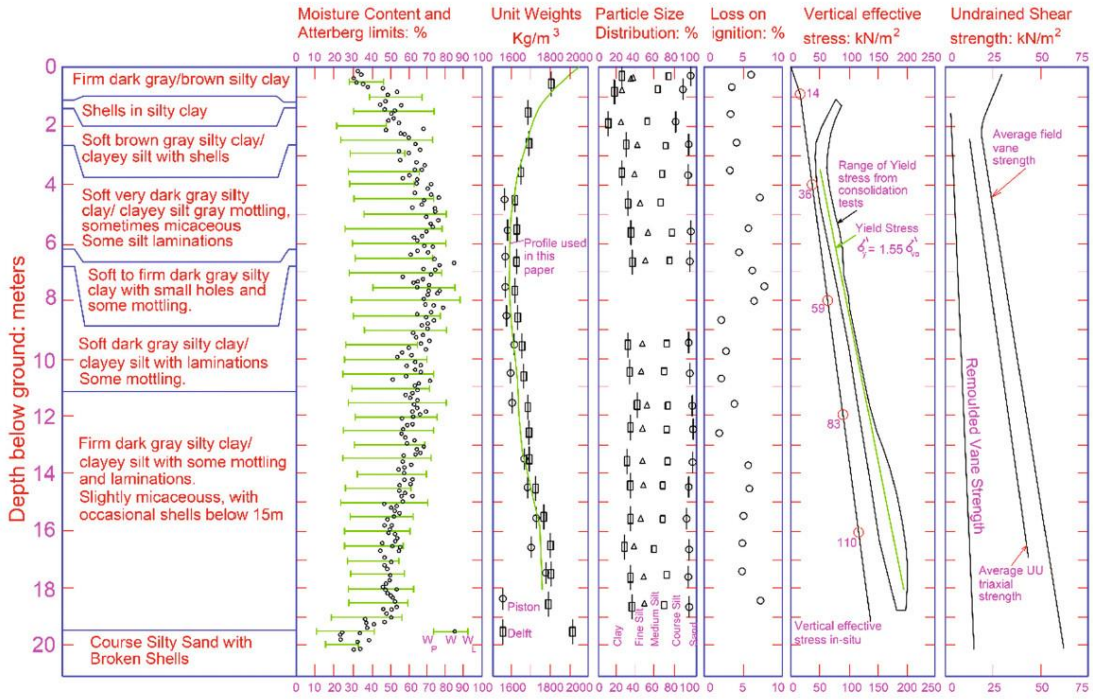


Figure 4.1 Key soil properties for Bothkennar soft clay (Nash et al., 1992a).

Finally, the influence of encasement depth and reinforcement hoop stresses upon the encased stone column-soil behaviour is investigated for a selected field trial data at the Bothkennar site (Serridge, 2013).

4.2 Field trials design

The Bothkennar site was owned and managed by the UK government through the Engineering and Physical Science Research Council (EPSRC) and subsequent to the field trials was taken over by RSPB (Scotland). This site was selected to install dry bottom feed vibro stone columns partially penetrating soft soil, beneath narrow footings in an attempt to advance the state of understanding of general behaviour of stone columns and their application in the ground improvement context. Historically, early involvement to commission field trials proved to be costly and difficult to implement so previous research was often undertaken with inadequate

soil investigations obtained for specific contracts rather than for preliminary stone column field research trials due to time and cost constraints.

Adequate soil parameters were not available for other research; moreover, none of the previous researches have addressed partially penetrating field trial installed with a dry bottom-feed method and their performance in a deep sensitive soft clay profile. The soft soil response at Bothkennar site, and associated stresses due to the stone columns installation were investigated by Serridge (2013). The main focus of this research is to predict the settlement performance of the ordinary stone columns, geosynthetic encased stone columns, and foundation response.

In the subsequent sections, the soil and column model, and the outcome of the sensitivity analysis are presented. The discussions include the influence of column spacing, column diameter, the full and partial length of the geogrid encasement, and influence of the encasement tensile stiffness upon the behaviour of stone columns. While the performance of Bothkennar field trials was measured for 10 months, it is important to investigate the influence of drained conditions to evaluate the impact of long-term soil behaviour upon the settlement performance and stone column failure mode.

The stone column design in Bothkennar site was made based on the following (Serridge, 2001):

Step 1: Calculate stone column ultimate load capacity based on factor of safety against bulging failure (Hughes and Withers, 1974).

Step 2: Calculate stone column length in accordance with Hughes and Withers (1974) observations.

Step 3: Calculate stress distribution between column and soil as defined by Baumann and Bauer (1974).

Step 4: Calculate pre-treatment settlement under applied load to demonstrate a requirement for stone column.

Step 5: Predict stone column settlement under the applied load using Priebe (1995) method.

A design treatment depth was found to be 5.5 m below foundation level based on step 2 (Serridge, 2013). However, column lengths of 3.7 m and 7.7 m with a stone column diameter of 750 mm were adopted in the trials to evaluate the length effect on column performance.

Table 4.1 and Figure 4.2 summarise the Bothkennar field trial footing arrangements and depths following above design steps. Two load increments were applied on top of the footings, given in Table 4.2. A further two load increments corresponding to 107 kPa and 125 kPa (average cumulative bearing pressures) were applied to Footing 4 and 6, to determine the ultimate bearing capacity of the stone columns. This research focusses on the settlement performance of the stone columns at serviceability load. A 50 kPa was adopted by Killeen (2012) as a serviceability load following the Jardine et al. (1995) trials at Bothkennar site (see subsequent Section 4.4.1- Ultimate bearing capacity of 138 KPa). Therefore, only the first two load cycles are adopted in this research to assess the stone column settlement behaviour. Concrete kentledge blocks were used on site to provide a uniformly distributed load on top of the Bothkennar field trials (Serridge, 2013) . Therefore, the external applied load is modelled in PLAXIS 3D as a uniformly distributed load on top of the footings.

Table 4.1 Summary of Bothkennar trial footing arrangements.

Trial footing	Dimensions (L x B)	Founding depth	Column length below foundation	Number of columns	Column spacing
	m	m	m		m
1	6 x 0.75	0.5	5.7	4	1.5
2	6 x 0.75	0.5	5.7	3	2.0
3	3 x 0.75	0.5	3.7	2	1.5
4	3 x 0.75	0.5	5.7	2	1.5
5	3 x 0.75	0.5	7.7	2	1.5
6	3 x 0.75	1.2	5.7	2	1.5
7	1.5 x 1.5	0.5	5.7	2	1.2

Table 4.2 Summary of loading increments applied to trial footings at Bothkennar.

Trial footing	Unit area per stone column (A_o)	1st Load increment	2nd Load increment
	m^2	kPa	kPa
1	1.125	35.5	72.0
2	1.500	32.9	67.1
3	1.125	33.1	67.8
4	1.125	34.9	71.1
5	1.125	32.1	67.0
6	1.125	34.2	69.6
7	1.125	32.7	67.0

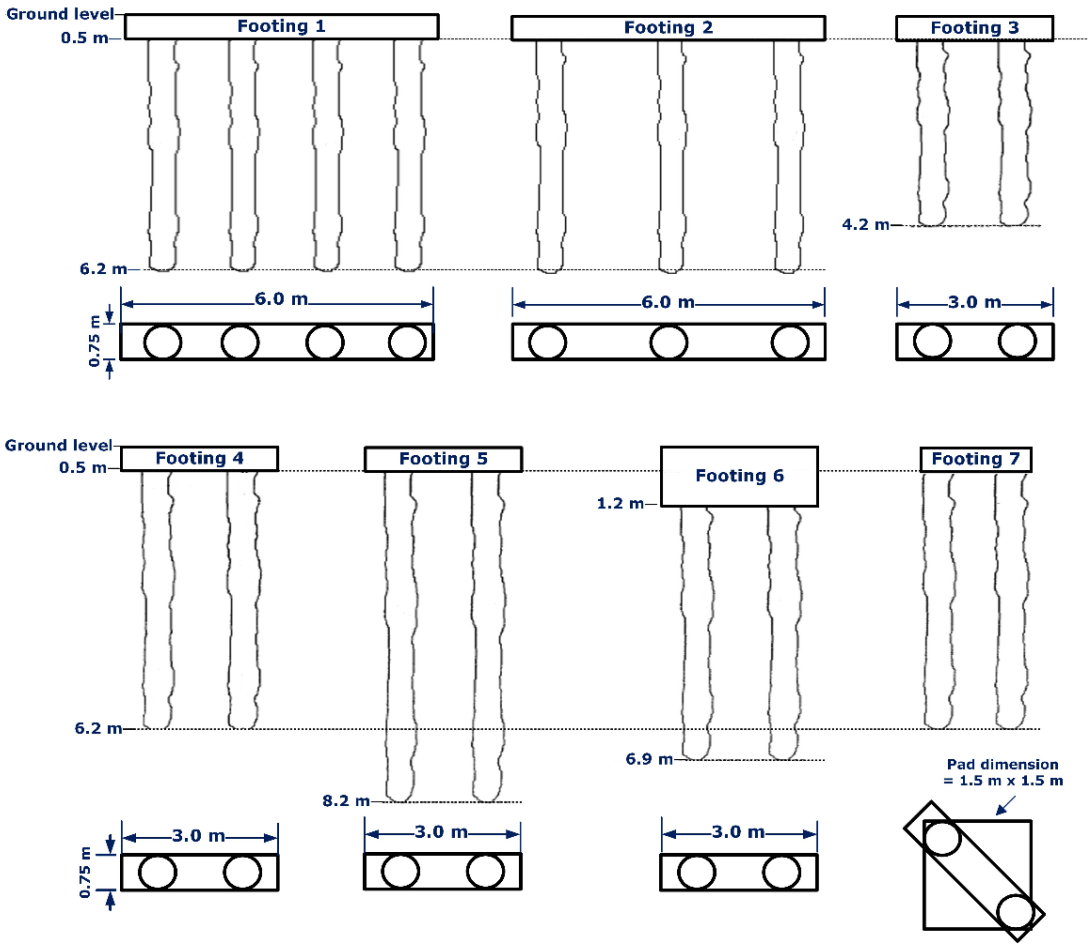


Figure 4.2 Bothkennar field trials (Serridge, 2013).

4.3 Bothkennar Numerical Analysis

A Hardening Soil (HS) model is considered more appropriate to model the Bothkennar stone column-soil composite field trials (see section 3.2.1). Mohr-Coulomb model is a simple model, and as such not capable of representing the complexity of the real soil behaviour. In drained conditions, the soil will continue dilating if a positive dilatancy angle is assigned to the soil as long as shear deformation occurs (PLAXIS, 2015). However, soils will reach a critical state at some point (critical state reached when shear deformation is occurring without any change in volume), therefore, in the HS model, the end of dilatancy (dilatancy cut-off at critical state condition) is considered in the model. Dilatancy cut-off

option is not available in Mohr-Coulomb (MC) model. The real behaviour of soil is highly nonlinear where both stiffness and soil strength are strain and stress level dependent (Potts and Zdravkovic, 1999). Soft and hard soils can both be simulated in the HS model, where better non-linear formulation of soil behaviour compared to that of the Mohr-Coulomb. In the HS model, different stiffnesses are assigned to the soil for different stress paths based on standard tests. Unlike MC model, there is a distinction between a primary loading and the unloading/reloading in the HS model and also a memory of pre-consolidation stress.

Field trials geometry, soils and material properties, foundation surcharge and mesh refinement and generation of model mesh need to be defined early in the PLAXIS 3D construction stage. When the model is completed and meshes generated then the initial stress condition and construction sequence in the calculation stages need to be built to calculate the associated stresses and relevant strains.

4.4 Hardening Soil model parameters

Soil parameters used in this research are presented in Table 4.3. For the purposes of building a numerical model in PLAXIS 3D, the soil profile is required. The soil profile has been stratified into a crust (stiff clay) underlain by a soft Carse Clay. McCabe and Killeen (2010) have divided the soft Carse Clay at Bothkennar site into upper and lower Carse Clay. However, the division of the soft Clay into two different layers is in contrast with Kamrat-Pietraszewska and Karstunen (2010) and Sexton and McCabe (2012) who suggest that the Carse Clay in Bothkennar site is only one layer. In the researcher opinion, there is very little data to justify the existence of an upper layer of Carse Clay, therefore only one Carse Clay layer has been adopted in the subsequent numerical analysis. It is worth noting, however, that there is a band of thin shelly layer (approximately 300 mm thick) at the base of the crust as reported by Nash et al. (1992a) and Serridge (2001).

This highlights the importance of the ground investigation of accurately capturing the presence of different layers across the site and beneath the foundation and their relevant properties. The material properties of the shelly layer were not investigated in depth by previous studies and lab tests, therefore, the shelly layer was ignored when modelling the soil profile by several researchers who conducted their studies on Bothkennar site (Castro et al., 2014; Killeen, 2012; Serridge, 2013). In this research, the crust layer is modelled as a drained material due to the fact that the crust layer is underlain by a shelly layer.

Table 4.3 Bothkennar field trials soil parameters (McCabe and Killeen, 2010).

Properties	Units	Crust	Carse Clay	Stone Backfill
Depth	m	0-1.2	1.2-14.5	-
Φ’	[°]	34	34	45
c’	[kPa]	3	1	1
Ψ	[°]	0	0	15
γ	[kN/m^3]	18	16.5	19
E_{50}^{ref}	[kPa]	1068	231	70000
E_{oed}^{ref}	[kPa]	1068	231	70000
E_{ur}^{ref}	[kPa]	5382	1164	210000
Over- consolidation ratio	[-]	1	1.5	-
Pre- overburden stress	[kPa]	15	0	-
m	[-]	1	1	0.3

Allman and Atkinson (1992) suggested a high critical state friction angle (Φ’) of 34° due to a high proportion of angular silt particles in the clay. Also, effective cohesion of 1 kPa for the clay is used for numerical stability. However, a slightly higher cohesion (c’) of 3 kPa is used for the weathered crust.

The variation of the yield stress ratio has been reported by Nash et al. (1992b) which is equivalent to the over consolidation ratio (OCR) measured in an oedometer, and in situ lateral earth pressure coefficient (K_o) with depth, suggesting that the erosion of the material may influenced the stress state of the Carse Clay. Additional factors such as the drop in the sea level and the fluctuating groundwater levels may have influenced the Carse Clay stress state. Nash et al. (1992b) reported the variation of Carse Clay initial void ratio (e_o), compression index (C_c), and swelling index (C_s) with depth. E_{50} and E_{oed} are secant stiffness in standard drained triaxial test and tangent stiffness for primary oedometer loading respectively derived from C_c while the unloading/reloading stiffness is derived from C_s.

In choosing the aggregate for the field trials, the aggregate properties were in line with the requirements of BRE specifying stone columns (BRE, 2000). In order to assign an appropriate friction angle for the stone column aggregate, reference was made to McCabe et al. (2009) who suggested the conventionally used value of Φ' = 40°, which may be conservative. The calculation of the angle of dilatancy, Ψ, is determined from an empirical relationship developed by Bolton (1986) where $\Psi \approx \Phi' - 30^0$, Φ' is the maximum effective angle of internal friction (Brinkgreve et al., 2018).

4.4.1 Bothkennar Hardening Soil model verification

A field trial described by Jardine et al. (1995) carried out at the Bothkennar site has been simulated using PLAXIS 3D code by McCabe and Killeen (2010) in order to substantiate the adoption of the geotechnical parameters detailed in Table 4.3. The development and validation of Bothkennar soil profile and the ability of PLAXIS 3D to capture the settlement behaviour of stone columns is described by Killeen (2012). The trials were for a pad footing at 0.75 m depth within the 1.2 m thick

surface 'crust' and without the support of stone columns. According to Jardine et al. (1995), a 2.2 m pad footing (square with 0.8 m thick) had been loaded in increments to failure over a period of 3 days using Kentledge blocks. A rigid interface element is suggested for a stone column to model the stone column-soil interaction on the basis that the surrounding soft soils is tightly interlocked with the stone column (Guetif et al., 2007; McCabe and Killeen, 2016).

The load-settlement curve for Jardine's trial is shown in Figure 4.3, together with PLAXIS 3D prediction and is closely aligned with that of McCabe and Killeen (2010). By investigating both load-settlement curves, it is evident that there is a good agreement affirming the selection of the adopted soil profile and material properties.

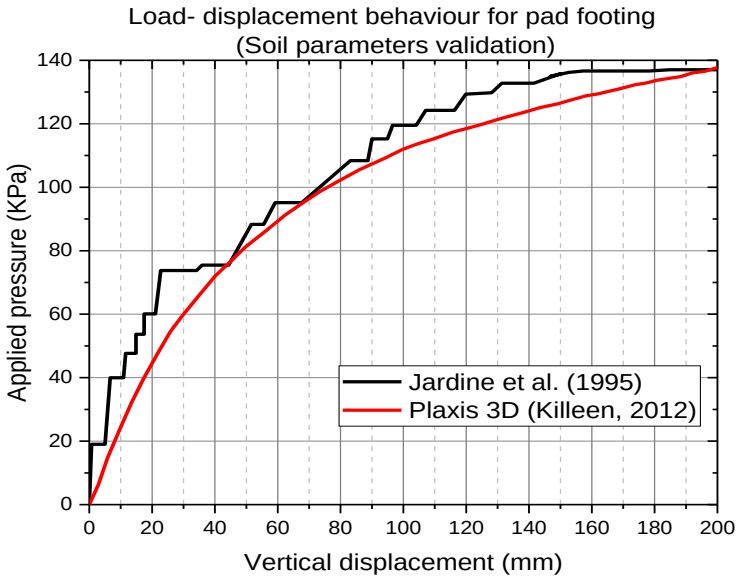


Figure 4.3 Validation of soil profile and parameters.

The numerical model validation for Bothkennar field trials is undertaken in this research using the soil parameters adopted by McCabe and Killeen (2010), where intensive investigation was carried out by the researchers to calibrate the soil model with Jardine et al. (1995) field trial. The measured vertical settlement

values indicated in Table 4.4 were recorded by Serridge (2001) after 5 months of placing each of the first and second load increments for the trial footings. The piezometers installed at different depths during the Bothkennar field trials were continued to measure pore water pressure due the installation of the stone columns in excess of pre-treatment values for up to 4 months (worst case scenario). Therefore, in this research, the predicted long term vertical settlement using PLAXIS 3D is compared with the measured vertical settlement values recorded by Serridge (2001) at the end of 5 months period for each of the load increments as shown in Table 4.4.

Table 4.4 Measured (Serridge, 2013) vs PLAXIS 3D vertical settlement prediction in drained and undrained condition for the field trials at Bothkennar site.

Trial footing no.	1st Load increment (kPa)	Measured (mm)	Drained (mm)	Undrained (mm)	2nd Load increment (kPa)	Measured(mm)	Drained (mm)	Undrained (mm)
1	35.5	27.5	16.5	15.0	72.0	50.0	55.0	56
2	32.9	25.0	18.0	16.0	67.1	42.5	57.0	57
3	33.1	17.5	14.0	13.0	67.8	37.5	37.5	39
4	34.9	20.0	12.0	11.5	71.1	42.5	42.5	41
5	32.1	22.0	9.5	8.0	67.0	40.0	35.0	31
6	34.2	24.0	11.0	11.0	69.6	45.0	40.0	36
7	32.7	20.0	12.0	10.5	67.0	42.5	43.5	39

PLAXIS 3D has been used in this research to predict the long term vertical settlement of Bothkennar field trials using the soil parameters outlined in Table 4.3. The PLAXIS 3D models a long-term behaviour of soft cohesive soil (generation of excess pore water pressure due to applied load) by two methods. The first method is loading in undrained conditions followed by another consolidation stage to allow the dissipation of excess pore pressure developed during loading. The second method is a drained analysis.

It can be seen in Table 4.4 that FEA slightly over-predicts the stiffness response of the field trials, especially at the first load increment. This may be attributed to the shell layer at the base of crust as reported by Jardine et al. (1995) and Serridge (2001).

The shell layer encountered on the site is not modelled in PLAXIS 3D; therefore, at first stage loading, the numerical analysis yields a relatively stiffer footing response. Another contributing factor to the stiffer response of PLAXIS 3D may be that some influence from footing 'bedding-in" effects at first load increment is likely to occur at low strain levels. While the stiffness parameters of the Hardening Soil model in PLAXIS 3D are derived from laboratory tests at high strain levels.

In conclusion, it can be seen that deriving the soil parameters from well characterised Bothkennar site and validating the adopted soil profile with Jardine et al. (1995) and Serridge (2001) is encouraging and provides confidence in PLAXIS 3D predicted performance used in the subsequent analysis.

4.5 Reinforcement material parameters

The lateral deformation at shallow depths is always accompanied by the vertical settlement of the stone columns under applied loads. If the stone column is encased with a geosynthetic material such as geotextile or geogrid, then a circumferential stress will be developed in the reinforcement due to the stretching of the material because of the lateral expansion of the stone column. Therefore, the reinforcement will provide a confinement stress to the column due to the developing of the circumferential stresses in the material.

There is a wide variety of the geosynthetic materials available to use in the ground improvement applications such as geotextiles, geomembrane, and geogrids. It is

well known that geogrid reinforcement is a stiffer material compared to a geotextile reinforcement. In the subsequent analysis, two types of geosynthetic materials were used to reinforce the stone columns. The first geogrid is called Secugrid 20/20 Q1 and the second type is a geogrid/geotextile composite which is called Combigrid 40/40 (both produced by Naue GmbH). A summary of the geosynthetic material properties is outlined in Table 4.5.

Table 4.5 Properties of the geogrid materials.

Property	Unit	Secugrid 20/20 Q1	Combigrid 40/40 Q1
Mass per unit area	g/m^2	155	240
Max. tensile strength	kN/m	20	40
Axial stiffness at 2% elongation, J	kN/m	400	800

The geogrid in PLAXIS 3D is a flexible element modelled as a linear elastic element which can only sustain tensile forces with no compression allowed. Geogrid is modelled as a slender element with an axial stiffness but without any bending stiffness (Brinkgreve et al., 2018). The axial stiffness modulus (J) of the geogrid is calculated at a strain of 2%.

4.6 Preliminary checks to assess the influence of distance to boundary

The pad footings considered in the subsequent FEA are embedded into the soil. The boundary of the soil undergoes no lateral movement as a condition. Therefore, it is of paramount importance to position the boundary at a sufficient distance from the pad footing to avoid influencing the results. A sensitivity analysis was conducted on a typical 3 m by 0.75 m pad footing to investigate the influence of the model boundary upon the accuracy of the analysis.

Three points were selected to measure the vertical displacement and the mean effective stress at 0, 1 m and 2 m below the centre of the pad footing, as shown in Figure 4.4. It is prudent to investigate the vertical settlement and associated stresses in the zone of interest as one of the primary objectives of this thesis is to investigate the settlement performance of the trial pad footings installed at the Bothkennar site. The soil profile of well characterised Bothkennar site is adopted in the sensitivity analysis. The sensitivity analyses were carried out in both drained and undrained conditions. In general, the predicted vertical settlements in drained conditions for Bothkennar field trials (see Table 4.4) were more onerous than undrained analysis with the exception of Footing 1 and Footing 3 at second load increment. The difference between the predicted vertical settlement in drained and undrained analysis at second load increment was marginal (about 1.8% to 3.8% for Footing 1 and Footing 3 respectively). However, in this sensitivity analyses, the stresses and displacements predicted in the drained analyses are more onerous than undrained analyses and therefore the results shown in Table 4.6 were calculated from the drained analyses.

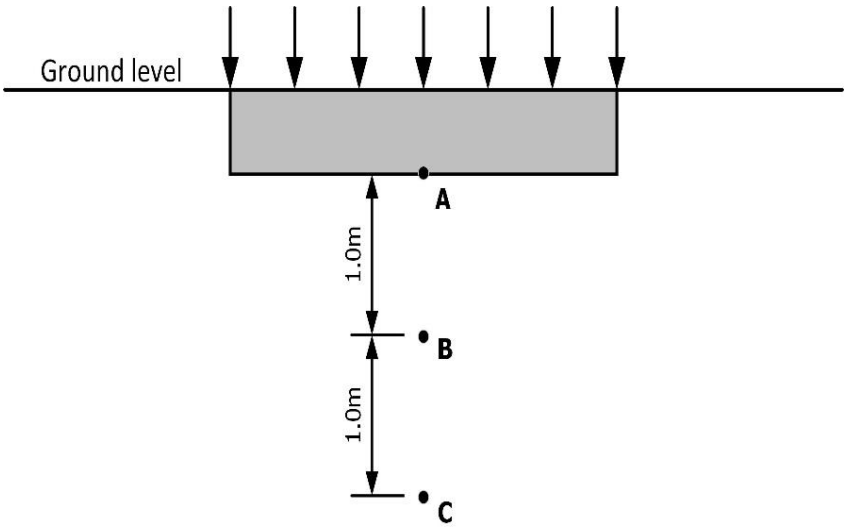


Figure 4.4 Measurement locations beneath footing

In the subsequent sensitivity analysis, the distance from the centre of the footing to the boundary ranged from 4 to 10 times the footing width (W). The effect of the boundary position from the centre of the footing is evaluated by comparing the normalised vertical displacements and mean effective stresses at Point A, B, and C:

$$\textit{Normalised vertical displacement, } u_z = \left(\frac{u_{z,1} - u_{z,2}}{u_{z,1}}\right) \times 100 \qquad (4.1)$$

$$\textit{Normalised mean effective stress, } P' = \left(\frac{P_{z,1} - P_{z,2}}{P_{z,1}}\right) \times 100 \qquad (4.2)$$

where $u_{z,1} - u_{z,2}$ is the difference between the vertical displacements where the boundary placed at different positions, for example at boundary 4W and 6W.

The appropriate positioning of the boundary is checked by the convergence of the settlement and the stress with the increasing boundary distance from the centre of the footing. The settlement performance of various footing arrangements and relevant sensitivity analysis in the subsequent FEA are examined at an average applied load of 33 kPa and 70 kPa. However, the influence of the boundary position was examined at 35 kPa to save the time of the analysis.

The stress and displacement at points A, B, and C for a range of boundary distances are shown in Table 4.6. It is clear that locating the boundary at a distance closer than 8 W (footing width (W) = 3 m) from the centre of the pad footing induces more vertical deflection in the footing. Furthermore, the lower boundary increased from 15 m to 20 m below the ground surface to investigate the influence of the boundary on the vertical settlement and mean effective stresses at points A, B, and C as shown on Table 4.6.

It can be seen that lowering the bottom boundary of the model has a minimal effect on the settlement and mean effective stresses. Therefore, positioning the boundary conservatively at a distance of 10 W from the centre of the footing is chosen for all subsequent analyses.

Table 4.6 Influence of the side boundary distance upon footing settlement.

Boundary distance (m)	Vertical displacement Uz (mm)			Normalised error %			Mean effective stress P' (kPa)			Normalised error %			No of elements
	A	B	C	A	B	C	A	B	C	A	B	C	
4 W	30	21.7	12.3	5.3	4.1	7.8	12.8	12.9	17.68	14.1	0.6	2.1	60376
6 W	28.4	20.8	11.25	3.2	1.0	3.1	11	12.82	17.3	1.8	0.2	1.7	34344
8 W	27.5	20.6	11.6	2.5	2.9	4.3	11.2	12.8	17.6	2.7	1.6	0.2	35513
10 W	28.2	21.2	12.1				11.5	13	17.64				35670

The coarseness of the mesh is selected as medium size, however, a very fine mesh is assigned to an area of interest such as large stress concentration zones beneath the footing.

Table 4.7 Influence of the lower boundary distance upon footing settlement.

Boundary distance (m)	Vertical displacement Uz (mm)			Normalised error %			Mean effective stress P' (kPa)			Normalised error %			No of elements
	A	B	C	A	B	C	A	B	C	A	B	C	
4 W	31	22	12.3	3.2	0.5	1.6	12.3	13	17.5	0.0	0.8	0.6	62074
6 W	30	21.9	12.1	2.3	0.9	2.5	12.3	12.9	17.6	4.1	0.0	0.6	39547
8 W	29.3	21.7	11.8	2.2	1.4	2.5	11.8	12.9	17.7	1.7	0.0	0.6	37651
10 W	28.67	21.4	12.1				11.6	12.9	17.8				40653

4.7 FEA and modelling issues

Within the constraints of the current research the stone columns have been 'wished-in-place', however K_o has been modified to reflects changes induced by the installation of the columns (see Section 2.8.3.1). The in situ coefficient of earth pressure at rest (K_o) at Bothkennar site was measured by Nash et al. (1992b) which records a variation from 1.5 in the crust layer to 0.75 at depth due post-

depositional process such as ageing. Killeen (2012) have used a three-dimensional FEA assuming a full confidence in the soil parameters and adopting K_o values recorded by Nash et al. (1992b) to match the measured settlement behaviour by Jardine et al. (1995) as detailed in Section 4.4.1. Therefore, to remain consistent with the approach of Killeen (2012), similar K_o values to the ones recorded by Nash et al. (1992b) have been used in the current research.

Owing the stone column installation process described in Section 2.6.1, the stone column material is tightly interlocked with surrounding soil, therefore it was assumed that a perfect bond (Rigid interface) occurs along the interface between the stone column aggregate and the surrounding soils. It is expected that using a lower interface reduction factor will yield a higher stone column settlement due to larger movement at the interface between soils and he column. It is deemed appropriate to model the column-soil interface in the subsequent analyses as tightly locked, in keeping with prior work of several other authors (Guetif et al., 2007; McCabe and Killeen, 2016).

4.8 Summary of the numerical analysis development and validation

A soil profile and set of soil parameters were developed for the Bothkennar site. The soil profile at Bothkennar is representative of many locations where the stone column technique is preferable over other geotechnical solutions. There is a growing interest in such soil profiles due to the presence of a crust layer at a shallow depth overlying soft clay.

Field load tests carried out by Jardine et al. (1995) and Serridge (2001) on single vibro stone columns founded in layered soils were simulated using PLAXIS 3D. The predicted settlement was compared against field measurements, it was clear from the comparison that PLAXIS 3D predicts the footing very well, which reflects the

ability of 3D analysis to model the footings and columns at discrete locations affirming the selection of the adopted soil profile and material parameters. However, the FEA slightly over-predicts the stiffness response of the field trials, especially at the first load increment. This may be attributed to the shell layer at the base of crust as reported by various researchers (Jardine et al. (1995) and Serridge (2001)).

A sensitivity analysis was carried out to investigate the influence of the side and lower boundaries' distances upon footing settlement. It was found that locating the side boundary at a distance between 8 W to 10 W (footing width (W) = 3 m) from the centre of the pad footing is sufficient to stop inducing more vertical deflection in the footing. It was also found that lowering the bottom boundary of the model has a minimal effect on the settlement and mean effective stresses.

4.9 Influence of column spacing (trial Footing 1 and 2) L/d= 7.5

The influence of stone column spacing upon the performance of the pad footings is examined at the locations of the trial footings 1 and 2 (column spacing of 1.5 m and 2.0 m, respectively - See

Table 4.1 for footing details). The response of the stone column to the two main load increments are discussed below.

4.9.1 Vertical settlement

Numerical analysis was carried out to predict the vertical settlement of the stone column. The predicted vertical settlement was compared against the settlement database of the Bothkennar field trial collated by Serridge (2001) as shown in Table 4.4, for the first and second load increments. The more widely spaced stone column (Footing 2) attracted more load than the more closely spaced column

(Footing 1) as shown in Figure 4.9 and as suggested by Serridge (2013). It can be seen from Table 4.4 that the predicted vertical settlement of Footing 1 is less than the settlement of Footing 2. However, the measured settlement during the field trials suggests a reverse trend to the predicted settlement carried out using the FEA.

One would expect that Footing 1 will provide a stiffer behaviour within the treated depth, associated with the closer columns (similar to the predicted settlement). The author is in agreement with the opinion of Serridge (2001) which suggests that the lesser measured settlement of Footing 1 compared to Footing 2 may be attributed to the following reasons:

(i) The disturbance of soft soils between the columns and the remoulding of sensitive Bothkennar soft clay due to the vibration associated with stone column installation are generally higher for closer columns. Therefore, this may attribute to the larger settlement measured during the field trials.

(ii) The 'reinforcing' effect of the higher frequency of stone columns in Footing 1 compared to Footing 2. Therefore, a higher stiffness per unit area of foundation might be considered as another factor.

The vertical settlement of Footing 2 predicted by the FEA is marginally higher than the recorded field measurements. The predicted vertical settlement of Footing 1 is less than the predicted settlement of Footing 2, which is in accordance with the expectations due to the effect of the closer column spacing on the column-clay composite stiffness within the treated depth.

The predicted load-settlement curves for Footing 1 and Footing 2 are shown in Figure 4.5 at both drained and undrained conditions. It is closer to reality to perform undrained analysis because the cohesive soil is in the undrained condition during load application followed by the consolidation stage to simulate the long-term behaviour. However, it is more time consuming than the drained analysis.

Therefore, engineers and researchers tend to use the drained method to simulate the long-term settlement performance of stone columns. It is important to highlight that the short-term behaviour under an initial undrained response is not separated from primary consolidation with the drained method therefore the short-term behaviour is less well understood than the long-term behaviour.

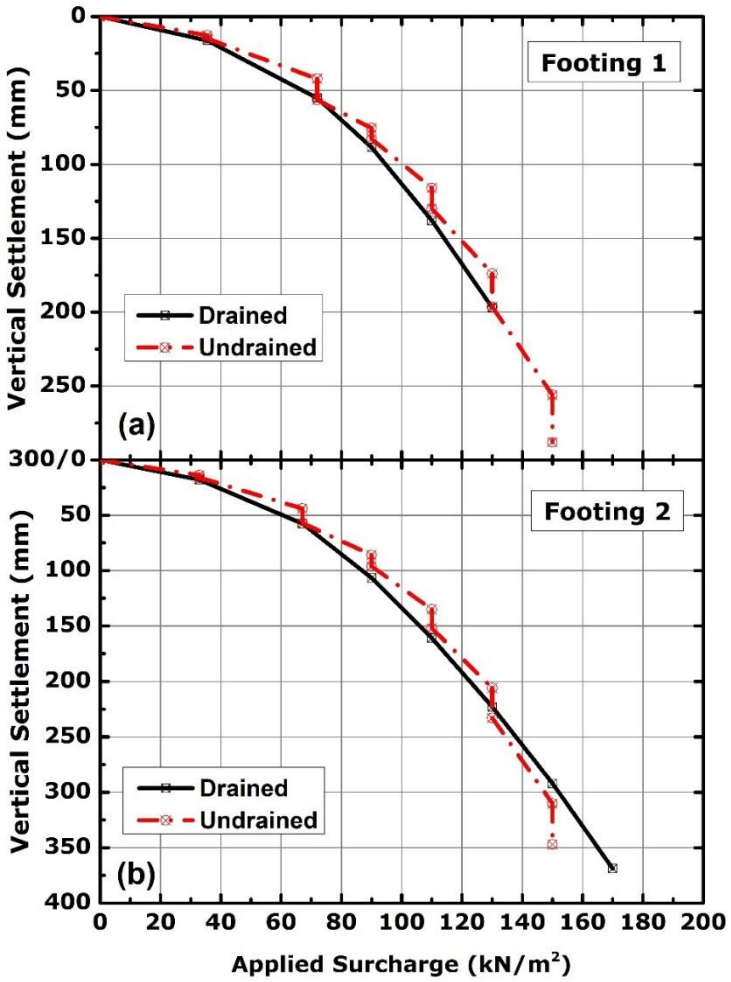


Figure 4.5 Load-displacement behaviour (a) Footing 1 and (b) Footing2.

The predicted short-term settlement for Footing 1 and Footing 2 is less than the long term settlement by 10% to 25% of the long-term settlement magnitude at applied pressure higher than 70 kPa (Figure 4.5). It appears that both drained and undrained methods predict a similar long-term settlement for Footing 1. Initially, both analyses predict similar settlement at lower loads. While the drained analysis

for Footing 2 predicts slightly higher settlement up to an applied pressure of 110 kPa.

Beyond this point the undrained analysis shows that the stone column starts yielding and the plastic deformation is more pronounced with higher applied pressures (>130 kPa). The rate of settlement increases thereafter at an approximately constant load. Applying a typical factor of safety in the range of 2.5 to 3 yields an allowable pressure in the range of 43 kPa to 52 kPa. Therefore, a working applied pressure of 50 kPa is considered satisfactory for the Bothkennar field trials to avoid excessive settlement.

It is very important to highlight that even if 50 kPa is considered satisfactory as a working applied pressure, the relevant settlement at 50 kPa is around 35 mm which exceeds typical tolerances of a narrow strip footing (25mm) supporting lightly loaded brick masonry structures (Meurant, 2013). An applied pressure of 40 kPa with associated settlement of around 25mm is considered acceptable for Bothkennar soils.

The influence of column spacing upon the footing and the ground surface vertical settlement is shown in Figure 4.6. As expected, the vertical settlement at ground level is decreased with distance from the centreline of the column for the main two load increments. The more widely spaced stone column (Footing 2) settled relatively more than the more closely spaced columns (Footing 1).

It can be seen in Figure 4.6 that during the application of the first load increment 35.5 kPa (Footing 1) and 32.9 kPa (Footing 2), the settlement decreases gradually in the surrounding soft soils with the distance increasing from the footing. The footing and the surrounding ground surface settlement is increased significantly during the application of the second load increment.

It appears that the applied load and the column spacing both play an important role in the magnitude of the settlement. Therefore, it is deemed reasonable to limit the applied load to 40 kPa for the field trials at Bothkennar site.

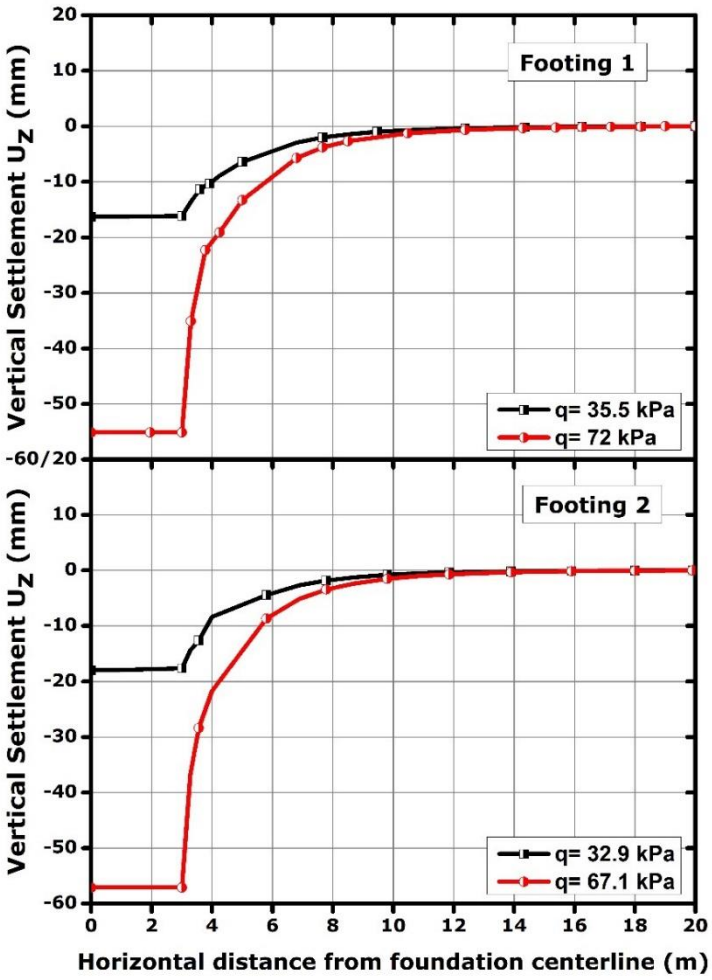


Figure 4.6 Influence of column spacing on the footing and ground vertical displacement in drained conditions- Footing 1 and Footing 2.

4.9.2 Lateral bulging

The bulging of the stone column is well understood for a single column and large group of stone columns. However, the bulging of small groups of stone columns is more complicated and not established yet. This may be attributed to the following reasons (Muir Wood et al., 2000):

- The loss of confinement at the peripheral stone columns.
- Vertical stress reduction with depth.

Many comparative studies were carried out by various researchers (Black, 2006; Kirsch, 2006; McCabe and Killeen, 2016; Satibi et al., 2009)) which highlighted the difference between the bearing capacity of small and large groups of stone columns, therefore no comparative study is included within the scope of this research. The variation of lateral column deflection (bulging) with depth at different applied loads for Footing 1 and Footing 2 are shown in Figure 4.8. The bulging of the stone columns for Footing 1 and Footing 2 is plotted for the column positioned at the footing edge where lateral confinement is relatively less than the middle columns (less confinement in the x-direction). The plotted bulging is toward the exterior and not between the piles to be consistent with the lateral bulging analyses of the subsequent foundations (worst case scenario). It appears that the maximum lateral bulging occurs at a depth equal to 2 times the column diameter which is in line with the values reported by Hughes and Withers (1974). This is clearly realistic due to the influence of crust layer over soft clay. Bulging of stone column took place in the soft clay underlying the crust layer.

Essentially the stone column in the ground behaves similarly to a column in a confined triaxial cell as shown in Figure 4.7. Substituting the angle of internal friction of the stone material into the equation of the plane of peak stress ratio gives the depth of maximum stress (maximum bulging). The depth of the maximum stress is about 2 times the diameter of the column below the base of the foundation using an angle of internal friction of the stone material =40˚ and column diameter of 0.75m. The depth of the maximum bulging calculated from a triaxial test analogy compares very well with the depth of maximum bulging predicted by the numerical analysis (Figure 4.8). This confirms the fact that the stress will transfer to the soil through the column shaft, which in turn leads to the

reduction in the stone column vertical stress. Thus, it is unlikely that the column would bulge near the top (Hughes and Withers, 1974).

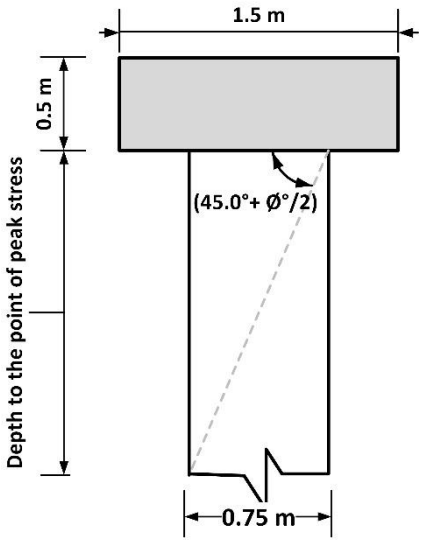


Figure 4.7 Triaxial test analogy

It can be seen in Figure 4.8 that lateral bulging for the more widely spaced stone column (Footing 2) is generally larger than that for the closely spaced columns (Footing 1). A very small lateral deformation in the x-direction (parallel to the foundation) occurs at the lower part of the column. The lateral deformation in the lower part of the column slightly increases with increasing column spacing. This can potentially be explained by the fact that the stress is transferred toward the column base (toe) in the x-direction due to the greater confinement provided by surrounding soil and the middle stone columns.

The numerical analyses suggested that larger stress transferred to the base of the columns under Footing 2 compared to the column beneath Footing 1 as shown in Figure 4.9. The calculated stresses using PLAXIS were approximately 55% of the applied stresses for Footing 1 and ranged between 87% to 99% of the applied stress for Footing 2 for applied loads between 35 kPa and 130 kPa (where applied

stresses are generated from the footing load (q) plus any additional stresses from footing and aggregate weights above the column toe level). The larger stress transferred to the base of column is attributed to the increase of the total share of load taken by the columns beneath Footing 2 due to the wider column spacing compared to the column spacing of Footing 1.

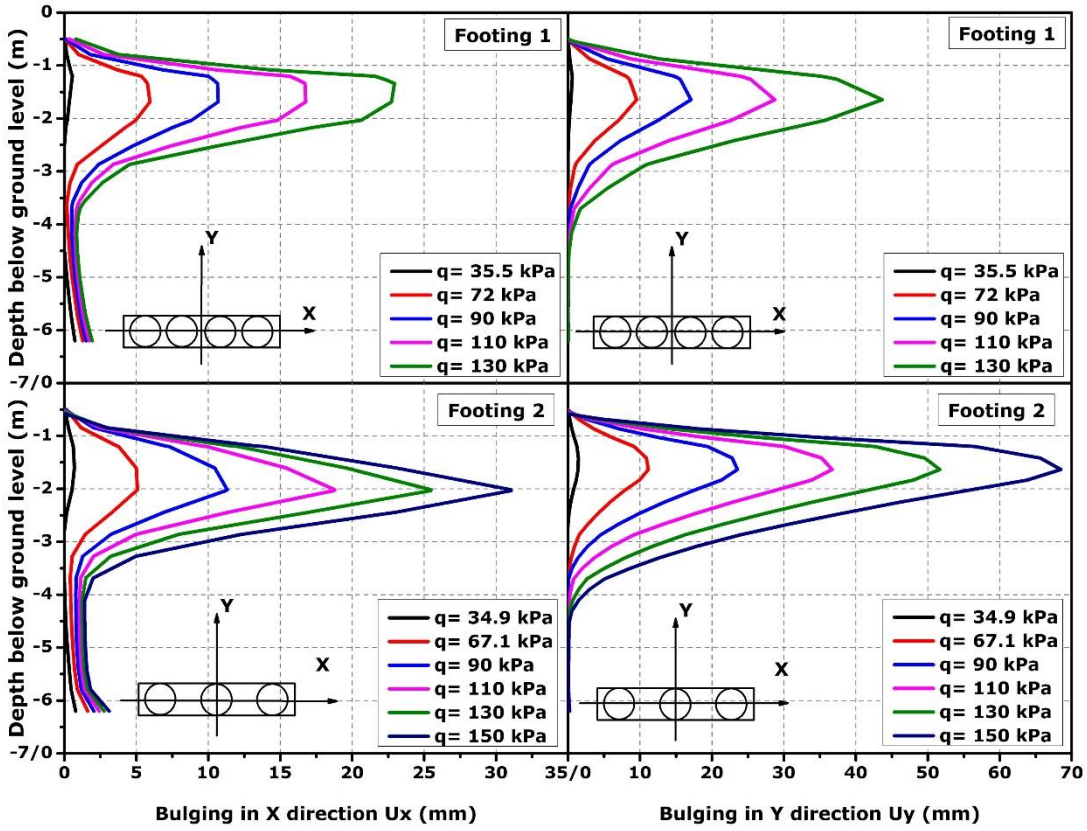


Figure 4.8 Influence of applied load on lateral bulging of the stone column for Footing 1 and 2- drained conditions.

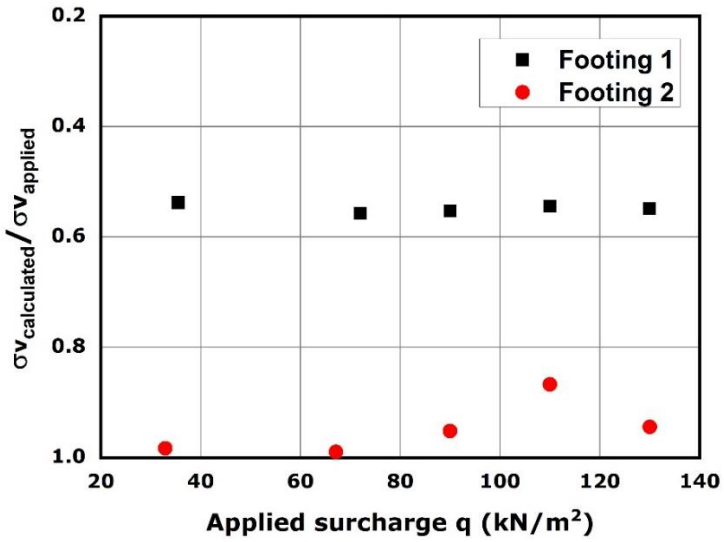


Figure 4.9 Vertical stress ratio at column base level for Footing 1 and Footing 2- Drained conditions.

4.9.3 Influence of geogrid encasement

In order to investigate the influence of the encasement, the following column arrangements are analysed:

1. Ordinary stone column (OSC) without reinforcement installed around the column.
2. Encased stone column (ESC) with a geosynthetic material installed around the column. Combigrid 40/40 Q1 geogrid (see Table 4.5) used in the subsequent analyses to investigate the influence of the column reinforcement on the column behaviour.

The long-term load-settlement behaviour of Footing 1 and Footing 2 is shown in Figure 4.10. The influence of reinforcement is quantified by measuring the reduction in the column settlement. The column capacity in drained and undrained conditions is similar for Footing 1. However, it appears that both drained and undrained methods predict similar behaviour for OSC and ESC (Footing 2) where

undrained method predicts plastic failure (PLAXIS 3D run stopped with plastic failure indicated in the program log) beyond 150 kPa and 200 kPa for OSC and ESC, respectively.

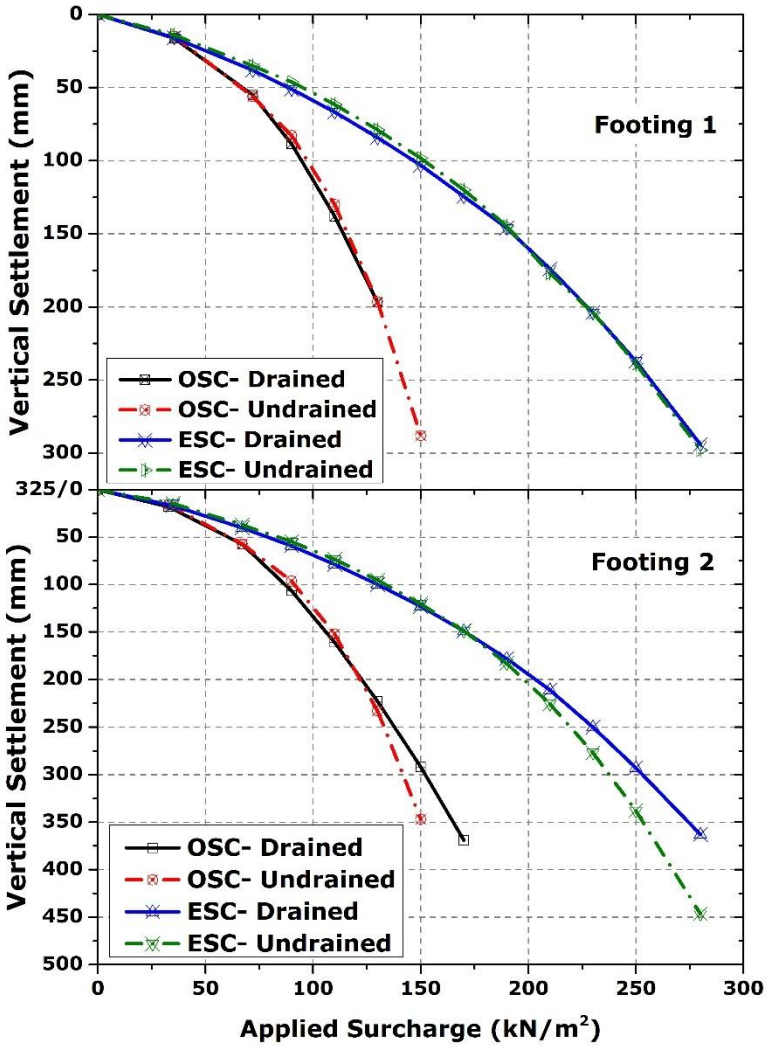


Figure 4.10 Load-displacement behaviour for OSC and ESC-Footing 1 and Footing 2.

It is appropriate to consider a safe working load of between 50 kPa to 60 kPa with encased stone columns to satisfy the typical tolerances of a narrow strip footing supporting lightly loaded brick masonry structures. However, a significant improvement in the settlement performance at a higher applied load is achieved by using an encased stone column.

Hoop stresses will be generated in the encasement as a result of the lateral expansion of stone column materials which leads to an overall increase in the column-soil system stiffness. A study of the hoop stresses magnitude is presented in the subsequent parametric studies of the reinforced stone columns. The vertical settlement is slightly reduced using ESC at applied load up to 70 kPa; however, the rate of reduction in the settlement of OSC is increased significantly at higher loads (larger than 70 kPa).

4.10 Influence of stone column length (trial Footings 3, 4, and 5):

Trial Footings 3 (L/d= 5), 4 (L/d= 7.5), and 5 (L/d= 10) correspond to the shortest, intermediate and longest column lengths, respectively. The influence of key design parameters such as the vertical settlement, lateral bulging, the influence of encasement and the encasement depths is investigated during the main two loading applications. This sensitivity analysis is carried out to determine the stone column efficiency in enhancing the footing settlement performance.

4.10.1 Vertical settlement

The increase in the vertical settlement of stone columns with applied loads is shown in Figure 4.11. During the application of the first load increment the predicted settlement is slightly less than the measured values in line with Section 4.4.1 which suggests that HS model is over-predicts the stiffness response at low loads. However, during the application of the second load increment, the predicted footing settlement agrees quite well with the settlement measured during the trials.

It is clear that the main difference between the drained and undrained analysis is that the undrained analysis initiates a larger vertical settlement beyond a yield

point. It can also be seen that the rate of settlement increases between the short-term and the long-term with the increase in applied load. It is important to highlight that both drained and undrained analyses reach failure (limit state) at a load over 180 kPa for Footings 3 to 5.

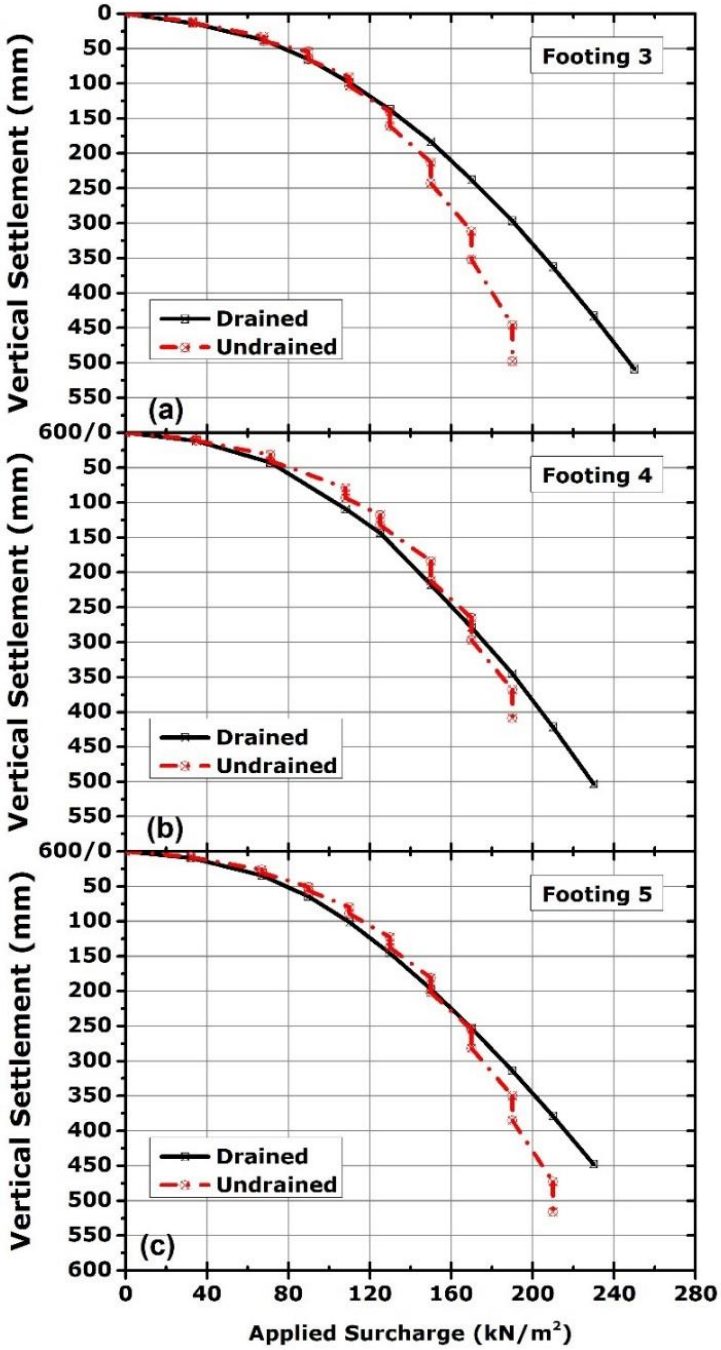


Figure 4.11 Load-displacement behaviour (a) Footing 3, (b) Footing 4 and Footing 5.

The predicted settlement in the undrained analysis is higher than the predicted settlement in the drained analysis at applied load of ≈ 130 kPa (Footing 3), and ≈ 170 kPa (Footing 4 and Footing 5), respectively. This may be attributed to the lateral bulging occurring at shallow depth (see Figure 4.12), where the undrained analyses predicted significantly higher lateral bulging than the drained analyses.

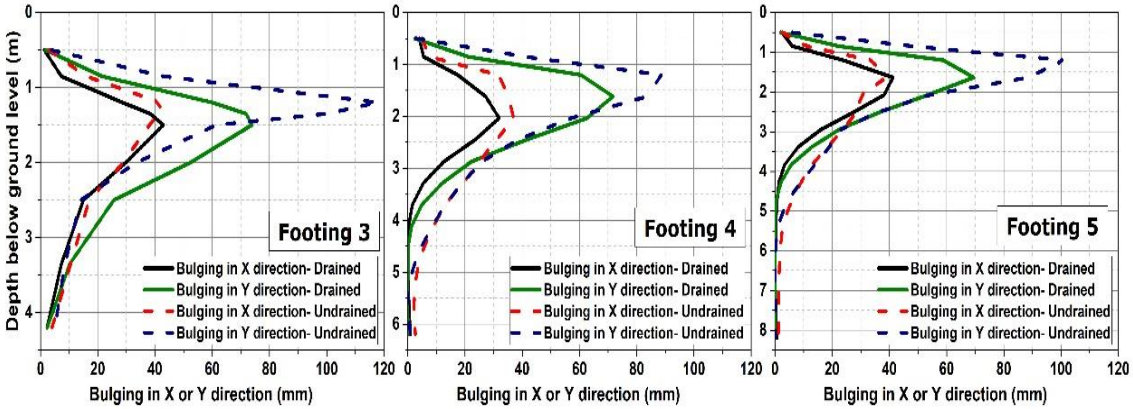


Figure 4.12 Column bulging of Footings 3, 4 and 5 at applied load= 190kPa.

The settlement of Footing 4 is marginally higher than the settlement of Footing 3 and Footing 5 under the second load increment which is in line with the field measurements. This may be attributed to the fact that Footing 4 bulged slightly more than Footings 3 and 5 and the applied load on top of Footing 4 is slightly more than on the other footings.

A critical column length of 5.5 m was calculated by Serridge (2013) based on Hughes and Withers (1974) for the Bothkennar field trials (see Section 4.2). The length of the column beyond the critical length was considered by Hughes and Withers (1974) not to contribute to enhancing the ultimate capacity of the column, but will contribute in reducing the column settlement. Footing 4 installed to the critical length and Footing 5 was installed to a length of 7.7 m, therefore, Footing

5 predicted settlement was relatively lower than Footing 4 which is in close agreement with the field observations of Hughes et al. (1976).

Also, if the remoulding of soft clay has taken place then this would influence the load transfer to the base of the column for longer columns. Another possible explanation is, with increasing the stone column length, the impact of the crust on footing settlement is clearly less as suggested by Serridge (2001).

The ground settlement profile from the centreline of the foundation is shown in Figure 4.13, Figure 4.14, and Figure 4.15 for Footings 3, 4, and 5, respectively. Footing 5 over the longer stone columns settled the least (around 9.5 mm under the first load increment), with Footing 4 settling marginally less than Footing 3 at the first load increment (around 14 mm compared with 16 mm for Footing 3).

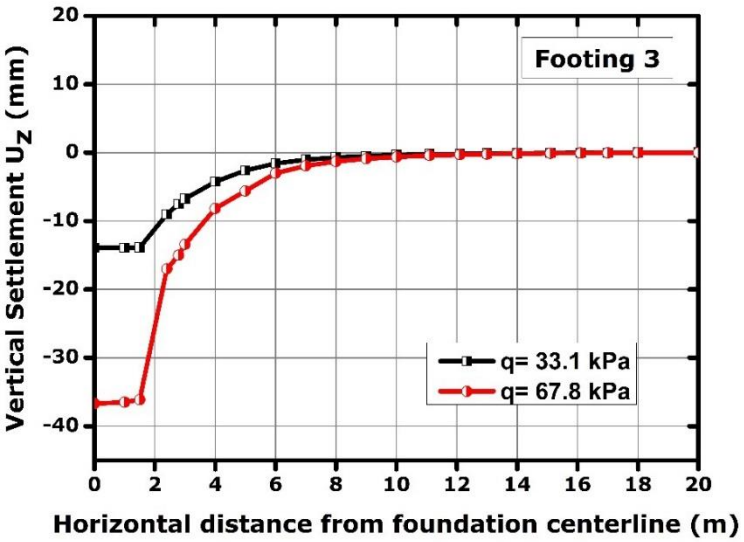


Figure 4.13 Influence of column length on the footing and ground vertical displacement in drained conditions- Footing 3.

A design treatment depth (calculated column length to resist applied load using Hughes and Withers (1974) method) for Bothkennar site of 5.5 m was calculated by Serridge (2013). Therefore, an investigation of the key design parameters in subsequent sections is performed on Footing 4 to evaluate their impact on the stone column behaviour.

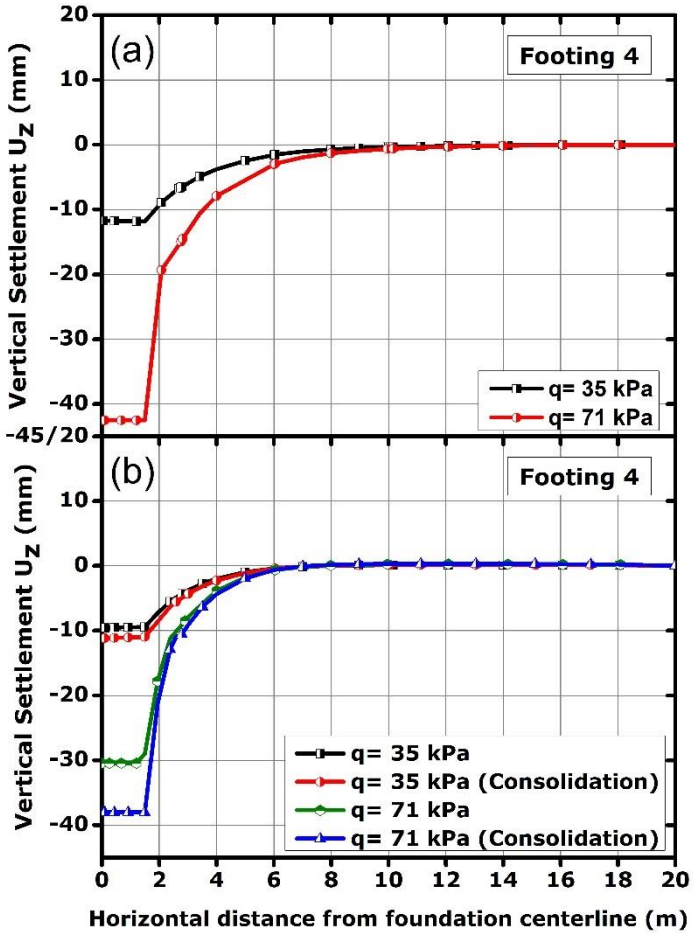


Figure 4.14 Influence of column length on the footing and ground vertical displacement in (a) drained and (b) undrained conditions- Footing 4.

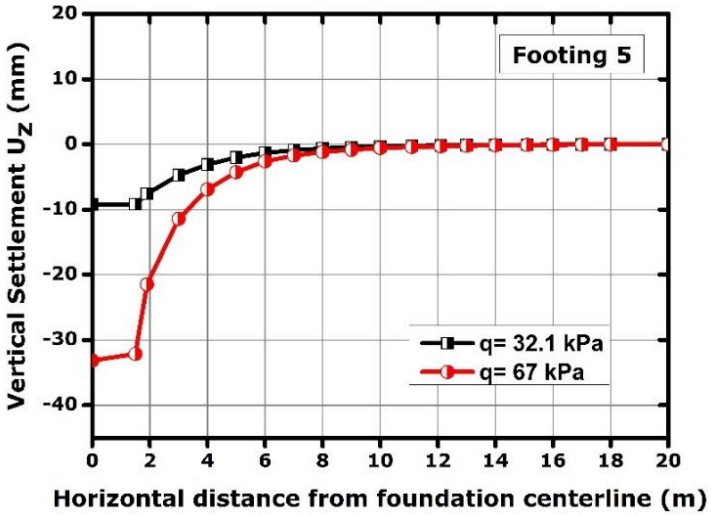


Figure 4.15 Influence of column length on the footing and ground vertical displacement in drained conditions - Footing 5.

The ground surface settlement profile with applied load for undrained analysis is shown in Figure 4.14. It is clearly shown that no ground settlement occurs at a distance of 2W (where W is the footing width) from the centreline of the footing, compared with around 2.6 W for drained analysis.

The vertical settlement at ground surface is marginally less in undrained analysis compared with drained analysis which may be attributed to the improvement of the soft soil strength during the consolidation process in undrained analysis. It is also worth noting that a small amount of heave (around 1 mm) is generated at a distance of around 2 times the footing dimension in undrained conditions.

4.10.2 Lateral Bulging

The influence of the ordinary stone column (OSC) length upon the lateral deformation of the stone column shaft beneath a 3 m by 0.75 m footing (footings 3, 4, and 5) is presented in Figure 4.16, Figure 4.17, and Figure 4.18.

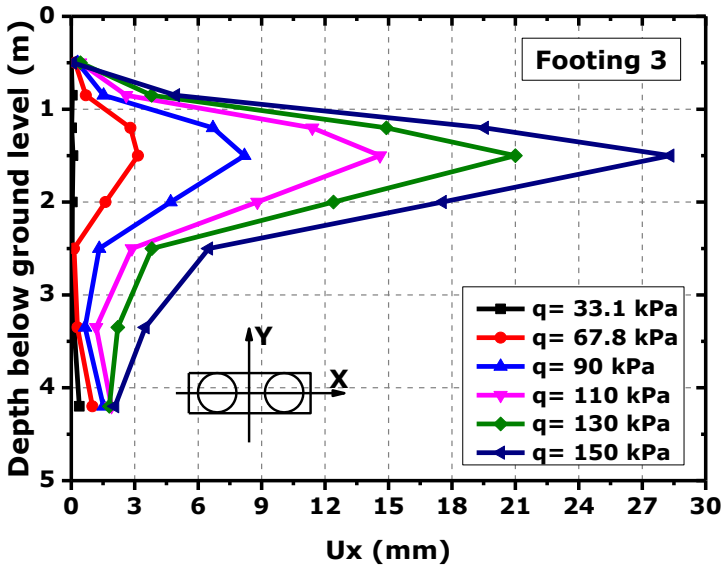


Figure 4.16 Lateral bulging (Ux) with depth observed in drained conditions- Footing 3.

The lateral displacement along the stone column shaft is calculated at various footing loads of up to 150 kPa. It can be seen that the column bulging occurs at

shallow depths where the lateral resistance is minimal. The lateral deflection is gradually increased with depth from the base level of the footing until reaching a maximum value at a depth of around two times the column diameter below the ground level.

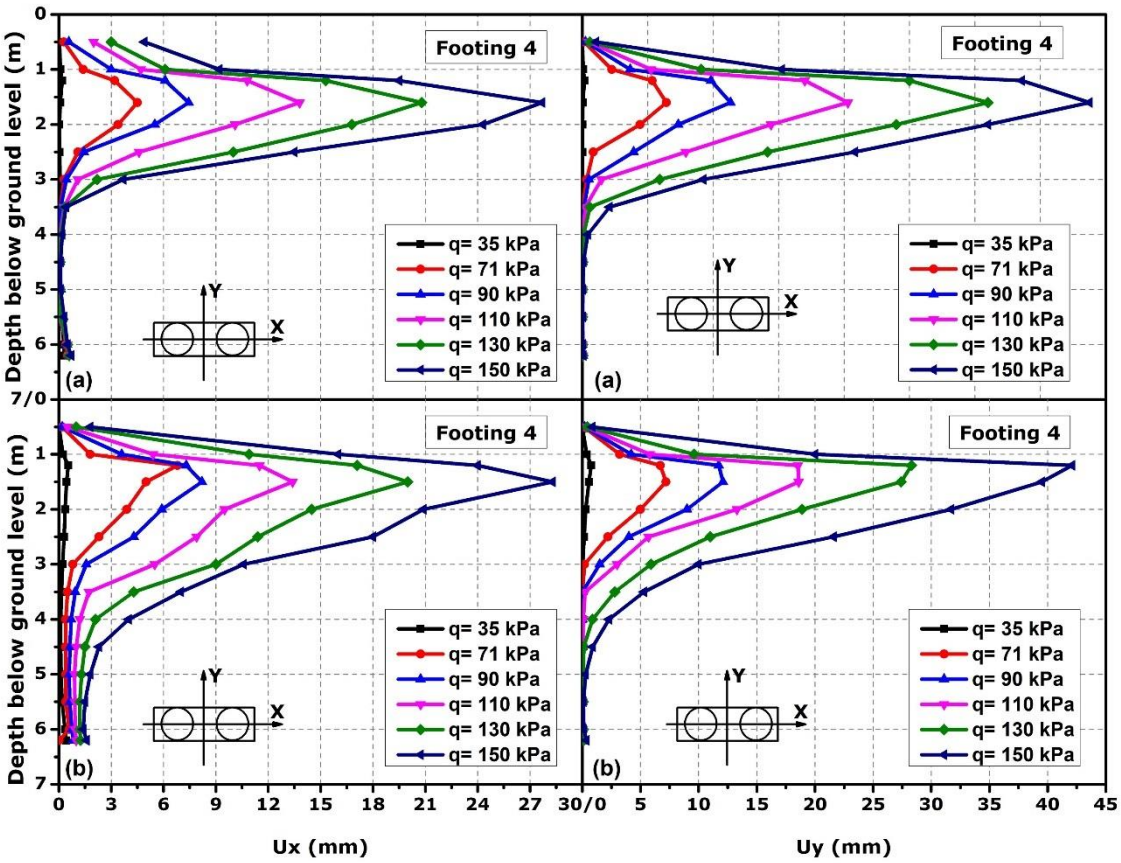


Figure 4.17 Lateral bulging with depth observed in (a) drained and (b) undrained conditions- Footing 4.

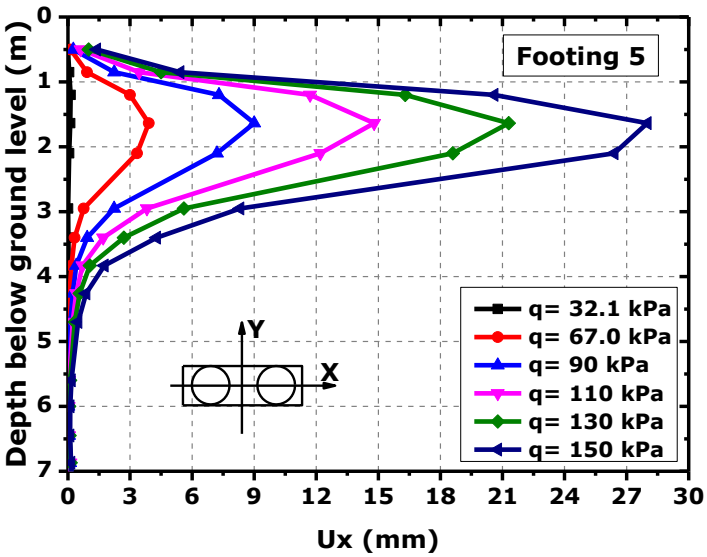


Figure 4.18 Lateral bulging (Ux) with depth observed in drained conditions- Footing 5.

The lateral deformation decreases thereafter with depth to reach zero at the column toe with the exception of Footing 3, where a very small lateral movement is still occurring at the toe level (less than 1 mm at working load of 40 kPa to 50 kPa). A possible explanation of the presence of lateral deformation at the toe of column (shorter column) is that there is a significant stress transfer to the toe of the column as shown in Figure 4.19. The effective vertical stress shown in Figure 4.19 is plotted for the two sides of the same column supporting Footing 3. The lateral deformation increases with the increase of the applied footing loads. McCabe and Killeen (2016) suggested that the dominant mode of failure for the short column is by punching through the soft soil due to high stresses transferred to the column base.

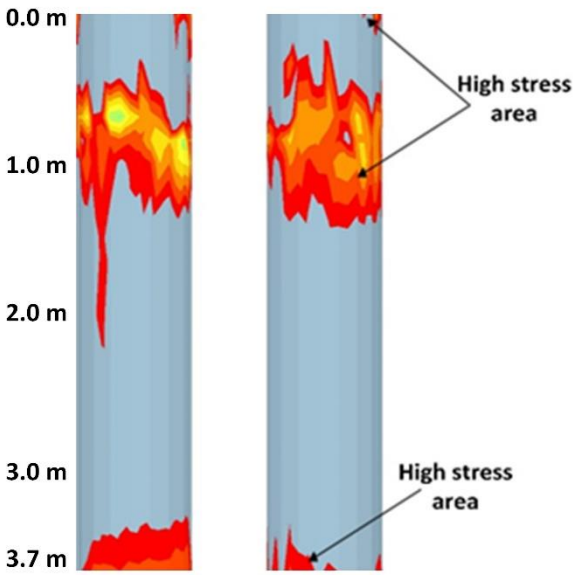


Figure 4.19 Effective vertical stress transfer to the column base in drained condition- Footing 3.

The influence of using drained and undrained analysis upon predicting the lateral deflection in both directions is compared in Figure 4.17. The analysis is again carried out on Footing 4 as explained earlier.

It can be seen that the lateral bulging in the direction of the stone columns (x-direction) is smaller compared with the lateral deformation in y-direction in both drained and undrained conditions. This is due to the lateral confinement provided by the adjacent column in x-direction. The lateral deflection of the stone column in undrained condition is slightly higher than the lateral deflection in drained condition in both x and y-directions at applied load of up to 90 kPa.

4.10.3 Influence of geogrid encasement

The effectiveness of the geogrid encasement upon the behaviour of the stone columns is shown in Figure 4.20. The influence is investigated using ordinary stone

column (OSC) without reinforcement and with encased stone columns (ESC) in drained and undrained conditions.

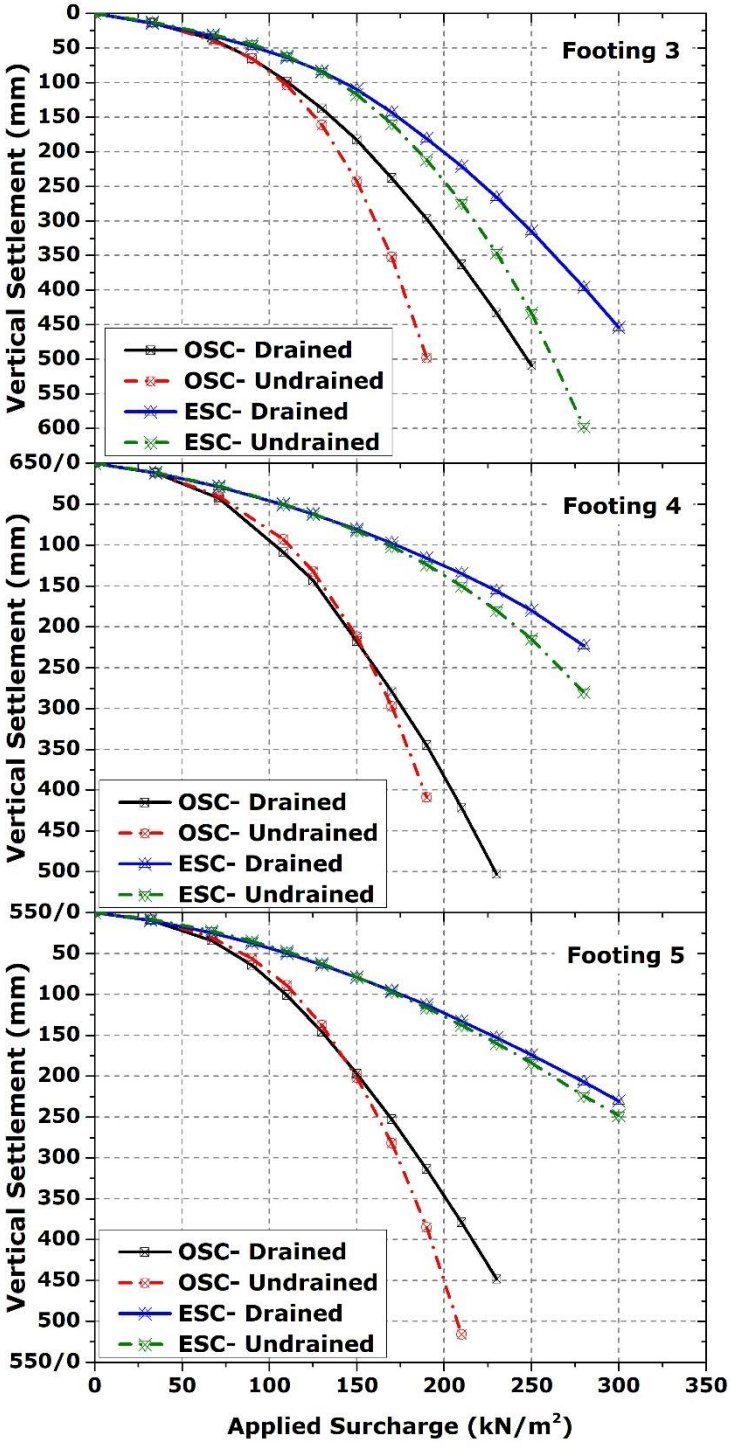


Figure 4.20 Load-displacement behaviour for OSC and ESC-Footing 3, 4 and 5.

The analysis is performed by applying a load on the trial Footings 3, 4, and 5 to assess the impact of column length upon the vertical settlement of the footing. All

the analyses were carried out by increasing the footing applied load until failure at the end of the analysis. The geogrid used in this investigation is the Combigrid 40/40 Q1 with a stiffness of 800 kN/m as outlined in Table 4.5.

It can be seen that the bearing capacity of the column increases with the use of geogrid as expected. The reduction in settlement becomes more significant after an applied pressure of 60 kPa. The increase in the initial elastic modulus is significant due to the additional confinement provided by the encasement. It appears that the settlement of ESC in drained and undrained conditions does not experience failure. While the OSC approached failure condition over a range of applied pressure approximately equal to 180 kPa to 230 kPa.

4.10.4 Influence of encasement depth

The improved performance of the trial footings is evaluated based on the vertical settlement, lateral bulging, footing and ground surface settlement, hoop stresses mobilised in a fully and partially encased stone column. The analysis is again carried out on Footing 4 as explained earlier in Section 4.10.1. The Combigrid 40/40 Q1 material is used with an encasement depth of 1 m (h/d= 1.3), 2m (h/d= 3.67), and a full length (h/d= 7.6) to investigate the influence of encasement depth upon the column behaviour. The influence of encasement depth upon the footing vertical settlement is shown in Figure 4.21.

It can be seen in Figure 4.21 that the vertical settlement of Footing 4 reduces with increasing the encasement length, while the use of a full-length encasement leads to a greater improvement in the vertical settlement of the stone column. The reduction in the vertical settlement is more pronounced at an applied pressure larger than 70 kPa for both drained and undrained analyses. Therefore, the column can carry higher loads to satisfy specific column settlement criteria by installing a

geogrid around the column. By way of example, the predicted vertical settlement of unreinforced stone column is around 110mm at 110kPa, meanwhile the column will settle only 50mm at 110 kPa if the column is reinforced deeper than 2 m below the head of the column.

The improvement of fully encased column and 2m encasement length is more effective than the 1 m encasement length, as both encasements develop a similar settlement trend up to around 120 kPa. The predicted improvement in the vertical settlement is slightly higher in the undrained analysis than that in the drained analysis at higher loads.

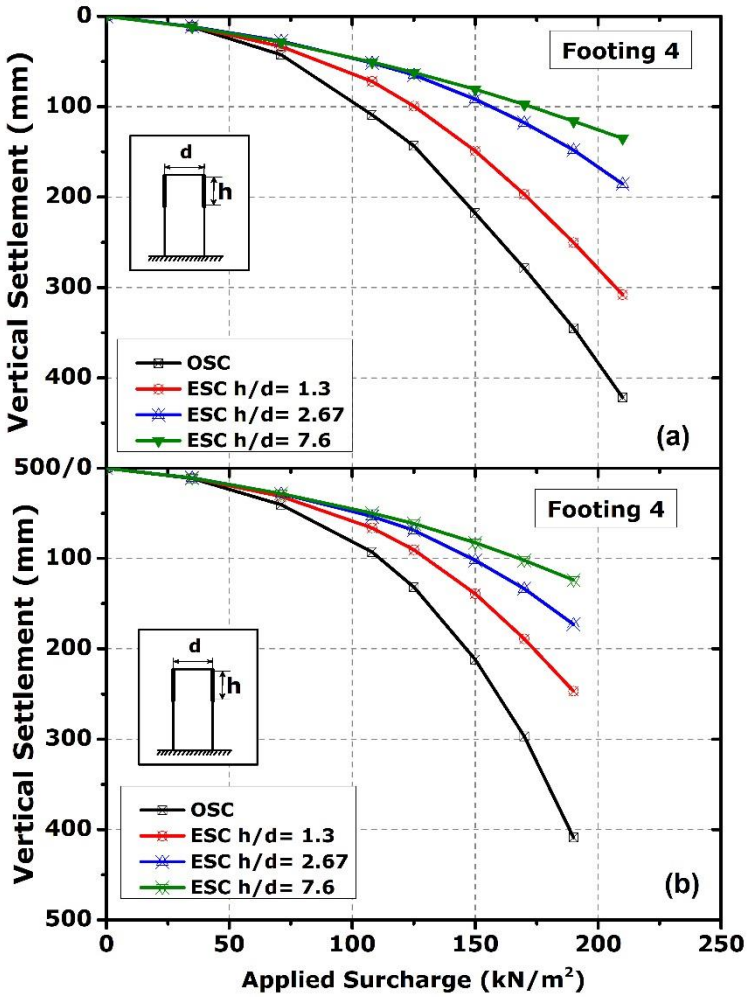


Figure 4.21 Influence of encasement depth upon vertical settlement in (a) drained and (b) undrained conditions.

The influence of 1 m of encasement depth upon the column behaviour is evaluated in the subsequent analysis (Figure 4.22). The analysis of the lateral bulging is modelled in the drained condition using PLAXIS 3D, as the undrained analysis shown in Figure 4.17 give a similar output with more time consuming analysis (for example, coupled analysis where undrained loading should be followed by a consolidation stage to simulate the long-term behaviour).

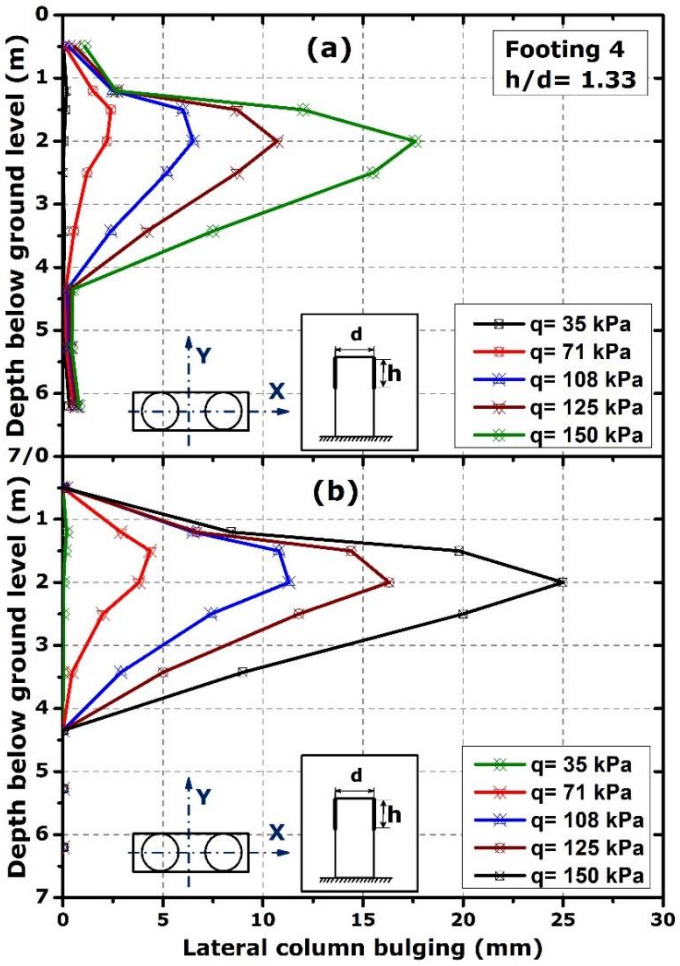


Figure 4.22 Lateral bulging (a) in x-direction, and (b) in y-direction with depth observed in drained conditions- h/d= 1.33.

The lateral bulging of the OSC (Figure 4.17) is significantly reduced in both directions (x and y) using a 1m length of encasement below the stone column head (Figure 4.22). The total reduction in the lateral bulging is around 37% in x-

direction and 45% in y-direction at 150 kPa. It is important to note that the column lateral bulging is not uniform in both directions. The influence of the partial encasement is substantial at the point of maximum bulging.

However, the reduction is not huge below the point of maximum bulging compared with OSC. It is interesting to note that the location of the maximum lateral bulging occurs beyond the end point of the encasement. Therefore, it is imperative to extend the encasement below the point of max lateral bulging as shown in the subsequent analyses.

The settlement profile for the footing and the soil at ground level in drained and undrained conditions is shown in Figure 4.23, respectively. It is interesting to note that the influence of encasing the top 1 metre of the stone column on the settlement of the footing and soil at the ground surface is marginal. However, the effect of the stone encasement is more pronounced for the second load increment.

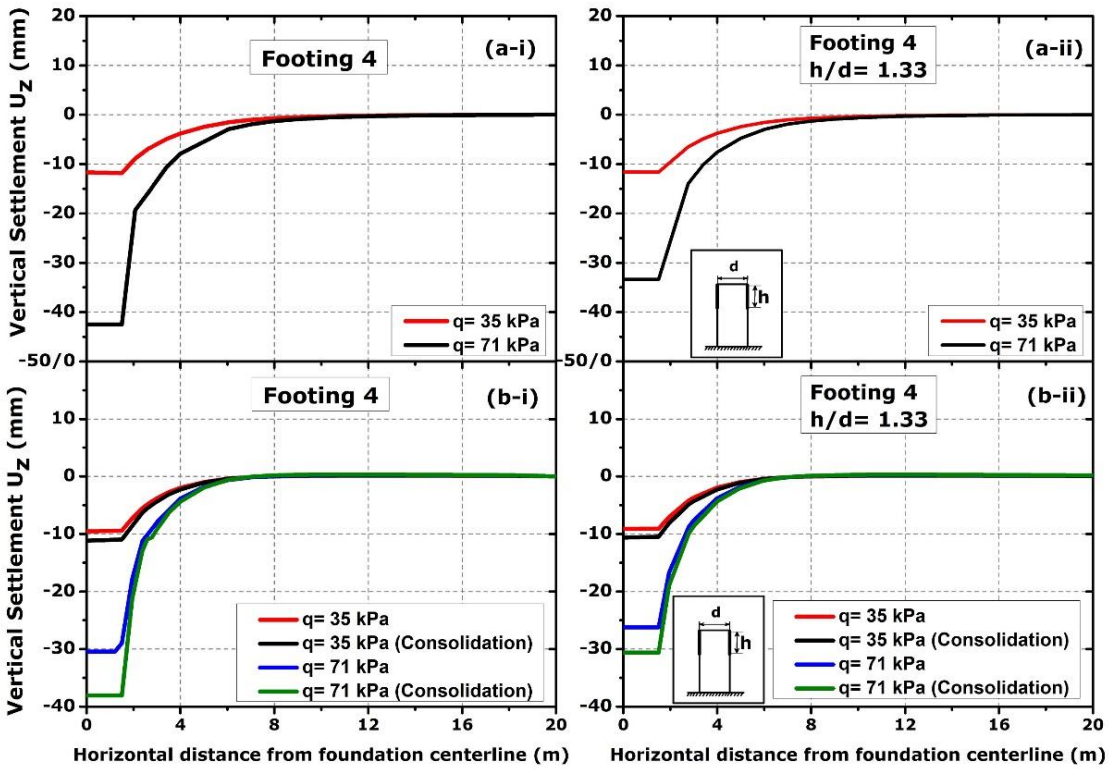


Figure 4.23 Settlement at the ground surface for (i) ordinary and (ii) reinforced stone columns with h/d=1.33 in (a) drained and (b) undrained conditions.

This is attributed to the footing 'bedding-in' effects which suggest that even with relatively low applied stress, the column will attract a significant proportion of the applied load and transfer the stress to the toe and to the soil below the toe level until the equilibrium is satisfied. At first load cycle, Figure 4.24 clearly shows that the maximum vertical stress is at toe level, meanwhile, the maximum vertical stress for the second load cycle is toward the mid-length and at the top of the column.

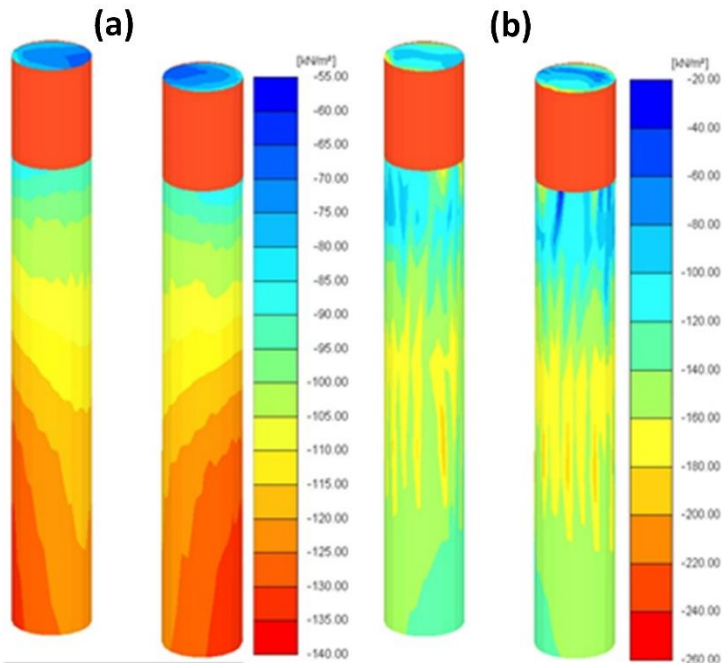


Figure 4.24 Vertical stress distribution (h/d=1.33): (a) 1st load cycle; (b) 2nd Load cycle.

Therefore, the reduction in the settlement is not significant under the first load increment even with using an encasement length of 1 m from the top of the column. Similarly, the difference in settlement between the footing and the surrounding soil is significantly reduced at the second load increment.

It is well established in Section 4.9.2 that the maximum lateral bulging occurred below the crust layer at a depth of 2 times the diameter of the column. Therefore,

it is prudent to extend the geogrid encasement below this depth to provide extra confinement to the column by developing a radial tension force in the geogrid (larger than 2 times the diameter of the column). The influence of encasing the stone column with a 2 m length of geogrid from the base level of the footing, upon the lateral bulging is shown in Figure 4.25.

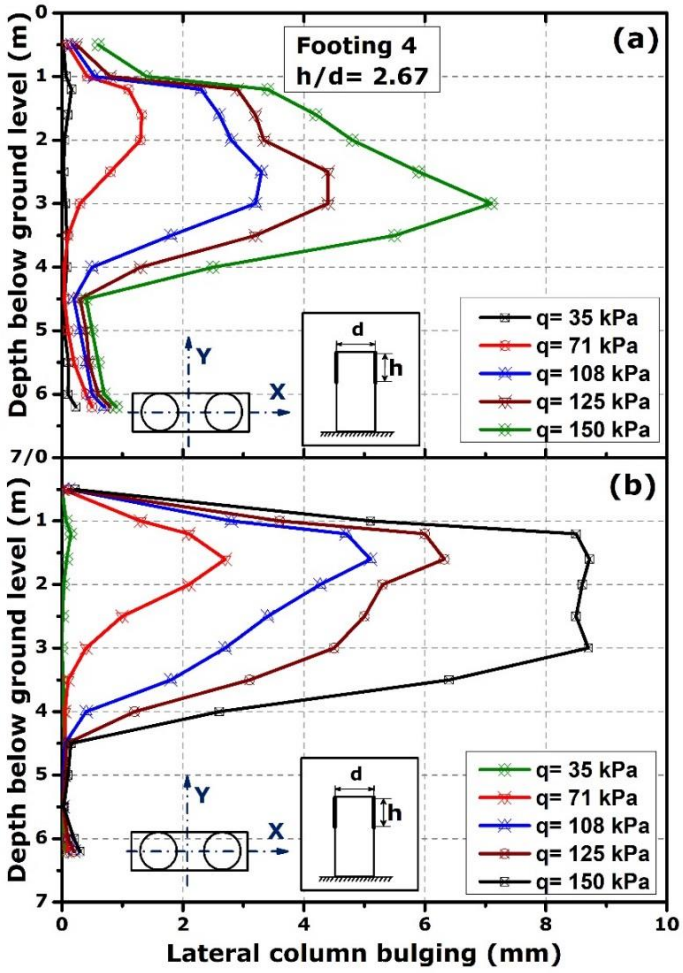


Figure 4.25 Lateral bulging in (a) x-direction, and (b) y-direction with depth observed in drained conditions- h/d= 2.67.

There is a significant reduction in the lateral bulging for ESC compared with the lateral bulging of the OSC shown in Figure 4.17. The more load applied, the more reduction in the lateral bulging. The lateral bulging reduces by 80% in both the X and y-direction at 150 kPa. It is perhaps worth noting that the ESC lateral deformation is more uniform compared with both OSC and ESC with 1 m of encasement; for example, the difference in the maximum lateral bulging in both

direction (x and y) is less than 2 mm at applied pressure of 150 kPa. It can be seen that the maximum lateral bulging (x-direction) is developed below the end point of the encasement. While the maximum lateral bulging location in y-direction is at two times the diameter of the column which is similar to the lateral bulging behaviour of OSC.

The influence of encasing the top 2 metres of the stone column on the settlement of Footing 4 is shown in Figure 4.26.

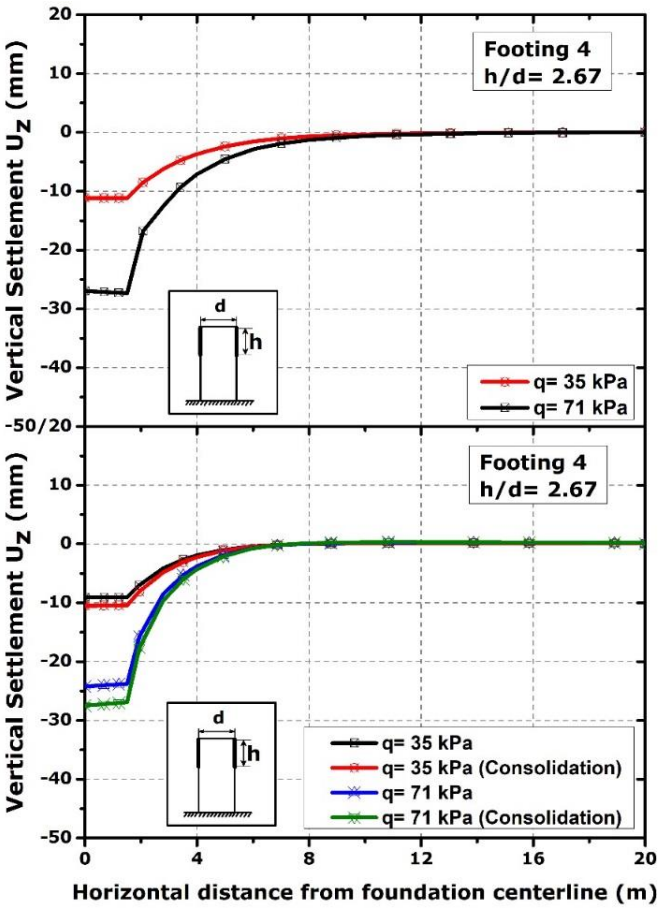


Figure 4.26 Settlement at the ground surface for an encasement of h/d= 2.67- drained and undrained conditions.

It can be seen that there is a slight reduction in the settlement of the stone column during the first load increment. Moreover, there is a reduction in the settlement of more than 20% under the second load increment. This emphasises the importance

of encasing the column from below the crust layer and below the depth of maximum lateral bulging upon the settlement performance of lightly loaded narrow footings supported by a small groups of stone columns.

Another interesting observation from this analysis is that the vertical settlement at ground level is reduced during the application of the first and second load increment which suggests that this depth of encasement is effective in reducing the footing settlement and the ground surface settlement. The reduction in the ground surface vertical settlement is approximately 50%. The variation of a fully encased stone column lateral bulging with depth is examined in drained conditions as shown in Figure 4.27.

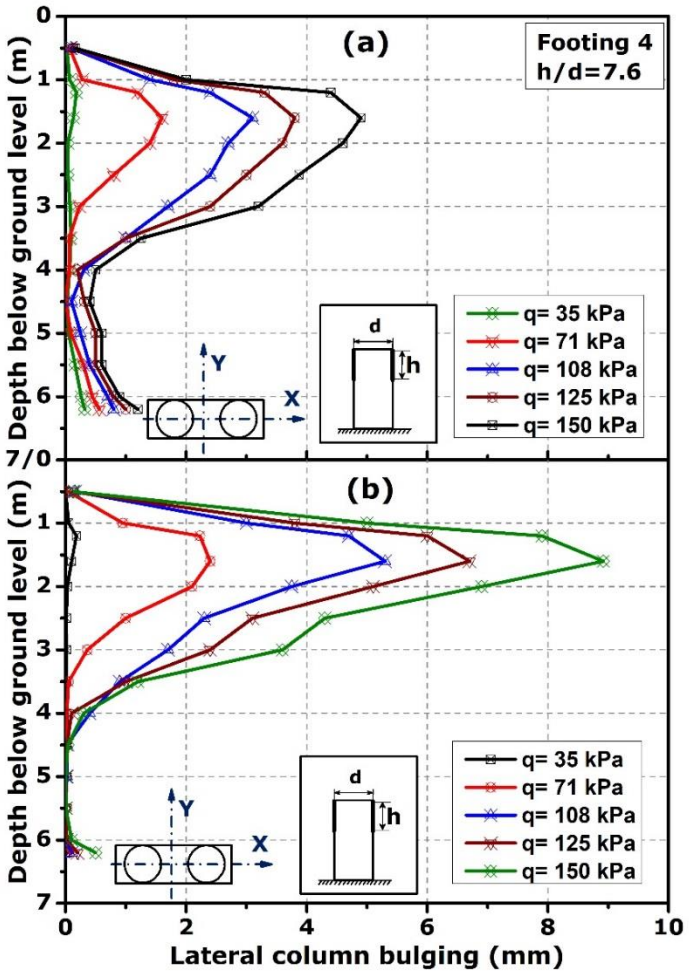


Figure 4.27 Lateral bulging (a) in x-direction, and (b) in y-direction with depth observed in drained conditions- h/d= 7.6.

It appears that the lateral bulging of the column is reduced across all column lengths compared with OSC (see Figure 4.17). It is clear that similar values of lateral bulging with depth were observed for the columns modelled with a 2 m length of encasement depth and fully encased columns. The lateral bulging of the fully reinforced column is reduced by 3.6 and 2.8 at X and Y directions, respectively, compared to 1 m column encasement as indicated in Figure 4.22 and Figure 4.27 (applied load = 150 kPa). However, the lateral bulging of fully encased column tends to increase with column length up to a maximum (L= 2 times the diameter of the column).

This may be attributed to the lack of confinement at shallow depths. It is perhaps worthy of note that the maximum lateral bulging occurs at a location of 2 times the column diameter despite using different encasement lengths. The column lateral bulging decreases thereafter to reach a minimum value coinciding with a slight lateral bulging at the column toe level.

The variation of the vertical settlement at ground level in both drained and undrained conditions is shown in Figure 4.28.

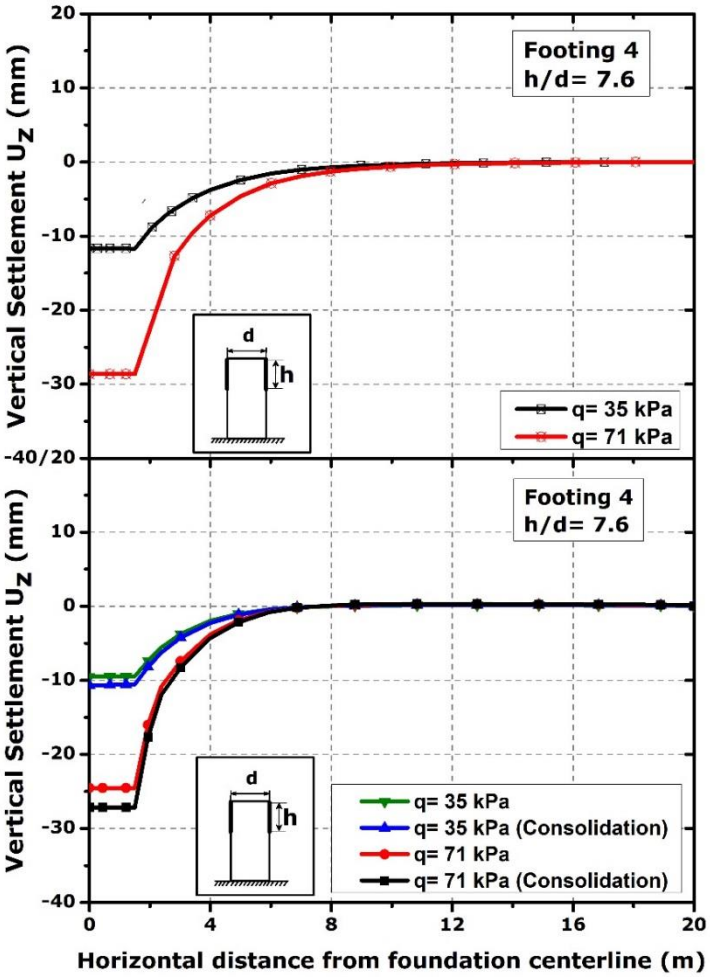


Figure 4.28 Settlement at the ground surface for an encasement of h/d= 7.6- drained and undrained conditions.

There is a significant reduction in both of the total footing settlement and the vertical settlement at ground surface compared with the OSC vertical settlement profile (Figure 4.14) which is again consistent with the findings of 2 m encasement length. The distribution of the hoop tension force generated in the geogrid due to the lateral confinement is shown in Figure 4.29 to Figure 4.31. It appears that a higher bulging occurs in the non-encased part of the column when the encasement depth is short.

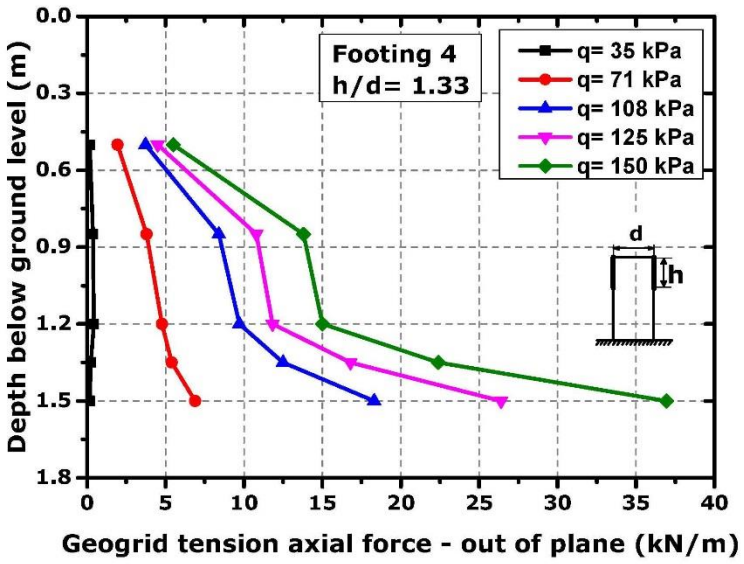


Figure 4.29 Influence of encasement depth on the hoop tension forces (h/d = 1.3)- drained conditions.

A more in depth analysis of the variation of hoop stresses with the column length reveals that the hoop tension forces developed in the geogrids are increased significantly with depth up to a maximum at the top of the soft clay for the 1 m column encasement length. Hoop tension forces remain relatively constant with the column length up to the end point of the encasement.

The distribution of the hoop tension forces is of similar trend to the lateral bulging for the 1 m encasement (see Figure 4.22) where both of the column lateral bulging and the geogrid tension forces are increasing with depth up to 1.5 m below the ground surface level. However, the distribution of the hoop tension forces is relatively constant across the encasement length for the 2 m encasement of the column.

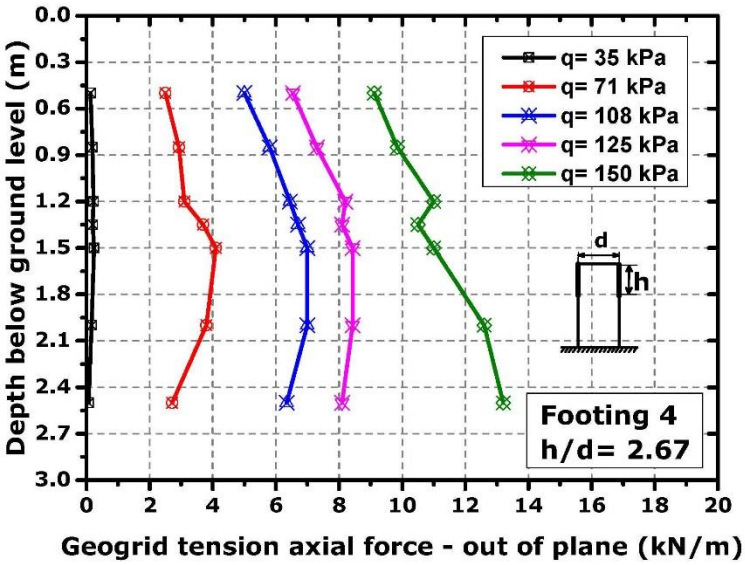


Figure 4.30 Influence of encasement depth on the hoop tension forces (h/d = 2.67)- drained conditions.

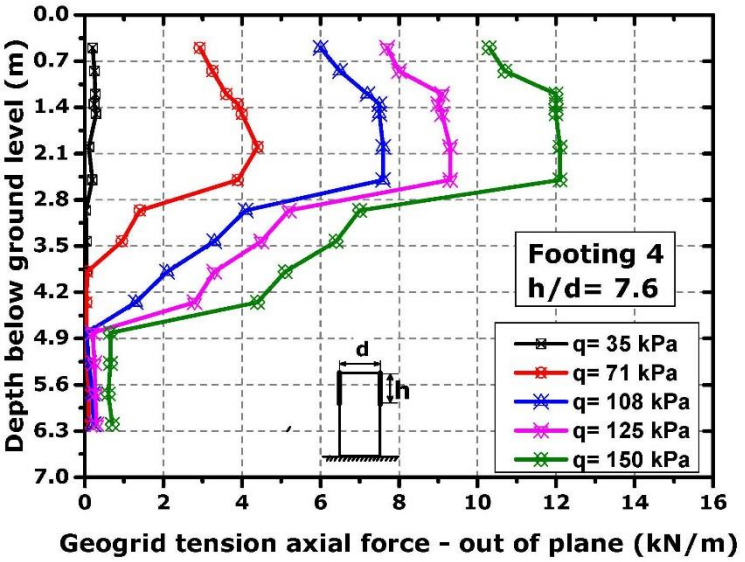


Figure 4.31 Influence of encasement depth on the hoop tension forces (h/d = 7.6)- drained conditions.

While the geogrid hoop tension force for fully encased column increases gradually until it reaches a maximum between 1.9 m and 2.6 m below the ground surface and then decreases gradually with column length to a minimum value.

The magnitude of the maximum hoop tension forces ranges from a low of 1 kN/m to 29 kN/m for different applied loads. The ultimate tension resistances of the most commercially available geogrids are much higher than the mobilised hoop

tension forces mobilised during the application of the loads. As columns are encased with a length below the maximum lateral bulging location it is deemed satisfactory to provide a sufficient lateral resistance to minimise the column lateral bulging. Furthermore, the encasement depth lower than 1 m below the top of the stone column is not effective in reducing the settlement of the stone column which is consistent with previous findings by Murugesan and Rajagopal (2006).

4.11 Effect of crust

Trial Footing 6 was installed at Bothkennar site (see

Table 4.1) with the intention of evaluating the impact of increasing the founding depth of the footing to the base of the crust upon the stone column behaviour. From reviewing the FEA of Footing 6, the following trends can be presented.

4.11.1 Vertical settlement

The variation of the vertical settlement with applied load for drained and undrained conditions is shown in Figure 4.32. Similar to other field trials, both drained and undrained analyses agree quite well where they yield the best match in the predicted settlement up to an applied pressure of 70 kPa. However, the rate of increase in the footing settlement is larger in the drained analysis compared with undrained analysis.

The predicted settlement for Footing 6 under the main two load increments is slightly lower than the settlement of Footing 4 but this trend reverses for an applied pressure higher than 71 kPa and 150 kPa for drained and undrained conditions where Footing 6 settled more compared with Footing 4 for the remaining of the load cycle. The author finds the higher settlement predicted for

Footing 6 as plausible because Footing 6 founding depth was at the top of the Carse Clay.

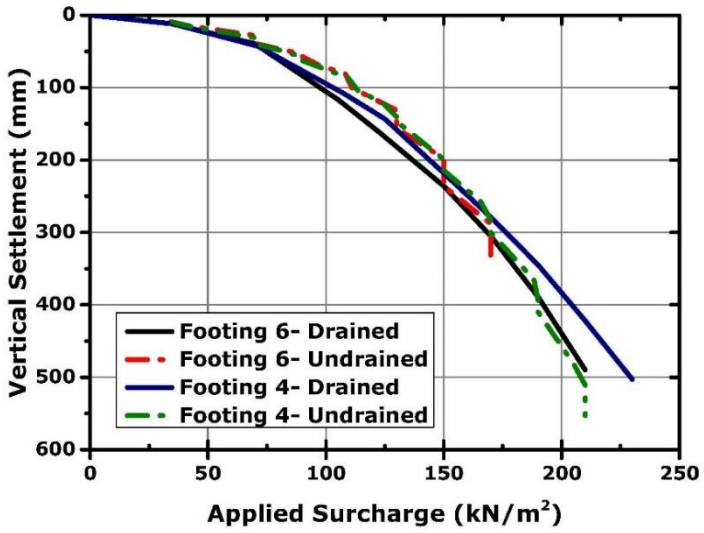


Figure 4.32 Load-displacement behaviour for pad Footing 4 and Footing 6.

Figure 4.33 shows the vertical displacement at the surface predicted from the centreline of the stone column. The settlement profile of Footing 6 at ground level was comparable to Footing 4 (see Figure 4.14) with identical column length and spacing. The difference in both the total and the ground profile settlement of Footings 4 and 6 is negligible.

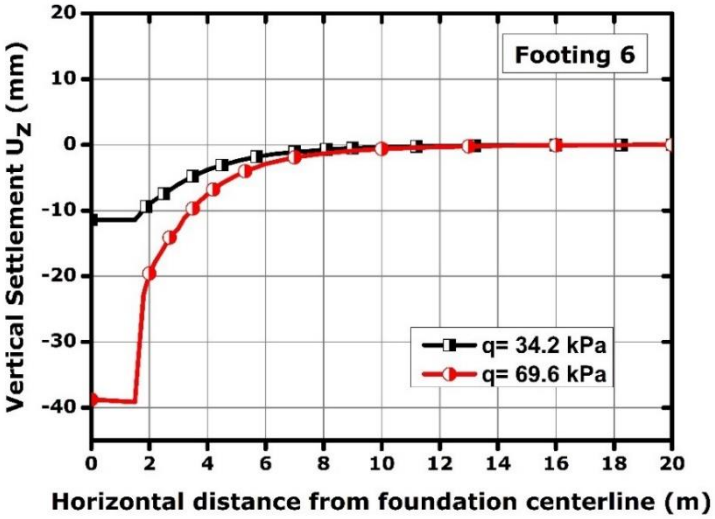


Figure 4.33 Influence of footing shape on the footing and ground vertical displacement in drained conditions- Footing 6.

4.11.2 Lateral Bulging

The influence of increase in the foundation depth on lateral bulging is shown in Figure 4.34. The lateral bulging of trial Footing 6 is similar to that of Footing 4 for an applied pressure up to 70 kPa. The lateral bulging of Footing 6 increases significantly under the subsequent applied loads to reach a maximum of 43 mm at an applied pressure of 150 kPa.

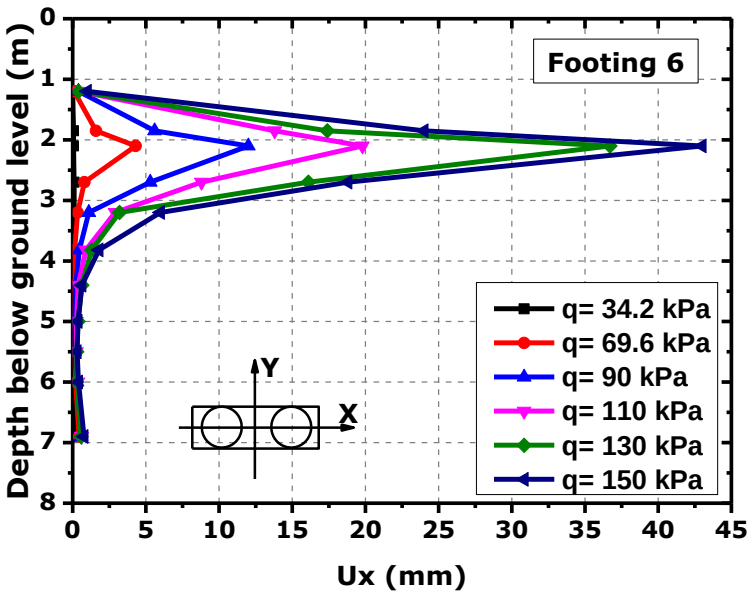


Figure 4.34 Lateral bulging (Ux) with depth observed in drained conditions- Footing 6.

The increase in the column bulging for Footing 6 (Footings 4 and 6 were placed at two depths corresponding to 0.5 m (in the crust) and 1.2 m (at the base of the crust) respectively below founding level) compared to Footing 4 suggests that the crust is effective in reducing the column lateral bulging. Therefore, it is important to consider the crust in the soft soil stratigraphy which is in agreement with Killeen (2012) who suggested that the modelling of the crust layer will yield a more realistic analysis to study the behaviour and settlement performance of small group of columns. Therefore, the increase in the vertical settlement of trial Footing

6 is due to the increase of column lateral bulging for an applied pressure range from over 70 kPa to 150 kPa.

4.11.3 Influence of geogrid encasement

The influence of fully encasing Footing 6 with geogrid upon the vertical settlement is shown in Figure 4.35. There is a significant improvement of the vertical settlement with reinforced stone column. It can be seen that using geogrid as reinforcement can improve the footing bearing capacity. It is also clear that the pressure applied on the footing can be increased from 70 kPa to 120 kPa to satisfy a settlement performance of 50mm with geogrid reinforcement.

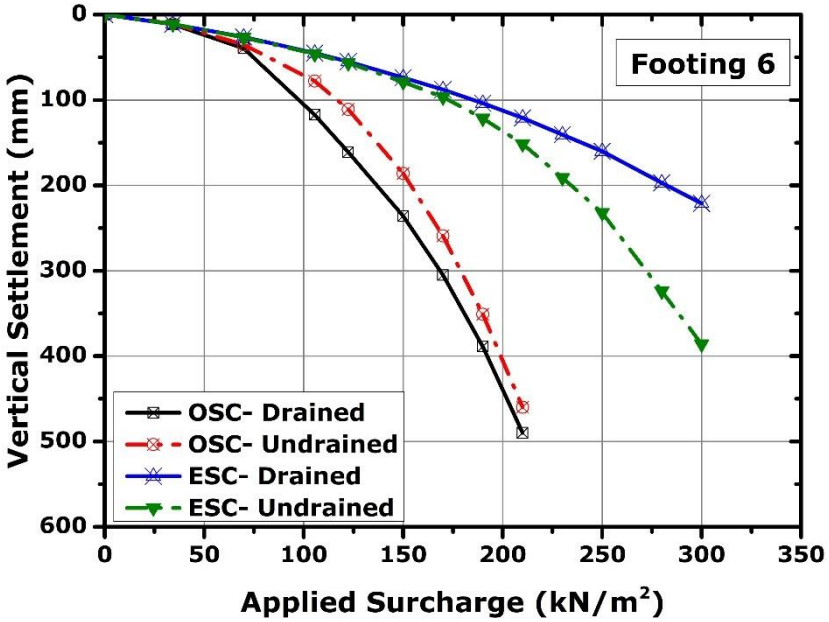


Figure 4.35 Load-displacement behaviour for OSC and ESC-Footing 6.

4.12 Investigation of footing shape

The influence of the footing shape upon the stone column behaviour is evaluated using field trial 7 constructed as a 1.5 m x 1.5 m pad with a corresponding area ratio similar to the trial strip footing number 3, 4, 5 and 6 supported by 2 stone columns of 5.7m length below the base of the footing.

4.12.1 Vertical settlement

The impact of footing shape on the vertical settlement of the footing is shown in Figure 4.36.

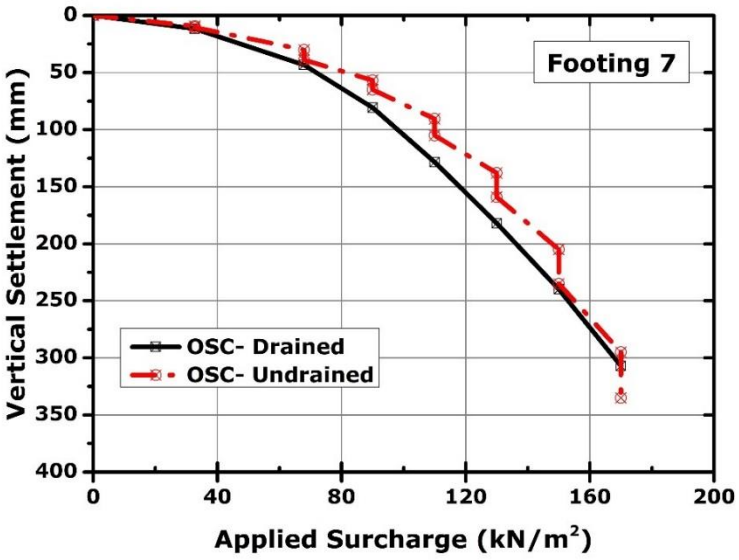


Figure 4.36 Load-displacement behaviour for pad Footing 7.

The predicted settlement in the FE analysis was comparable (slightly more) to the trial Footing 4 settlement. Trial Footing 7 is identical to trial Footing 4 column length, area ratio, and founding depth. This is consistent with the findings by Serridge (2001) during the monitoring of Bothkennar trial footings.

It is important to note that the stress bulb beneath Footing 4 and 7 is different. As the stress depth influence is around 6.0 m below the base of Footing 7, whereas it is around 2.7 m below the founding depth of trial Footing 4. This suggests that the crust may be playing an important role in masking the beneficial contribution of the smaller footing dimensions, to a certain extent.

The footing and ground settlement profile with depth is shown in Figure 4.37. It can be seen that the settlement profile was comparable again with Footing 4 which

again highlights the influence of the crust as a salient feature of the Bothkennar soil profile.

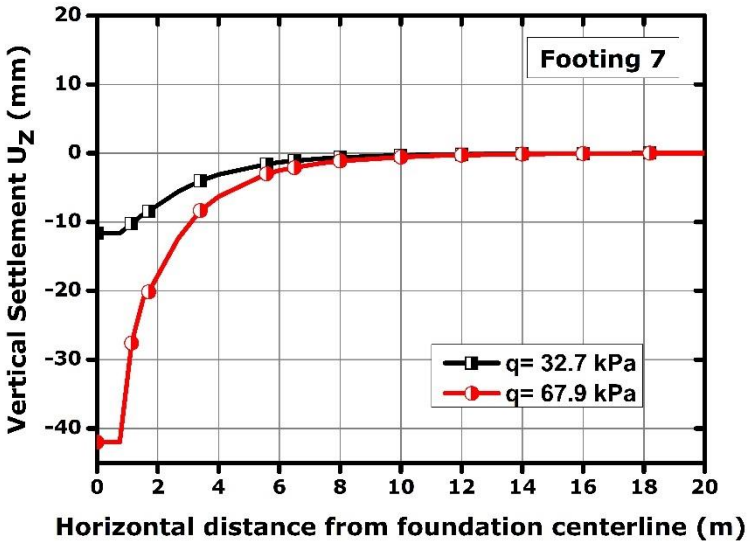


Figure 4.37 Influence of footing shape on the footing and ground vertical displacement in drained conditions- Footing 7

4.12.2 Lateral Bulging

The lateral bulging of Footing 7 in the x and y directions in drained conditions is shown in Figure 4.38 and Figure 4.39, respectively.

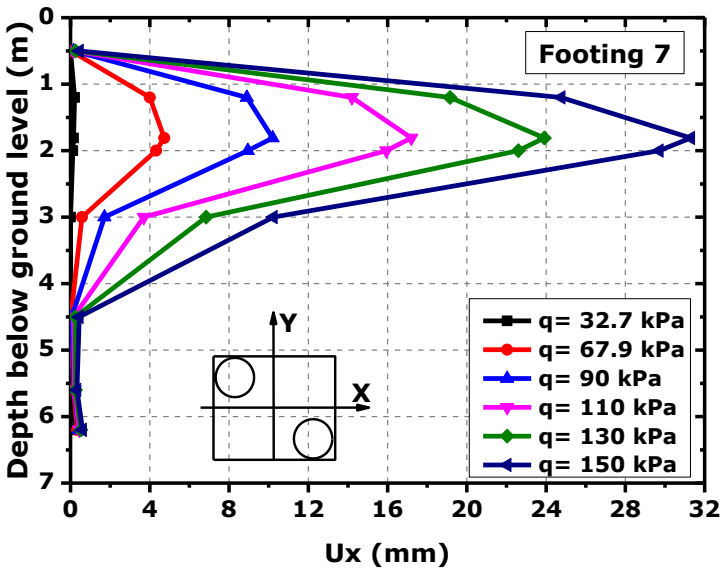


Figure 4.38 Lateral bulging (Ux) with depth observed in drained conditions- Footing 7.

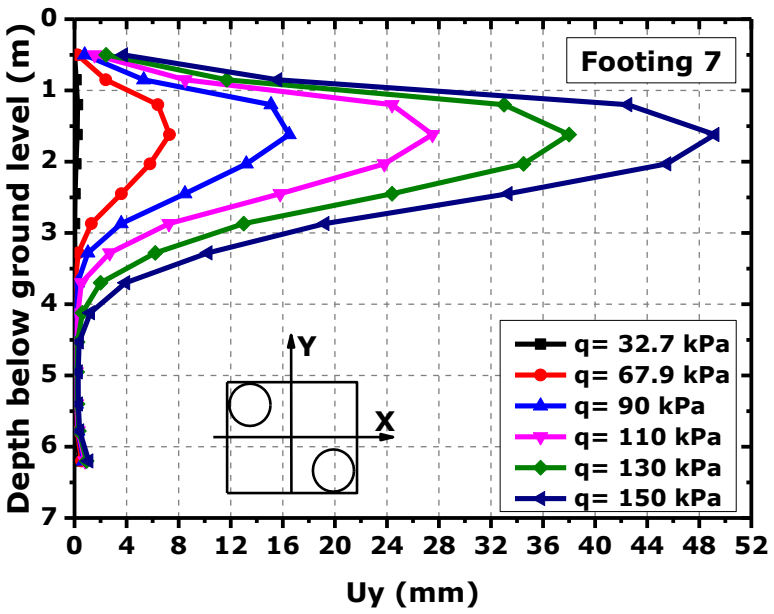


Figure 4.39 Lateral bulging (Uy) with depth observed in drained conditions- Footing 7.

The maximum lateral bulging is once again located at 2 times the diameter of the column. The lateral bulging of Footing 7 is slightly higher than the bulging of Footing 4 in both directions. This is due, in part, to the confinement associated with a particular column arrangement, as the columns in Footing 4 appear to have a tighter confinement than Footing 7.

4.12.3 Influence of geogrid encasement

The influence of using full length column encasement upon the settlement performance of trial Footing 7 is shown in Figure 4.40. It appears that the impact of encasing stone columns beneath Footing 7 upon the vertical settlement is again similar to trial Footing 4.

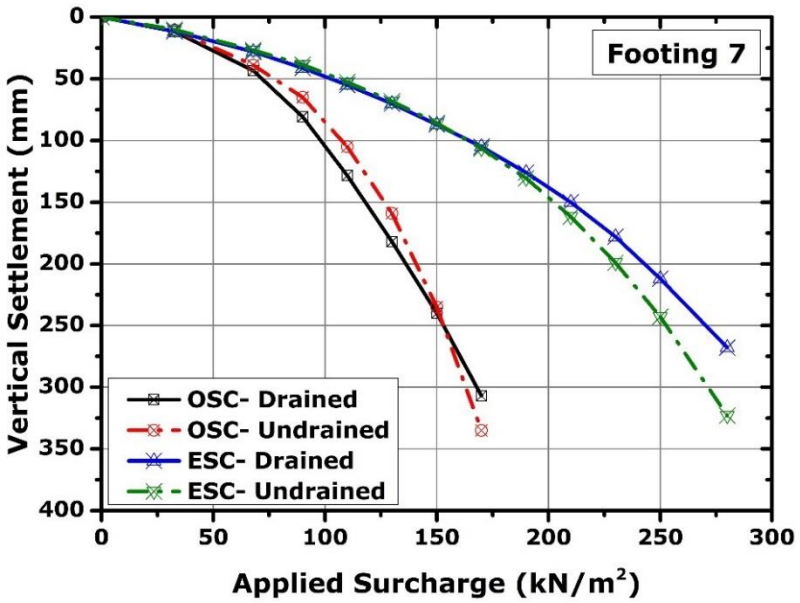


Figure 4.40 Load-displacement behaviour for OSC and ESC-Footing 7.

4.13 Review of Priebe (1995) method

The Priebe (1995) method is considered one of the most popular methods to assess the settlement behaviour of stone columns in the UK. In this method, a reduction factor can be calculated based on the area replacement ratio as a function of the stone friction angle. This reduction factor considers the column material compressibility under loading and also takes account for the effect of increasing overburden on the column bearing capacity.

The reduction factor should be applied to the untreated settlement within treated depth. Moreover, untreated soil layer settlement must be added to the reduced settlement in the treated zone to calculate the total post treatment settlement associated with soft soil improvement by installing the stone columns. The author used the Priebe (1995) method to estimate the post settlement of Bothkennar field trials (see Appendix A). In contrast to Serridge (2001) who used the basic reduction factor in calculating the post treatment settlement of the field trials at Bothkennar field (see Figure 2.22), the post treatment settlement of the field trials in Appendix A has been calculated considering the influence of the column material

compressibility and the effect of increasing overburden on the stone column (see Figure 2.23 and Figure 2.24). The predicted post treatment settlements for all field trials under first and second load increments are summarised in Table 4.8 and Table 4.9.

The settlement calculated using the Priebe method ranged from 4 mm to 7.5 mm and 12 mm to 19 mm for the first and second load increments, respectively. It appears that the modified settlement improvement factor suggested by Priebe (1995) underestimates the settlement performance of the field trials at Bothkennar site. This may be attributed to the ground surface heave and the sensitivity of the Bothkennar soft soil, with remoulding occurring during installation of the stone columns.

The Priebe method does not capture these two important Bothkennar soil features (i.e. installation effects). Moreover, most of the Priebe analysis is applicable on wide spread loads associated with slabs and embankments structures where the column behaviour is stiffer due to the greater confining actions provided by the installation of the adjacent columns compared to a single stone column installed beneath isolated foundations.

Table 4.8 Estimated post treatment settlements of trial footings under first load increment.

Trial footing	Load (kN/m²)	A_o (m²)	Stone column diameter (m)	Ac (m²)	A/Ac	Friction angle of Stone φ (°)	Pre-treatment settlement (mm)	Post-treatment settlement (mm)	Measured post-treatment settlement (mm)
1	33.5	1.13	0.75	0.44	2.56	42.5	16.2	6.6	27.5
2	32.9	1.5	0.75	0.44	3.41	42.5	15.9	6.9	25.0
3	33.1	1.13	0.75	0.44	2.56	42.5	13.3	5.7	17.5
4	34.9	1.13	0.75	0.44	2.56	42.5	14.8	6.2	20.0
5	32.1	1.13	0.75	0.44	2.56	42.5	13.6	5.5	22.0
6	34.2	1.13	0.75	0.44	2.56	42.5	13.8	4.2	24.0
7	32.7	1.13	0.75	0.44	2.56	42.5	19.3	7.6	22.0

Table 4.9 Estimated post treatment settlements of trial footings under second load increment.

Trial footing	Load (kN/m²)	A_o (m²)	Stone column diameter (m)	Ac (m²)	A/Ac	Friction angle of Stone φ (°)	Pre-treatment settlement (mm)	Post-treatment settlement (mm)	Measured post-treatment settlement (mm)
1	72	1.13	0.75	0.44	2.56	42.5	34.9	17.1	50.0
2	67.1	1.5	0.75	0.44	3.41	42.5	32.5	16.6	42.5
3	67.8	1.13	0.75	0.44	2.56	42.5	27.1	13.6	37.5
4	71.1	1.13	0.75	0.44	2.56	42.5	30.2	14.8	42.5
5	67.8	1.13	0.75	0.44	2.56	42.5	28.8	14.1	40.0
6	69.6	1.13	0.75	0.44	2.56	42.5	28	12.2	45.0
7	67	1.13	0.75	0.44	2.56	42.5	39.6	19.0	42.5

4.14 Influence of column diameter and strength

The influence of key design parameters such as the column diameter upon the settlement performance of Footing 4 in drained analysis is shown in Figure 4.41. It can be seen than the larger column diameter settled the least (keeping the column spacing over the column diameter constant s/d= 2.0). This may be explained as more stone is used to build the larger diameter column than the smaller diameter column therefore more area is treated by the larger column diameter.

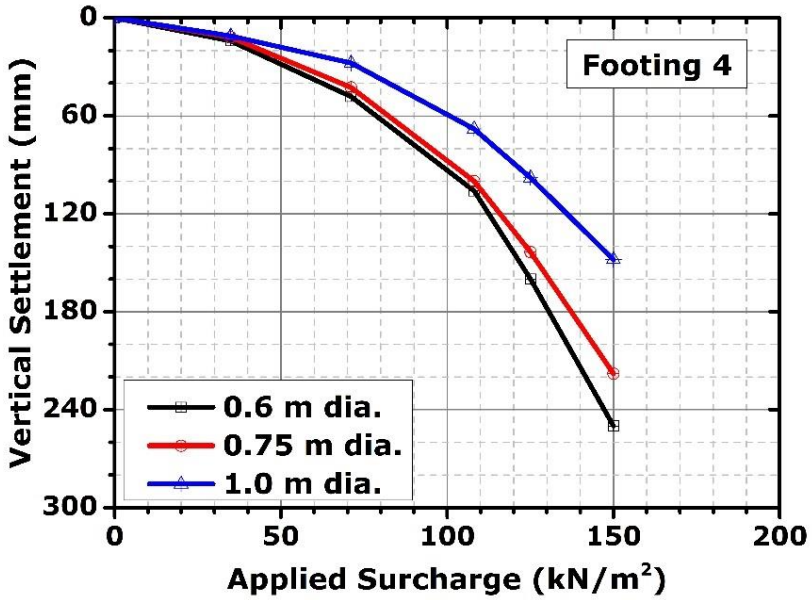


Figure 4.41 Influence of column diameter upon footing settlement- drained conditions.

The variation of vertical displacement with loads is illustrated in Figure 4.42. A negligible settlement improvement is observed with increasing column strength (angle of internal friction) at working applied pressure (lower than 50 kPa). However, it can be seen that increasing the column strength leads to significant improvement in settlement at ultimate pressure (higher than 150 kPa). This may be explained as the column load increases, the column is in a plastic state where

the angle of internal friction is mobilised. Therefore, the effect of angle of friction is more pronounced on columns with the largest degree of plasticity.

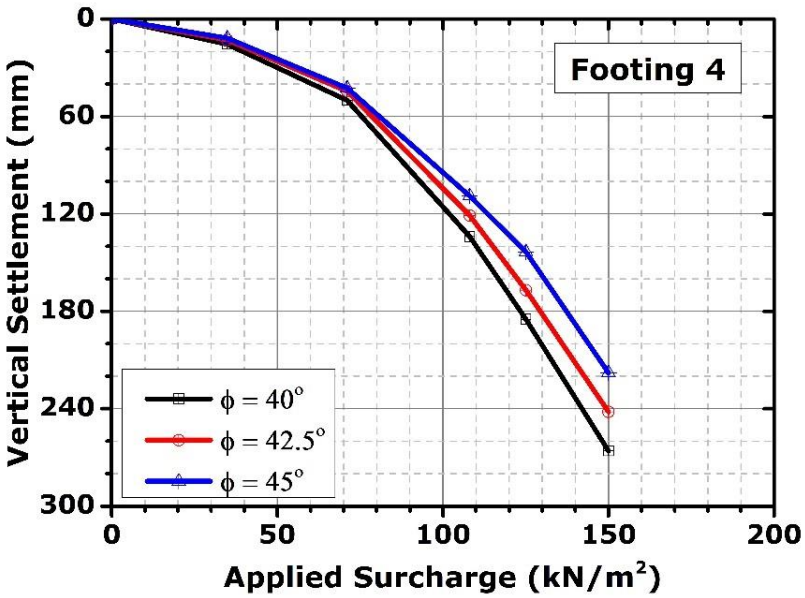


Figure 4.42 Influence of column strength upon footing settlement- drained conditions.

4.15 Influence of reinforcement stiffness

Two different geogrid materials are used to encase the column in this analysis, as shown in Table 4.5. The column bearing capacity increases significantly by encasing the column with a geosynthetic material. It can be seen that as the geogrid stiffness increases leads to better improvement in the column settlement (Figure 4.43).

It was shown earlier that the geogrid material will enhance column lateral confinement by generation of hoop tension forces. Drained conditions analysis agrees quite well with the undrained analysis. The settlement improvement is more pronounced at higher loads where the contribution of geogrids in resisting the lateral bulging is increasing due to more hoop tension forces being generated.

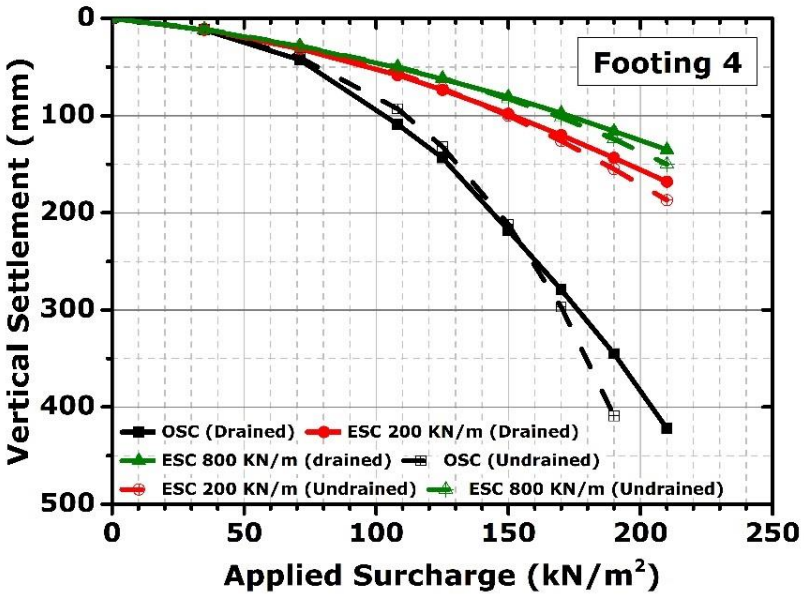


Figure 4.43 Influence of geogrid encasement on Load-displacement behaviour for OSC and ESC.

4.16 Summary of results

Various arrangements of footings and columns were analysed over a typical range of applied loads to investigate the influence of key design parameters such as column length, spacing, footing shape and the crust layer on footing behaviour at the Bothkennar site. The vertical settlement, the settlement at the ground surface, the lateral bulging, the encasement and their depth were examined for a select number of trial footings at the Bothkennar site. The main findings from this research are summarised as follows:

- It was found that a working applied pressure of 50 kPa is deemed satisfactory for the Bothkennar field trial (and could be used as a guidance when designing a pad footing supported by stone columns in soft soils) applying a typical factor of safety in the range of 2.5 to 3. It is inferred that the applied working load should be limited to satisfy a typical settlement

performance of columns installed beneath a narrow footing supporting lightly loaded structure.

- For all the trials, the ground settlement profile indicates that the settlement at ground level would diminish at a distance in the range of 2 to 3 of the footing width measured from the centreline of the footing for undrained and drained analysis, respectively.
- Analysis of Footing 6 (founded at the base of the crust) predicts a settlement similar to that of Footing 4 (founded at 0.5m depth in the crust) for the first two load increments. However, the rate of settlement increased significantly compared with Footing 4 at higher loads which is in line with the expectations due to the founding depth in soft soil (i.e. base of crust) and also demonstrates the sensitivity of foundation depth within the crust.
- The predicted settlement for Footing 7 was comparable (slightly more) to that of the trial Footing 4 settlement. This may be explained on the basis that the stress depth influence is deeper for Footing 7 compared with Footing 4. This suggests that the crust may be playing an important role in masking some of the beneficial contribution of the smaller footing dimensions.
- The settlement performance of larger diameter stone column is superior to that of a smaller diameter (keeping s/d= 2.0 ratio constant) due to the larger treated area associated with larger column diameter (larger proportion of soil replacement).
- The estimated settlement calculated in accordance with Priebe (1995) design charts significantly underestimated the settlement of the trial footings. This may be attributed to the high energy used in column installation which leads to soft soil disturbance contributing to less settlement prediction than the trial footings. In order to err on the side of caution, Priebe method outcomes should be verified against field tests or

with a numerical analysis when stone columns installed in sensitive clays or where a crust layer is available at shallow depths.

- The lateral bulging of Bothkennar field trials stone columns is analogous to Hughes and Withers (1974) laboratory findings, Hughes et al. (1976) field findings and the case where a triaxial sample is failed (height to width ratio = 2). It was observed that the stone column suffers a severe lateral bulging near the top of the column. The lateral bulging is constrained by the crust presence at the upper part of the column. However, bulging of the stone column is still taking place in the soft clay underlying the crust layer at the point of peak stress.
- Trial Footing 1 laterally bulged less than trial Footing 2 and settled slightly less than Footing 2. This may be attributed to the increase in the area ratio which leads to an increase in the total load taken by the column. Therefore, for a similar column length, the shear resistance along the side of the column is similar (if shear resistance is fully mobilised) and the increase in the column load will increase the column load resisted at the base, which consequently increase the column vertical settlement. Similarly, higher lateral bulging is associated with larger area ratio (Footing 2).
- For the shortest column (Footing 3) to the longest column (Footing 5), the lateral bulging is similar. However, the lateral bulging for Footing 3 is gradually reduced from a maximum to a minimum value of between 0.5 mm to 2 mm correspondent to the applied loads. This confirms that the load is transferring to the column toe. Therefore, it appears that the dominant mode of failure for the short column is by punching through the soft soil. This is consistent with the analyses carried out in Chapter 5 using the punching and compression ratios and the findings of McCabe and Killeen (2016).

- Footing 6 constructed at the top of the soft soil (base of the crust) laterally bulged the most. The large bulging can be explained as the crust does not contribute significantly in reducing the lateral bulging in contrast to other footings. Therefore, there is a potential of raising the site level by using a compacted fill at the expected depth of bulging to avoid bulging failure where sensitive or very soft clays are present. It is important that the base of the foundation is constructed as far as possible from the soft clay However, other factors such as construction time, cost, and safety must also be considered to develop a proper foundation solution. This will enable the engineers to specify stone column solutions in lieu of other expensive geotechnical solutions such as piling.
- The use of geogrid encasement around the column improves the column bearing capacity and their stress-displacement behaviour (the serviceability performance). The greater the length of encasement used, the more the total and the relative vertical settlement between the footing and the surrounded soils are reduced
- The encasement of the top metre of the column reduces the lateral bulging considerably. However, the lateral bulging reduced significantly by extending the encasement below the maximum lateral bulging zone (around 2 times the diameter of the column).
- The lateral bulging becomes more uniform where similar lateral bulging occurs in both directions (x and y) if encasement depth extends below the maximum lateral bulging position.
- The magnitude of the maximum predicted hoop tension forces ranges from a low of 1 kN/m to 29 kN/m for different applied loads and is much lower than the tension resistance of the most commercially available geogrids.

CHAPTER 5

SIMPLIFIED ANALYTICAL MODEL FOR STONE COLUMNS

5.1 Introduction

The results from the numerical analysis regarding the settlement performance, column bulging, and encasement depth for small groups of stone columns are placed in context in Chapter 4. A simplified design method is proposed which allows to investigate the influence of installing an unlimited column grid below an unlimited loaded area upon settlement performance. The improvement in settlement due to the installation of a small group of stone columns is also investigated in this chapter.

The mode of deformation is identified in this chapter using punching and compression ratios for different area ratios and coefficients of the lateral stress. The modes of deformation such as punching, bulging and block behaviour are also identified and compared with FEA conducted by other researchers (Black, 2006; Kirsch, 2006; McCabe and Killeen, 2016; Satibi et al., 2009).

In current practice, the numerical analysis is often used to investigate the stone column settlement performance (Al Ammari and Clarke, 2016). A series of analytical and empirical design methods are available to address the settlement improvement associated with stone column installation. In the UK, most designs use Priebe's method to assess settlement improvement (Priebe, 1995). In this research, a numerical study of axisymmetric model (an efficient mathematical

means of modelling stone column grids) using Hardening Soil model is performed and compared with the derived analytical model to understand effectiveness of stone columns. The study is carried out with the intent to provide practicing engineers with a simple tool for assessing the foundation settlement in soft soils.

The focus of this chapter is to propose a simplistic analytical model that can predict the settlement improvement in the soft soils due to the installation of vibro stone columns. The design of stone columns in soft clays is usually governed by performance (settlement) rather than the column bearing capacity to support applied load (Killeen (2012) and (Priebe, 1976)). An analytical approach developed by Satibi et al. (2009) was modified in the current study to assess the performance of an infinite grid of floating stone columns. Furthermore, the analytical model is used in conjunction with the design charts developed by Priebe (1995) to predict the settlement of single pad and strip footings

This approach is used to calculate the critical stone column length defined as the minimum required length to resist the applied load solely by a floating stone column (ignoring toe resistance contribution). Although the existence of a critical column length at failure condition was reported by several researchers such as McKelvey et al. (2004) and Wehr (2004), this finding is not supported in the current study because the critical length determined in this research is based on the serviceability limit state rather than the ultimate limit state. The critical length in this study refers to the length where the entire foundation load is resisted by the floating stone column and no load is transferred to the underlying soil. However, the critical lengths calculated by various others (McKelvey et al. (2004) and Wehr (2004)) were at failure condition rather than at serviceability condition. The analytical approach is based on the unit cell concept where a uniformly distributed load is applied on the top of the stone column, as shown in Figure 5.1.

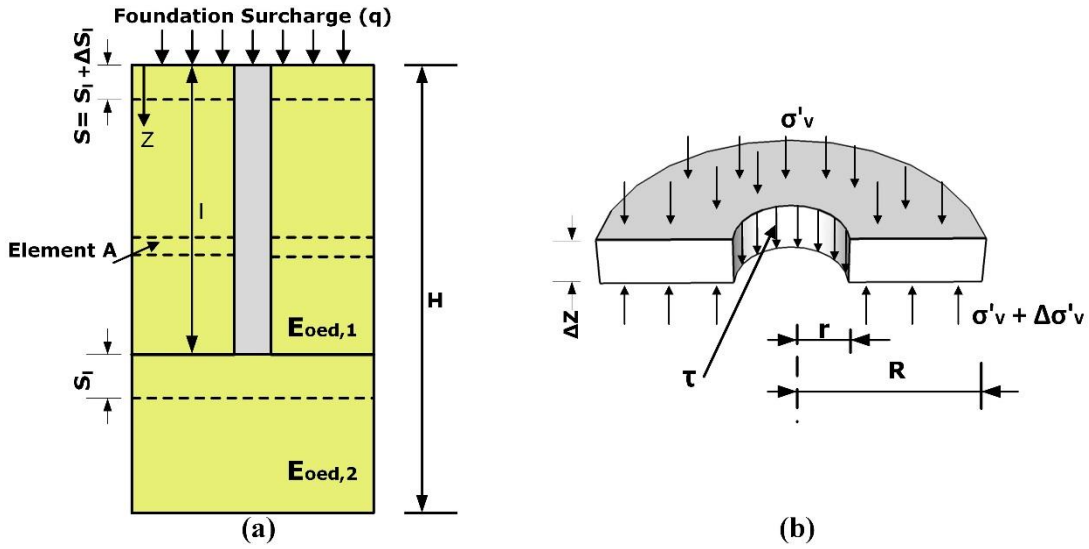


Figure 5.1 Settlement analysis of one cell of an infinite grid of floating stone columns (a) vertical cross section (b) vertical effective force equilibrium of element A.

Figure 5.1 (a) and (b) show the vertical cross section of the axisymmetric cell and an element A illustrating the effective vertical forces in equilibrium within the column. The effectiveness of the footing or embankment constructed on top of the floating stone columns is then investigated by using a relative settlement reduction ratio (RSR).

The RSR ratio is defined as:

$$\mathbf{RSR} = \frac{S_o - S}{S_o} \qquad (5.1)$$

where the subscript "0" means no stone column is installed thus S_o is soft soil surface total settlement without improvement in the ground due to stone column installation. S refers to the total settlement at the surface of the soft soil improved by stone columns. It needs to be emphasized that the use of an advanced method such as the FEA for detailed design is important to evaluate the effectiveness of the stone column as a ground improvement method. The advantage of the FEA is

that the behaviour of the stone columns solution can be captured more accurately than other methods such as the Priebe (1995) method due to its capability of capturing all the factors influencing the effectiveness of the stone columns solutions, rather than treating each layer individually (Killeen, 2012). However, analytical design methods based on more simplified material models compared to PLAXIS models would be more practical and easier to use by the practitioners and the industry when assessing the effectiveness of a stone column solution. A program was written by the author in Visual Basic to model circular cell geometry as illustrated in Figure 5.1 to predict the RSR (See Appendix B).

5.2 Analytical model derivations

Stone columns have been increasingly used to support embankments especially when a settlement/differential settlement is involved. Several researchers such as Pulko and Majes (2005) and Sexton et al. (2016) have indicated that the settlement of infinite grid of floating stone columns can be simulated by using unit cell model (concept). Different types of stone columns have been used, each with different rigidities, and using different installation processes and materials. The analytical model adopted in this research is based on the rigid column theory (Satibi, 2009). The soft soil settlement due to the foundation applied load is based on the Hooke's law of elasticity where the soil is idealised as linear elastic, uniform, and isotropic if no stone column is installed. Hence;

$$\boldsymbol{S_o = S_l + \Delta S_o = (q\,.(H - l))/E_{oed,2} + (q\,.l)/E_{oed,1}} \qquad (5.2)$$

ΔS_0 refers to the partial soft soil settlement up to a depth of l (l is the stone column length, if installed). Settlement of the soft soil below the stone column toe level, S_l. The embankment/foundation surcharge including the external applied load (q), and H is the soft soil layer thickness. E_{oed} is defined as the oedometer or constrained modulus of the soft soil layer. It should be noted that the previous investigations such as that by Balaam and Brown (1977) demonstrated that using

an elastic analysis will slightly under-predict the settlement performance of stone columns at working loads.

If an embankment/foundation is constructed over a soft soil and improved with the stone column, then soft soil settlement can be determined by the equilibrium of the effective vertical stress. Considering floating condition with the ground water at the ground surface, the effective vertical stresses in Figure 5.1b can be written as follows:

$$\left[(-\boldsymbol{\sigma}'_v + (\boldsymbol{\sigma}'_v + \Delta\boldsymbol{\sigma}'_v) - \boldsymbol{\gamma}'.\Delta\boldsymbol{z}) \,.\boldsymbol{\pi}\left(\boldsymbol{R}^2 - \boldsymbol{r}^2\right)\right] - \boldsymbol{2\pi r}.\boldsymbol{\tau}\Delta\boldsymbol{z} = \boldsymbol{0} \qquad (5.3)$$

where R is the radius of the circular cell, r is the stone column radius, γ' is the effective unit weight of the soil and τ is the stone column unit shaft friction. In terms of the soil mechanics theory, the ultimate skin friction on the stone column shaft (if it is modelled as a rigid column) can be evaluated in soft to firm clays in terms of the effective vertical stress using the following equation (Terzaghi et al., 1996).

$$\boldsymbol{\tau} = \boldsymbol{RF}.\boldsymbol{\acute{\sigma}_v} \qquad (5.4)$$

where RF is the lateral reduction factor representing the reduction in the effective angle of friction with increasing depth up to the residual value. On the assumption that during column installation surrounding soft clay is in a remoulded state and the cohesion intercept is zero.

$$\boldsymbol{RF} = \boldsymbol{K_s}\,.\boldsymbol{\tan\delta} \qquad (5.5)$$

where K_s is the final coefficient of horizontal soil pressure after stone column installation and δ is the average value of the angle of friction between stone column and soil. The reduction factor (RF), calculated on the basis of load tests, is found to vary from about 0.1 to 0.5 in soft to medium clay. Moreover, the values of the reduction factor range from about 0.25 to 0.5 for short columns where the

length to width ratio of less than 10 to 12 (Terzaghi et al., 1996; Tomlinson and Woodward, 2014). Satibi (2009) derived his analytical model using the coefficient of lateral pressure K_s to model the column installation effect. However, the author has used RF parameter in lieu of K_s because the stone column can be considered in most construction applications as a short column normally installed in soft soils to improve their compressibility and strength, accordingly.

There are a few methods to simulate the stone column installation effects. However, Priebe's approach (Priebe, 1995) is the most accepted method in the industry. It is based on the increase in the coefficient of lateral earth pressure (K_s=1.0) to simulate the stone column installation.

Satibi (2009) derived the column critical length and settlement after improvement as follows:

$$\boldsymbol{l_{critical} = \sqrt{\frac{2\,.\,q}{\beta\,.\,\gamma'}}} \qquad (5.6)$$

$$\boldsymbol{S = S_l + \frac{\left(q+\gamma'\,.l+\frac{\gamma'}{\beta}\right)}{E_{oed,1}\,.\beta}\,.\left(1 - e^{-\beta l}\right) - \frac{\gamma'\,.l}{E_{oed,1}\,.\beta} - \frac{\gamma'\,.l^2}{2\,.\,E_{oed,1}}} \qquad (5.7)$$

Critical stone column length $l_{critical}$ is the column length that satisfies the criteria where the entire embankment/foundation load is resisted by the floating stone column and no load is transferred to the soil where β can be calculated as follows:

$$\boldsymbol{\beta = \left(\frac{2r}{R^2 - r^2}\right)\,.RF} \qquad (5.8)$$

and E_{oed} is the oedometer modulus of the soft soil layers taken as tangent modulus and can be determined by a power law relation (Brinkgreve et al., 2014):

$$\boldsymbol{E_{oed} = E_{oed}^{ref}\,.\left(\frac{\sigma'_v}{p^{ref}}\right)^m} \qquad (5.9)$$

where E_{oed}^{ref} = tangent stiffness for primary oedometer loading at the reference pressure p^{ref}=100kPa.

m= power for stress level dependency of stiffness.

According to Stroud and Butler (1975), oedometer modulus E_{oed} can be estimated from the following equation:

$$\boldsymbol{E_{oed} = \frac{1}{m_v}} \qquad (5.10)$$

E_{oed}^{ref} can be determined using a recommended coefficient of volume compressibility for high compressible clays m_v= 0.6 x 10^{-3} m^2/kN (Carter and Bentley, 1991). Satibi et al. (2009) has used E_{oed}^{ref} = 1 MPa; however, a typical design input of E_{oed}^{ref}= 1.5 MPa is used in this analysis for a soft sensitive clay (taken m= 1 and $P_{ref} = 100\ kPa$). Therefore, above equation (5.9) reduces to E_{oed}= 15. σ_v'. The effective stress σ_v' is calculated at the middle of the soft soil layer and includes an additional applied load. The oedometer modulus of soft soil can be determined as follows:

$$\boldsymbol{E_{oed,1} = 15\ (0.5\ l\ \gamma' + 0.5\ q\ )} \qquad (5.11)$$

$$\boldsymbol{E_{oed,2} = 15\ (0.5\ (H + l)\gamma' + 0.5\ q\ )} \qquad (5.12)$$

Therefore, the settlement after ground improvement in equation (5.7) can be calculated using above oedometer moduli in equations (5.11) and (5.12). The effectiveness of the footing system constructed over stone columns can be investigated based on the RSR factor in equation (5.1).

5.3 Settlement improvement analysis

The main objective of this section is to examine the improvement in the settlement performance of the footing/embankment due to the installation of stone columns in the soft clay. A hypothetical soft soil profile is considered in the build-up of the analytical model to perform a comparison between the analytical model and the FEA. The soil and stone material properties (Table 5.1) used in the FEA are

representative of most of the soft soils where the use of the stone columns as an improvement technique is of growing interest.

Table 5.1 Material parameters for models.

Properties		Soft Soil	Stone
φ'	[°]	25	45
c'	kPa	0.1	0.1
ψ	[°]	0	15
γ	kN/m^3	16.5	19
$E_{50}^{ref} = E_{oed}^{ref}$	MPa	1.5	70
E_{ur}^{ref}	MPa	4.5	210
υ_{ur}	[-]	0.2	0.2
m	[-]	1	0.5

The proposed analytical approach has been used to predict the critical length of the stone column and to assess their effectiveness (Table 5.2), with the radius of the circular cell lies in the range (R) = 0.5 to 0.75 m and a stone column radius of r = 0.3 m. In this analysis, the soft soil has the effective unit weight of 6.5 kN/m^3 and the effective angle of internal friction equal to 25°.

Table 5.2 Analytical model predicted critical column length $L_{critical}$ and L/d ratio.

	$L_{critical}$			**L/d**		
	Column spacing s (m)			**Column spacing s (m)**		
RF	1.0	1.2	1.5	1.0	1.2	1.5
0.42	3.13	4.06	5.37	5.22	6.77	8.95
0.5	2.86	3.72	4.92	4.76	6.2	8.2

It is interesting to note that the critical column length suggested by the analytical model is consistent with the findings of Hughes and Withers (1974), Narasimha Rao et al. (1992), McKelvey et al. (2004), and Black (2006). Hughes 1974 suggested that the column shorter than 4d would fail by punching where it was found that the shear stress and end bearing pressure are lower than the bulging capacity for columns shorter than L<4d. A critical column length appears to exist

between 5 to 7 times the column diameter beyond which no further increase in ultimate capacity is gained (Narasimha Rao et al., 1992). McKelvey et al. (2004) suggests that there is some merit in installing columns longer than the bearing capacity critical column length to control settlement. The findings of Black (2006) are consistent with McKelvey et al. (2004) who carried out a laboratory study on small groups of columns and suggested that the ratio between the critical column length to the column diameter exists and lies in the range L/d= 6-10. As a result of these studies, it is suggested that the column critical length lies in the range L/d= 4 to 10. The column critical length predicted by the analytical model suggests that it lies in the range L/d= 4.76 to 8.95, as shown in Table 5.2.

The reduction factor is set to be equal to 0.42 where the coefficient of lateral earth pressure K_s is set to be equal to 1.0 in order to account for the installation effect of the stone columns, which is consistent with the value proposed by Priebe (1995). However, a value of the lateral earth pressure of K_s=1.2 (equates to RF= 0.5) is used to investigate the impact of the column installation effect on reducing the footing settlement. The reduction factors of 0.42 and 0,5 were derive based on that the soft soil is a non-dilating soil therefore $\tan\delta = \sin\varphi'$ for ultimate skin friction as indicated by Satibi (2009), and Vermeer and Sutjiadi (1985).

A numerical parametric study is carried out using PLAXIS 2D code and compared with the analytical model to examine the impact of various key parameters such as soil layer thickness and stone column spacing upon the column-foundation settlement performance.

Finite Element program PLAXIS 2D is used to model the stone column behaviour where the soil and the stone are both modelled using the Hardening Soil model. The stone column reinforced foundation has been analysed by the axisymmetric

soil model similar to that used in the analytical approach. The geometry and mesh used in FE analysis are shown in Figure 5.2. The external boundary has a radius of 0.5 m to 0.75 m to simulate typical column spacing of 1.0 m to 1.5 m and the stone column radius is equal to 0.3m.

A vibrating poker is normally used to install the stone column (Bottom-feed system) with a fixed diameter of 430mm in the soft soils. It is most common that the column diameter of 600 mm is constructed using such poker diameter. The completed column diameter is alwayes greater than the initial diameter of the vibrating poker depending upon the soil type, soil strength, stone size, constuction method and the characteristic of the vibrating poker.

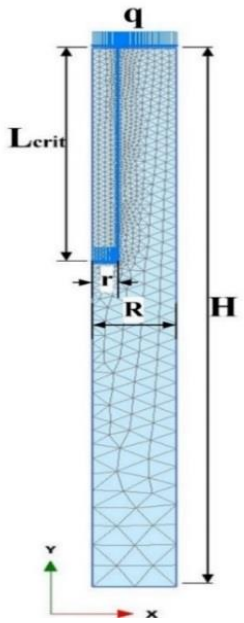


Figure 5.2 FE mesh and geometry.

In the subsequent FE and analytical analyses, the settlement behaviour of various configurations of soft soil thickness and stone column spacing is examined for an applied pressure up to 50 kPa, a typical working stress for a stone columns installed in the soft clay. Boundary conditions are applied by preventing the horizontal displacement at the vertical side of the mesh and preventing both the

vertical and horizontal movements at the bottom. The ground water level is set to be at the ground level.

The Hardening Soil model is used for the soft soil and stone column materials. The influence of stone column installed in soft clay with different soft soil thickness upon the relative settlement reduction ratio (RSR) is shown in Figure 5.3 to Figure 5.8 and Figure 5.10 to Figure 5.13. The effectiveness of stone columns is evaluated using the relative reduction in settlement (RSR). As the stone column length increases, the RSR ratio increases. A similar trend in the RSR ratio is observed for both of the FE and analytical model analyses.

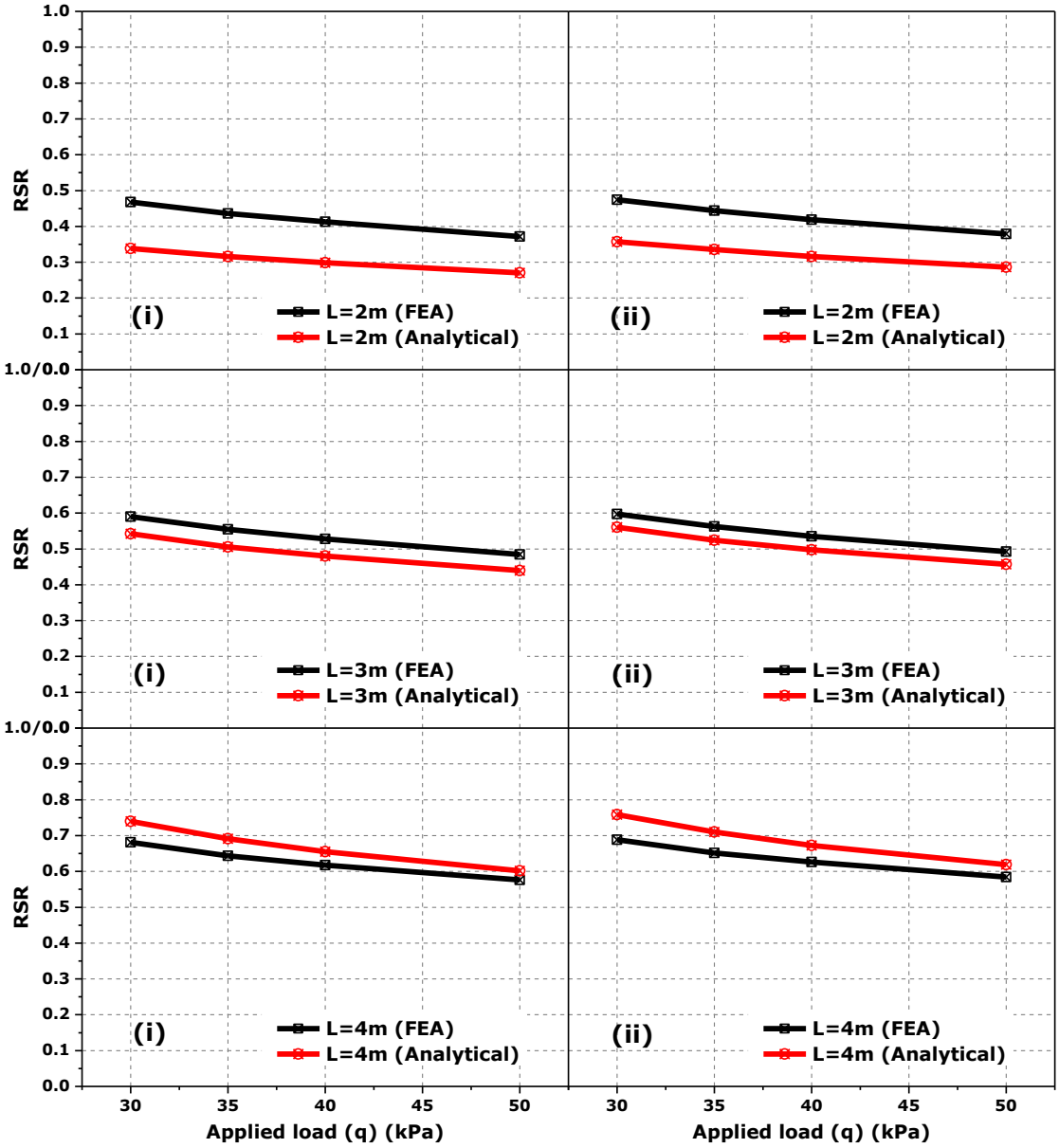


Figure 5.3 Variation of RSR with column length for (i) RF= 0.42 and (ii) RF= 0.5 for soft soil thickness of H= 10 m and column spacing of s= 1.0 m.

The results indicate that the stone columns significantly improve the settlement performance of the footings in the range from approximately 21% to 75% (see Figure 5.3 to Figure 5.5). In general, the effectivness of installing the stone columns is between 42% to 61% at the critical column length for the soft soil thickness H = 10 m (see Figure 5.13).

The predictions from both the analytical model and the FEA agree relatively well. It can be also seen that the FE analysis and the analytical model predicted close RSR values at various column lengths.

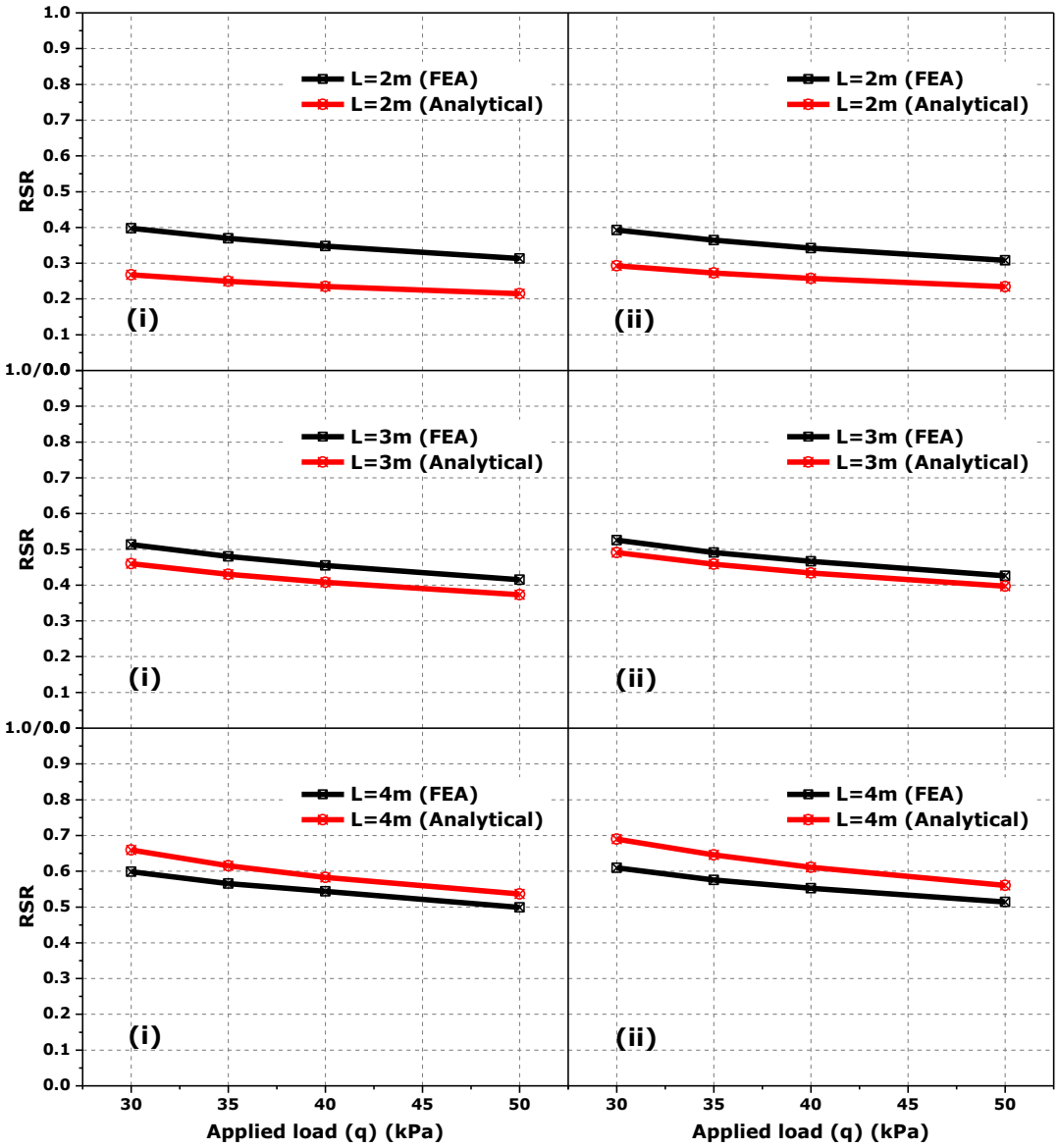


Figure 5.4 Variation of RSR with column length for (i) RF=0.42 and (ii) RF= 0.5 for soft soil thickness of H= 10 m and column spacing of s= 1.2 m.

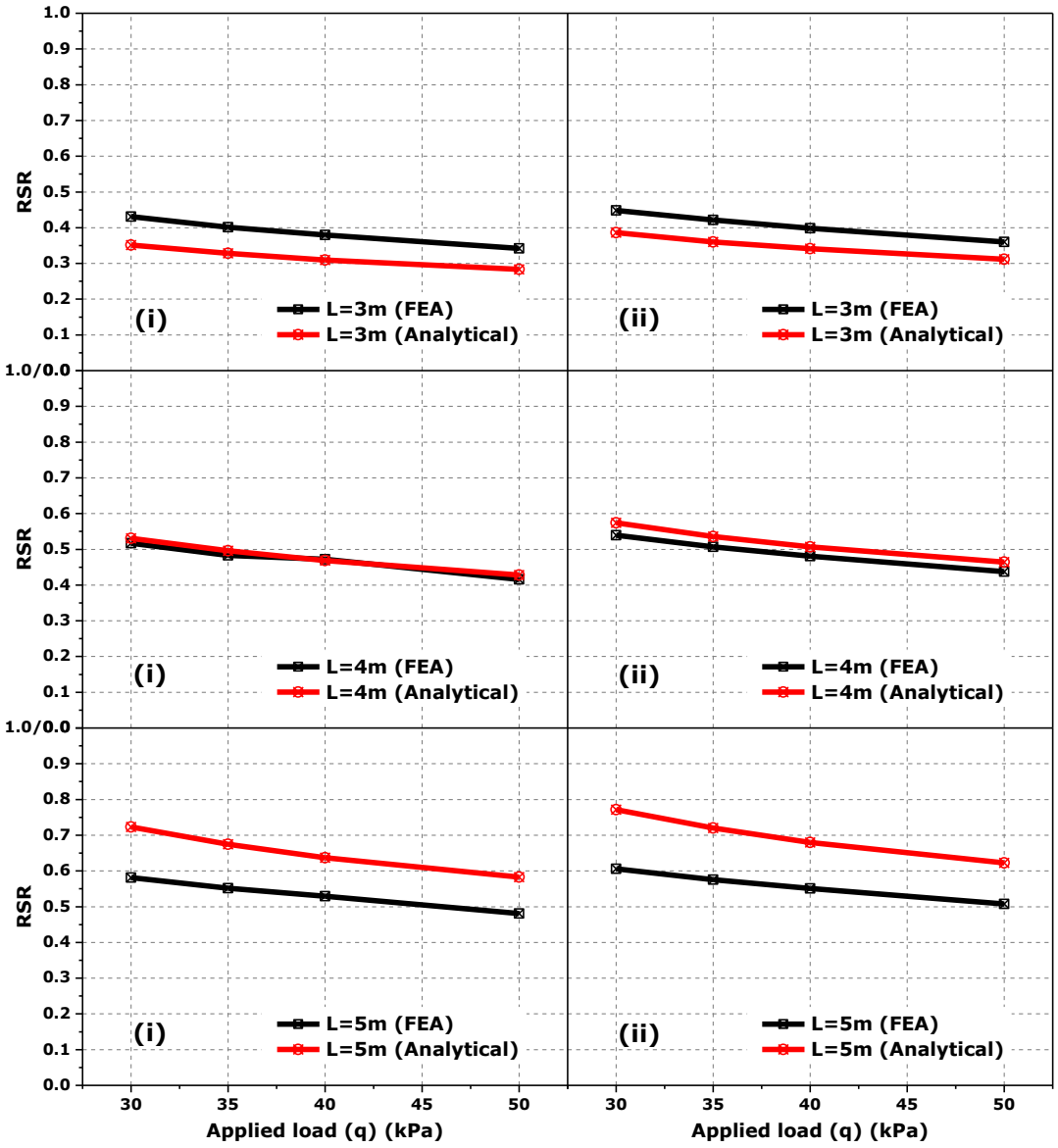


Figure 5.5 Variation of RSR with column length for (i) RF= 0.42 and (ii) RF= 0.5 for soft soil thickness of H= 10 m and column spacing of s=1.5 m.

As outlined previously in Section 5.2, the analytical model is derived on the basis of critical column length and, therefore, the RSR can only be predicted for a column length up to a critical length. The influence of increasing the soft soil thickness (H) from 10 m to 14.5 m upon the RSR is shown in Figure 5.6 to Figure 5.8, respectively.

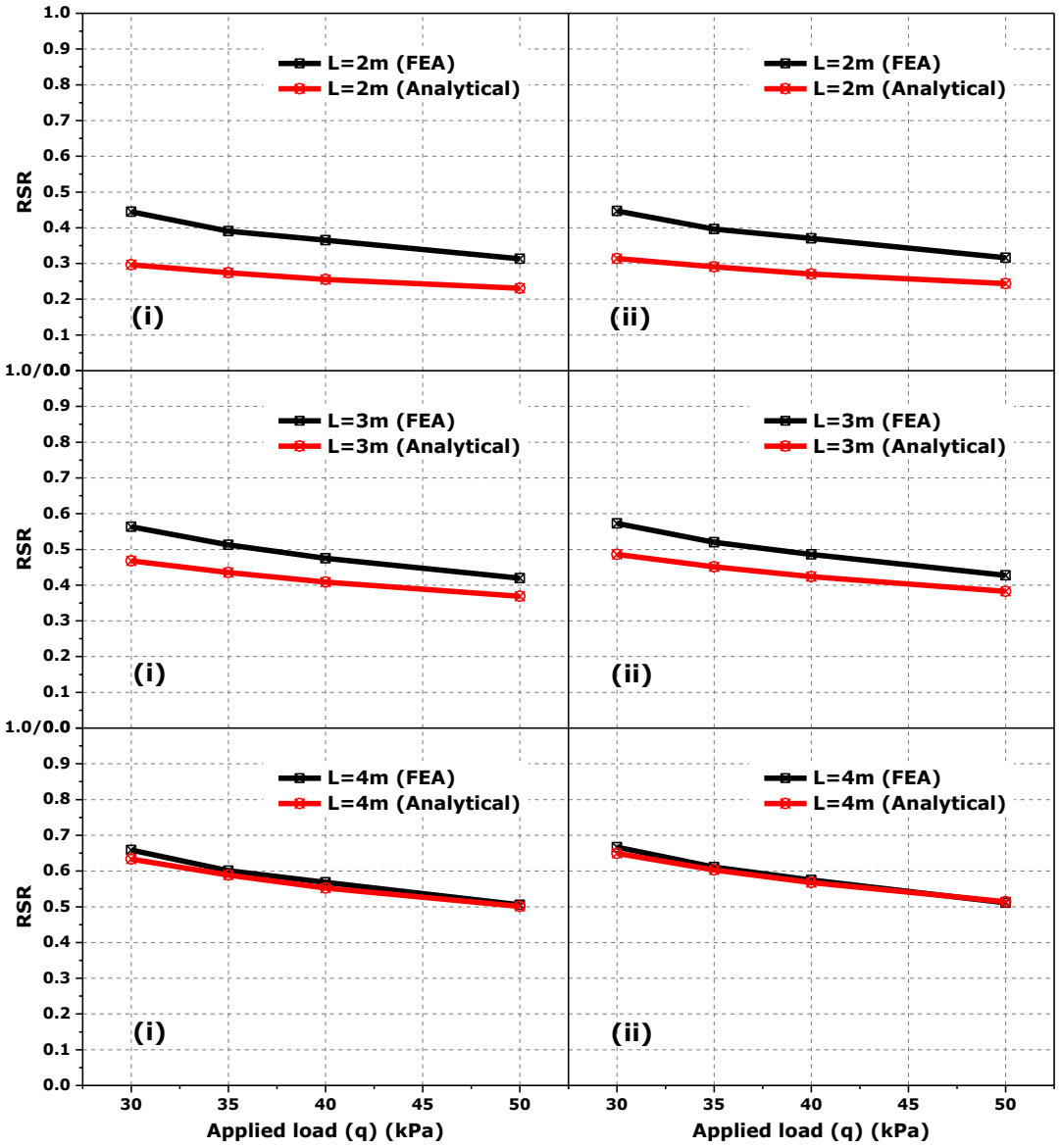


Figure 5.6 Variation of RSR with column length for (i) RF= 0.42 and (ii) RF= 0.5 for soft soil thickness of H= 14.5 m and column spacing of s= 1.0 m.

While all plots indicate that all column arrangement exhibit similar variations of RSR with column length, the rate of the improvement in the settlement performance slightly reduces for applied pressures higher than 40 kPa.

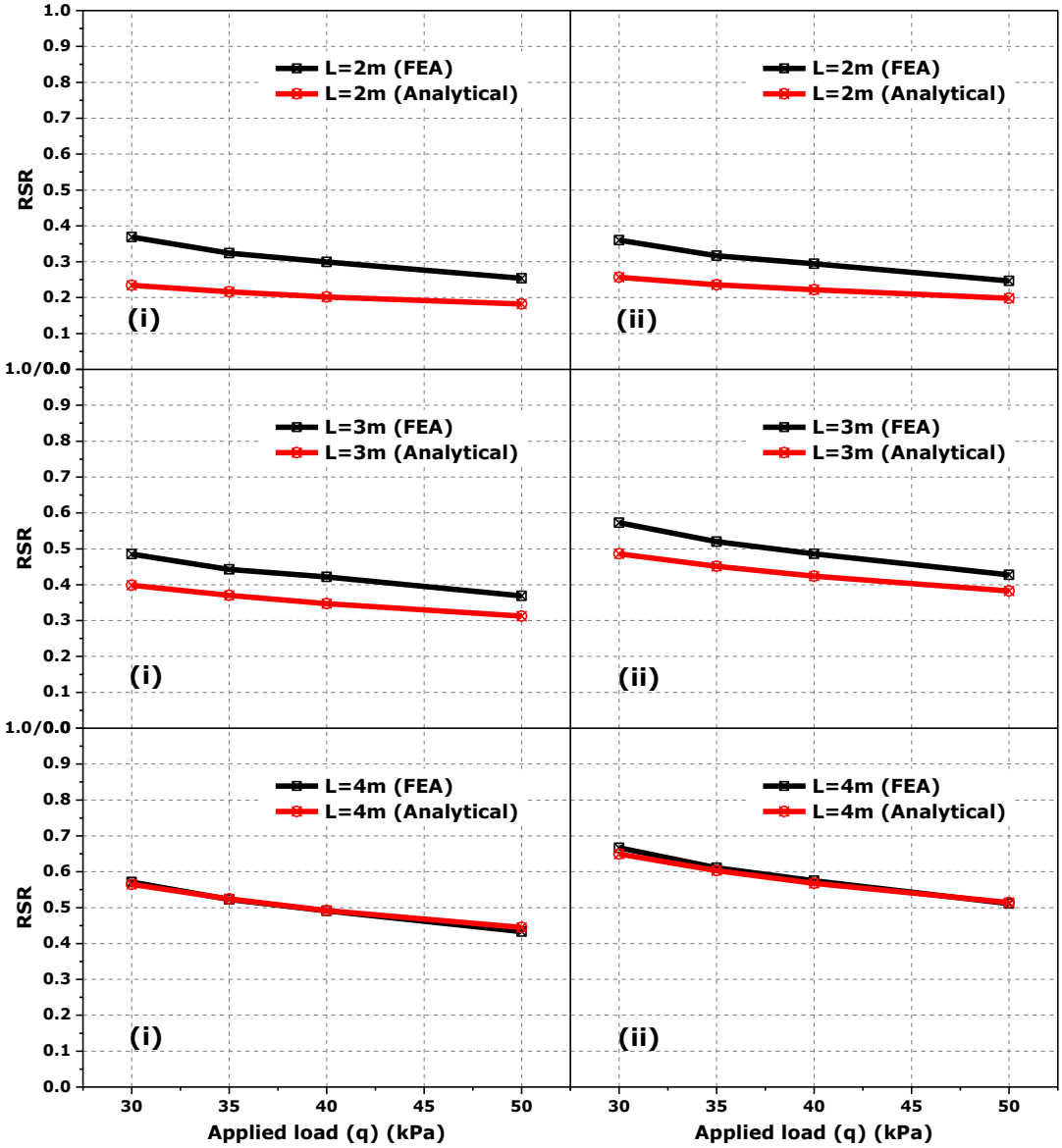


Figure 5.7 Variation of RSR with column length for (i) RF= 0.42 and (ii) RF= 0.5 for soft soil thickness of H= 14.5 m and column spacing of s= 1.2 m.

This suggests that heavily loaded columns are deforming at shallow depths and only transfer a small proportion of the load to the toe of the columns. The reduction in the settlement ratio with length, corresponding to a column spacing of 1.5 m, is less than 1.2 m. The RSR values from the numerical analysis are compared with those from the analytical method.

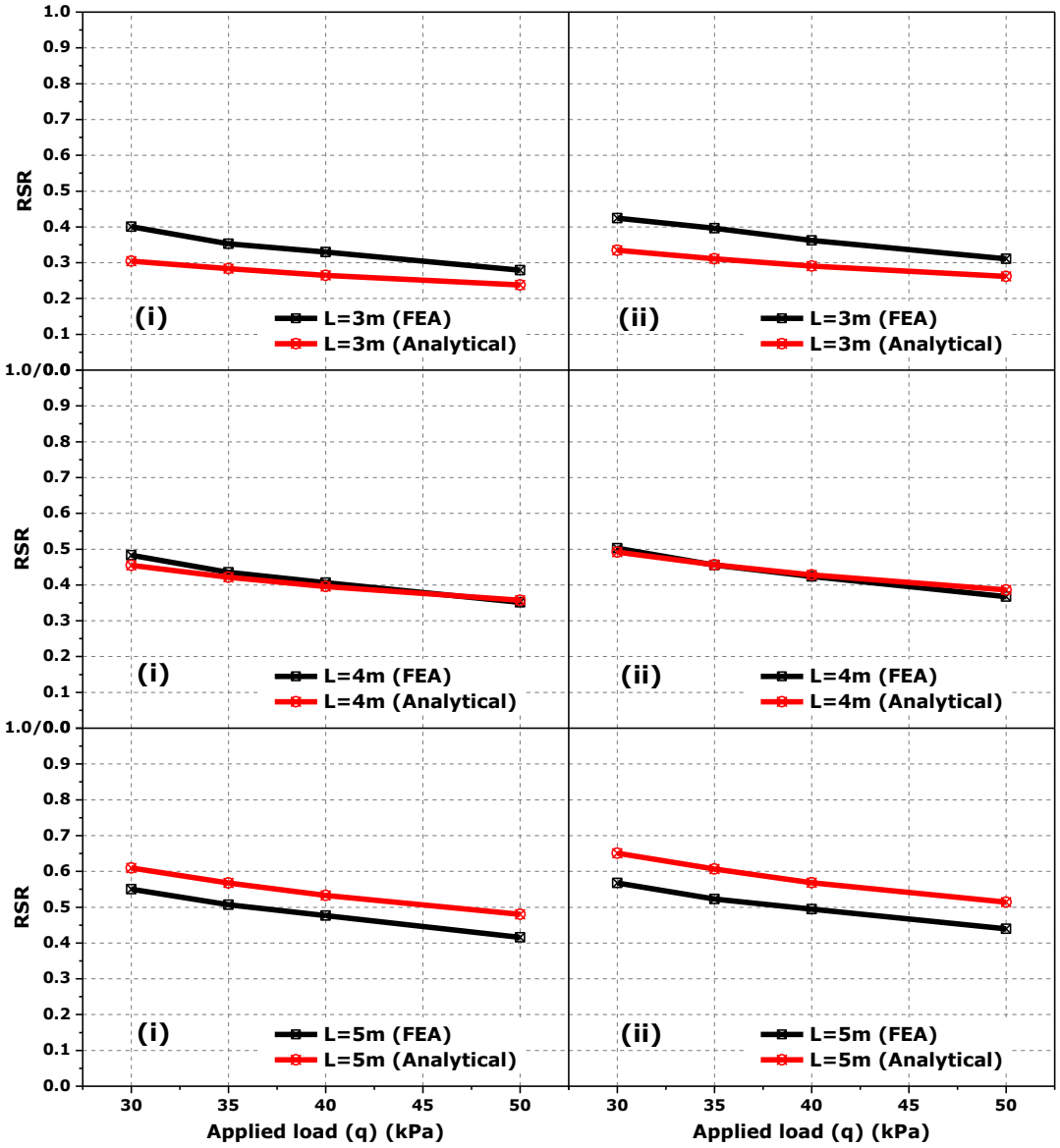


Figure 5.8 Variation of RSR with column length for (i) RF= 0.42 and (ii) RF= 0.5 for soft soil thickness of H= 14.5 m and column spacing of s=1.5 m.

The variation of the RSR with applied load ranges from 1% to 13% at the column lengh up to the the critical column length. The distribution of plastic points along a cross section of column spacing corresponding to 1.0 m, 1.2 m, 1.5 m, and 2 m is shown in Figure 5.9. Plastic points represent stone elements which lie on the MC failure line.

It can be seen that the plastic point extends deeper for the higher area ratio (area ratio (A/A_c) is the ratio of area of unit cell to stone column area). The extent of plastic points increases for wider columns (higher area ratio) may be explained by the fact that the average column load increases for wider columns. This suggests that columns are in more of a plastic state for higher area ratio and hence the column plasticity reduces the ability of load transfer to column base and, consequently, leads to a lower improvement in the RSR ratio corresponding to the higher area ratio.

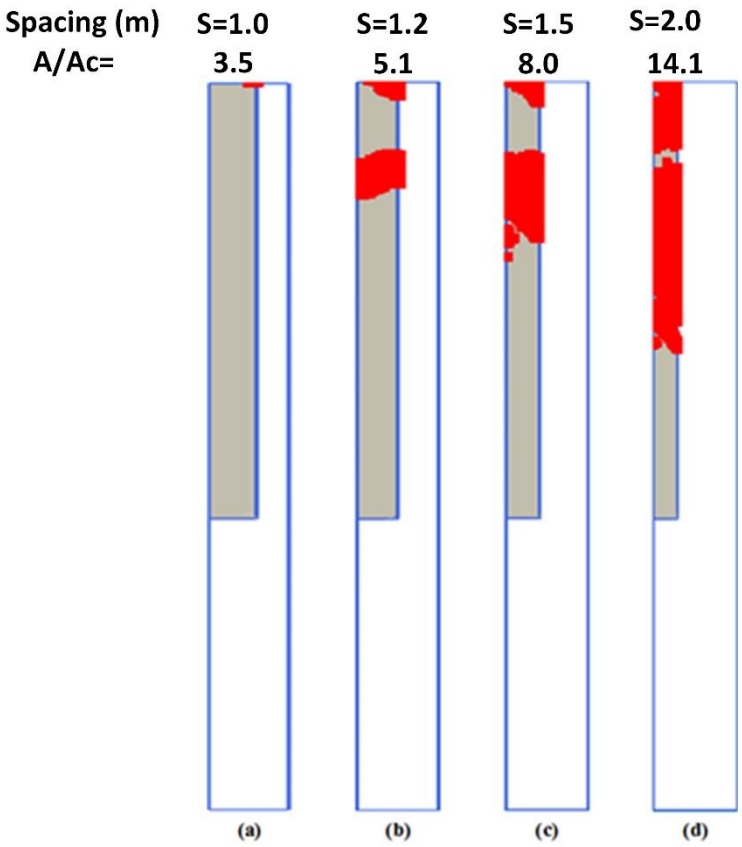


Figure 5.9 Distribution of plastic points within a cross-section of (a) A/A_c= 3.5, (b) A/A_c=5.1, (c) A/A_c=8.0, and (d) A/A_c= 14.1 for column length of 6 m.

The variation of the RSR – determined by FE analysis and analytical model- with applied load for a unit cell and column spacing of s= 1.0 m, s= 1.2 m, and s= 1.5 m (soft soil thickness of H= 20 m) are shown in Figure 5.10, Figure 5.11, and Figure 5.12, respectively.

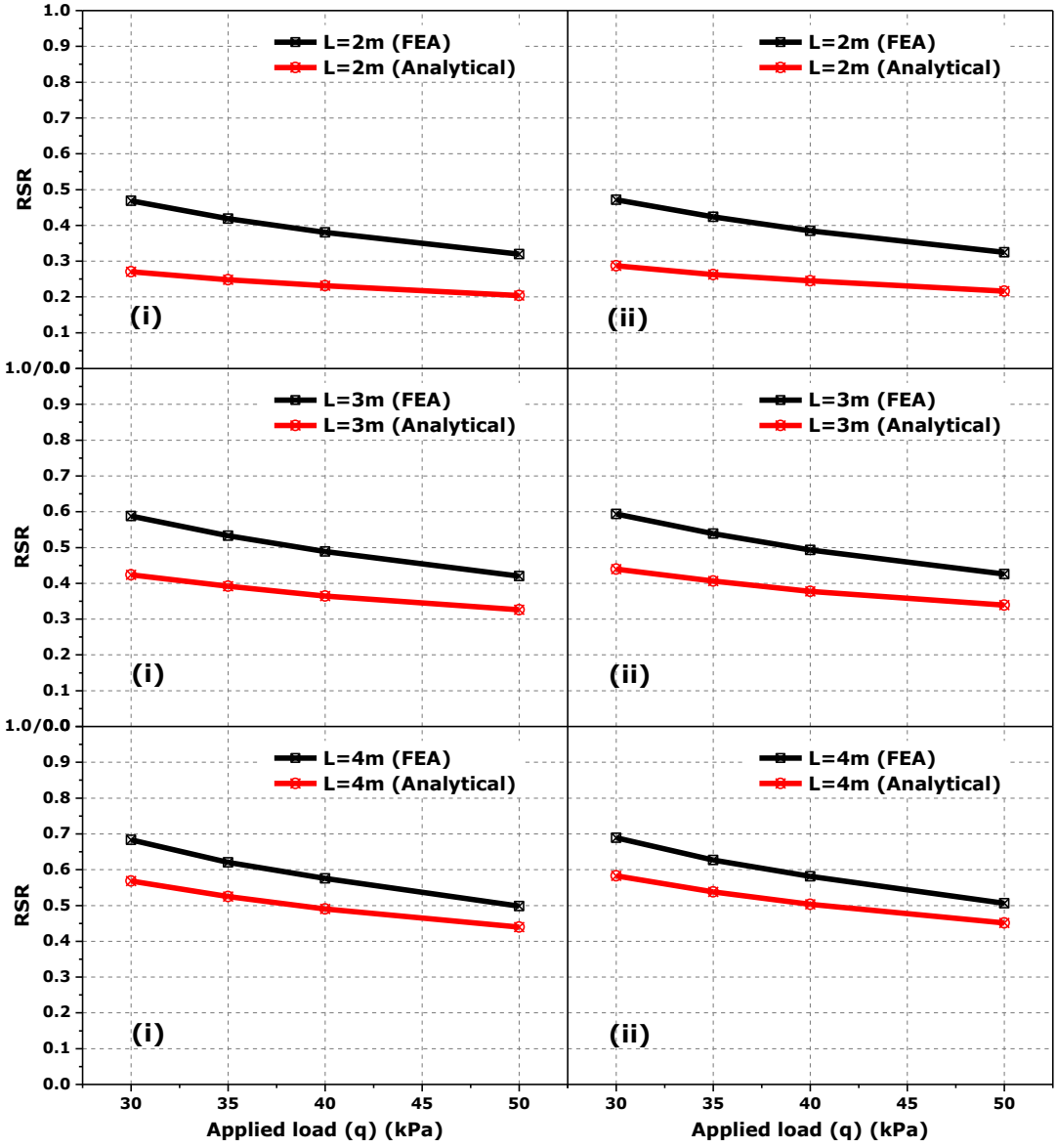


Figure 5.10 Variation of RSR with column length for (i) RF= 0.42 and (ii) RF= 0.5 for soft soil thickness of H= 20 m and column spacing of s=1.0 m.

The difference between the RSR values predicted by both FE and analytical models are found to be negligible (up to 4%) at the critical column length (Figure 5.13) with the exception of soft soil thickness column spacing s= 1.0 m, where the variation in predicting RSR was no greater than 9% at the critical column length. It is can be seen from Figure 5.10 that the agreement between the analytical and

numerical models, in predicting RSR, breaks down at closley-spaced columns where the difference in predicting the RSR is up to 19%.

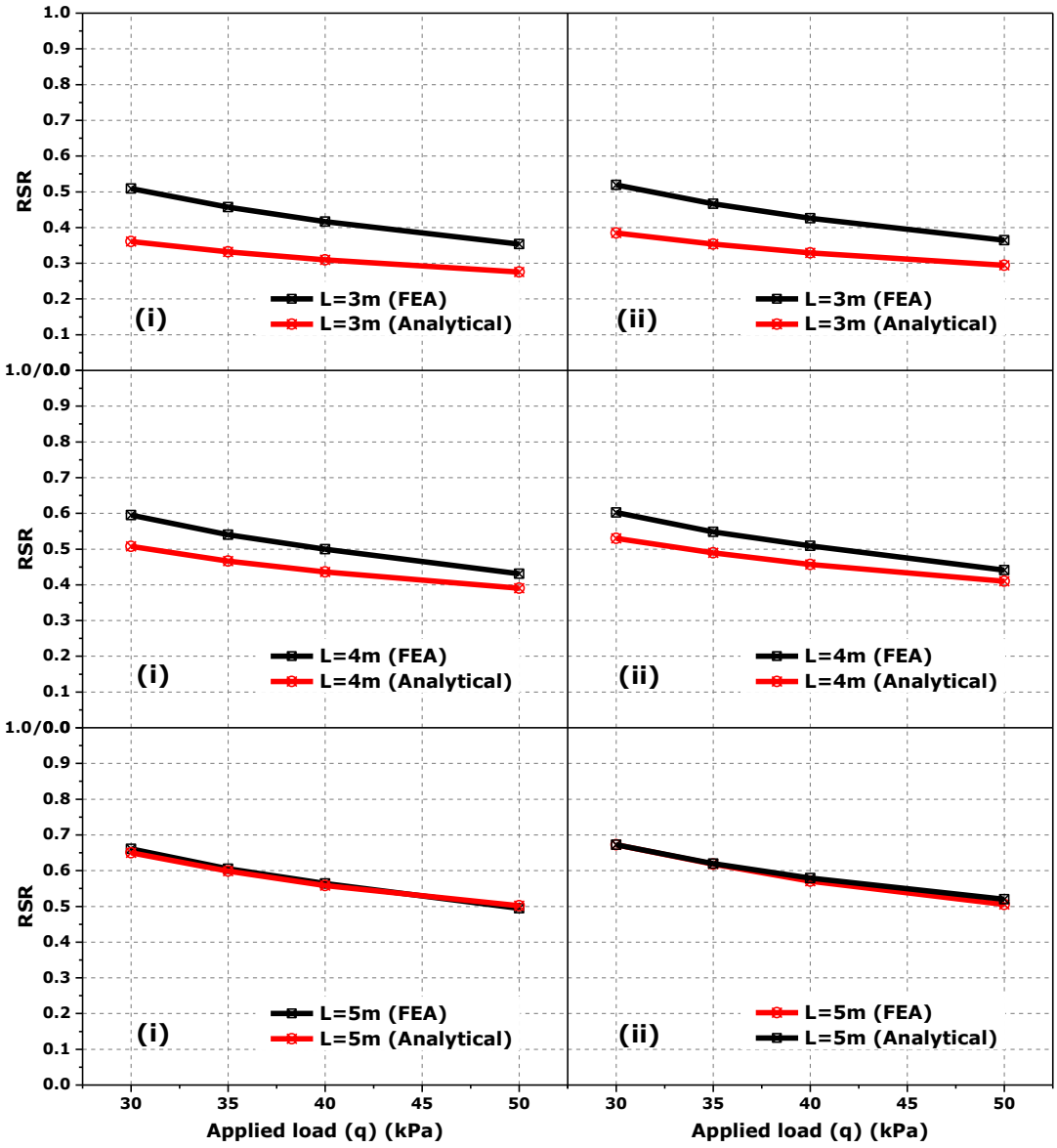


Figure 5.11 Variation of RSR with column length for (i) RF= 0.42 and (ii) RF= 0.5 for soft soil thickness of H= 20 m and column spacing of s=1.2 m.

It may be attributed to that closely-spaced columns are acting with the surrounding soils as a 'Block'. The FE analysis is capable of capturing the presence of a 'Block' behaviour and therefore, capable of modelling more realistic soil-column interaction than the analytical model. In the subsequent FE analysis, a

'Block' mechanism of various column spacings is investigated to examine their infulence upon the footing settlement performance.

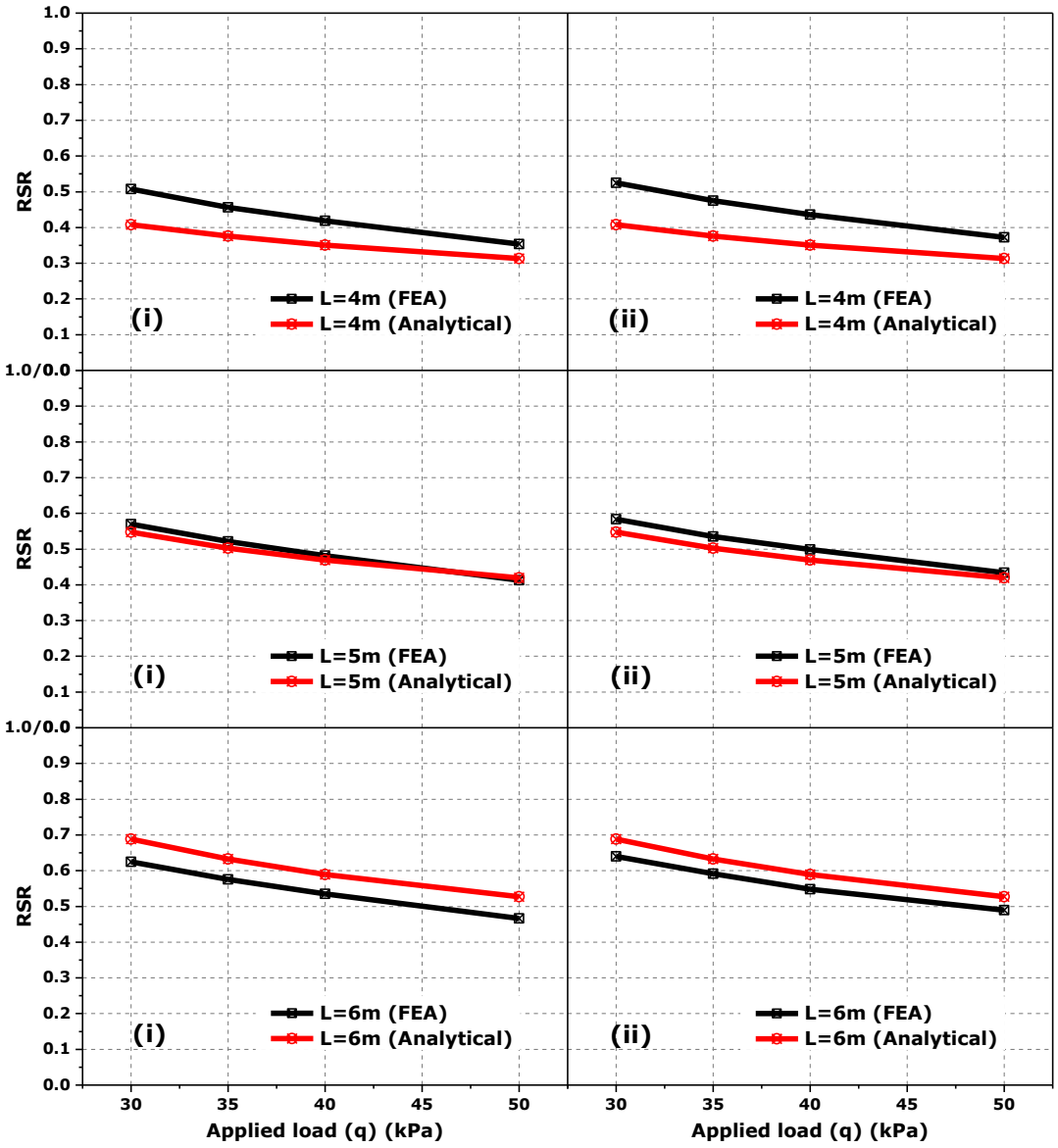


Figure 5.12 Variation of RSR with column length for (i) RF= 0.42 and (ii) RF= 0.5 for soft soil thickness of H= 20 m and column spacing of s= 1.5 m.

It is interesting to note that increasing the soft soil thickness from H=10 m to H= 14.5 m and H= 20 m has a slight impact on the RSR, where column effectivness

lies in the range of 17% to 60% at different column lengths (Figure 5.3 to Figure 5.8 and Figure 5.10 to Figure 5.13).

The effects of column installation upon settlement improvement is investigated by increasing the lateral coefficient pressure in the soft clay from K_s= 1.0 (RF= 0.42) to K_s= 1.2 (RF= 0.5). The influence of increasing the reduction factor is shown in Figure 5.3 to Figure 5.8 and Figure 5.10 to Figure 5.12. It is evident that increasing K_s over 1.0 is of minor significance upon the RSR predictions.

In general, it can be seen that increasing RF slightly enhances the settlement performance predicted by the analytical model. The range of increase is between 1% and 5%. However, a slight decrease in the RSR ratio (between 1 and 5%) is observed in FE analysis. This may be explained as the settlement of untreated footing benefits more than the footing improved with the stone column installed by increasing lateral coefficient pressure and hence RSR decreases slightly.

In fact, a light increase in RSR is observed for closed space columns with the soft soil thickness of H= 20 m. This suggests that the RSR is less dependent on the confinement pressure provided by the surrounded soils than other parameters such as column length, soft soil thickness and applied loads.

The variation of RSR with the ratio of column critical length to the soft soil thickness ($l_{critical}$/H) at applied pressure of 50 kPa is shown in Figure 5.13. In general, it can be seen that the effectiveness of reinforcing soft soils by stone columns is with column critical length in the range of 0.35 to 0.6 times soft soil thickness. However, effectiveness predicted in this simplified method need to be assessed alongside the total and differential settlements to evaluate if ground improvement is satisfying specific project performance criteria.

A good agreement exisits between both the FE analysis and the analytical model in predicting the RSR for all coefficients of lateral pressure (simulate column

installation) when the soft layer thickness over the critical column length ratio ($H/L_{critical}$) = 2 to 5.

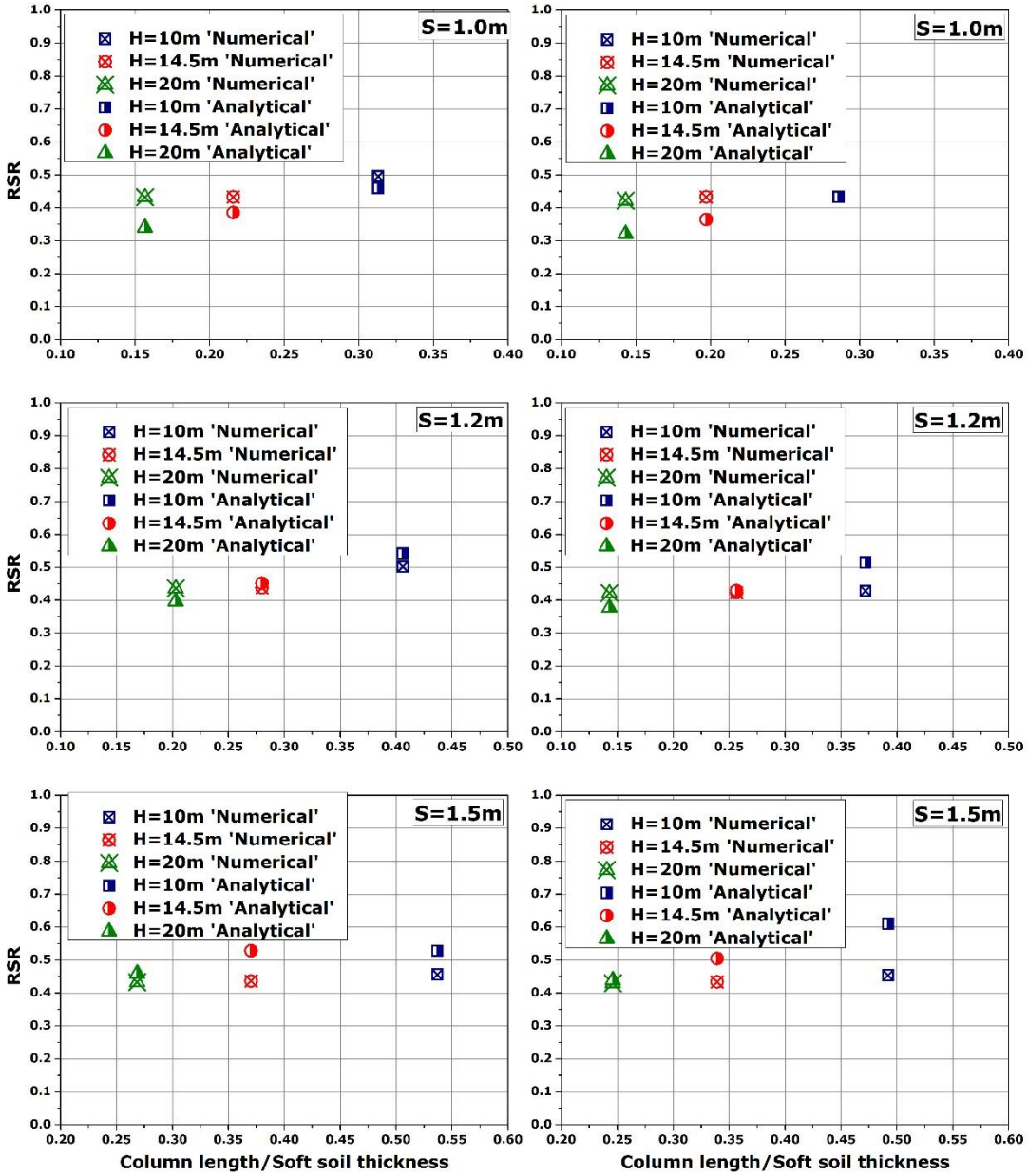


Figure 5.13 Variation of RSR with critical column length to the soil thickness ($l_{critical}/H$) for (i) RF= 0.42 and (ii) RF= 0.5 at applied pressure= 50 kPa.

5.3.1 Settlement improvement of single and strip footings

In general, the bearing capacity of stone columns is a less stringent design criterion than the settlement in soft soils (see Section 5.1). Considerable advances have been made in the soft soils constitutive models to incorporate the effect of bonding, creep and anisotropy in FEA. However, there is very limited use of such models by industry practitioners in ground improvement designs due to their complexity and the requirements of detailed and expensive soil investigations which are not always available.

The most common design methods in stone column practice involve some empiricism in formulae derivations and many simplifying assumptions. It was worthwhile to carry out some modifications on the simplified analytical model in Section 5.2 to calculate the settlement improvement in stone columns under single and strip footings. Design charts developed by Priebe (1995) are used to predict the settlement of single pad and strip footings (Figure 2.25).

The total settlement of an unlimited column grid below a widely-loaded area before ground improvement (see equation 5.2) is used to calculate the settlement of spread and strip footings by applying Priebe's (1995) design charts reduction factor (Figure 2.25). The reduction factor (settlement of spread/strip footing over infinitely large group total settlement) can be calculated if the stone column diameter and length are known (see Figure 5.14). The settlement reduction factor is considered an acceptable approximation if the area ratio (A/A_c) is up to 10.

The main modifications of Satibi et al. (2009) analytical model which are adopted in this research can be summarised below:

1- The use of reduction factor RF in lieu of $K_s \,.\, tan\,\delta$ to simulate short columns (length over width ratio < 10 to 12).

2- Apply additional settlement factor to calculate the settlement of spread footings (see Figure 5.14).

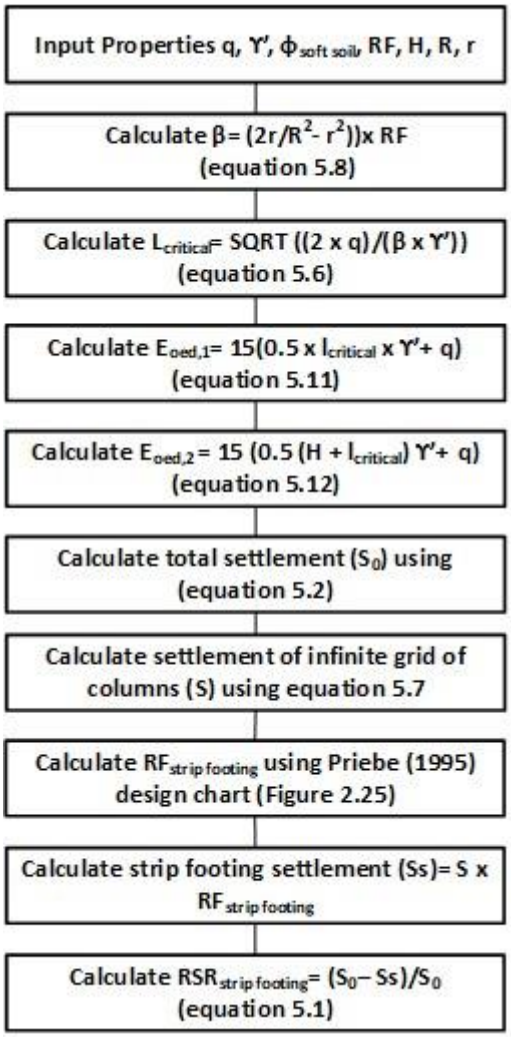


Figure 5.14 Simplified analytical model program used to predict the settlement of strip/spread footings

The various configurations of footings analysed are outlined in Figure 5.15. The RSR was predicted by analysing various column configurations such as single column, 2x2, 3x3 groups and a row of 2 columns under pad footing. The footings are 0.6 m thick and the depth of the footing is 0.6 m below ground surface. A typical bottom feed stone column diameter of 0.6 m installed in soft soils with a critical length in accordance with equation 5.6. A square grid of columns spaced

at 1.0, 1.2, and 1.5 m is used in the analyses. The footing overhang is located at half the column spacing (0.5xs) from the centreline of the outer row. The settlement performance of different stone column arrangements was calculated at 50kPa using soil properties in Table 5.1. The effectiveness of stone columns was measured using the reduced settlement ratio, (RSR), which is defined in Section 5.2.

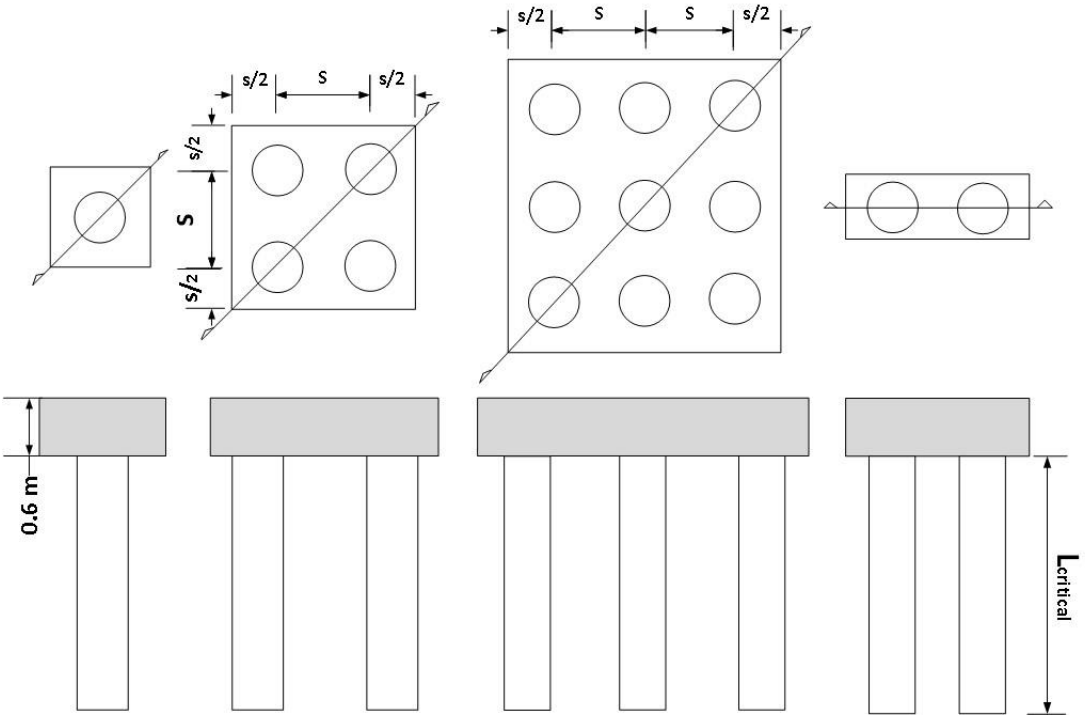


Figure 5.15 Column configurations to examine RSR of single footings.

The influence of column arrangement upon RSR is shown in Figure 5.16 and Figure 5.17. It can be seen that the maximum difference between RSR predicted by FEA and analytical model is 14% in some arrangements. Most of the results predicted less than 10% difference in calculated RSR using FEA compared to the analytical model. Therefore, this simplistic analytical model tool could be used to estimate the effectiveness of the stone columns installed under single footings at preliminary design stage, however, the settlement of the footing should be verified by measurements made after the construction of sacrificial or working stone columns.

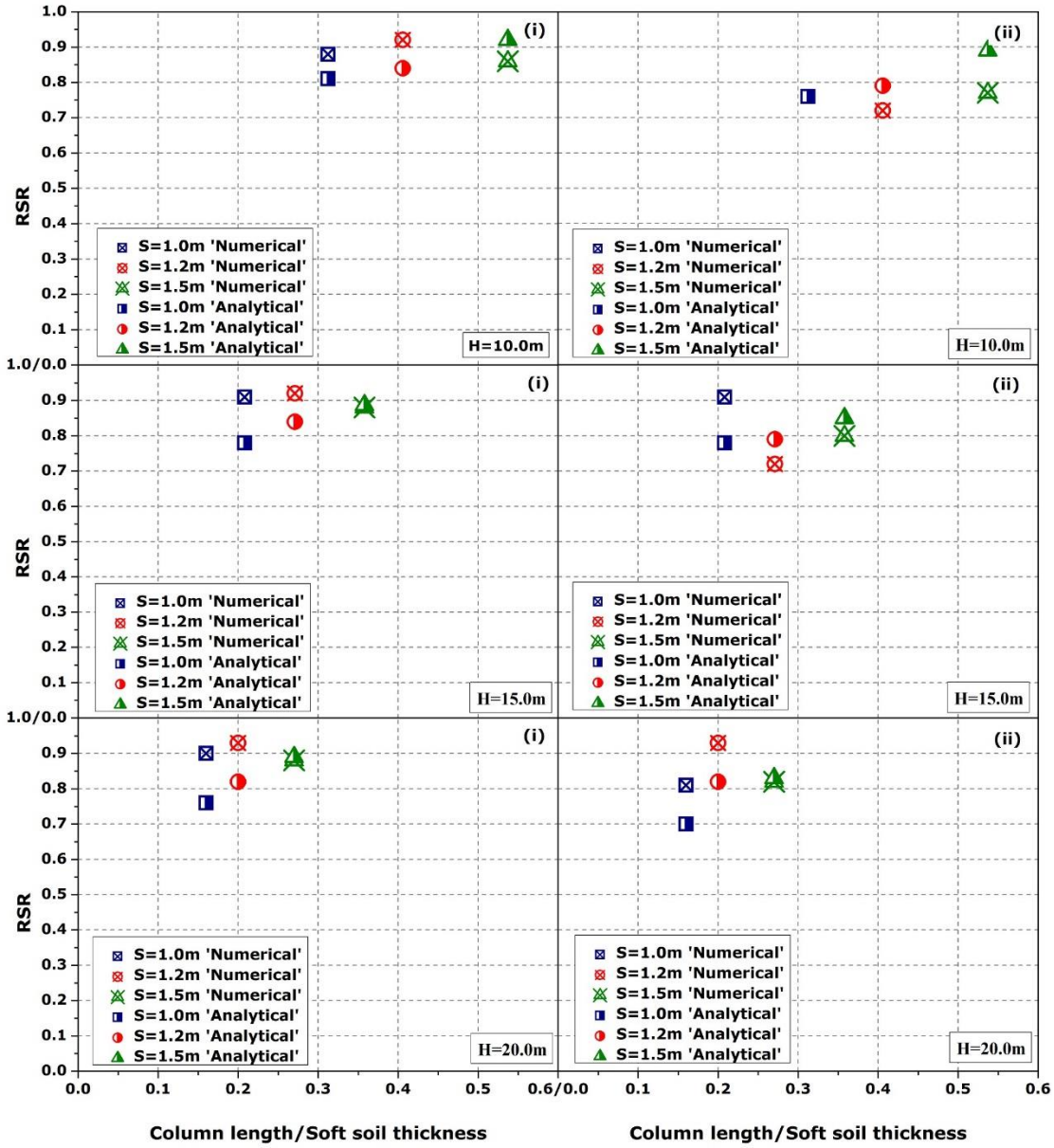


Figure 5.16 Variation of RSR with critical column length to the soil thickness ($l_{critical}$/H) for (i) Single footing and (ii) 2x2 group.

The stone columns constructed to support pad and strip footings are more effective than the stone columns beneath a wide loaded area in reducing the foundation settlement with a column critical length in the range of 0.6 to 0.93 times the soft soil thickness as indicated in Figure 5.16 and Figure 5.17. Therefore, installing stone columns to support pad footings is more effective in reducing settlement

compared to an infinite grid of columns supporting an infinitely wide load as shown in Figure 5.13.

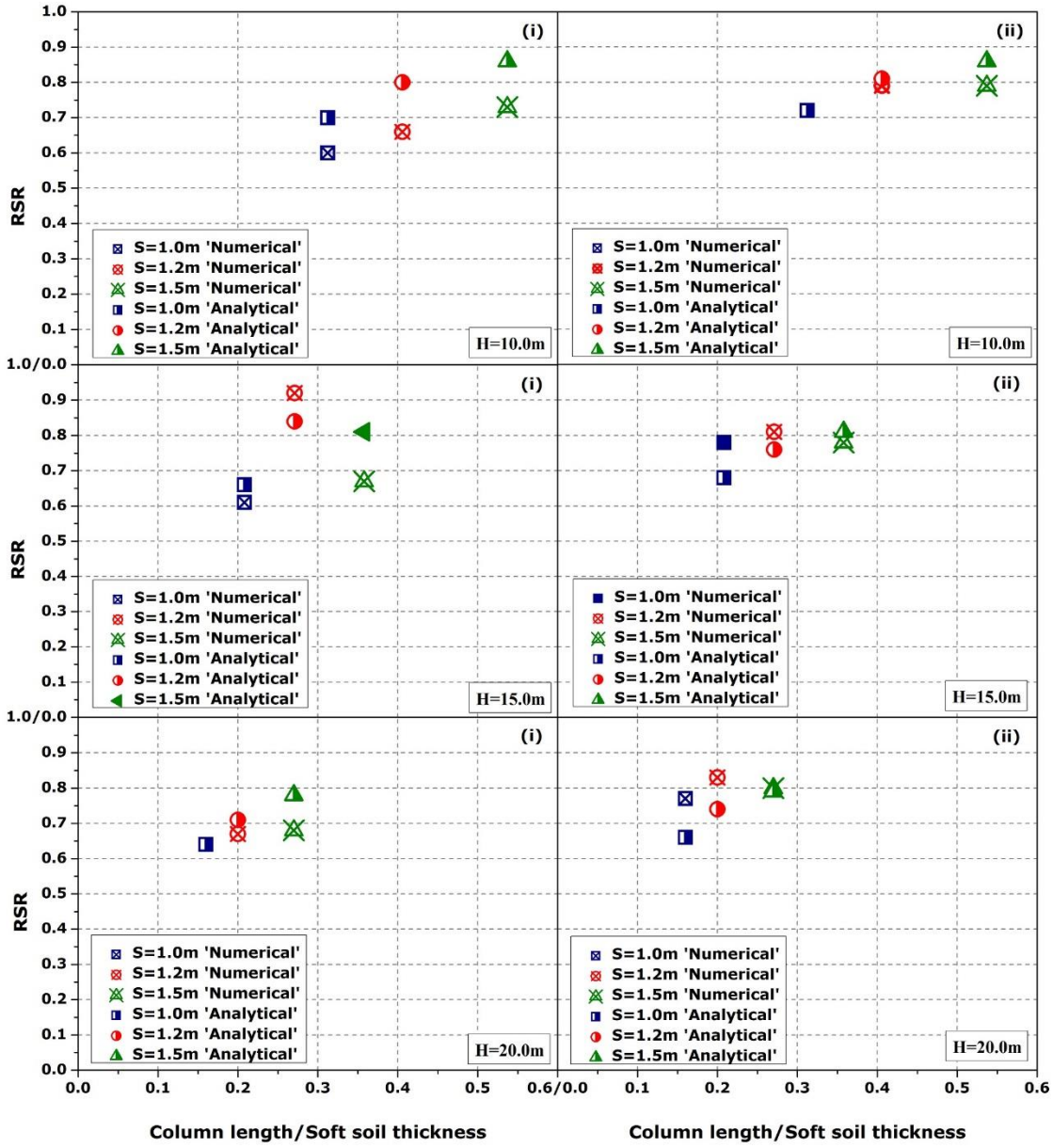


Figure 5.17 Variation of RSR with critical column length to the soil thickness ($l_{critical}$/H) for (i) 3x3 group and (ii) 2-column footing.

5.4 Definition of compression and punching ratios

It was identified by the seminal work of Hughes and Withers (1974) and Muir Wood et al. (2000) that the stone column can deforms in four modes: bulging, punching,

shearing and bending. Compression and punching ratios were used by McCabe and Killeen (2016) to identify the stone column different modes of deformation.

The compression and punching ratios are derived from the footing settlement at the surface ($U_{footing}$), vertical displacement of the soil surrounding the base of the stone columns averaged over a square zone with a width equal to column spacing (U_{soil}), and the column settlement (U_{toe}) as shown in Figure 5.18. The compression ratio is a very important parameter to measure the load transfer to depth and is defined as the column compression ($U_{footing}$-U_{toe}) normalised by $U_{footing}$.

$$\textbf{\textit{Compression ratio}} = \frac{U_{footing} - U_{toe}}{U_{footing}} \qquad (5.13)$$

A higher compression ratio suggests that the column deforming along their shaft and may be bulging at shallow depths. The compression ratio is limited in capturing column punching. Therefore, a punching ratio parameter is introduced to measure the relative settlement at the toe level of the column (U_{toe} – U_{soil}) normalised by the toe movement (U_{toe}). Punching ratio originally developed by McCabe and Killeen (2016) was normalising the relative settlement at the column base by the ground surface settlement. The compression of the column was included in the punching ratio developed by McCabe and Killeen (2016). It is considered more efficient by the researcher to normalise the relative settlement at the column base by the base movement when investigating the column punching. In order to compare the punching of the columns into soft soil layer, the punching ratio is used to quantify the proportion of loads transferred to the column base.

$$\textbf{\textit{Punching ratio}} = \frac{U_{toe} - U_{soil}}{U_{toe}} \qquad (5.14)$$

Compression and punching ratios are calculated using PLAXIS 2D to investigate the stone column mode of failure.

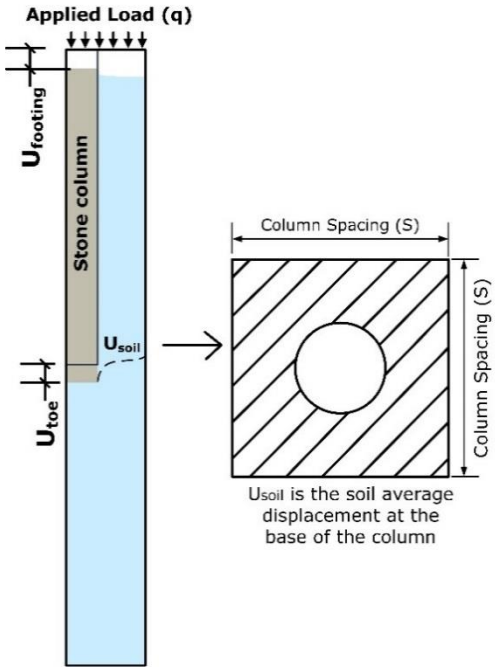


Figure 5.18 Displacements of footing, at column toe, and soil surrounding base of columns.

5.4.1 Deformational behaviour

5.4.1.1 Soft soil layer thickness

In this section, the mode of deformation will be discussed in terms of the influences of column length, soft soil thickness and lateral coefficient pressure (installation effect) with respect to area ratio (A/A_c). The variation of the punching ratio with the column length, lateral coefficient pressure, and area ratio for the soft soil thickness of 10 m and an applied load of 50 kPa is shown in Figure 5.19. It can be seen that the punching ratios are the largest for short columns at an area ratio of A/A_c= 3.53. In general, the punching ratio is decaying with increasing column length.

It can also be seen that columns at all area ratios larger than A/A_c= 3.53 exhibit a similar variation of punching ratio with the column length up to L= 2 m (up to L= 3 m for high area ratio) where punching ratios are observed to increase with column length.

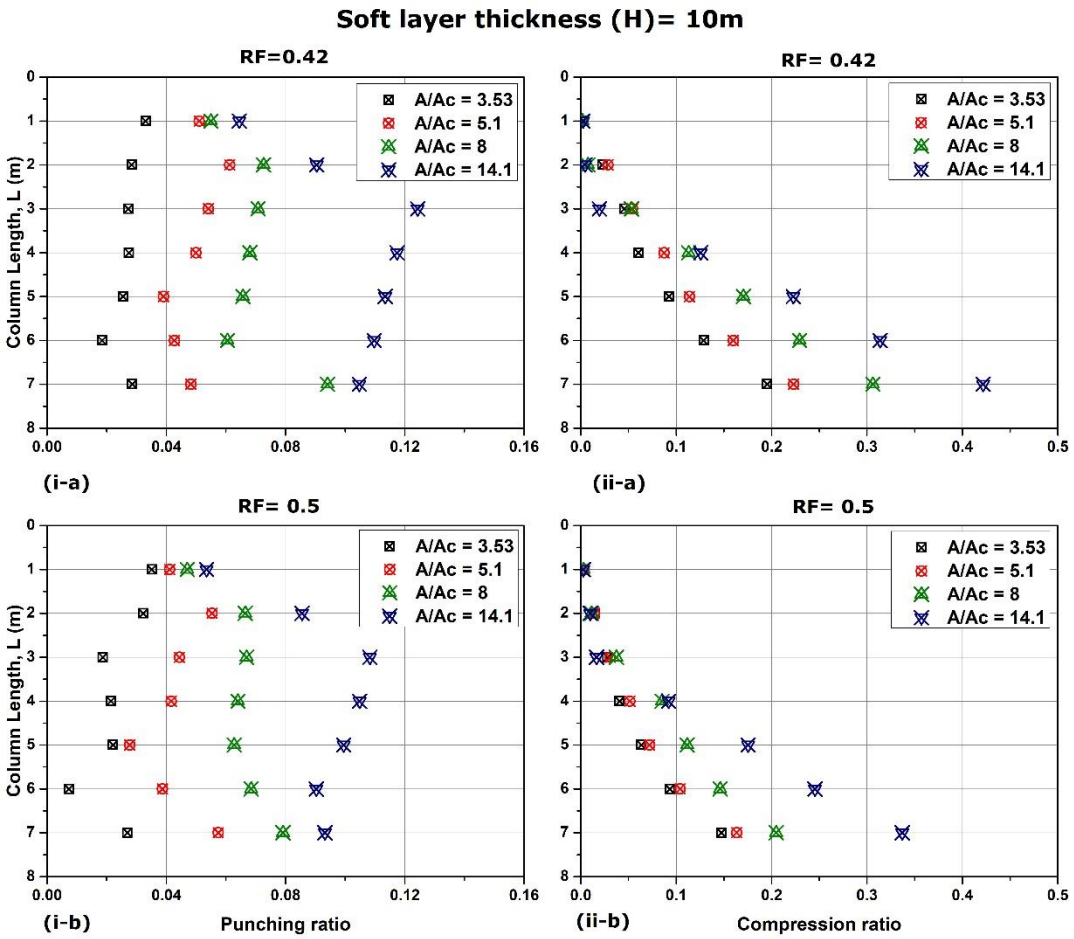


Figure 5.19 Variation of (a) punching and (b) compression ratios for lateral coefficient (i) RF= 0.42, and (ii) RF= 0.5 with column length for unit cell model.

It appears that the column is not deforming along the column shaft where punching and compression ratios increase with depth, therefore, punching is the dominant mode of deformation for shorter columns. It is evident that an increase in the area ratio leads to an increase in the punching ratio with increasing column length up to L= 2 m (up to L= 3 m for high area ratio).

It appears that punching is the dominant mode of deformation for such short columns, which implies that columns mobilised a full shaft resistance along the shaft and end bearing resistance at the base of the column. An increase in the area ratio of columns corresponds to an increase in the column loads due to the

larger space between columns. Columns of similar length can resist similar shear force along the shaft if they are punching. Therefore, an increase in the column area ratio leads to an increase in the load portion transferred to the column toe and reflects the loss in the lateral confinement associated with the increasing of area ratio, which consequently leads to punching ratio increase for the higher area ratio.

The column at low area ratios continue to exhibit relatively low punching ratio for column lengths L> 2 m. The compression ratios also remain relatively low, which indicates that the lower area ratio columns do not deform significantly compared to higher area ratio columns. The punching ratio for an area ratio of A/A_c= 3.53 is lower than other higher area ratios coupled with relatively lower compression ratio which suggests that block behaviour occurred for groups of closely-spaced columns and is characterised by a slight increase in the punching ratio coupled with the increase in compression ratio.

A further investigation was carried out by the author based on FE analysis results. It is found that the soil settlement is uniform at the toe level where the settlement of the soft soil is similar to the settlement at the base of the column, as shown in Figure 5.20.

The increase in lateral pressure coefficient from K_s= 1.0 to K_s= 1.2 coupled with a reduction in the compression ratio suggests that columns are transferring the foundation loads to depth when lateral coefficient pressure increases due to column installation (Figure 5.21-i and Figure 5.21-ii). The influence of the area ratio upon punching and compression ratios for soft soil thickness of H=14.5 m is shown in Figure 5.21.

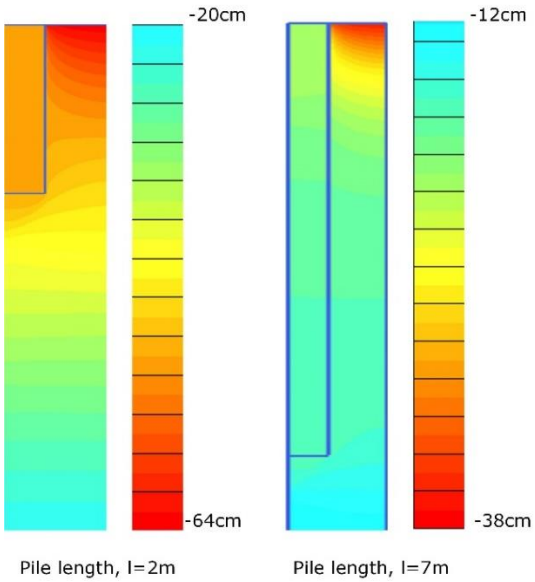


Figure 5.20 Vertical displacement for q= 50 kPa with column length L= 2m and L= 7m (A/A_c= 3.53).

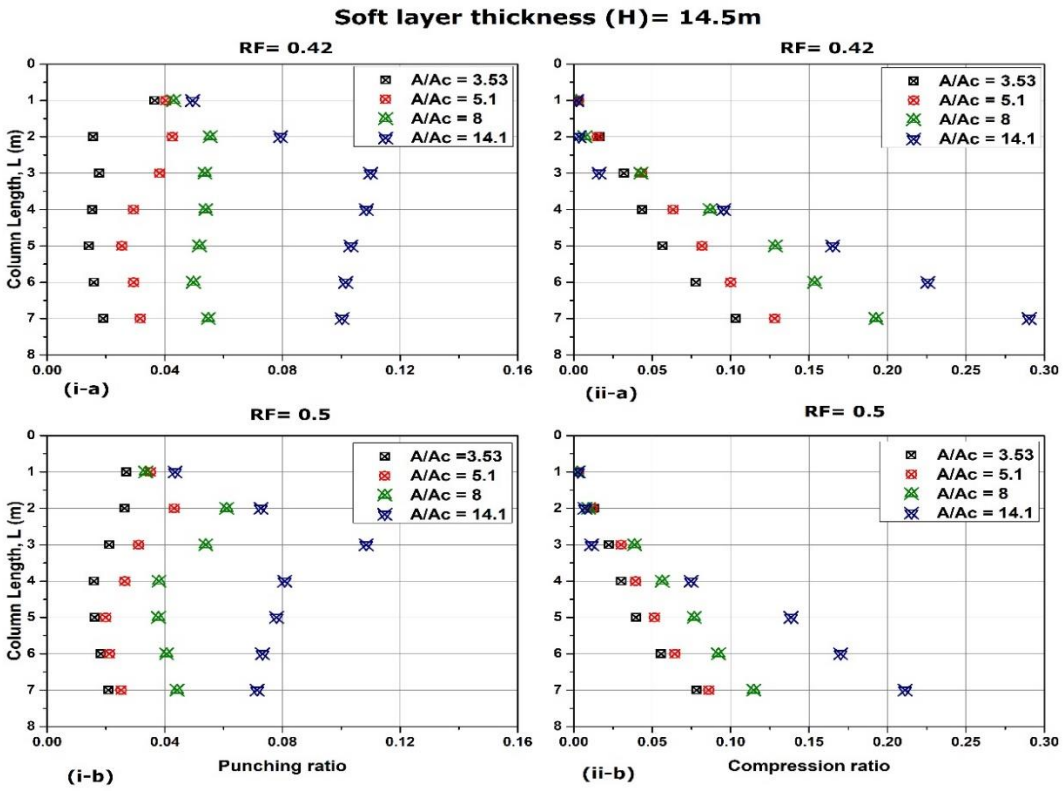


Figure 5.21 Variation of (a) punching and (b) compression ratios for lateral coefficient (i) RF= 0.42, and (ii) RF= 0.5 with column length for unit cell model.

It was established previously that punching failure is the dominant mode of deformation for short columns. Furthermore, punching and compression ratios are lower for thicker soft soil of H= 14.5 m compared to H= 10 m, as the rigid layer is deeper. Therefore, the column toe movement is larger which leads to a higher punching ratio.

Punching ratios for columns at high area ratios (A/A_c > 8.0) decay with depth for column lengths L > 3 m. This is coupled with relatively high compression ratios, which is consistent with the findings of McCabe and Killeen (2016). The increase in compression ratios indicated that columns may be bulging closer to the ground level. The influence of columns bulging upon the punching ratio is that columns cannot transfer applied loads to the base of the columns which consequently leads to a lower punching ratio.

Punching ratio for columns with area ratio lower than 3.53 is relatively lower than other area ratios, which is again similar to the findings from the layer thickness of 10 m. Punching failure is normally characterised by the higher punching ratio; however, it is indicated by Black (2006) and Satibi (2009) that 'Block' failure does not occur if the punching ratio is low and both column and surrounding soils deform uniformly. Punching and compression ratios variation for layer thickness of H= 20 m with column length is shown in Figure 5.22.

The column mode of deformation is similar to the above findings for layer thicknesses of H=10m and 14.5m. It can also be seen that punching and compression ratios are less than those with layer thickness of H=10m and H=14.5m.

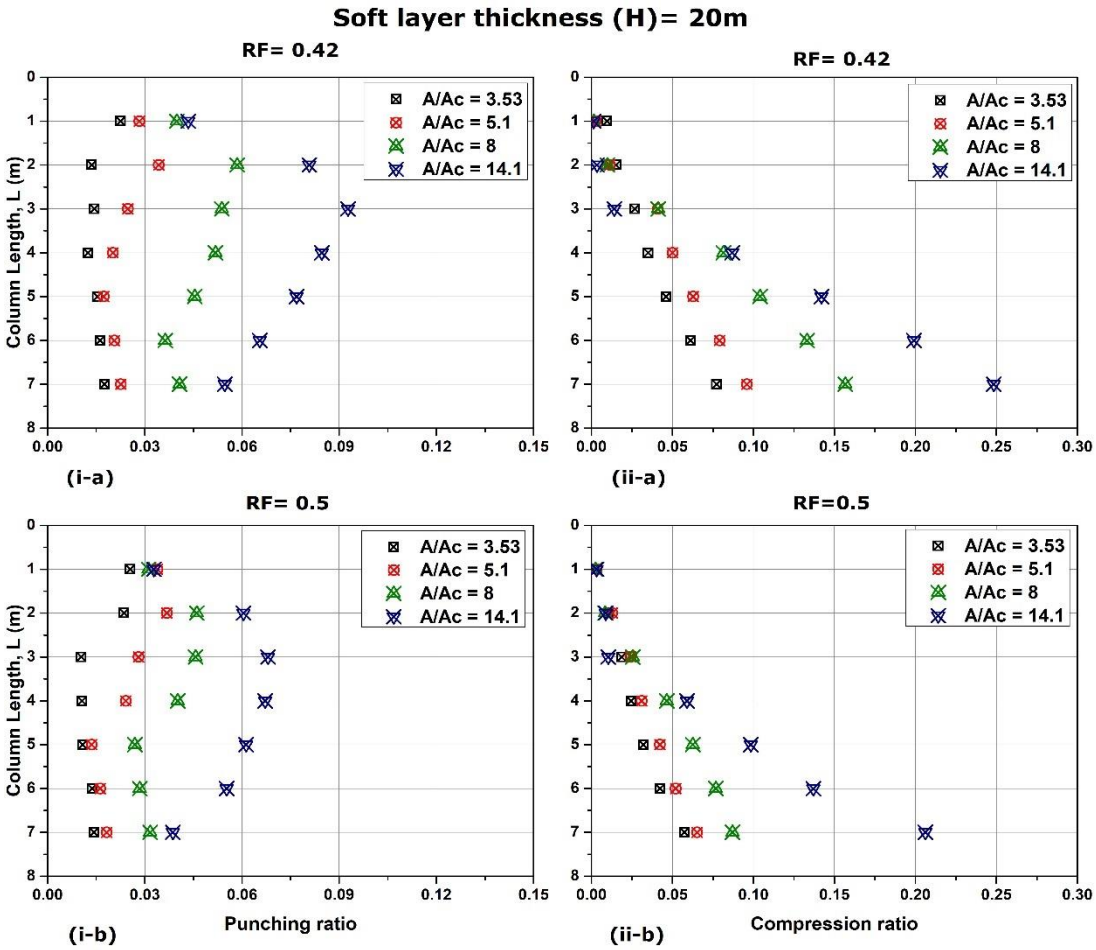


Figure 5.22 Variation of (a) punching and (b) compression ratios for lateral coefficient (i) RF= 0.42, and (ii) RF= 0.5 with column length for unit cell model

The existence of a block mechanism in conjunction with optimum area ratio (<3.53) where soil is more confined proved to have a detrimental effect on the settlement reduction and to prevent an excessive column deformation (see Figure 5.23).

Although these findings need additional modelling and field experiments to improve our understanding on how to incorporate the block mechanism alongside the optimum area ratio in the design. It appears that a trade-off exists between the column length and the area ratio (either short column length with low area ratio or long columns with high area ratio). However, other factors such as

construction time, cost, and safety must also be considered to develop a proper foundation solution.

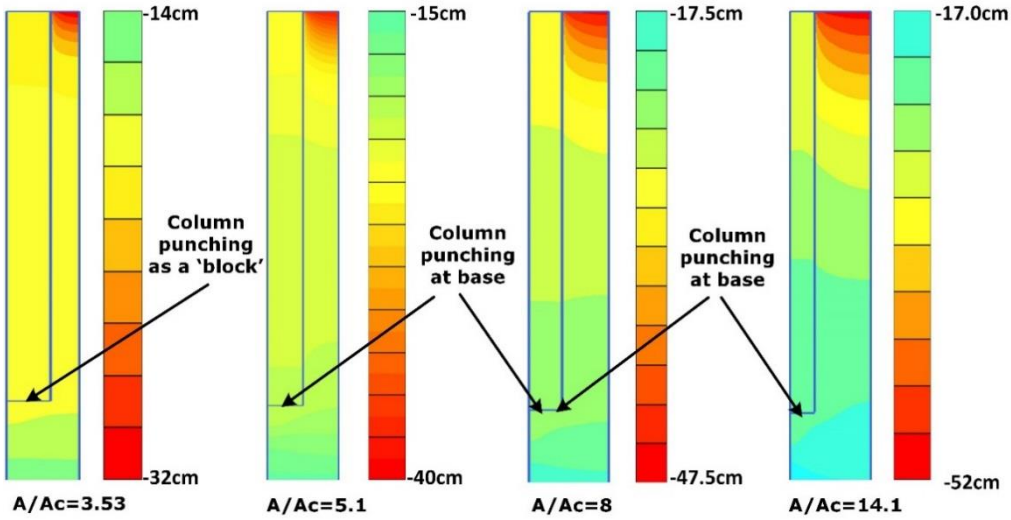


Figure 5.23 Block failure with different area ratio (L= 6 m and q= 50 kPa).

5.4.1.2 Influence of the coefficient of lateral soil pressure

The installation effect of stone columns can be modelled using K-Pressure procedure as described in Section 2.8.3.1. The influence of increasing lateral pressure coefficient from K_s= 1.0 (RF= 0.42) to 1.2 (RF= 0.5) upon the deformational behaviour is investigated (see Figure 5.19, Figure 5.21, and Figure 5.22). It appears that increasing lateral coefficient pressure, leads to a reduction in the punching and compression ratios for various layer thicknesses and area ratios. However, it can be seen that increasing lateral coefficient pressure has a minor impact on column deformation behaviour which is consistent with the findings by Kirsch (2006). Kirsch (2006) performed FEA for a group of stone columns and observed that increasing the coefficient of lateral soil pressure improves column settlement but has no effect on the deformation behaviour of columns.

5.5 Summary of the results

In this chapter, the analytical model developed by Satibi (2009) is modified to predict the foundation relative settlement reduction ratio (RSR) and compared with the FEA to evaluate the influence of installing a stone column upon the settlement performance of a footing. The effectivness of the stone columns was quantified using a RSR, which was identified as the ratio of the reduced footing settlement due to the column istallation to that of the total footing settlement without reinforcing. The analytical model was primarly used to calculate the effectiveness of stone columns installed to support widespread loads beneath ground bearing slabs. The analytical model was further developed by introducing Priebe (1995) factors to enable the calculation of spread and pad footings RSR.

The main contributions achieved by the work presented in this chapter are summarised below:

1- The analytical model derived by Satibi (2009) has been modified by the researcher to calculate the effectiveness of installing infinite grid of columns supporting an infinitely wide load. It was observed that the effectiveness (in terms of RSR) of the stone columns lies in the range 35% to 60%. The RSR ratio predicted by the FE analysis agrees quite well with the analytical model when the soft layer thickness over critical column length ratio ($H/L_{critical}$) = 2 to 5.

2- The analytical model is further modified by introducing Priebe (1995) factors to enable the calculation of spread and pad footings RSR. The simplified design analytical method was developed to calculate the RSR of a small group of stone columns from column diameter, column spacing, coefficentof lateral stress, column, layer thickness, external applied

pressure, and critical column length. It appears that the simplified analytical model yields reasonable results when predicting the settlement improvement of small group footings due to the installation of stone columns.

The maximum difference between RSR predicted by FEA and analytical model is 14%, however, the majority of the results predicted less than 10% difference between the two models. The effectiveness of stone column constructed to support pad and strip footings is with column critical length in the range of 0.6 to 0.94 times soft soil thickness. Therefore, installing stone columns to support pad footings is more effective in reducing settlement compared to an infinite grid of columns supporting an infinitely wide load.

3- The deformational behaviour of the stone column was examined in this chapter using compression ratio and newley defined punching ratio. Area ratios were found to have a significant influence on the mode of deformation of the columns. As the degree of plasticity is increasing within a widely-spaced columns, this reduces the ability of load transfer to the column base and, consequently, leads to a lower effectivness in reducing the settlement performance corresponding to a higher area ratio.

Punching and compression ratio has been used in this thesis to examine the mode of deformation of the stone column. It is evident in this analysis that the short column is tranferring significant portion of the applied load to the base of the column and is characterised by a high punching ratio and low compression ratio. This is consistent with the lateral bulging analyses carried out in Chapter 4 (see Section 4.10.2). Therefore, the mode of failure of short columns can be identified by punchnig. In contrast, long columns

are bulging along the shaft and are characterised by a low punching ratio and a high compression ratio. Thus, they cannot transfer load to the base.

It appears that the area ratio and column length are the key parameters governing the defomational behaviour of stone column (bulging, punching, and 'Block' behaviour). While the increase in the lateral pressure coefficient of soil improves the effectiveness of stone columns for a given area ratio, it appears that it does not alter the mode of deformation. The existence of a block mechanism (characterised by low punching and compression ratios where closed-spaced columns act together and punch as a block into the underlying soil) in conjunction with an optimum area ratio (<3.53), where soil is more confined, proved to have a detrimental effect on the settlement reduction and to prevent excessive column deformation.

Finally, it appears that the block mechanism should be used to optimise the stone column design either by choosing a short length column with low area ratio or a long column with high area ratio. However, other factors such as construction time, cost, and safety must also be considered. The modified analytical model could be used to estimate the effectiveness of the stone columns installed under footings at preliminary design stage, however, the settlement of the footing should be verified by measurements made after the construction of sacrificial or working stone columns

CHAPTER 6

CONCLUSIONS

6.1 Introduction

A series of FEA were undertaken to examine the influence of the lateral earth pressure coefficient upon the granular fill material arching above column-like elements. Moreover, numerical analyses were carried out to investigate the influence of key design parameters upon the behaviour of small groups of stone columns used to support shallow footings for lightly loaded low- rise structures. The advanced Hardening Soil model in PLAXIS code is adopted in this research. The material parameters and soil profile were taken from a well characterised Zaeske's model test (2001) and the Bothkennar (soft clay research site) (Serridge, 2001), which formed the basis of this thesis.

It was necessary to arrive at a reliable methodology to capture the embankment arching and arching distribution over the embankment height. The profile of normalised earth pressure coefficient (K/K_p) on a vertical profile at the midpoint between piles was used to investigate granular embankment material arching. It was found that the earth pressure coefficient K normalised by the passive earth pressure coefficient K_p plotted on a vertical profile at the midpoint between piles can be a very useful tool to study the embankment material arching. Furthermore, the K/K_p method can be used to perform a sensitivity analysis and to measure the

effect of number of key design variables on the arching when analysing piled-embankment system.

The monitoring of the Bothkennar field trials was carried out over a period of around 10 months, which enabled the author to perform a long-term FEA and predict the settlement under drained and undrained conditions. It was found that the long-term settlement performance of the trial footings at Bothkennar site can be accurately modelled using either a drained or undrained analysis (coupled analysis) up to a working load between 40 kPa to 50 kPa. It was observed that the long-term settlement difference between the drained and undrained analysis becomes more noticeable beyond an applied pressure of around 50 kPa with a distinct difference between short- term (undrained) and long-term loading. It was found that if a stiff crust layer is present on site, then a numerical analysis should be carried out to investigate the influence of the crust on the vertical settlement and lateral bulging of columns. The main conclusions of this thesis are summarised in this chapter.

6.2 Piled-embankments

A parametric FEA study was carried out in PLAXIS 2D to examine the influence of several key design parameters upon the behaviour of a granular embankment supported by piles installed in soft soils. The key conclusions are:

- The predicted minimum embankment height necessary to mobilise a full embankment arching using the method of the normalised earth pressure coefficient (K/K_p) on a vertical profile at the midpoint between piles is in agreement with the specified minimum height criteria for full arching conditions recommended by the British Standards BS8006. It is clear that

the minimum height criteria recommended by the German standard underestimates the embankment height required for full arching condition.

- It is evident from the results of the FEA that both plane of equal settlement and the K/K_p profile at mid- point methods can be used to determine the initiation of arching in the embankment and also can characterize the embankment arching. Therefore, a minimum embankment height can be determined using both the plane of equal settlement and the K/K_p profile at mid-point methods.

Additionally, it is concluded that:

- There is no evidence of arching above $z/s \approx 0.95$ to 1.1 for a normalised embankment height of between $h/s = 2.3$ and 1.25, respectively. Therefore, the embankment height is one of the key parameters when assessing the embankment soil arching.
- The increase in the granular embankment angle of internal friction leads to more efficient load distribution within the embankment material where the higher the effective angle of internal friction ,φ', results in a lower soft soil settlement accompanied with a lower K value at the same embankment height. Therefore, it is important to use a granular material with high effective angle of internal friction φ' to reduce soft soil settlement and for better load distribution within embankment material.
- The settlement of the foundation soils is less dependent on the angle of dilatation ψ compared to that of the angle of internal friction φ'. However, both angles have similar effect, to some extent, on the settlement of the founding soils where the higher subsoil surface settlement is obtained for reduced φ' and ψ angles.
- Generally, the stress concentration ratio increases with the increase of geogrid tensile stiffness. However, there is a limit beyond which increasing

the geogrid stiffness will not influence the stress concentration ratio. For the conditions simulated in this thesis, the limit was between 3000 kN/m to 5000 kN/m.

- It was found that a capping ratio of between 10% to 25% is necessary to ensure a stable piled-embankment behaviour.

6.3 Stone columns

The influence of key design parameters such as column length, spacing, footing shape and the presence of crust layer at shallow depth on footing behaviour at the Bothkennar site was investigated in this thesis. The influence of key design parameters was examined by predicting the footing vertical settlement, lateral bulging distribution with depth, and the encasement impact on the footing performance for a selected number of trial footings at the Bothkennar site.

6.3.1 Settlement

The measured and predicted settlement was recorded at the top of the seven trial footings. The main findings from this research are summarised as follows:

- It was found that a working applied pressure of 50 kPa is deemed satisfactory for the Bothkennar field trial (and could be used as a guidance when designing a pad footing supported by stone columns in soft soils) applying a typical factor of safety in the range of 2.5 to 3. It is inferred that the applied working load should be limited to satisfy a typical settlement performance (around 25mm subject to structure type) of columns installed beneath a narrow footing supporting a lightly loaded structure.
- For all the trials, the ground settlement profile indicates that the settlement at ground level would diminish at a distance in the range of 2 to 3 of the

footing width measured from the centreline of the footing for undrained and drained analysis, respectively.

- The design curves developed by Priebe (1995) were used to estimate the vertical settlement of the footings at the Bothkennar site. The settlement calculated by the Priebe (1995) method was adapted to match the numerical analysis results. It was found the Priebe (1995) method significantly under-predicts the settlement of the trial footings by 55% to 73% (see Appendix A) which can be attributed to soil disturbance as a result of the high energy used in the column installation which contributed to less settlement prediction than the field trials. In order to err on the side of caution, either a time limit should be specified for the poker during column installation to avoid sensitive soil disturbance or Priebe calculation method should be verified against field tests if stone columns installed in sensitive clays similar to Bothkennar site.

6.3.2 Bulging

The lateral bulging of stone columns at the Bothkennar field trials was analogous to the laboratory findings by Hughes and Withers (1974) and the field findings by Hughes et al. (1976) and the failure mode of a conventional triaxial sample (height to width ratio = 2). It was observed that the stone column suffers a severe lateral bulging near the top of the column (around two times the column diameter below ground surface). This research is the first comprehensive three-dimensional FEA study of the influence of the crust on lateral bulging of the ordinary and reinforced stone columns constructed to support narrow footings.

The key conclusions from Bothkennar field trials and the relevant numerical analysis are as follows:

- The maximum lateral bulging for trial Footing 1 occurs at shallow depths (around two times the column diameter below ground surface) below the crust layer. Footing (Footing 1) with the closer column spacing bulging and vertical settlement is less than trial Footing 2. This may be explained by the increase of the total load taken by the column due to the increase of the area replacement ratio (larger spacing). Therefore, for a similar column length and diameter, the shear resistance along the side of the column is similar (if shear resistance is fully mobilised) and the increase in the column load will increase the column load resisted at the base (see Figure 4.8), which consequently increases the column vertical settlement. If the ultimate applied load was higher than the soft soil shear resistance across the sides of the column shaft, then the failure would occur. Therefore, a careful consideration of the applied load will reduce bulging and will yield a better column performance.
- For the shortest column (Footing 3) to the longest column (Footing 5), the lateral bulging is similar. However, the lateral bulging for Footing 3 is gradually reduced from a maximum to a minimum value of between 0.5 mm to 2 mm correspondent to the applied loads. This confirms that the load is transferring to the column toe. Therefore, it appears that the dominant mode of failure for the short column is by punching through the soft soil. This is consistent with the analyses carried out in Chapter 5 using the punching and compression ratios.

6.3.3 Encasement

The influence of the stone columns encased by geogrids upon the settlement performance of the trial footings constructed at Bothkennar site was investigated

in PLAXIS 3D. The influence of key design parameters such as number of columns, column length, footing shape and depth upon the column settlement was also evaluated in this research. To the Author's knowledge, this research is the first comprehensive 3D numerical study of the key design parameters affecting the encased stone columns in a sensitive soft clay such as soft soils at Bothkennar site in short and long-term conditions. The key conclusions are as follows:

- The encasement of the top metre of the column reduces the lateral bulging considerably. However, the lateral bulging can be reduced further compared to partial encasement by extending the encasement below the maximum lateral bulging zone (around 2 times the diameter of the column). The lateral bulging of a fully reinforced column is reduced by 3.6 and 2.8 in X and Y directions, respectively, compared to 1 m column encasement as indicated in Figure 4.22 and Figure 4.27 (applied load = 150 kPa).
- The lateral bulging becomes more uniform where similar lateral bulging occurs in both directions (x and y) if encasement depth extends below the maximum lateral bulging position. It was found that encasing the column below the maximum lateral bulging zone is considered sufficient to reduce the lateral bulging and increase the column bearing capacity (ultimate resistance).

Additionally, it is concluded that the use of geogrid encasement around the column improves the column bearing capacity and their stress-displacement behaviour (the serviceability performance). The greater the length of encasement used, the more the total and the relative vertical settlement between the footing and the surrounded soils are reduced.

The magnitude of the maximum predicted hoop tension forces ranges from 1 kN/m to 29 kN/m for different applied pressures. The hoop tension forces were much

lower than the tension resistance of the most commercially available geogrids. Therefore, a geogrid with a tension resistance of 50 kN/m (factor of safety = 1.5) would be sufficient to resist the mobilised tension forces within the geogrid due to the applied load on the Bothkennar field trials.

6.3.4 Crust effect

The effect of the crust on the column behaviour has found to be:

- Footing 6 (founded at the base of the crust) analysis predicts a settlement similar to that of Footing 4 (founded at 0.5m depth in the crust) for first two load increments. However, the rate of settlement increased significantly compared with Footing 4 at higher loads which is in line with the expectations due to the founding depth in soft soil (i.e. base of crust) and also demonstrates the sensitivity of foundation depth within the crust on the column behaviour.
- The predicted settlement for Footing 7 (1.5 m x 1.5 m pad with a corresponding area ratio similar to the trial strip Footing 4) was comparable (slightly more) to that of the trial Footing 4 settlement. This may be explained on the basis that the stress depth influence is deeper for Footing 7 compared with Footing 4. This suggests that the crust may be playing an important role in masking some of the beneficial contribution of the smaller footing dimension.
- The lateral bulging is constrained by the crust presence at the upper part of the column, however, bulging of the stone column is still taking place in the soft clay underlying the crust layer at the point of peak stress.
- Footing 6 constructed at the top of the soft soil (base of the crust) laterally bulged the most. The large bulging can be explained as the crust does not

contribute significantly in reducing the lateral bulging in contrast to other footings. Therefore, there is a potential of using a compacted fill within the expected depth of bulging to avoid bulging failure where sensitive or very soft clays present. This will enable the engineers to specify stone columns solution in lieu of other expensive geotechnical solution such as piling option.

6.4 Simplified design method

The modified analytical model was used to predict the effectiveness of installing stone columns beneath foundation. The results were then compared with the FEA to validate the analytical model accuracy in predicting the effectiveness of stone column solution. The effectiveness of the stone columns was quantified using a relative settlement reduction ratio (RSR), which was identified as the ratio of the reduced footing settlement due to the column installation to that of the total footing settlement without reinforcing. The analytical model was primarly used to calculate the effectiveness of stone columns installed to support widespread loads beneath ground bearing slabs. The analytical model was further developed by introducing Priebe (1995) factors to enable the calculation of spread and pad footings RSR. The main findings of the simplified analytical model can be summarised as follow:

- The effectiveness of the stone columns (RSR) lies in the range of 35% to 60%.
- The RSR ratio predicted by the FEA agrees well with the analytical model when the soft layer thickness over critical column length ratio ($H/L_{critical}$) = 2 to 5.
- It appears that the simplified analytical model yields reasonable results when predicting the settlement improvement of small group footings due

to the installation of stone columns. The maximum difference between RSR predicted by FEA and analytical model is 14%, however, the majority of the results predicted less than 10% difference between the two models.

- The relative settlement reduction ratio of a stone column constructed to support pad and strip footings is in the range of 0.6 to 0.94. This implies that the stone column constructed to support pad and spread footings were more effective in reducing settlement compared to an infinite grid of columns supporting an infinitely wide load.

Additionally, it is concluded that the stone column design should be carried out to choose the optimum column length and area ratio to select either a short length column with the low area ratio or a long column with the high area ratio. Ground conditions such as the depth of rigid layer together with other factors such as construction time, cost, and safety must be considered. The existence of a block mechanism (characterised by low punching and compression ratios where a closed-spaced of columns act together and punch as a block into the underlying soil) in conjunction with optimum area ratio (<3.53) where soil is more confined proved to have a detrimental effect on the settlement reduction and to prevent an excessive column deformation. Punching and compression ratios were used in this research to examine the mode of deformation of the stone column. The mode of failure of short columns can be identified by punching (characterised by a high punching ratio and a low compression ratio). In contrast, long columns were bulging in their upper regions (characterised by a low punching ratio and a high compression ratio). This suggests that a smaller proportion of the load transferred to the base of long columns. Finally, it is concluded that the increase in the lateral pressure coefficient of soil improves the settlement performance of the pad

foundation for a given area ratio. Meanwhile, the mode of deformation was not altered by increasing the lateral pressure coefficient.

6.5 Recommendations for future research

This research was focussed on the arching behaviour of piled-embankment system and considered the influence of founding soil and embankment base reinforcement on the piled-embankment response to the applied external load. Whilst the current study has given an important contribution to the greater understanding of the influence of the key design parameters upon the partial depth stone column beneath a narrow, shallow footings using dry bottom-feed technique, further research and development could be undertaken in the future:

- Piled-embankment system has been analysed under static loading condition. The stability of soil arching during cyclic and dynamic loading could be investigated using physical and numerical models.
- The degree of secondary consolidation settlement (creep) reduction due to the installation of stone columns is not well understood and calls for further investigation.
- The installation effects associated with column-like elements have been touched on in this research. Further research and development are required regarding excessive remoulding of sensitive soft soils and consequently the soil strength reduction because of column installation. Therefore, rigorous field monitoring system is essential to evaluate the influence of installation effects on different soil types.
- The process of installing stone columns imposes complex changes on the surrounded soil (i.e. stress regime, increase the soil stiffness due to the poker displacing effect, and soil remoulding). More field measurements

are essential to validate the results presented in Chapter 5 using the modified analytical model.

REFERENCES

ABOSHI, H., ICHIMOTO, E., ENOKI, M. & HARADA, K. 1979. The compozer—A method to improve characteristics of soft clays by inclusion of large diameter sand columns. *Proceedings International Conference on Soil Reinforcement: Reinforced Earth and Other Techniques.,* 1**,** PP. 211-216.

AL-REFEAI, T. 1992. Strengthening of soft soil by fibre-reinforced sand column. *Proceedings, international symposium on earth reinforcement, VI, Rotterdam***,** 677-682.

AL AMMARI, K. & CLARKE, B. Predicting the effect of vibro stone column installation on performance of reinforced foundations. International Journal of Civil, Environmental, Structural, Construction and Architectural Engineering, 2016. World Academy of Science, Engineering and Technology, 111-117.

ALLMAN, M. & ATKINSON, J. 1992. Mechanical properties of reconstituted Bothkennar soil. *Geotechnique,* 42**,** pp. 289-301.

ALPHAN, I. 1967. The empirical evaluation of the coefficient Ko and Kor. *Soils and foundations,* 7**,** pp. 31-40.

ARIYARATHNE, P. & LIYANAPATHIRANA, D. 2015. Review of existing design methods for geosynthetic-reinforced pile-supported embankments. *Soils and Foundations,* 55**,** 17-34.

BABU, M. R. D., NAYAK, S. & SHIVASHANKAR, R. 2013. A Critical Review of Construction, Analysis and Behaviour of Stone Columns. *Geotechnical and Geological Engineering,* 31**,** 1-22.

BALAAM, N. P. & BOOKER, J. R. 1985. Effect of stone column yield on settlement of rigid foundations in stabilized clay. *International Journal for Numerical and Analytical Methods in Geomechanics,* 9**,** 331-351.

BALAAM, N. P. & BROWN, P. T. 1977. Settlement analysis of soft clay reinforced with granular piles.

BARKSDALE, R. D. & BACHUS, R. C. 1983. Design and Construction of Stone Columns. Virginia, USA: Fedral Highway Administration, National technical Information Service.

BAUMANN, V. & BAUER, G. 1974. The performance of foundations on various soils stabilized by the vibro-compaction method. *Canadian Geotechnical Journal,* 11**,** 509-530.

BERGADO, D. & LONG, P. 1994. Numerical analysis of embankment on subsiding ground improved by vertical drains and granular piles. *Proceedings of the international conference on soil mechanics and foundation engineering-International society for soil mechanics and foundation engineering,* 4**,** pp. 1361-1361.

BERGADO, D. T. & LAM, F. L. 1987. Full scale load test of granular piles with different densities and different proportions of gravel and sand on soft Bangkok Clay. *Soils and foundations,* 27**,** 86-93.

BJERRUM, L. 1973. Problems of soil mechanics and construction on soft clays and structurally unstable soils (collapsible, expansive and others). *Proc. of 8th Int. Conf. on SMFE,* 3**,** 111-159.

BLACK, J. A. 2006. *The settlement performance of a footing supported on soft clay reinforced with vibrated stone columns.* PhD, Queen's University of Belfast.

BOLTON, M. D. 1986. The strength and dilatancy of sands. *Géotechnique,* 36**,** 65-78.

BOUASSIDA, M., ELLOUZE, S. & HAZZAR, L. 2009. Investigating Priebe's method for settlement estimation of foundation resting on soil reinforced by stone columns.

BOUSSINESQ, J. 1885. *Applications des potentials à l'étude de l'équilibre et du mouvement des solides élastiques*.

BRE, B. R. E.-. 2000. Specifying vibro stone columns. Garston, UK.

BRINKGREVE, R., ENGIN, E. & SWOLFS, W. 2014. PLAXIS 2014. *PLAXIS bv, The Netherlands*.

BRINKGREVE, R., ENGIN, E. & SWOLFS, W. 2018. PLAXIS Material Models Manual The Netherlands: PLAXIS bv.

BRINKGREVE, R. B. 2005. Selection of soil models and parameters for geotechnical engineering application. *Soil constitutive models: Evaluation, selection, and calibration.*

BRITISH STANDARD BS8006 2010. Code of practice for strengthened/reinforced soils and other fills. *British Standard Institution, London*.

BRITISH STANDARD BS5930 2015. Code of practice for ground investigations. British Standard Institution, London.

BURLAND, J. & BURBRIDGE, M. 1985. Settlement of foundations on sand and gravel. *Institution of Civil Engineers, Proceedings, Pt 1,* 76.

BURLAND, J. B. 1969. Contribution to Discussion. *In-situ Investigation on Soils and Rocks*.

CARLSSON, B. 1987. Reinforced soil, principles for calculation. *Terratema AB, Linköping*.

CARTER, M. & BENTLEY, S. P. 1991. *Correlations of soil properties,* London, Pentech press publishers.

CASTRO, J. 2017a. Groups of encased stone columns: Influence of column length and arrangement. *Geotextiles and Geomembranes,* 45**,** 68-80.

CASTRO, J. 2017b. Modeling stone columns. *Materials,* 10**,** 782.

CASTRO, J., KARSTUNEN, M. & SIVASITHAMPARAM, N. 2014. Influence of stone column installation on settlement reduction. *Computers and Geotechnics,* 59**,** 87-97.

CASTRO, J., KARSTUNEN, M., SIVASITHAMPARAM, N. & SAGASETA, C. 2013. Numerical analyses of stone column installation in Bothkennar clay. *Proc. International Conference on Installation Effects in Geotechnical Engineering, Rotterdam.*

CHEN, R., TANG, L., LING, D. & CHEN, Y. 2011. Face stability analysis of shallow shield tunnels in dry sandy ground using the discrete element method. *computers and Geotechnics,* 38**,** 187-195.

DEBATS, J., GUETIF, Z. & BOUASSIDA, M. 2003. Soft soil improvement due to vibro-compacted columns installation. *Proc. International Workshop on Geotechnics of soft soils-Theory and practice. Noordwijkerhout-Netherlands***,** 551-556.

DUNCAN, J. M. & CHANG, C. Y. 1970. Nonlinear Analysis of Stress and Strain in Soils. *Soil Mech. Found. Eng., ASCE,* 96**,** 1629-1653.

EBGEO 2004. EBGEO Emfehlungen für Bewehrungen aus Geokunststoffen Bewehrte Erdköper auf punkt - oder linienförmigen Tragglieder. *EBGEO, Kapitel 6.9, Stand.*

ELSAWY, M. 2010. *Highway Embankment Constructed on Soft Soil Improved by Stone Columns with Geosynthetic Materials.* Universität Duisburg-Essen, Ehem. Fachbereich Bauwissenschaften» Bauingenieurwesen.

ELSHAZLY, H., HAFEZ, D. & MOSSAAD, M. 2006. Back-calculating vibro-installation stresses in stone-column-reinforced soils. *Proceedings of the Institution of Civil Engineers-Ground Improvement,* 10**,** 47-53.

ELSHAZLY, H., HAFEZ, D. & MOSSAAD, M. 2008. Reliability of conventional settlement evaluation for circular foundations on stone columns. *Geotechnical and Geological Engineering,* 26**,** 323.

FANG, Q., TSUCHIYA, T. & YAMAMOTO, T. 2002. Finite difference, finite element and finite volume methods applied to two-point boundary value problems. *Journal of Computational and Applied Mathematics,* 139**,** 9-19.

FAYED, A. L., SOROUR, T. M. & SHEHATA, H. F. 2017. Study of the Behavior of Floating Stone Columns in Soft Clay Formations Using Numerical Modeling. *International Congress and Exhibition" Sustainable Civil Infrastructures: Innovative Infrastructure Geotechnology"***,** 236-251.

GÄB, M., SCHWEIGER, H. F., KAMRAT-PIETRASZEWSKA, D. & KARSTUNEN, M. 2010. Numerical analysis of a floating stone column foundation using different constitutive models. *Geotechnics of Soft Soils: Focus on Ground Improvement: Proceedings of the 2nd International Workshop held in Glasgow, Scotland, 3-5 September 2008***,** 137.

GABA, A., HARDY, S., DOUGHTY, L., POWRIE, W. & SELEMETAS, D. 2017. *Guidance on embedded retaining wall design,* London, UK, Construction Industry Research and Information Association (CIRIA).

GIBSON, R. E. & ANDERSON, W. F. 1961. In situ measurement of soil properties with the pressuremeter. *Civil engineering and public works review,* 56**,** 615-618.

GOUGHNOUR, R. R. & BAYUK, A. A. 1979a. Analysis of stone column-soil matrix interaction under vertical load. *Coll. Int. Renforcements des Sols***,** 279-285.

GOUGHNOUR, R. R. & BAYUK, A. A. 1979b. A field study of long-term settlements of loads supported by stone columns in soft ground. *Proceedings, international conference on soil reinforcement, Paris***,** 279-285.

GREENWOOD, D. A. 1970. Mechanical improvement of soils below ground surface. *Proceeding on the conference on Ground Engineering* 2**,** 11-22.

GREENWOOD, D. A. & KIRSCH, K. 1984. Specialist ground treatment by vibratory and dynamic methods. *Advances in piling and ground treatment, Proceeding of International Conference***,** 17-45.

GUETIF, Z., BOUASSIDA, M. & DEBATS, J. 2007. Improved soft clay characteristics due to stone column installation. *Computers and Geotechnics,* 34**,** 104-111.

GUIDO, V. A., KNUEPPEL, J. D. & SWEENY, M. A. 1987. Plate Loading Tests on Geogrid-reinforced Earth Slabs. 216-225.

HAN, G.-X., GONG, Q.-M. & ZHOU, S.-H. 2014. Soil arching in a piled embankment under dynamic load. *International Journal of Geomechanics,* 15**,** 04014094.

HAN, J. 1999. Design and construction of embankments on geosynthetic reinforced platforms supported by piles. *Proceedings of***,** 66-84.

HAN, J. 2015. Recent research and development of ground column technologies.

HAN, J. & AKINS, K. 2002. Use of geogrid-reinforced and pile-supported earth structures. *Deep Foundations 2002: An International Perspective on Theory, Design, Construction, and Performance.*

HAN, J. & COLLIN, J. 2005. Geosynthetic support systems over pile foundations. *Geosynthetics Research and Development in Progress.*

HAN, J. & GABR, M. 2002. Numerical analysis of geosynthetic-reinforced and pile-supported earth platforms over soft soil. *Journal of Geotechnical and Geoenvironmental Engineering,* 128**,** 44-53.

HAN, J. & WAYNE, M. 2000. Pile-soil-interactions in geosynthetic reinforced platform/piled embankments over soft soil. *Rep. No. 000777, Presentation and CD-Print at 79th Annual Transportation Research Board Meeting*.

HANDY, R. L. 1985. The arch in soil arching. *Journal of Geotechnical Engineering,* 111**,** 302-318.

HANDY, R. L. 1987. Closure to "The Arch in Soil Arching" by Richard L. Handy (March, 1985, Vol. 111, No. 3). *Journal of Geotechnical Engineering,* 113**,** 275-277.

HENKE, S. & GRABE, J. 2006. Simulation of pile driving by 3-dimensional finite-element analysis. *Proceedings of 17th European Young Geotechnical Engineers' Conference. V. Szavits-Nossan, Croatian Geotechnical Society*.

HEWLETT, W. & RANDOLPH, M. 1988. Analysis of piled embankments. *International Journal of Rock Mechanics and Mining Sciences and Geomechanics Abstracts,* 25**,** 297-298.

HIGHT, D., BOND, A. & LEGGE, J. 1992. Characterization of the Bothkennaar clay: an overview. *Geotechnique,* 42**,** 303-347.

HU, W. 1995. *Physical modelling of group behaviour of stone column foundations.* University of Glasgow.

HUGHES, J. M. O. & WITHERS, N. J. 1974. Reinforcing of soft cohesive soils with stone columns. *Ground Engineering,* 7.

HUGHES, J. M. O., WITHERS, N. J. & GREENWOOD, D. A. 1976. *A field trial of the reinforceing effect of a stone column in soil. Ground treatment by deep Compaction.,* London, Institution of Civil Engineers.

IGLESIA, G. R., EINSTEIN, H. H. & WHITMAN, R. V. 1999. Determination of vertical loading on underground structures based on an arching evolution concept. *Geo-Engineering for Underground Facilities***,** 495-506.

INSTITUTION OF CIVIL ENGINEERS 1992. Bothkennar soft clay test site: characterisation and lessons learned. *Geotechnique,* 42**,** 159-378.

ISHIKURA, R., OCHIAI, H., OMINE, K., YASUFUKU, N. & KOBAYASHI, T. 2006. Estimation of the settlement of improved ground with floating-type cement-treated columns. *Proceedings of Fourth International Conference on Soft Soil Engineering***,** 625-635.

JAKY, J. 1948. Pressure in silos. *2nd ICSMFE.*

JARDINE, R. J., LEHANE, B. M., SMITH, P. R. & GILDEA, P. A. 1995. Vertical loading experiments on rigid pad foundations at Bothkennar. *Geotechnique,* 45**,** 573-597.

JOHNSON, A. 2012. *Recommendations for Design and Analysis of Earth Structures Using Geosynthetic Reinforcements-EBGEO*, John Wiley & Sons.

JONES, C., LAWSON, C. & AYRES, D. Geotextile reinforced piled embankments. Proceedings of the 4th International Conference on Geotextiles: Geomembranes and Related Products. Rotterdam: AA Balkema, 1990a. 155-160.

JONES, C. J. F. P., LAWSON, C. R. & AYRES, D. J. 1990b. Geotextile reinforced piled embankments *Proc 4th International Conference on Geotextiles, Geomembranes and Related Products,* 29**,** 155-160.

KATSIKADELIS, J. & NERANTZAKI, M. 1999. The boundary element method for nonlinear problems. *Engineering Analysis with Boundary Elements,* 23**,** 365-373.

KEMPFERT, H.-G., STADEL, M. & ZAESKE, D. 1997. Design of geosynthetic-reinforced bearing layers over piles. *Bautechnik,* 74**,** 818-825.

KEMPFERT, H. G. 2003. Ground improvement methods with special emphasis on column-type techniques. *Proceedings, international workshop on geotechnics of soft soils—theory and practice***,** 101-112.

KEMPFERT, H. G. 2006. *Schriftenreihe Geotechnik: Bodengewölbe unter ruhender und nichtruhender Belastung bei Berücksichtigung von Bewehrungseinlagen aus Geogittern. Heft 19.* Universität Kassel.

KEMPFERT, H. G. & GEBRESELASSIE, B. 2006. *Excavations and foundations in soft soils,* Berlin, Springer-Verlag

KEMPFERT, H. G., GÖBEL, C., ALEXIEW, D. & HEITZ, C. 2004. German recommendations for reinforced embankments on pile-similar elements. *EuroGeo3-Third European Geosynthetics Conference, Geotechnical Engineering with Geosynthetics***,** 279-284.

KEMPTON, G., RUSSELL, D., PIERPOINT, N. D. & JONES, C. J. F. P. 1998. Two- and three- dimensional numerical analysis of the performance of piled embankment. *6th International Conference on Geosynthetics.*

KEYHOSROPUR, L., SOROUSH, A. & IMAM, R. 2011. A study on the behaviour of a geosynthetic encased stone columns group using 3D numerical analysis. *2011 Pan-Am CGS Geotechnical Conf.***,** 1-7.

KHABBAZIAN, M., KALIAKIN, V. N. & MEEHAN, C. L. 2009. 3D numerical analyses of geosynthetic encased stone columns. *Contemporary Topics in Ground Modification, Problem Soils, and Geo-Support.*

KILLEEN, M. 2012. *NUMERICAL MODELLING OF SMALL GROUPS OF STONE COLUMNS.* College of Engineering and Informatics, National University of Ireland, Galway.

KIRSCH, F. 2006. Vibro stone column installation and its effect on ground improvement. *Proceedings of the International Conference on Numerical Modelling of Construction Processes in Geotechnical Engineering for Urban Environment***,** 115-124.

LAMBE, W. T. & WHITMAN, R. V. 1979. Soil Mechanics, SI Version. John Wiley.

LANCELLOTA, R. 1995. In situ investigations. *Geotechnical Engineering. Balkema, Rotterdam,* 436.

LANCELLOTTA, R. 2014. *Geotechnical engineering*, CRC Press.

LEE, J. & PANDE, G. 1998. Analysis of stone - column reinforced foundations. *International Journal for Numerical and Analytical Methods in Geomechanics,* 22**,** 1001-1020.

LEE, Y. N. & JIN, B. I. 1979. Measurement and prediction of K0. *Korean Society of Civil Engineering***,** 226-233.

LIU, H., NG, C. W. & FEI, K. 2007. Performance of a geogrid-reinforced and pile-supported highway embankment over soft clay: case study. *Journal of Geotechnical and Geoenvironmental Engineering,* 133**,** 1483-1493.

LO, S., ZHANG, R. & MAK, J. 2010. Geosynthetic-encased stone columns in soft clay: a numerical study. *Geotextiles and Geomembranes,* 28**,** 292-302.

LOVE, J. & MILLIGAN, G. 2003. Design methods for basally reinforced pile-supported embankments over soft ground. *Ground Engineering,* 36.

LOW, B. K., TANG, S. K. & CHOA, V. 1994. Arching in piled embankments. *Journal of Geotechnical Engineering - ASCE,* 120**,** 1917-1938.

MAGNAN, J.-P. 1994. Methods to reduce the settlement of embankments on soft clay: a review. *Vertical and Horizontal Deformations of Foundations and Embankments:***,** 77-91.

MALARVIZHI, S. & ILAMPARUTHI, K. 2004. Load versus settlement of clay bed stabilized with stone and reinforced stone columns. *Proceedingns of GeoAsia–2004, Seoul, Korea***,** 322-329.

MALARVIZHI, S. & ILAMPARUTHI, K. 2006. Modeling of geogrid encased stone column. *Proceedings of the 2 nd International Congress on Computational Mechanics and Simulation (ICCMS-06), IIT Guwahati, India*.

MALARVIZHI, S. & ILAMPARUTHI, K. 2007. Comparative study on the behavior of encased stone column and conventional stone column. *Soils and Foundations,* 47**,** 873-885.

MARFURT, K. J. 1984. Accuracy of finite-difference and finite-element modeling of the scalar and elastic wave equations. *Geophysics,* 49**,** 533-549.

MARSTON, A. & ANDERSON, A. 1913. The Theory of Loads on Pipes in Ditches. *Bulletin 31, Iowa Engineering Experiment Station, Iowa*.

MCCABE, B., KILLEEN, M. & EGAN, D. 2008. Challenges faced in 3-d finite element modeling of stone column construction. *Proc. Joint Symposium on Concrete Research and Bridge and Infrastructure Research in Ireland***,** 393-400.

MCCABE, B. & KILLEEN, M. M. 2010. A numerical study of factors affecting the performance of stone columns supporting rigid footings on soft clay. *7th European Conference on Numerical Methods in Geotechnical Engineering*.

MCCABE, B., NIMMONS, G. & EGAN, D. 2009. A review of field performance of stone columns in soft soils. *Proceedings of the Institution of Civil Engineers-Geotechnical engineering,* 162**,** 323-334.

MCCABE, B. A. & KILLEEN, M. M. 2016. Small Stone-Column Groups: Mechanisms of Deformation at Serviceability Limit State. *International Journal of Geomechanics***,** 04016114.

MCKELVEY, D., SIVAKUMAR, V., BELL, A. & GRAHAM, J. 2004. Modelling vibrated stone columns in soft clay. *Proceedings of the ICE-Geotechnical Engineering,* 157**,** 137-149.

MCKELVEY, J. A. 1994. The Anatomy of Soil Arching. *Geotextiles and Geomembranes,* 13**,** 317-329.

MCNULTY, J. W. 1965. An experimental study of arching in sand. DTIC Document.

MEURANT, G. 2013. *Soil mechanics of earthworks, foundations and highway engineering*, Elsevier.

MITCHELL, J. K. & HUBER, T. R. 1985. Performance of a stone column foundation. *Journal of Geotechnical Engineering,* 111**,** 205-223.

MUIR WOOD, D., HU, W. & NASH, D. 2000. Group effects in stone column foundations: model tests. *Geotechnique,* 50**,** 689-698.

MURUGESAN, S. & RAJAGOPAL, K. 2006. Numerical analysis of geosynthetic encased stone column. *Proceedings of the 8th International Conference on Geosynthetics, Yokohama, Japan***,** 1681-1684.

MURUGESAN, S. & RAJAGOPAL, K. 2008. Shear load tests on stone columns with and without geosynthetic encasement. *Geotechnical Testing Journal,* 32**,** 76-85.

MURUGESAN, S. & RAJAGOPAL, K. 2009. Studies on the behavior of single and group of geosynthetic encased stone columns. *Journal of Geotechnical and Geoenvironmental Engineering,* 136**,** 129-139.

NAJJAR, S. S., SADEK, S. & MAAKAROUN, T. 2010. Effect of sand columns on the undrained load response of soft clays. *Journal of Geotechnical and Geoenvironmental Engineering,* 136**,** 1263-1277.

NARASIMHA RAO, S., MADHIYAN, M. & PRASAD, Y. 1992. Influence of bearing area on the behavior of stone columns. *Proceedings of Indian Geotechnical Confererence***,** 235-237.

NASH, D., POWELL, J. & LLOYD, I. 1992a. Initial investigations of the soft clay test site at Bothkennar. *Geotechnique,* 42**,** 163-181.

NASH, D., SILLS, G. & DAVISON, L. 1992b. One-dimensional consolidation testing of soft clay from Bothkennar. *Geotechnique,* 42**,** 241-256.

NAUGHTON, P. 2007. The significance of critical height in the design of piled embankments. *Part of Geo-Denver***,** 13-23.

NIKOLIĆ, M., ROJE-BONACCI, T. & IBRAHIMBEGOVIĆ, A. 2016. Overview of the numerical methods for the modelling of rock mechanics problems. *Tehnički vjesnik,* 23**,** 627-637.

O'RIORDAN, N. J., SEAMAN, J. W., BRIDGES, T. R. L. & CENTRE, G. E. R. 1994. *Highway Embankments Over Soft Compressible Alluvial Deposits: Guidelines for Design and Construction*, Transport Research Laboratory, Bridges and Ground Engineering Resource Centre.

OBRZUD, R. & TRUTY, A. 2018. The hardening soil model-a practical guidebook z soil. *PC100701 Rep*.

PEIRÓ, J. & SHERWIN, S. 2005. Finite difference, finite element and finite volume methods for partial differential equations. *Handbook of materials modeling.* Springer.

PLAXIS, B. 2015. PLAXIS material models manual. Delft, Netherlands: PLAXIS, University of Technology.

POTTS, D. & ZDRAVKOVIC, L. 1999. Finite element analysis in geotechnical engineering—theory Thomas Telford, London.

POTTS, V. & ZDRAVKOVIC, L. 2008. Finite element analysis of arching behaviour in soils. *Proceedings of the 12th International Conference on Computer Methods and Advances in Geomechanics***,** 3642-3649.

POULOS, H. 2007. Design charts for piles supporting embankments on soft clay. *Journal of Geotechnical and Geoenvironmental Engineering,* 133**,** 493-501.

POULOS, H. G. & MATTES, N. S. 1969. Settlement of single compressible pile. *Journal of soil Mechanics & Foundations Division. American Society of Civil Engineers (ASCE),* 95**,** 189-207.

PRIEBE, H. J. 1976. An evaluation of settlement reduction in soil improved by vibroreplacement. *en alemán). Bautechnik***,** 160-162.

PRIEBE, H. J. 1991. Vibro-replacement: Design criteria and quality control. Deep Foundation Improvements: Design, Construction and Testing. *ASTM STP 1089.* Philadelphia: ASTM.

PRIEBE, H. J. 1995. The design of vibro replacement. *Ground Engineering,* 28**,** 31.

PULKO, B. & MAJES, B. 2005. Simple and accurate prediction of settlements of stone column reinforced soil. *PROCEEDINGS OF THE INTERNATIONAL CONFERENCE ON SOIL MECHANICS AND GEOTECHNICAL ENGINEERING,* 16**,** 1401.

RANDOLPH, M. F., CARTER, J. & WROTH, C. 1979a. Driven piles in clay-the effects of installation and subsequent consolidation. *Geotechnique,* 29**,** 361-393.

RANDOLPH, M. F., STEENFELD, J. & WROTH, P. 1979b. *The effect of pile type on design parameters for driven piles*, Cambridge University Engineering Department.

RANJAN, G. & RAO, A. 2007. *Basic and applied soil mechanics*, New Age International.

RATHMAYER, H. 1975. Piled embankment supported by single pile caps. *Proceedings of Conference on Soil Mechanics and Foundation Engineering***,** pp. 283-290.

REID, W. & BUCHANAN, N. 1984. Bridge approach support piling. *Piling and ground treatment***,** 267-274.

RUSSELL, D., NAUGHTON, P. & KEMPTON, G. 2003. A new design procedure for piled embankments. *Proceedings of the 56th Canadian Geotechnical Conference and 2003 NAGS Conference,* 1**,** 858-865.

SATIBI, S. 2009. *Numerical analysis and design criteria of embankments on floating piles*, Institut für Geotechnik der Universität Stuttgart IGS.

SATIBI, S., LEONI, M., VERMEER, P. A. & VAN DER MEIJ, R. 2009. On the numerical analysis of piled embankments. *Geotechnics of Soft Soils - Focus on Ground Improvement.*

SCHERZINGER, T. 1991. *Materialverhalten von seetonen- Ergebnisse von laboruntersuchungen und ihre bedeutung fur das Bauen in weichem baugrund.* Universität Fridericiana.

SCHOFIELD, A. N. 1980. Geotechnical Engineering Notes.

SCHWEIGER, H. & PANDE, G. 1986. Numerical analysis of stone column supported foundations. *Computers and Geotechnics,* 2**,** 347-372.

SERRIDGE, C. J. 2001. *A review of vibro stone columns in soft clay (Incorporating field trials of partial depth stone columns beneath a raft foundation at Bothkennar soft clay research site).* MSc, University of Bolton.

SERRIDGE, C. J. 2013. *An Evaluation of partial depth dry bottom-feed vibro stone columns to support shallow footings in deep soft clay deposits.* PhD, Anglia Ruskin.

SEXTON, B. G., MCCABE, B. A., KARSTUNEN, M. & SIVASITHAMPARAM, N. 2016. Stone column settlement performance in structured anisotropic clays: the influence of creep. *Journal of Rock Mechanics and Geotechnical Engineering,* 8**,** 672-688.

SHERIF, M. A. & KOCH, D. E. 1970. Coefficient of earth pressure at rest as related to soil recompression ratio and liquid limit. *Highway Research Record*.

SIVAKUMAR, V., GLYNN, D., BLACK, J. & MCNEILL, J. 2007. A laboratory model study of the performance of vibrated stone columns in soft clay. *Proceedings of the 14th European Conference on Soil Mechanics and Geotechnical Engineering, Madrid, Spain***,** 24-27.

SKEMPTON, A. & BJERRUM, D. 1957. A contribution to the settlement analysis of foundations on clay.

SLOCOMBE, B. C. & BELL, A. L. 1998. Setting on a dispute: Discussion on Russel and Pierpoint paper. *Ground Engineering***,** 34-36.

STROUD, M. & BUTLER, F. 1975. The standard penetration test and the engineering properties of glacial materials. *Symposium on Engineering Properties of Glacial Materials, Midland Geotechnical Society*.

TAYLOR, D. W. 1948. Fundamentals of soil mechanics. *Soil Science,* 66**,** 161.

TERZAGHI, K. 1943. Theoretical soil mechanics.

TERZAGHI, K., PECK, R. B. & MESRI, G. 1996. *Soil mechanics in engineering practice*, John Wiley & Sons.

THORBURN, S. 1975. Building structures supported by stabilized ground. *Geotechnique,* 25**,** 83-94.

THORBURN, S. & MACVICAR, R. 1968. Soil stabilization employing surface and depth vibrators. *The structural engineer,* 46**,** 309-316.

TOMLINSON, M. & WOODWARD, J. 2014. *Pile design and construction practice*, CRC Press.

UESHITA, K. & MEYERHOFF, G. 1968. Surface displacement of an elastic layer under uniformly distributed loads. *Highway Research Record*.

VAN EEKELEN, S., BEZUIJEN, A. & OUNG, O. 2003. Arching in piled embankments; experiments and design calculations. *Foundations: Innovations, observations, design and practice***,** 885-894.

VAN EEKELEN, S., BEZUIJEN, A. & VAN TOL, A. 2013. An analytical model for arching in piled embankments. *Geotextiles and Geomembranes,* 39**,** 78-102.

VAN EEKELEN, S., JANSEN, H., VAN DUIJNEN, P., DE KANT, M., VAN DALEN, J., BRUGMAN, M., VAN DER STOEL, A. & PETERS, M. 2010. The Dutch design guideline for piled embankments. *Proceedings of 9ICG, Brazil***,** 1911-1916.

VAN EEKELEN, S. J. & BRUGMAN, M. H. 2016. *Design guideline basal reinforced piled embankments*, CRC Press.

VAN EEKELEN, S. V., BEZUIJEN, A. & VAN TOL, A. 2011. Analysis and modification of the British Standard BS8006 for the design of piled embankments. *Geotextiles and Geomembranes,* 29**,** 345-359.

VAN IMPE, W. & SILENCE, P. 1986. Improving of the bearing capacity of weak hydraulic fills by means of geotextiles. *Proceedings of the 3rd International Conference on Geotextiles, Vienna, Austria***,** 1411-1416.

VAN IMPE, W. F. & DEBEER, E. 1983. Improvement of settlement behaviour of soft layers by means of stone columns. *Proceedings, 8th European Conference on Soil Mechanics and Foundation Engineering: Improvement of Ground,* 1**,** 309-312.

VERMEER, P. & SUTJIADI, W. The uplift resistance of shallow embedded anchors. International conference on soil mechanics and foundation engineering. 11, 1985. 1635-1638.

VERMEER, P. A. & BRINKGREVE, R. B. J. 2008. Handbook of the finite element code for soil and rock analysis "PLAXIS". Balkema, Rotterdam.

VESIC, A. S. 1972. Expansion of cavities in infinite soil mass. *Journal of Soil Mechanics and Foundations Division,* 98**,** pp. 265.

WATTS, K. 2000. Specifying vibro stone columns. *British Research Establishment (BRE) Report, Watford, UK*.

WEHR, J. 2004. Stone columns–single columns and group behavior. *Proceedings of 5th international conference on ground improvement technologies, Kuala Lumpur***,** 329-340.

YU, H.-S. 2013. *Cavity expansion methods in geomechanics*, Springer Science & Business Media.

ZAESKE, D. 2001. *Zur Wirkungweise von unbewehrten und bewerhrten mineralischen tragschichten über pfahlartigen Gründungselementen.* PhD, Universität Kassel.

ZHUANG, Y. 2009. *Numerical modelling of arching in piled embankments including the effects of reinforcement and subsoil.* University of Nottingham.

ZHUANG, Y., ELLIS, E. A. & YU, H.-S. 2010. Plane strain FE analysis of arching in a piled embankment. *Proceedings of the Institution of Civil Engineers-Ground Improvement,* 163**,** 207-215.

ZIENKIEWICZ, O., KELLY, D. & BETTESS, P. 1977. The coupling of the finite element method and boundary solution procedures. *International journal for numerical methods in engineering,* 11**,** 355-375.

Appendix A:

Prediction of the settlement performance of stone columns (after Priebe, 1995), utilising updated spreadsheet, for average applied second pressure increment in Bothkennar field trials (Footing 1 to Footing 7), together with explanatory notes for stress distribution and (pre-treatment) settlement analysis.

Determination of Improvement Factors (Priebe 1995)

Contract Name: Bothkennar, Trial Footing 1
Contract Number: Trial run
Calculation Reference: 0.75 m wide x 6.0 m long footing

P_o = 72 kN/m²
A_o = 1.13 m²
Founding Depth = 0.5 m
ϕ_c = 42.5
E_c = 40 MN/m²

Layer Ref.	d m	Dia. m	A_o/A_c	E_s MN/m²	γ_s kN/m³	υ_s	n_0	E_c/E_s	K_{ac}	$(A_c/A_o)_1$	$\Delta(A_o/A_c)$	A_c/A_o	n_1	$\Sigma(\gamma_s.\Delta d)$	P_c/P_s	P_c	K_{oc}	f_d	n_2
								Column Compressibility						Overburden Constraint					
	0.50				18														
1	1.00	0.75	2.56	20	9	0.33	4.43	2.00	0.19	0.16	5.41	0.13	1.78	11.25	7.20	292	0.32	1.09	1.93
2	2.00	0.75	2.56	20	9	0.33	4.43	2.00	0.19	0.16	5.41	0.13	1.78	18	7.20	292	0.32	1.15	2.04
3	3.00	0.75	2.56	20	9	0.33	4.43	2.00	0.19	0.16	5.41	0.13	1.78	27	7.20	292	0.32	1.24	2.20
4	4.00	0.75	2.56	20	9	0.33	4.43	2.00	0.19	0.16	5.41	0.13	1.78	36	7.20	292	0.32	1.35	2.39
5	5.00	0.75	2.56	20	9	0.33	4.43	2.00	0.19	0.16	5.41	0.13	1.78	45	7.20	292	0.32	1.47	2.62
6	5.50	0.75	2.56	20	9	0.33	4.43	2.00	0.19	0.16	5.41	0.13	1.78	51.75	7.20	292	0.32	1.59	2.82
7	6.00	0.75	2.56	20	9	0.33	4.43	2.00	0.19	0.16	5.41	0.13	1.78	56.25	7.20	292	0.32	1.67	2.97
8	6.20	0.75	2.56	20	9	0.33	4.43	2.00	0.19	0.16	5.41	0.13	1.78	59.4	7.20	292	0.32	1.74	3.09

A_o = Area per stone column
A_c = Cross sectional area of stone column
d = depth to bottom of layer from ground level
Δd = Layer Thickness
K_{oc} = Coeficient of Earth Pressure at rest of column
K_{ac} = Coeficient for Active Earth Pressure of column
E_c = Modulus of Stone Column
E_s = Modulus of Soil

n_0 = Basic improvement factor
n_1 = Improvement factor with Column Compressibility
n_2 = Improvement factor with Overburden Constraint
P_o = Imposed Stress
P_c = Imposed Stress on Column
P_s = Imposed Stress on Soil
γ_s = Unit Weight of soil
υ_s = Poissions Ratio
ϕ_c = Friction angle of Stone Column

Calculation Sheet Page 1 of 2

Determination of Settlement Beneath Pad/Strip Foundation

Contract Name: Bothkennar, Trial Footing 1
Contract Number: Trial run

P_o = 72 kN/m²
A_o = 1.13 m²
Improvement factor = n2 (n0, n1 or n2)
B = 0.75 m
L = 6 m
Time = 25 years

depth m	Δd m	z m	z/B	P_o kN/m²	P_o/σ_v	Soil Profile		Cohesive Soils: Consolidation m_v	μ	ρ_c	Cohesive Soils: Immediate C_u	E_s/C_u	ρ_i	Granular Soils: Immediate SPT N	ρ_i	Granular Soils: Creep f_t	$\rho_i + \rho_c$	ρ_T	Improvement: Vibro y/n	Priebe n2	ρ_{Tn}
0.50	0.50	0.25	0.333	57	5.06	NAT	Cohesive	0.45	1	12.80	20	150	0.00		0.00	1.48	0.00	12.80	y	1.93	6.62
1.50	1.00	1	1.333	27	1.48	NAT	Cohesive	0.5	1	13.32	20	150	0.00		0.00	1.48	0.00	13.32	y	2.04	6.53
2.50	1.00	2	2.667	13	0.48	NAT	Cohesive	0.6	1	7.78	20	150	0.00		0.00	1.48	0.00	7.78	y	2.20	3.53
3.50	1.00	3	4.000	2	0.06	NAT	Cohesive	0.45	1	0.97	20	150	0.00		0.00	1.48	0.00	0.97	y	2.39	0.41
4.50	1.00	4	5.333	0	0.00	NAT	Cohesive	0.19	1	0.00	20	150	0.00		0.00	1.48	0.00	0.00	y	2.62	0.00
5.00	0.50	4.75	6.333	0	0.00	NAT	Cohesive	0.25	1	0.00	20	150	0.00		0.00	1.48	0.00	0.00	y	2.82	0.00
5.50	0.50	5.25	7.000	0	0.00	NAT	Cohesive	0.35	1	0.00	20	150	0.00		0.00	1.48	0.00	0.00		1.00	0.00
5.70	0.20	5.6	7.467	0	0.00	NAT	Cohesive	0.35	1	0.00	20	150	0.00		0.00	1.48	0.00	0.00		1.00	0.00

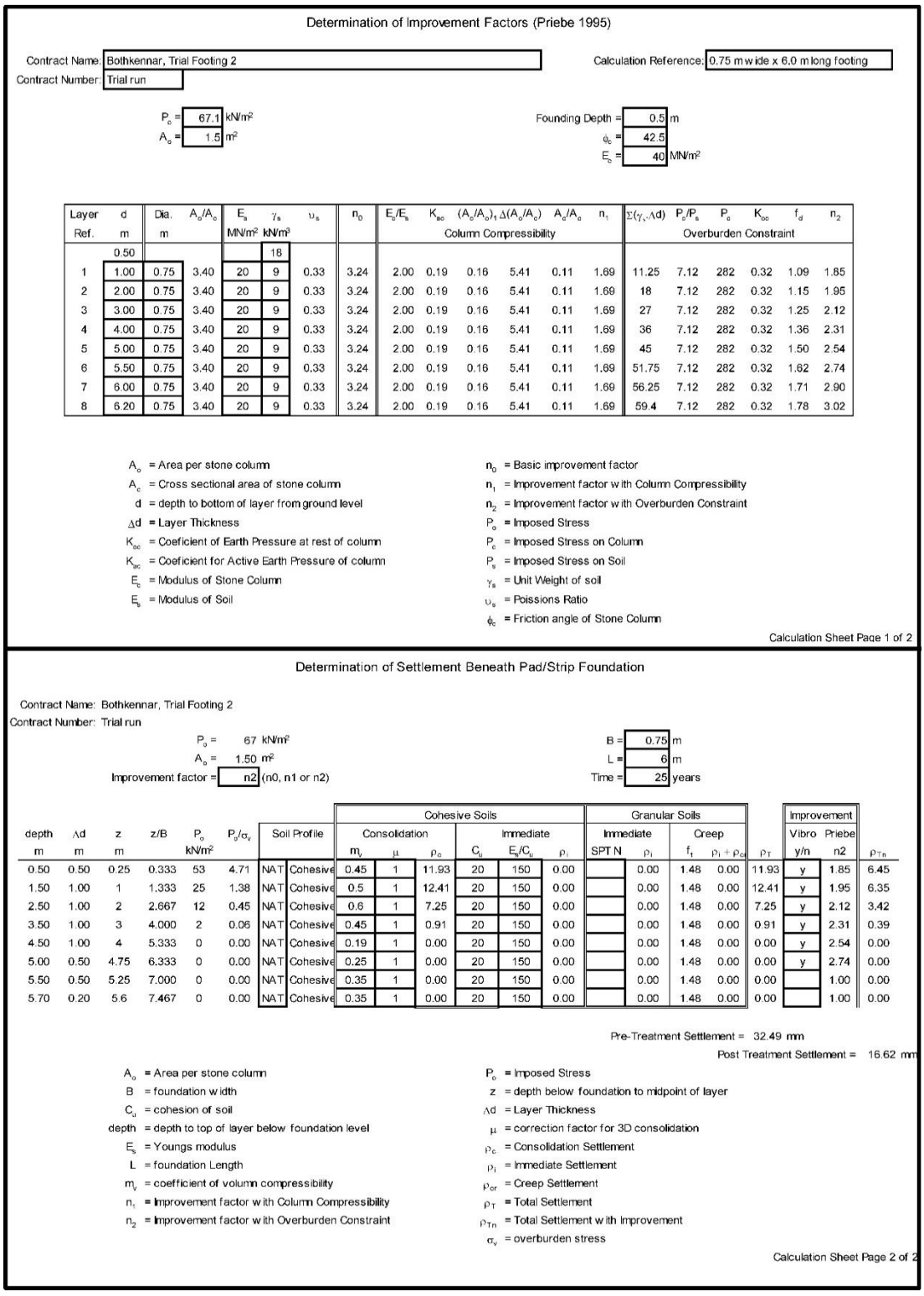
Pre-Treatment Settlement = 34.87 mm
Post Treatment Settlement = 17.09 mm

A_o = Area per stone column
B = foundation width
C_u = cohesion of soil
depth = depth to top of layer below foundation level
E_s = Youngs modulus
L = foundation Length
m_v = coefficient of volumn compressibility
n_1 = Improvement factor with Column Compressibility
n_2 = Improvement factor with Overburden Constraint

P_o = Imposed Stress
z = depth below foundation to midpoint of layer
Δd = Layer Thickness
μ = correction factor for 3D consolidation
ρ_c = Consolidation Settlement
ρ_i = Immediate Settlement
ρ_{cr} = Creep Settlement
ρ_T = Total Settlement
ρ_{Tn} = Total Settlement with Improvement
σ_v = overburden stress

Calculation Sheet Page 2 of 2

Figure A.1 Vertical settlement prediction using Priebe (1995) method- Footing 1.



Determination of Improvement Factors (Priebe 1995)

Contract Name: Bothkennar, Trial Footing 2
Contract Number: Trial run
Calculation Reference: 0.75 m wide x 6.0 m long footing

P_o = 67.1 kN/m²
A_o = 1.5 m²
Founding Depth = 0.5 m
ϕ_c = 42.5
E_c = 40 MN/m²

Layer Ref.	d m	Dia. m	A_c/A_o	E_s MN/m²	γ_s kN/m³	υ_s	n_0	E_c/E_s	K_{so}	$(A_c/A_o)_1$	$\Delta(A_c/A_o)$	A_c/A_o	n_1	$\Sigma(\gamma_s \cdot \Delta d)$	P_c/P_s	P_c	K_{oc}	f_d	n_2
	0.50				18			Column Compressibility						Overburden Constraint					
1	1.00	0.75	3.40	20	9	0.33	3.24	2.00	0.19	0.16	5.41	0.11	1.69	11.25	7.12	282	0.32	1.09	1.85
2	2.00	0.75	3.40	20	9	0.33	3.24	2.00	0.19	0.16	5.41	0.11	1.69	18	7.12	282	0.32	1.15	1.95
3	3.00	0.75	3.40	20	9	0.33	3.24	2.00	0.19	0.16	5.41	0.11	1.69	27	7.12	282	0.32	1.25	2.12
4	4.00	0.75	3.40	20	9	0.33	3.24	2.00	0.19	0.16	5.41	0.11	1.69	36	7.12	282	0.32	1.36	2.31
5	5.00	0.75	3.40	20	9	0.33	3.24	2.00	0.19	0.16	5.41	0.11	1.69	45	7.12	282	0.32	1.50	2.54
6	5.50	0.75	3.40	20	9	0.33	3.24	2.00	0.19	0.16	5.41	0.11	1.69	51.75	7.12	282	0.32	1.62	2.74
7	6.00	0.75	3.40	20	9	0.33	3.24	2.00	0.19	0.16	5.41	0.11	1.69	56.25	7.12	282	0.32	1.71	2.90
8	6.20	0.75	3.40	20	9	0.33	3.24	2.00	0.19	0.16	5.41	0.11	1.69	59.4	7.12	282	0.32	1.78	3.02

A_o = Area per stone column
A_c = Cross sectional area of stone column
d = depth to bottom of layer from ground level
Δd = Layer Thickness
K_{so} = Coeficient of Earth Pressure at rest of column
K_{ac} = Coeficient for Active Earth Pressure of column
E_c = Modulus of Stone Column
E_s = Modulus of Soil

n_0 = Basic improvement factor
n_1 = Improvement factor with Column Compressibility
n_2 = Improvement factor with Overburden Constraint
P_o = Imposed Stress
P_c = Imposed Stress on Column
P_s = Imposed Stress on Soil
γ_s = Unit Weight of soil
υ_s = Poissions Ratio
ϕ_c = Friction angle of Stone Column

Calculation Sheet Page 1 of 2

Determination of Settlement Beneath Pad/Strip Foundation

Contract Name: Bothkennar, Trial Footing 2
Contract Number: Trial run

P_o = 67 kN/m²
A_o = 1.50 m²
Improvement factor = n2 (n0, n1 or n2)
B = 0.75 m
L = 6 m
Time = 25 years

depth m	Δd m	z m	z/B	P_o kN/m²	P_o/σ_v	Soil Profile	Cohesive Soils: Consolidation m_v	μ	ρ_c	Cohesive Soils: Immediate C_u	E_u/C_u	ρ_i	Granular Soils: Immediate SPT N	ρ_i	Creep f_t	Creep $\rho_i + \rho_{cr}$	ρ_T	Improvement Vibro y/n	Improvement Priebe n2	ρ_{Tn}
0.50	0.50	0.25	0.333	53	4.71	NAT Cohesive	0.45	1	11.93	20	150	0.00		0.00	1.48	0.00	11.93	y	1.85	6.45
1.50	1.00	1	1.333	25	1.38	NAT Cohesive	0.5	1	12.41	20	150	0.00		0.00	1.48	0.00	12.41	y	1.95	6.35
2.50	1.00	2	2.667	12	0.45	NAT Cohesive	0.6	1	7.25	20	150	0.00		0.00	1.48	0.00	7.25	y	2.12	3.42
3.50	1.00	3	4.000	2	0.06	NAT Cohesive	0.45	1	0.91	20	150	0.00		0.00	1.48	0.00	0.91	y	2.31	0.39
4.50	1.00	4	5.333	0	0.00	NAT Cohesive	0.19	1	0.00	20	150	0.00		0.00	1.48	0.00	0.00	y	2.54	0.00
5.00	0.50	4.75	6.333	0	0.00	NAT Cohesive	0.25	1	0.00	20	150	0.00		0.00	1.48	0.00	0.00	y	2.74	0.00
5.50	0.50	5.25	7.000	0	0.00	NAT Cohesive	0.35	1	0.00	20	150	0.00		0.00	1.48	0.00	0.00		1.00	0.00
5.70	0.20	5.6	7.467	0	0.00	NAT Cohesive	0.35	1	0.00	20	150	0.00		0.00	1.48	0.00	0.00		1.00	0.00

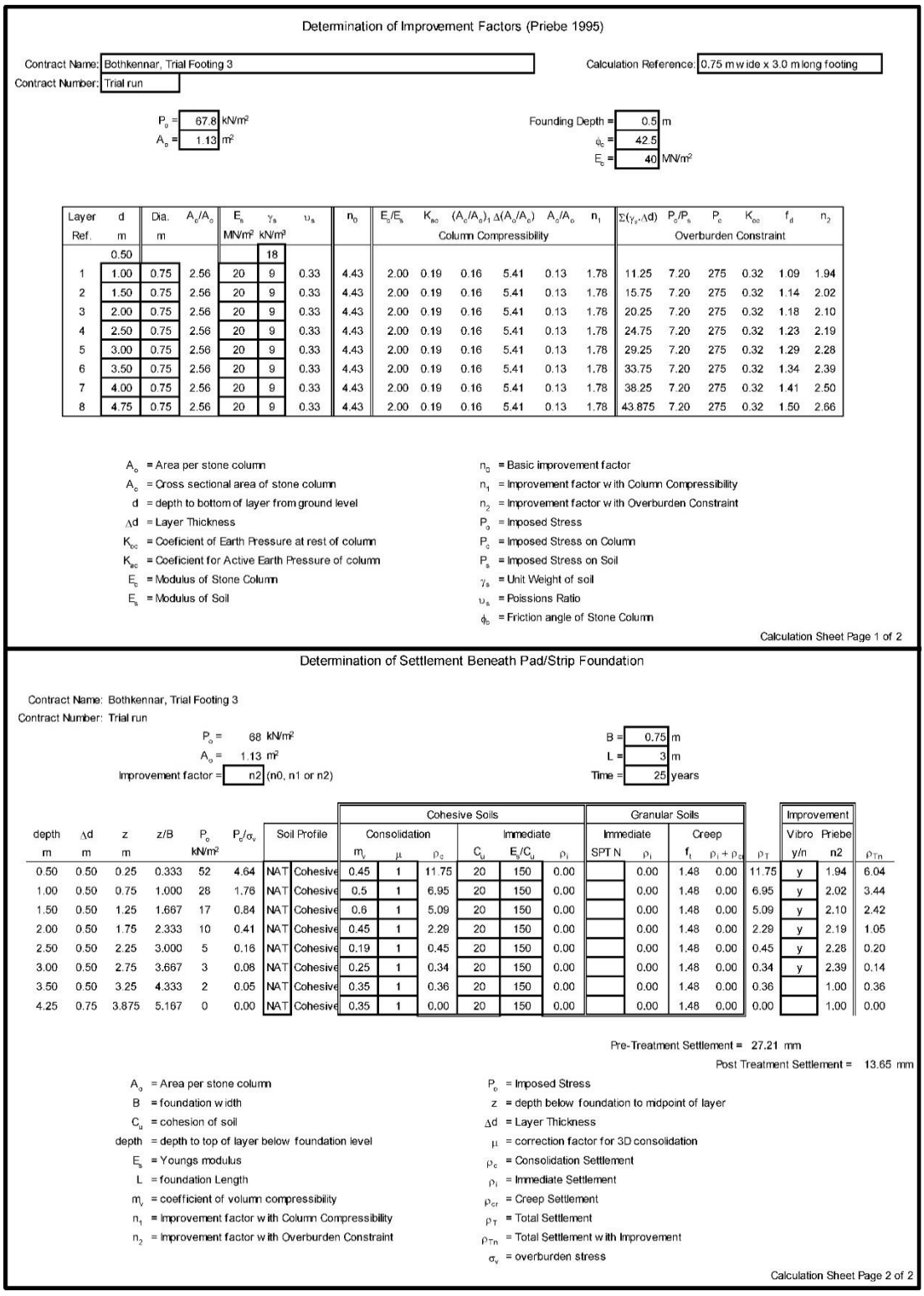
Pre-Treatment Settlement = 32.49 mm
Post Treatment Settlement = 16.62 mm

A_o = Area per stone column
B = foundation width
C_u = cohesion of soil
depth = depth to top of layer below foundation level
E_s = Youngs modulus
L = foundation Length
m_v = coefficient of volumn compressibility
n_1 = Improvement factor with Column Compressibility
n_2 = Improvement factor with Overburden Constraint

P_o = Imposed Stress
z = depth below foundation to midpoint of layer
Δd = Layer Thickness
μ = correction factor for 3D consolidation
ρ_c = Consolidation Settlement
ρ_i = Immediate Settlement
ρ_{cr} = Creep Settlement
ρ_T = Total Settlement
ρ_{Tn} = Total Settlement with Improvement
σ_v = overburden stress

Calculation Sheet Page 2 of 2

Figure A.2 Vertical settlement prediction using Priebe (1995) method- Footing 2.



Determination of Improvement Factors (Priebe 1995)

Contract Name: Bothkennar, Trial Footing 3
Contract Number: Trial run
Calculation Reference: 0.75 m wide x 3.0 m long footing

P_o = 67.8 kN/m²
A_o = 1.13 m²

Founding Depth = 0.5 m
ϕ_c = 42.5
E_c = 40 MN/m²

Layer Ref.	d m	Dia. m	A_c/A_o	E_s MN/m²	γ_s kN/m³	υ_s	n_0	E_c/E_s	K_{ac}	$(A_c/A_o)_1$	$\Delta(A_c/A_o)$	A_c/A_o	n_1	$\Sigma(\gamma_s.\Delta d)$	P_c/P_s	P_c	K_{oc}	f_d	n_2
								Column Compressibility						Overburden Constraint					
	0.50				18														
1	1.00	0.75	2.56	20	9	0.33	4.43	2.00	0.19	0.16	5.41	0.13	1.78	11.25	7.20	275	0.32	1.09	1.94
2	1.50	0.75	2.56	20	9	0.33	4.43	2.00	0.19	0.16	5.41	0.13	1.78	15.75	7.20	275	0.32	1.14	2.02
3	2.00	0.75	2.56	20	9	0.33	4.43	2.00	0.19	0.16	5.41	0.13	1.78	20.25	7.20	275	0.32	1.18	2.10
4	2.50	0.75	2.56	20	9	0.33	4.43	2.00	0.19	0.16	5.41	0.13	1.78	24.75	7.20	275	0.32	1.23	2.19
5	3.00	0.75	2.56	20	9	0.33	4.43	2.00	0.19	0.16	5.41	0.13	1.78	29.25	7.20	275	0.32	1.29	2.28
6	3.50	0.75	2.56	20	9	0.33	4.43	2.00	0.19	0.16	5.41	0.13	1.78	33.75	7.20	275	0.32	1.34	2.39
7	4.00	0.75	2.56	20	9	0.33	4.43	2.00	0.19	0.16	5.41	0.13	1.78	38.25	7.20	275	0.32	1.41	2.50
8	4.75	0.75	2.56	20	9	0.33	4.43	2.00	0.19	0.16	5.41	0.13	1.78	43.875	7.20	275	0.32	1.50	2.66

A_o = Area per stone column
A_c = Cross sectional area of stone column
d = depth to bottom of layer from ground level
Δd = Layer Thickness
K_{oc} = Coeficient of Earth Pressure at rest of column
K_{ac} = Coeficient for Active Earth Pressure of column
E_c = Modulus of Stone Column
E_s = Modulus of Soil

n_0 = Basic improvement factor
n_1 = Improvement factor with Column Compressibility
n_2 = Improvement factor with Overburden Constraint
P_o = Imposed Stress
P_c = Imposed Stress on Column
P_s = Imposed Stress on Soil
γ_s = Unit Weight of soil
υ_s = Poissons Ratio
ϕ_c = Friction angle of Stone Column

Calculation Sheet Page 1 of 2

Determination of Settlement Beneath Pad/Strip Foundation

Contract Name: Bothkennar, Trial Footing 3
Contract Number: Trial run

P_o = 68 kN/m²
A_o = 1.13 m²
Improvement factor = n2 (n0, n1 or n2)

B = 0.75 m
L = 3 m
Time = 25 years

depth m	Δd m	z m	z/B	P_o kN/m²	P_o/σ_v	Soil Profile		Cohesive Soils: Consolidation m_v	μ	ρ_c	Cohesive Soils: Immediate C_u	E_s/C_u	ρ_i	Granular Soils: Immediate SPT N	ρ_i	Granular Soils: Creep f_t	$\rho_i + \rho_{cr}$	ρ_T	Improvement: Vibro y/n	Priebe n2	ρ_{Tn}
0.50	0.50	0.25	0.333	52	4.64	NAT	Cohesive	0.45	1	11.75	20	150	0.00		0.00	1.48	0.00	11.75	y	1.94	6.04
1.00	0.50	0.75	1.000	28	1.76	NAT	Cohesive	0.5	1	6.95	20	150	0.00		0.00	1.48	0.00	6.95	y	2.02	3.44
1.50	0.50	1.25	1.667	17	0.84	NAT	Cohesive	0.6	1	5.09	20	150	0.00		0.00	1.48	0.00	5.09	y	2.10	2.42
2.00	0.50	1.75	2.333	10	0.41	NAT	Cohesive	0.45	1	2.29	20	150	0.00		0.00	1.48	0.00	2.29	y	2.19	1.05
2.50	0.50	2.25	3.000	5	0.16	NAT	Cohesive	0.19	1	0.45	20	150	0.00		0.00	1.48	0.00	0.45	y	2.28	0.20
3.00	0.50	2.75	3.667	3	0.08	NAT	Cohesive	0.25	1	0.34	20	150	0.00		0.00	1.48	0.00	0.34	y	2.39	0.14
3.50	0.50	3.25	4.333	2	0.05	NAT	Cohesive	0.35	1	0.36	20	150	0.00		0.00	1.48	0.00	0.36		1.00	0.36
4.25	0.75	3.875	5.167	0	0.00	NAT	Cohesive	0.35	1	0.00	20	150	0.00		0.00	1.48	0.00	0.00		1.00	0.00

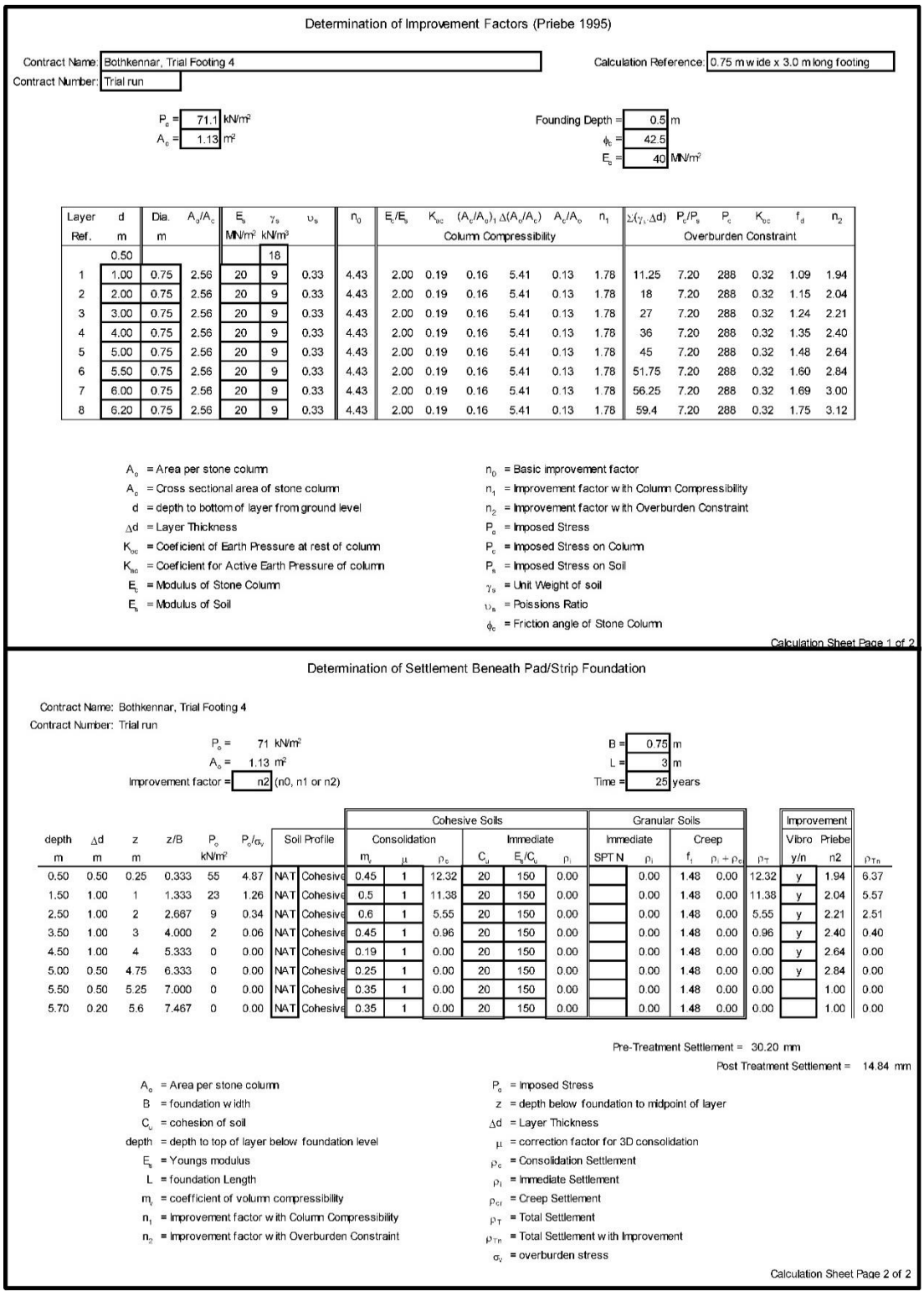
Pre-Treatment Settlement = 27.21 mm
Post Treatment Settlement = 13.65 mm

A_o = Area per stone column
B = foundation width
C_u = cohesion of soil
depth = depth to top of layer below foundation level
E_s = Youngs modulus
L = foundation Length
m_v = coefficient of volumn compressibility
n_1 = Improvement factor with Column Compressibility
n_2 = Improvement factor with Overburden Constraint

P_o = Imposed Stress
z = depth below foundation to midpoint of layer
Δd = Layer Thickness
μ = correction factor for 3D consolidation
ρ_c = Consolidation Settlement
ρ_i = Immediate Settlement
ρ_{cr} = Creep Settlement
ρ_T = Total Settlement
ρ_{Tn} = Total Settlement with Improvement
σ_v = overburden stress

Calculation Sheet Page 2 of 2

Figure A.3 Vertical settlement prediction using Priebe (1995) method- Footing 3.



Determination of Improvement Factors (Priebe 1995)

Contract Name: Bothkennar, Trial Footing 4
Contract Number: Trial run
Calculation Reference: 0.75 m wide x 3.0 m long footing

P_o = 71.1 kN/m²
A_o = 1.13 m²

Founding Depth = 0.5 m
ϕ_c = 42.5
E_c = 40 MN/m²

Layer Ref.	d m	Dia. m	A_c/A_o	E_s MN/m²	γ_s kN/m³	υ_s	n_0	E_c/E_s	K_{ac}	$(A_c/A_o)_1$	$\Delta(A_c/A_o)$	A_c/A_o	n_1	$\Sigma(\gamma_i \cdot \Delta d)$	P_c/P_s	P_c	K_{oc}	f_d	n_2
	0.50				18			Column Compressibility						Overburden Constraint					
1	1.00	0.75	2.56	20	9	0.33	4.43	2.00	0.19	0.16	5.41	0.13	1.78	11.25	7.20	288	0.32	1.09	1.94
2	2.00	0.75	2.56	20	9	0.33	4.43	2.00	0.19	0.16	5.41	0.13	1.78	18	7.20	288	0.32	1.15	2.04
3	3.00	0.75	2.56	20	9	0.33	4.43	2.00	0.19	0.16	5.41	0.13	1.78	27	7.20	288	0.32	1.24	2.21
4	4.00	0.75	2.56	20	9	0.33	4.43	2.00	0.19	0.16	5.41	0.13	1.78	36	7.20	288	0.32	1.35	2.40
5	5.00	0.75	2.56	20	9	0.33	4.43	2.00	0.19	0.16	5.41	0.13	1.78	45	7.20	288	0.32	1.48	2.64
6	5.50	0.75	2.56	20	9	0.33	4.43	2.00	0.19	0.16	5.41	0.13	1.78	51.75	7.20	288	0.32	1.60	2.84
7	6.00	0.75	2.56	20	9	0.33	4.43	2.00	0.19	0.16	5.41	0.13	1.78	56.25	7.20	288	0.32	1.69	3.00
8	6.20	0.75	2.56	20	9	0.33	4.43	2.00	0.19	0.16	5.41	0.13	1.78	59.4	7.20	288	0.32	1.75	3.12

A_o = Area per stone column
A_c = Cross sectional area of stone column
d = depth to bottom of layer from ground level
Δd = Layer Thickness
K_{oc} = Coeficient of Earth Pressure at rest of column
K_{ac} = Coeficient for Active Earth Pressure of column
E_c = Modulus of Stone Column
E_s = Modulus of Soil

n_0 = Basic improvement factor
n_1 = Improvement factor with Column Compressibility
n_2 = Improvement factor with Overburden Constraint
P_o = Imposed Stress
P_c = Imposed Stress on Column
P_s = Imposed Stress on Soil
γ_s = Unit Weight of soil
υ_s = Poissions Ratio
ϕ_c = Friction angle of Stone Column

Calculation Sheet Page 1 of 2

Determination of Settlement Beneath Pad/Strip Foundation

Contract Name: Bothkennar, Trial Footing 4
Contract Number: Trial run

P_o = 71 kN/m²
A_o = 1.13 m²
Improvement factor = n2 (n0, n1 or n2)

B = 0.75 m
L = 3 m
Time = 25 years

depth m	Δd m	z m	z/B	P_o kN/m²	P_o/σ_v	Soil Profile		Cohesive Soils: Consolidation m_v	μ	ρ_c	Cohesive Soils: Immediate C_u	E_s/C_u	ρ_i	Granular Soils: Immediate SPT N	ρ_i	Granular Soils: Creep f_t	$\rho_i + \rho_{cr}$	ρ_T	Improvement: Vibro y/n	Priebe n2	ρ_{Tn}
0.50	0.50	0.25	0.333	55	4.87	NAT	Cohesive	0.45	1	12.32	20	150	0.00		0.00	1.48	0.00	12.32	y	1.94	6.37
1.50	1.00	1	1.333	23	1.26	NAT	Cohesive	0.5	1	11.38	20	150	0.00		0.00	1.48	0.00	11.38	y	2.04	5.57
2.50	1.00	2	2.667	9	0.34	NAT	Cohesive	0.6	1	5.55	20	150	0.00		0.00	1.48	0.00	5.55	y	2.21	2.51
3.50	1.00	3	4.000	2	0.06	NAT	Cohesive	0.45	1	0.96	20	150	0.00		0.00	1.48	0.00	0.96	y	2.40	0.40
4.50	1.00	4	5.333	0	0.00	NAT	Cohesive	0.19	1	0.00	20	150	0.00		0.00	1.48	0.00	0.00	y	2.64	0.00
5.00	0.50	4.75	6.333	0	0.00	NAT	Cohesive	0.25	1	0.00	20	150	0.00		0.00	1.48	0.00	0.00	y	2.84	0.00
5.50	0.50	5.25	7.000	0	0.00	NAT	Cohesive	0.35	1	0.00	20	150	0.00		0.00	1.48	0.00	0.00		1.00	0.00
5.70	0.20	5.6	7.467	0	0.00	NAT	Cohesive	0.35	1	0.00	20	150	0.00		0.00	1.48	0.00	0.00		1.00	0.00

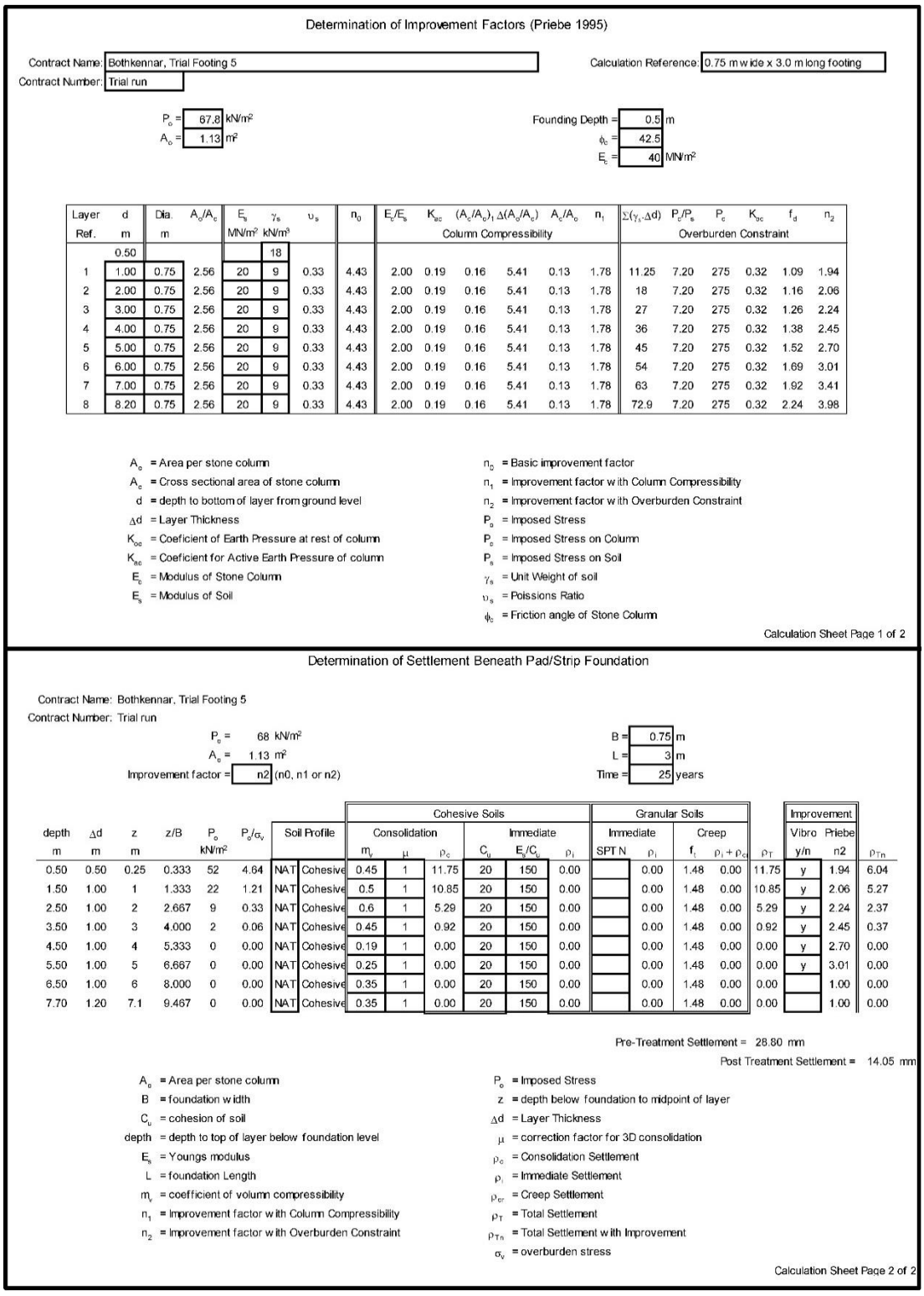
Pre-Treatment Settlement = 30.20 mm
Post Treatment Settlement = 14.84 mm

A_o = Area per stone column
B = foundation width
C_u = cohesion of soil
depth = depth to top of layer below foundation level
E_s = Youngs modulus
L = foundation Length
m_v = coefficient of volumn compressibility
n_1 = Improvement factor with Column Compressibility
n_2 = Improvement factor with Overburden Constraint

P_o = Imposed Stress
z = depth below foundation to midpoint of layer
Δd = Layer Thickness
μ = correction factor for 3D consolidation
ρ_c = Consolidation Settlement
ρ_i = Immediate Settlement
ρ_{cr} = Creep Settlement
ρ_T = Total Settlement
ρ_{Tn} = Total Settlement with Improvement
σ_v = overburden stress

Calculation Sheet Page 2 of 2

Figure A.4 Vertical settlement prediction using Priebe (1995) method- Footing 4.



Determination of Improvement Factors (Priebe 1995)

Contract Name: Bothkennar, Trial Footing 5
Contract Number: Trial run
Calculation Reference: 0.75 m wide x 3.0 m long footing

P_o = 67.8 kN/m²
A_o = 1.13 m²
Founding Depth = 0.5 m
ϕ_c = 42.5
E_c = 40 MN/m²

Layer Ref.	d m	Dia. m	A_c/A_c	E_s MN/m²	γ_s kN/m³	υ_s	n_0	E_c/E_s	K_{ac}	$(A_c/A_c)_1$	$\Delta(A_c/A_c)$	A_c/A_c	n_1	$\Sigma(\gamma_s.\Delta d)$	P_c/P_s	P_c	K_{oc}	f_d	n_2
	0.50				18			Column Compressibility						Overburden Constraint					
1	1.00	0.75	2.56	20	9	0.33	4.43	2.00	0.19	0.16	5.41	0.13	1.78	11.25	7.20	275	0.32	1.09	1.94
2	2.00	0.75	2.56	20	9	0.33	4.43	2.00	0.19	0.16	5.41	0.13	1.78	18	7.20	275	0.32	1.16	2.06
3	3.00	0.75	2.56	20	9	0.33	4.43	2.00	0.19	0.16	5.41	0.13	1.78	27	7.20	275	0.32	1.26	2.24
4	4.00	0.75	2.56	20	9	0.33	4.43	2.00	0.19	0.16	5.41	0.13	1.78	36	7.20	275	0.32	1.38	2.45
5	5.00	0.75	2.56	20	9	0.33	4.43	2.00	0.19	0.16	5.41	0.13	1.78	45	7.20	275	0.32	1.52	2.70
6	6.00	0.75	2.56	20	9	0.33	4.43	2.00	0.19	0.16	5.41	0.13	1.78	54	7.20	275	0.32	1.69	3.01
7	7.00	0.75	2.56	20	9	0.33	4.43	2.00	0.19	0.16	5.41	0.13	1.78	63	7.20	275	0.32	1.92	3.41
8	8.20	0.75	2.56	20	9	0.33	4.43	2.00	0.19	0.16	5.41	0.13	1.78	72.9	7.20	275	0.32	2.24	3.98

A_o = Area per stone column
A_c = Cross sectional area of stone column
d = depth to bottom of layer from ground level
Δd = Layer Thickness
K_{oc} = Coeficient of Earth Pressure at rest of column
K_{ac} = Coeficient for Active Earth Pressure of column
E_c = Modulus of Stone Column
E_s = Modulus of Soil

n_0 = Basic improvement factor
n_1 = Improvement factor with Column Compressibility
n_2 = Improvement factor with Overburden Constraint
P_o = Imposed Stress
P_c = Imposed Stress on Column
P_s = Imposed Stress on Soil
γ_s = Unit Weight of soil
υ_s = Poissions Ratio
ϕ_c = Friction angle of Stone Column

Calculation Sheet Page 1 of 2

Determination of Settlement Beneath Pad/Strip Foundation

Contract Name: Bothkennar, Trial Footing 5
Contract Number: Trial run

P_o = 68 kN/m²
A_o = 1.13 m²
Improvement factor = n2 (n0, n1 or n2)
B = 0.75 m
L = 3 m
Time = 25 years

depth m	Δd m	z m	z/B	P_o kN/m²	P_o/σ_v	Soil Profile		Cohesive Soils: Consolidation m_v	μ	ρ_c	Cohesive Soils: Immediate C_u	E_u/C_u	ρ_i	Granular Soils: Immediate SPT N	ρ_i	Granular Soils: Creep t_t	$\rho_i + \rho_c$	ρ_T	Improvement: Vibro y/n	Improvement: Priebe n2	ρ_{Tn}
0.50	0.50	0.25	0.333	52	4.64	NAT	Cohesive	0.45	1	11.75	20	150	0.00		0.00	1.48	0.00	11.75	y	1.94	6.04
1.50	1.00	1	1.333	22	1.21	NAT	Cohesive	0.5	1	10.85	20	150	0.00		0.00	1.48	0.00	10.85	y	2.06	5.27
2.50	1.00	2	2.667	9	0.33	NAT	Cohesive	0.6	1	5.29	20	150	0.00		0.00	1.48	0.00	5.29	y	2.24	2.37
3.50	1.00	3	4.000	2	0.06	NAT	Cohesive	0.45	1	0.92	20	150	0.00		0.00	1.48	0.00	0.92	y	2.45	0.37
4.50	1.00	4	5.333	0	0.00	NAT	Cohesive	0.19	1	0.00	20	150	0.00		0.00	1.48	0.00	0.00	y	2.70	0.00
5.50	1.00	5	6.667	0	0.00	NAT	Cohesive	0.25	1	0.00	20	150	0.00		0.00	1.48	0.00	0.00	y	3.01	0.00
6.50	1.00	6	8.000	0	0.00	NAT	Cohesive	0.35	1	0.00	20	150	0.00		0.00	1.48	0.00	0.00		1.00	0.00
7.70	1.20	7.1	9.467	0	0.00	NAT	Cohesive	0.35	1	0.00	20	150	0.00		0.00	1.48	0.00	0.00		1.00	0.00

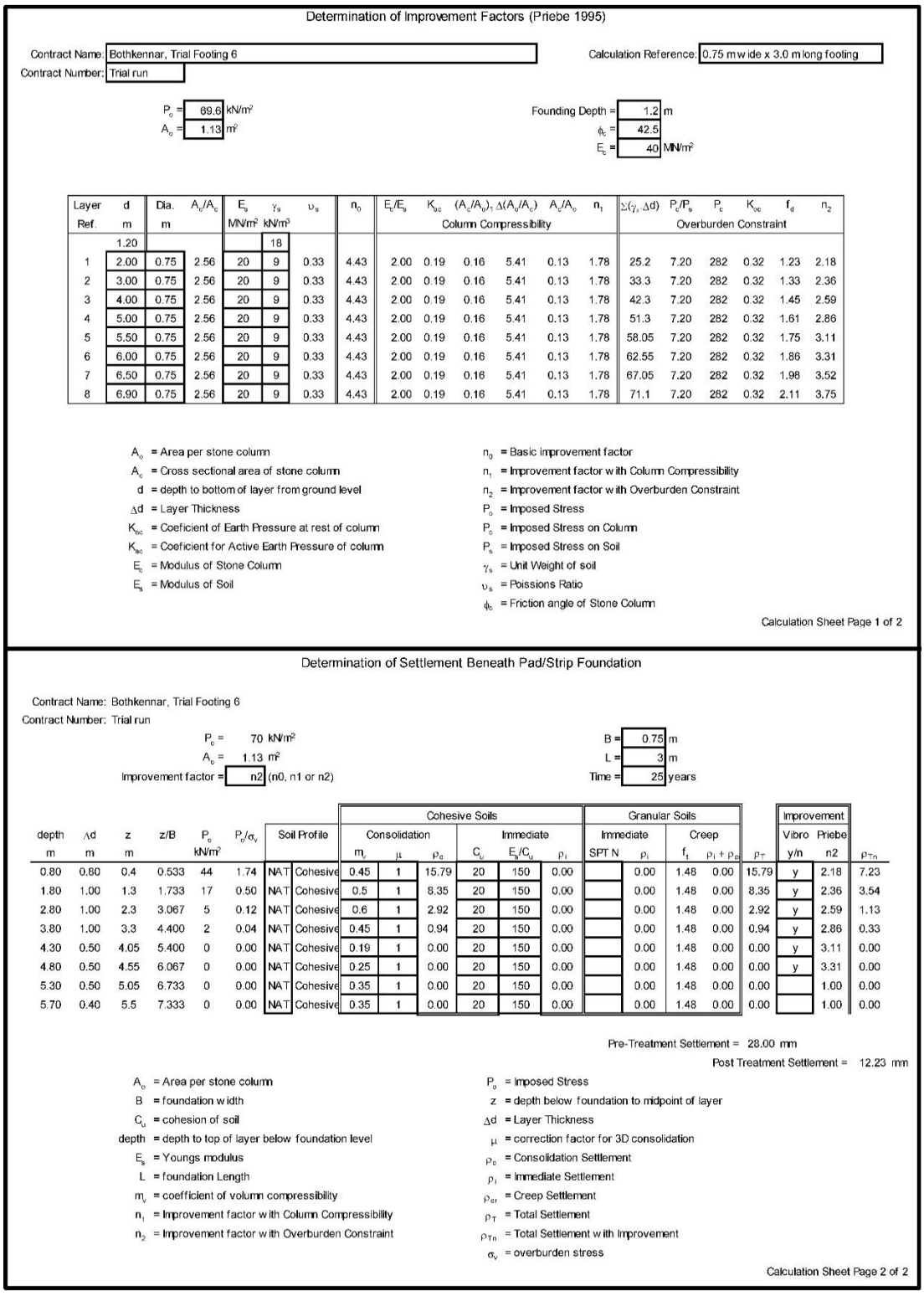
Pre-Treatment Settlement = 28.80 mm
Post Treatment Settlement = 14.05 mm

A_o = Area per stone column
B = foundation width
C_u = cohesion of soil
depth = depth to top of layer below foundation level
E_s = Youngs modulus
L = foundation Length
m_v = coefficient of volumn compressibility
n_1 = Improvement factor with Column Compressibility
n_2 = Improvement factor with Overburden Constraint

P_o = Imposed Stress
z = depth below foundation to midpoint of layer
Δd = Layer Thickness
μ = correction factor for 3D consolidation
ρ_c = Consolidation Settlement
ρ_i = Immediate Settlement
ρ_{cr} = Creep Settlement
ρ_T = Total Settlement
ρ_{Tn} = Total Settlement with Improvement
σ_v = overburden stress

Calculation Sheet Page 2 of 2

Figure A.5 Vertical settlement prediction using Priebe (1995) method- Footing 5.



Determination of Improvement Factors (Priebe 1995)

Contract Name: Bothkennar, Trial Footing 6
Contract Number: Trial run
Calculation Reference: 0.75 m wide x 3.0 m long footing

P_o = 69.6 kN/m²
A_o = 1.13 m²
Founding Depth = 1.2 m
ϕ_c = 42.5
E_c = 40 MN/m²

Layer Ref.	d m	Dia. m	A_o/A_c	E_s MN/m²	γ_s kN/m³	υ_s	n_0	E_c/E_s	K_{ac}	$(A_c/A_o)_1$	$\Delta(A_o/A_c)$	A_c/A_o	n_1	$\Sigma(\gamma_s \Delta d)$	P_c/P_s	P_c	K_{oc}	f_d	n_2
								Column Compressibility						Overburden Constraint					
	1.20				18														
1	2.00	0.75	2.56	20	9	0.33	4.43	2.00	0.19	0.16	5.41	0.13	1.78	25.2	7.20	282	0.32	1.23	2.18
2	3.00	0.75	2.56	20	9	0.33	4.43	2.00	0.19	0.16	5.41	0.13	1.78	33.3	7.20	282	0.32	1.33	2.36
3	4.00	0.75	2.56	20	9	0.33	4.43	2.00	0.19	0.16	5.41	0.13	1.78	42.3	7.20	282	0.32	1.45	2.59
4	5.00	0.75	2.56	20	9	0.33	4.43	2.00	0.19	0.16	5.41	0.13	1.78	51.3	7.20	282	0.32	1.61	2.86
5	5.50	0.75	2.56	20	9	0.33	4.43	2.00	0.19	0.16	5.41	0.13	1.78	58.05	7.20	282	0.32	1.75	3.11
6	6.00	0.75	2.56	20	9	0.33	4.43	2.00	0.19	0.16	5.41	0.13	1.78	62.55	7.20	282	0.32	1.86	3.31
7	6.50	0.75	2.56	20	9	0.33	4.43	2.00	0.19	0.16	5.41	0.13	1.78	67.05	7.20	282	0.32	1.98	3.52
8	6.90	0.75	2.56	20	9	0.33	4.43	2.00	0.19	0.16	5.41	0.13	1.78	71.1	7.20	282	0.32	2.11	3.75

A_o = Area per stone column
A_c = Cross sectional area of stone column
d = depth to bottom of layer from ground level
Δd = Layer Thickness
K_{oc} = Coeficient of Earth Pressure at rest of column
K_{ac} = Coeficient for Active Earth Pressure of column
E_c = Modulus of Stone Column
E_s = Modulus of Soil

n_0 = Basic improvement factor
n_1 = Improvement factor with Column Compressibility
n_2 = Improvement factor with Overburden Constraint
P_o = Imposed Stress
P_c = Imposed Stress on Column
P_s = Imposed Stress on Soil
γ_s = Unit Weight of soil
υ_s = Poissions Ratio
ϕ_c = Friction angle of Stone Column

Calculation Sheet Page 1 of 2

Determination of Settlement Beneath Pad/Strip Foundation

Contract Name: Bothkennar, Trial Footing 6
Contract Number: Trial run

P_o = 70 kN/m²
A_o = 1.13 m²
Improvement factor = n2 (n0, n1 or n2)
B = 0.75 m
L = 3 m
Time = 25 years

depth m	Δd m	z m	z/B	P_o kN/m²	P_o/σ_v	Soil Profile		Cohesive Soils: Consolidation m_v	μ	ρ_c	Cohesive Soils: Immediate C_u	E_s/C_u	ρ_i	Granular Soils: Immediate SPT N	ρ_i	Granular Soils: Creep f_t	$\rho_i + \rho_{cr}$	ρ_T	Improvement: Vibro y/n	Priebe n2	ρ_{Tn}
0.80	0.60	0.4	0.533	44	1.74	NAT	Cohesive	0.45	1	15.79	20	150	0.00		0.00	1.48	0.00	15.79	y	2.18	7.23
1.80	1.00	1.3	1.733	17	0.50	NAT	Cohesive	0.5	1	8.35	20	150	0.00		0.00	1.48	0.00	8.35	y	2.36	3.54
2.80	1.00	2.3	3.067	5	0.12	NAT	Cohesive	0.6	1	2.92	20	150	0.00		0.00	1.48	0.00	2.92	y	2.59	1.13
3.80	1.00	3.3	4.400	2	0.04	NAT	Cohesive	0.45	1	0.94	20	150	0.00		0.00	1.48	0.00	0.94	y	2.86	0.33
4.30	0.50	4.05	5.400	0	0.00	NAT	Cohesive	0.19	1	0.00	20	150	0.00		0.00	1.48	0.00	0.00	y	3.11	0.00
4.80	0.50	4.55	6.067	0	0.00	NAT	Cohesive	0.25	1	0.00	20	150	0.00		0.00	1.48	0.00	0.00	y	3.31	0.00
5.30	0.50	5.05	6.733	0	0.00	NAT	Cohesive	0.35	1	0.00	20	150	0.00		0.00	1.48	0.00	0.00		1.00	0.00
5.70	0.40	5.5	7.333	0	0.00	NAT	Cohesive	0.35	1	0.00	20	150	0.00		0.00	1.48	0.00	0.00		1.00	0.00

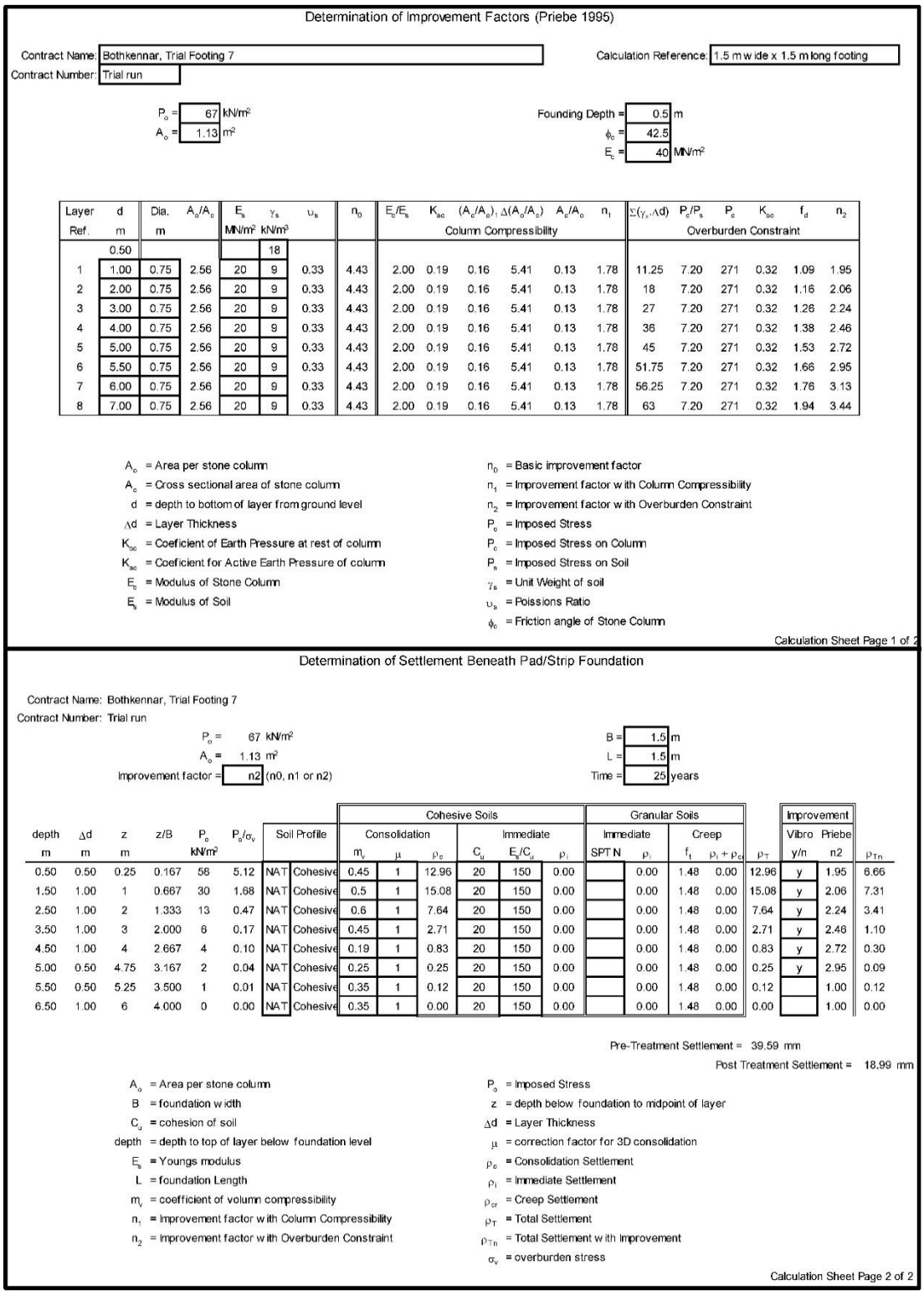
Pre-Treatment Settlement = 28.00 mm
Post Treatment Settlement = 12.23 mm

A_o = Area per stone column
B = foundation width
C_u = cohesion of soil
depth = depth to top of layer below foundation level
E_s = Youngs modulus
L = foundation Length
m_v = coefficient of volumn compressibility
n_1 = Improvement factor with Column Compressibility
n_2 = Improvement factor with Overburden Constraint

P_o = Imposed Stress
z = depth below foundation to midpoint of layer
Δd = Layer Thickness
μ = correction factor for 3D consolidation
ρ_c = Consolidation Settlement
ρ_i = Immediate Settlement
ρ_{cr} = Creep Settlement
ρ_T = Total Settlement
ρ_{Tn} = Total Settlement with Improvement
σ_v = overburden stress

Calculation Sheet Page 2 of 2

Figure A.6 Vertical settlement prediction using Priebe (1995) method- Footing 6.



Determination of Improvement Factors (Priebe 1995)

Contract Name: Bothkennar, Trial Footing 7
Contract Number: Trial run
Calculation Reference: 1.5 m wide x 1.5 m long footing

P_o = 67 kN/m²
A_o = 1.13 m²
Founding Depth = 0.5 m
ϕ_c = 42.5
E_c = 40 MN/m²

Layer Ref.	d m	Dia. m	A_o/A_c	E_s MN/m²	γ_s kN/m³	υ_s	n_0	E_c/E_s	K_{ac}	$(A_c/A_o)_1$	$\Delta(A_o/A_c)$	A_c/A_o	n_1	$\Sigma(\gamma_s.\Delta d)$	P_c/P_s	P_c	K_{ac}	f_d	n_2
	0.50				18			Column Compressibility						Overburden Constraint					
1	1.00	0.75	2.56	20	9	0.33	4.43	2.00	0.19	0.16	5.41	0.13	1.78	11.25	7.20	271	0.32	1.09	1.95
2	2.00	0.75	2.56	20	9	0.33	4.43	2.00	0.19	0.16	5.41	0.13	1.78	18	7.20	271	0.32	1.16	2.06
3	3.00	0.75	2.56	20	9	0.33	4.43	2.00	0.19	0.16	5.41	0.13	1.78	27	7.20	271	0.32	1.26	2.24
4	4.00	0.75	2.56	20	9	0.33	4.43	2.00	0.19	0.16	5.41	0.13	1.78	36	7.20	271	0.32	1.38	2.46
5	5.00	0.75	2.56	20	9	0.33	4.43	2.00	0.19	0.16	5.41	0.13	1.78	45	7.20	271	0.32	1.53	2.72
6	5.50	0.75	2.56	20	9	0.33	4.43	2.00	0.19	0.16	5.41	0.13	1.78	51.75	7.20	271	0.32	1.66	2.95
7	6.00	0.75	2.56	20	9	0.33	4.43	2.00	0.19	0.16	5.41	0.13	1.78	56.25	7.20	271	0.32	1.76	3.13
8	7.00	0.75	2.56	20	9	0.33	4.43	2.00	0.19	0.16	5.41	0.13	1.78	63	7.20	271	0.32	1.94	3.44

A_o = Area per stone column
A_c = Cross sectional area of stone column
d = depth to bottom of layer from ground level
Δd = Layer Thickness
K_{ac} = Coeficient of Earth Pressure at rest of column
K_{ac} = Coeficient for Active Earth Pressure of column
E_c = Modulus of Stone Column
E_s = Modulus of Soil

n_0 = Basic improvement factor
n_1 = Improvement factor with Column Compressibility
n_2 = Improvement factor with Overburden Constraint
P_o = Imposed Stress
P_c = Imposed Stress on Column
P_s = Imposed Stress on Soil
γ_s = Unit Weight of soil
υ_s = Poissions Ratio
ϕ_c = Friction angle of Stone Column

Calculation Sheet Page 1 of 2

Determination of Settlement Beneath Pad/Strip Foundation

Contract Name: Bothkennar, Trial Footing 7
Contract Number: Trial run

P_o = 67 kN/m²
A_o = 1.13 m²
Improvement factor = n2 (n0, n1 or n2)

B = 1.5 m
L = 1.5 m
Time = 25 years

depth m	Δd m	z m	z/B	P_o kN/m²	P_o/σ_v	Soil Profile		Cohesive Soils: Consolidation m_v	μ	ρ_c	Cohesive Soils: Immediate C_u	E_s/C_u	ρ_i	Granular Soils: Immediate SPT N	ρ_i	Granular Soils: Creep f_t	$\rho_i + \rho_c$	ρ_T	Improvement: Vibro y/n	Priebe n2	ρ_{Tn}
0.50	0.50	0.25	0.167	58	5.12	NAT	Cohesive	0.45	1	12.96	20	150	0.00		0.00	1.48	0.00	12.96	y	1.95	6.66
1.50	1.00	1	0.667	30	1.68	NAT	Cohesive	0.5	1	15.08	20	150	0.00		0.00	1.48	0.00	15.08	y	2.06	7.31
2.50	1.00	2	1.333	13	0.47	NAT	Cohesive	0.6	1	7.64	20	150	0.00		0.00	1.48	0.00	7.64	y	2.24	3.41
3.50	1.00	3	2.000	6	0.17	NAT	Cohesive	0.45	1	2.71	20	150	0.00		0.00	1.48	0.00	2.71	y	2.46	1.10
4.50	1.00	4	2.667	4	0.10	NAT	Cohesive	0.19	1	0.83	20	150	0.00		0.00	1.48	0.00	0.83	y	2.72	0.30
5.00	0.50	4.75	3.167	2	0.04	NAT	Cohesive	0.25	1	0.25	20	150	0.00		0.00	1.48	0.00	0.25	y	2.95	0.09
5.50	0.50	5.25	3.500	1	0.01	NAT	Cohesive	0.35	1	0.12	20	150	0.00		0.00	1.48	0.00	0.12		1.00	0.12
6.50	1.00	6	4.000	0	0.00	NAT	Cohesive	0.35	1	0.00	20	150	0.00		0.00	1.48	0.00	0.00		1.00	0.00

Pre-Treatment Settlement = 39.59 mm
Post Treatment Settlement = 18.99 mm

A_o = Area per stone column
B = foundation width
C_u = cohesion of soil
depth = depth to top of layer below foundation level
E_s = Youngs modulus
L = foundation Length
m_v = coefficient of volumn compressibility
n_1 = Improvement factor with Column Compressibility
n_2 = Improvement factor with Overburden Constraint

P_o = Imposed Stress
z = depth below foundation to midpoint of layer
Δd = Layer Thickness
μ = correction factor for 3D consolidation
ρ_c = Consolidation Settlement
ρ_i = Immediate Settlement
ρ_{cr} = Creep Settlement
ρ_T = Total Settlement
ρ_{Tn} = Total Settlement with Improvement
σ_v = overburden stress

Calculation Sheet Page 2 of 2

Figure A.7 Vertical settlement prediction using Priebe (1995) method- Footing 7.

Stress Distribution Beneath Main Foundations

Beneath pad / strip foundations a Bousinessq stress distribution is used.

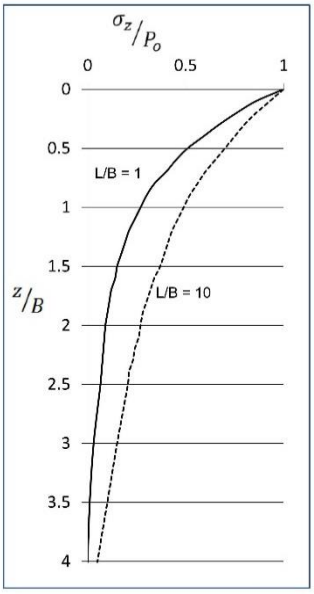


Figure A.8 Mean vertical stress (σ_z) at a depth Z beneath a rectangular area (L x B) loaded to a uniform bearing pressure of P_0, after Boussinesq (1885).

Settlement Determination

Cohesive Soils

Immediate Settlement – Ueshita and Meyerhof (1968)

The solution of immediate (undrained) settlements within clays is provided by Ueshita and Meyerhof (1968). The solution provides the settlement at the corner of a loaded area, and in order to determine the maximum settlement at the centre of a loaded area the principle of superposition should be applied. The expression used by Ueshita and Meyerhof (1968) is as follows:

$$\rho_I = \{q.B.I\}/E_u$$

where,

q = Uniform applied pressure

B = Foundation width

I = Influence Factor (Figure 1)

E_u = Undrained shear modulus

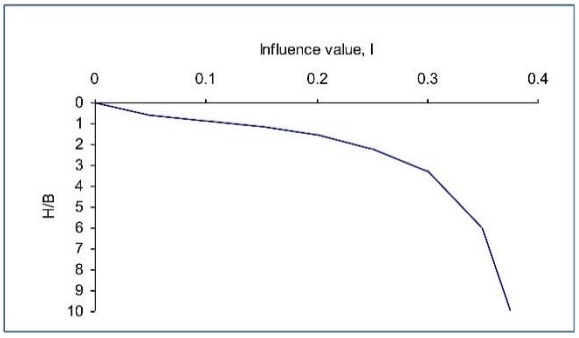


Figure A.9 Influence values (I) based on L/B = 1, for various soil layer thickness (H), after Ueshita and Meyerhoff (1968).

Consolidation Settlements - Oedometer or M_v Method

Where cohesive soils are encountered, oedometer tests are often carried out to determine the consolidation characteristics of the soils. For a given pressure increase above the effective vertical stress at the depth the sample was collected, the m_v value can be measured (coefficient of volume compressibility). Using this m_v value the change in thickness/settlement for a soil layer is obtained using the following expression:

$$\rho_{oed} = m_v.H.\Delta\sigma$$

where,

m_v = Coefficient of volume compressibility

H = Initial thickness of soil layer

$\Delta\sigma$ = Change in stress

Skempton and Bjerrum (1957) have taken this a stage further by stating that the settlements predicted by the above equation do not take into account the fact that soils beneath structures are not laterally confined as with the oedometer tests. They introduced a semi-empirical correction factor (μ), to give the consolidation settlement as:

$$\rho_c = \mu.\rho_{oed}$$

Granular Soils

Immediate Settlements – Burland and Burbridge (1985)

Based on the statistical analysis of observed settlements, Burland and Burbridge (1985) proposed that the average immediate settlement for a foundation founded on the surface of normally consolidated sands is given by:

$$\rho_i = f_s.f_l.q`.B^{0.7}.I_c$$

where,

q` = Average gross effective foundation pressure (kN/m^2)

B = Width of foundations (m)

I_c = Compressibility index

$= (1.71)/(N^{1.4})$

f_s = Shape factor

$= [\{1.25.(L/B)\}/\{(L/B)+0.2\}]$

f_l = Thickness factor

$= (H_s/Z_l).\{2-(H_s/Z_l)\}$ for $H_s < Z_l$

$= 1$ for $H_s > Z_l$

where,

N = Average SPT value over depth of influence

L = Foundation length (m)

B = Foundation breadth (m)

Z_I = Depth of influence (Figure 2)

H_s = Thickness of sand below foundation (m)

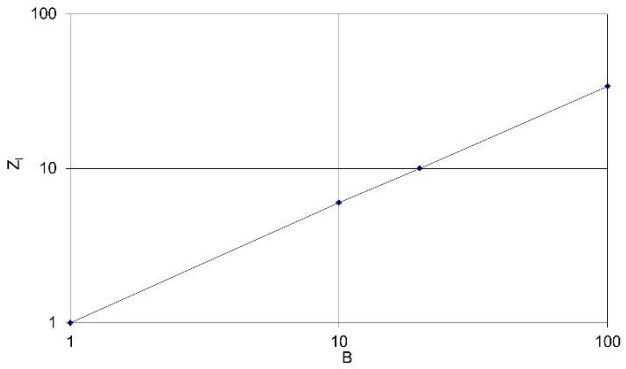


Figure A.10 Depth of influence, after Burland and Burbridge (1985).

Creep Settlements

A correction is applied to the immediate settlement in granular soils to obtain the long term (or creep) settlement. The correction is given by the term:

$$f_t = 1 + R_3 + R_t.\log_{10}(t/3)$$

where,

R_3 = 0.3 for static loads and 0.7 for fluctuating loads

R_t = 0.2 for static loads and 0.8 for fluctuating loads

The corrected immediate settlement is then given by:

$$\rho_t = f_t.\rho_i$$

Appendix B:

A program was written by the author in Visual Basic (Figure B.1) to model the circular cell geometry as illustrated in Figure 5.1. The analytical model was used to predict the relative settlement reduction ratio (RSR) in Chapter 5.

```
Dim P_r As Double
Dim R As Double
Dim Y_soft_soil As Double
Dim RF As Double
Dim H As Double
Dim Beta As Double
Dim Load As Double
Dim S As Double
Dim S0 As Double
Dim TOL As Double
Dim l_crit As Double
Dim Eoed1 As Double
Dim Eoed2 As Double
Dim t1 As Double
Dim t2 As Double
Dim t3 As Double
Dim t4 As Double
Dim t5 As Double
Dim SF As Double
Dim Ss As Double
Dim rsr As Double

Private Sub initilize()
   P_r = 0.3
   R = 0.75
   Y_soft_soil = 6.5
   RF = 0.42
   H = 10
   SF = 0.4
End Sub

Private Sub calculate()
  Beta = ((2 * P_r) / (R * R - P_r * P_r)) * RF
  S = 0
  S0 = 0
    Load = 50
    l_crit = Sqr((2 * Load) / (Beta * Y_soft_soil))
    Eoed1 = 15 * (0.5 * l_crit * Y_soft_soil + 0.5 * Load)
    Eoed2 = 15 * (0.5 * (H + l_crit) * Y_soft_soil + 0.5 * Load)
    t1 = (Load * (H - l_crit)) / Eoed2
    t2 = (Load + (Y_soft_soil * l_crit) + (Y_soft_soil / Beta)) / (Eoed1 * Beta)
    t3 = 1 - Exp(-Beta * l_crit)
    t4 = (Y_soft_soil * l_crit) / (Eoed1 * Beta)
    t5 = (Y_soft_soil * l_crit ^ 2) / (2 * Eoed1)
    S = t1 + t2 * t3 - t4 - t5
    Ss = S * SF


  S0 = 0
    Load = 50
    t1 = (Load * (H - l_crit)) / Eoed2
    t2 = (Load * l_crit) / Eoed1
    S0 = t1 + t2
    rsr = (S0 - Ss) / S0

End Sub
Private Sub Form_Load()
   Call initilize
   Call calculate
   Open "output.txt" For Output As #1
     Write #1, "Beta=", Beta
     Write #1, "Load=", Load
     Write #1, "l_crit=", l_crit
     Write #1, "Eoed1=", Eoed1
     Write #1, "Eoed2=", Eoed2
     Write #1, "S0=", S0
     Write #1, "S=", S
     Write #1, "Ss=", Ss
     Write #1, "rsr=", rsr
  Close #1
End Sub
```

Figure B.1 Simplified analytical model program used to predict the RSR.

Appendix C:

Conference Papers

1. Al-Ani, W., Wanatowski, D. and Chan, S., 2014. Numerical analysis of piled embankments on soft soils. Proceedings of Geo-Shanghai Conference. Geotechnical Special Publication, ASCE.

2. Al-Ani, W., Wanatowski, D., Chan, S.H. and Serridge, C.J., 2015. Numerical modelling of stone columns in soft soils. In Proceedings of the XVI ECSMGE. Geotechnical Engineering for Infrastructure and Development.

3. Al-Ani, W. and Wanatowski, D., 2017, September. Settlement analysis of floating stone columns. In Proceedings of the 19th International Conference on Soil Mechanics and Geotechnical Engineering (pp. 2469-2472). International Society for Soil Mechanics and Geotechnical Engineering.

NUMERICAL ANALYSIS OF PILED EMBANKMENTS ON SOFT SOILS

Wisam Al-Ani[1], Dariusz Wanatowski[2] MASCE and Swee Huat Chan[3]

[1]PhD student, The University of Nottingham, United Kingdom
[2]Associate Professor, The University of Nottingham Ningbo China
[3]Assistant Professor, The University of Nottingham Malaysia Campus,

ABSTRACT: The construction of embankments on soft soils is a common problem. Soft soil cannot sustain external loads without having large deformations. Piled embankments system provides a possible solution for the construction of roads and rail over soft soils. Until now the system behaviour can only be described by analytical models such as those included in British or German Codes. This paper describes research undertaken to investigate the effects of pile embankment construction in soft soils. Experimental results are used to help investigate arching effect developed due to differential settlement between pile and surrounding soft soil. Numerical parametric study was carried out to examine impact of various soil parameters on the pile-embankment system behaviour. The outcome of parametric study implemented using numerical analysis has been investigated and discussed throughout this paper. Based on the numerical analysis carried out in this research, it was found that the earth pressure coefficient normalized by the passive earth pressure K_p plotted on a vertical profile at the midpoint between piles gave a good illustrations of arching behaviour. The findings presented in this paper can be considered as guides for numerical analysis and design criteria of soil arching for embankments constructed over piles.

1. INTRODUCTION

Geometry, load transfer mechanism (arching) and embankment stability are the main factors to consider in piled embankment system design. Embankment stability can be checked using most common slope stability methods such as Bishop's method and Fellenius's method. Construction requirements, system stability and soil arching phenomenon are the main factors which dictates embankment geometry. Both embankment stability and geometry are well defined, however uncertainties lie with load transfer mechanism through soil arching. Therefore, any improvement in piled embankment system design should address to soil arching and how to measure this aspect of design.

Arching action has been recognised by many published standards and papers in civil engineering. As stated by Handy (1987), in civil engineering is defined as the transfer of stress from a yielding part of soil mass to adjoining less-yielding or restrained parts of mass. Lack of a standard design has led to the development of many design theories and methods (Love and Milligan, 2003; Van Eekelen et al, 2003 and many others). Additionally, soil-structure interaction is complex and the precise mechanism by which load transfers occur remains unknown. Current procedures such as BS8006 and German method EBGEO 2004 section 6.9 gives

significant difference in the design results. However, it is both on safe side compared to measurements. The piles that support embankment are generally assumed as rigid piles. For the design of embankment on floating piles further studies of the floating piled embankment is required, although some studies on floating piled embankment exist (Poulos, 2007 and Satibi et al, 2008).

Construction of embankments over soft soils for highways and rail embankments impose a significant load over wide area. The soft soils and other compressible soils are quite challengeable subject normally face geotechnical engineers. Several challenges include potential bearing failure, intolerable settlement, large lateral pressure and movement, global or local instability and soil arching (Han and Jabr, 2002). Geotextile reinforcement stabilise arching effect by which called membrane effect. Structures settlement may be minimised considerably with shorter piles installed in soft soils.

In 1943, Terzaghi was one of the first researchers to define soil arching in his text "Theoretical Soil Mechanics". He describes the arching effects based on his experiment from which came the 'trapdoor' theory. Although arching effect has been acknowledged for decades, it still needs to be investigated due to various design uncertainties.

As shown in FIG. 1, Terzaghi initially proposed vertical shear planes at either side of a 'trapdoor'. Hewlett and Randolph (1988) derived theoretical solution based on observations from experimental tests of arching in a granular soil attempting to investigate arching in cohesionless soil. Semicircular arch proposed by Hewlett and Randolph for piled embankments.

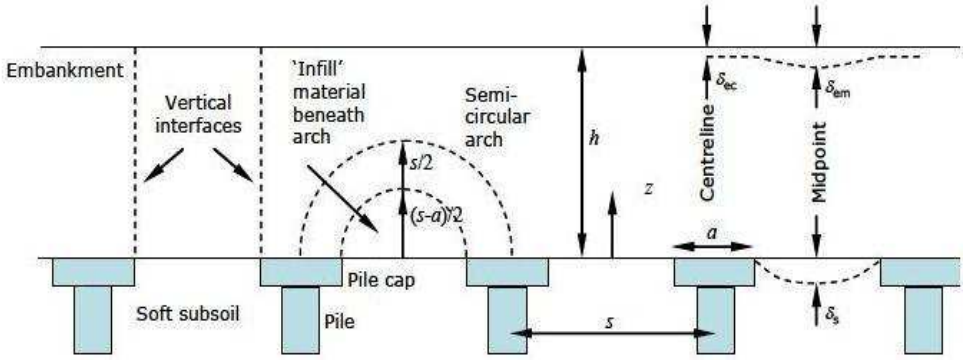


FIG. 1. Piled embankment showing potential arching mechanisms

(Zhuang, 2009).

2. PLAXIS SOIL PARAMETERS

A very useful set of laboratory model tests were performed at University of Kassel. As described by Zaeske (2001) and Kempfert et al. (2004), four piles placed in a

square grid in a 40 cm thickness of soft soil are arranged in a 1.1m x 1.1m box as shown in FIG. 2. Pile size was 16cm and centre to centre spacing of 50cm, which correspond to an area of replacement ratio of 10%.

In separate experiments, sand was placed on top of the piles to represent embankment in two thicknesses: 35cm and 70cm. However, 70cm test is chosen to verify numerical analysis. All simulations are performed with the finite element code Plaxis 2D.

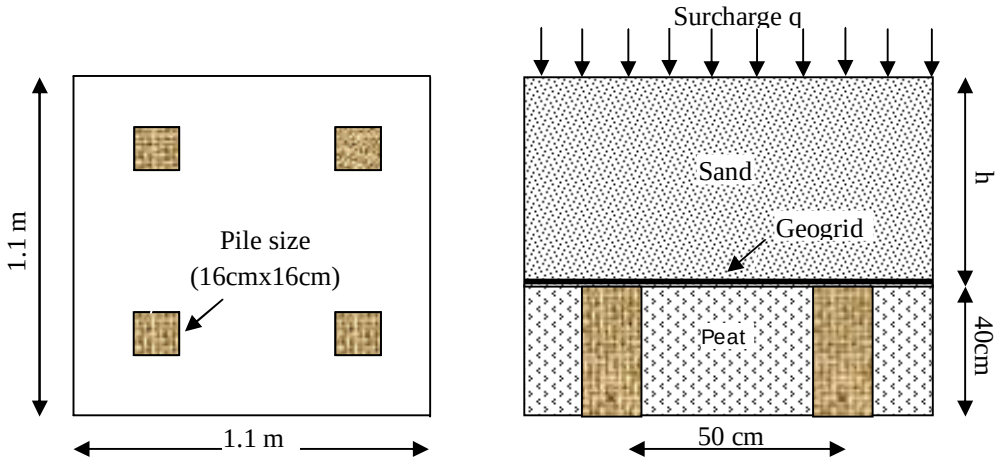


FIG. 2. Zaeske (2001) Model test dimensions and configuration: (a) plan view of piles; (b) Section view.

The advanced elastic-plastic Hardening soil (HS) model in Plaxis was chosen to simulate the behaviour of the sand and peat. The HS model is an extension of the hyperbilc model developed by Duncan and Chang (1970). The sand and peat properties used in the soil model as described by Zaeske (2001) and Kempfert et al. (2004) are presented in Table 1.

Table 1. Soil parameters for Hardening Soil model

	Properties	**Sand**	**Peat**
Φ′	[°]	**38**	**24**
c′	**[kPa]**	**0.1**	**8.5**
Ψ′	[°]	**11**	**0**
γ′	[kN/m^3]	**18**	**8**
E^{ref}	[MPa]	**23**	**1.7**
E^{ref}	[MPa]	**28**	**0.85**
E^{ref}	[MPa]	**112**	**12.75**
v_{ur}	[-]	**0.2**	**0.2**
m	[-]	**0.5**	**1**
R_{inter}	[-]	**1**	**0.35**

The system has been simulated as axisymmetric and 3D models. Half of the geometry is selected to reflect the effect of symmetry. The nodes on the lateral boundaries have been restrained in the x-direction only but the nodes on the bottom boundary have restrained in both x and y-directions. The finite element mesh was generated automatically with six- node elements for axisymmetric model.

3. FINITE ELEMENT ANALYSIS

3.1 Soil Primary Compression

The soil stress increase within a normally consolidated soil during the sedimentation process (Lambe and Whitman 1969). The ratio of the lateral effective stress to the vertical effective stress is known as the coefficient of the lateral earth pressure K_o, is given by

$$K_o = \frac{\acute{\sigma_h}}{\acute{\sigma_v}} \tag{1}$$

$$\acute{\sigma_v} = \sigma_v - u \text{ and } \acute{\sigma_h} = \sigma_h - u \tag{2}$$

where $\acute{\sigma_h}$ and $\acute{\sigma_v}$ represent effective lateral and vertical stresses respectively, σ_h and σ_v represent lateral and vertical stresses respectively. There are two ways to obtain K_o which is either from laboratory test carried out on undisturbed sample or field tests. However, in absence of tests or for simplicity K_o value can be readily estimated from the well known Jaky 1944 empirical formula:

$$K_o = 1 - \sin\acute{\varphi} \tag{3}$$

where φ′ is soil effective angle of internal friction. However, there are also empirical equations to estimate the K_0 in soft soils in particular. The Jaky's formula which is widely accepted among engineers and researchers is underestimating the K_o value. In order to find out the right approach to calculate accurate figure for K_o, measured K_0 values from Scherzinger 1991 and published work by Alphan 1967, Lee and Jin 1979 and Sherif and Koch 1970 (FIG. 3) compared with Jaki formula. Jaki formula k_o value lies far away from the range of measured K_0 by Scherzinger hence K_0 calculated based on Scherzinger is recommended in this research.

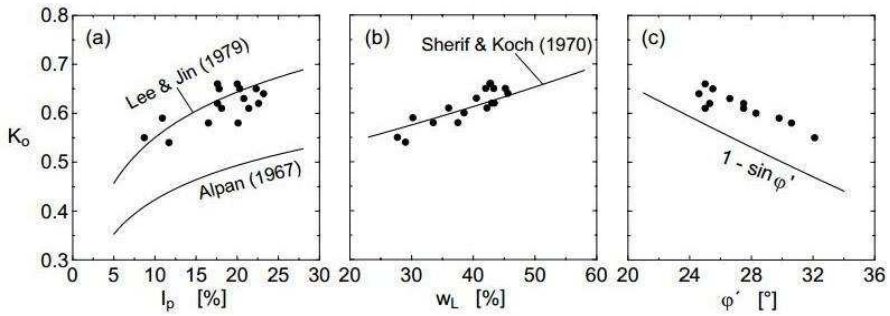


FIG. 3. Empirical equations after Kempfert 2006 to estimate K0 from (a) plasticity index I_p, (b) Liquid limit W_L and (c) Effective angle of friction φ′ (data from Scherzinger 1991)

3.2 Validation of Soil Model

A well- documented set of laboratory model tests were performed by Zaeske (2001) was simulated using Plaxis in order to substantiate the use of parameters in Table 1. Firstly, the initial stresses were generated under K_o conditions. Then, pile sector was activated to represent pile installation (wish in place). The embankment fill was then added to simulate embankment's construction on the top of the piles. If embankment was reinforced with basal geotextile, it was applied simultaneously with the embankment construction. Last stage in computation procedure was placing an external surcharge on to top of the embankment. Finite element mesh of various stages of analysis is shown in FIG. 4.

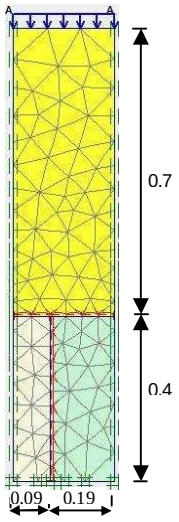


FIG. 4. FE- Axi-symmetric model mesh used for the calculations

The pile load and geogrid tensile force versus embankment load responses of the model test recorded by Zaeske (2001) are shown in FIG. 5 together with the Plaxis 2D prediction.

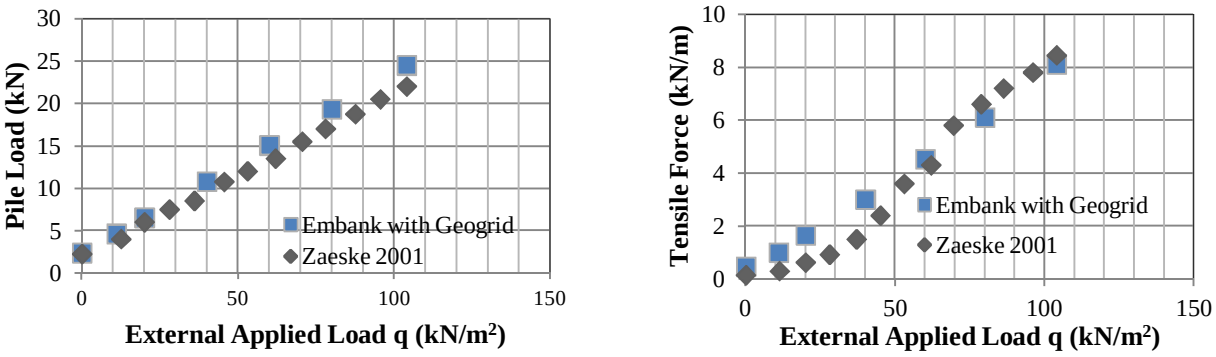


FIG. 5. Validation of soil profile and parameters for Zaeske (2001) model test.

It is clear that both curves are in good agreement with Zaeske (2001) model test, affirming the selection of the adopted soil profile and material parameters.

4. MIDPOINT OF EARTH PRESSURE COEFFICIENT

It is found the earth pressure coefficient (K= $\frac{\sigma'_h}{\sigma'_v}$) plotted on a vertical profile at the midpoint between piles (the right-hand boundary of the mesh in FIG.4) gave a good 'illustration' of arching behaviour (Zhuang, 2009). Earth pressure coefficient (K) midpoint profile has been used to investigate embankment material arching and compare it with a semi-circular arch in shown in FIG.1 developed by Terzaghi (1943). In this research, K profile has been normalized by passive earth pressure K_p (taking the standard Rankine value and ignoring the small cohesive element of strength K_p =(1+sin φ)/(1-sin φ)) plotted upward from the base of embankment normalised by spacing (s). This approach will provide direct results whether the soil is in plastic state comparing this with FIG. 1.

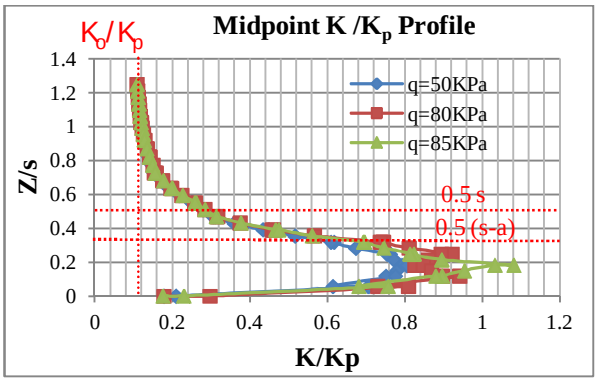
5.0 RESULTS

Zaeske (2001) model test shown in Fig. 2 is revisited, which shows the influence of key parameters variation upon the normalized K value. Fig. 6 shows the profiles plotted with z – vertical distance upwards from the base of the embankment normalized by s. The profile as plotted do extend to the top of the embankment, values of 0.5(s-a) and 0.5s are highlighted on the z/s axis. Subplot (a) shows the effect of increased embankment surcharge (q) keeping angle of friction (φ'), embankment height (h) and dilatation angle (ψ) constant. Subplots (b) and (c) again show variation of embankment angle of friction whilst keeping other soil properties constant. In order to measure embankment surcharge affects, surcharge in subplots (c) increased to 85kPa.

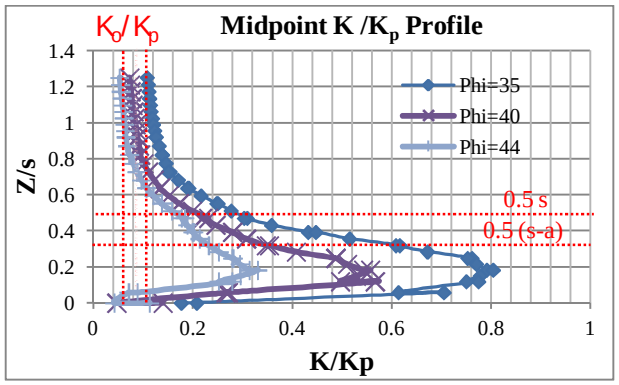
Referring to FIG. 6 (a) for (z/s) >1.0, K= K_0 , and thus has not been modified by the formation of the arch. Embankment where h/s= 1.25, K increases with depth for z/s< 1.0, reaching K_p just below z ≈ 0.5(s-a) for the higher surcharge of 85kPa. Comparing this with a semicircular arch in FIG. 1, the upper limit of the effect of arching is about 2.0 times higher, but the passive limit is only reached (q= 85kPa) below the inner radius of the arch, where the 'infill material is evidently in a plastic state. Subplot (e) where h/s=2.3 suggests for (z/s) >0.9, K= K_0 , and thus has not been modified by the formation of the arch. Comparing this with a semicircular arch in FIG. 1, the upper limit of the effect of arching is about 1.8 times higher, but the passive limit is only reached (q= 85kPa) below the inner radius of the arch, where the 'infill material is evidently in a plastic state. Therefore, even the data show similar trends to lower embankment however embankment modified by arching at lower level than for the lower embankments.

Effective cohesion can be assumed zero for granular embankment. Hence, evaluation is focused on the variation of φ' and ψ to investigate the influence of shear

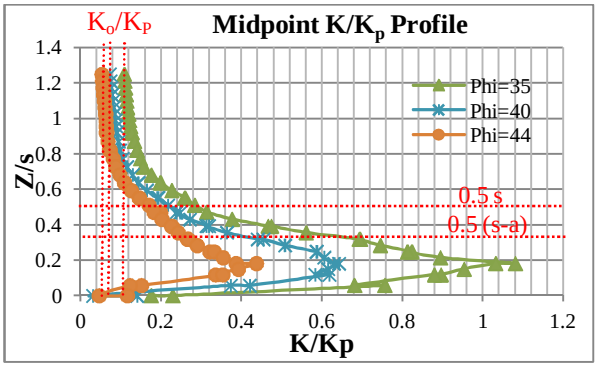
parameters. In order to assess the influence of φ', all other parameter are kept constant. Moreover, dilation angle ψ has been taken as zero and 8° to assess its influence on piled embankment system behaviour. φ' has an influence on subsoil surface settlement as illustrated in FIG.7 (a). The higher the angle of friction is the less subsoil surface settlement. FIG. 7 (b) shows that pile loads have a proportional relationship with the embankment angle of internal friction and the portion of external loads transferring to pile. Therefore, φ' has significant influence on embankment soil arching. FIG.6 (subplots b to e) shows the effect of increased friction angle.



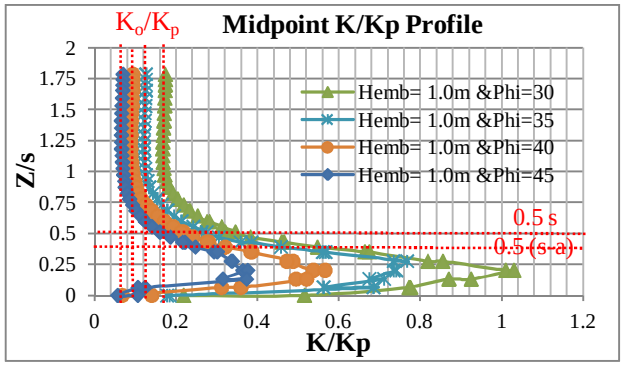
(a) h=0.7m, Ψ=0° and Φ= 35°



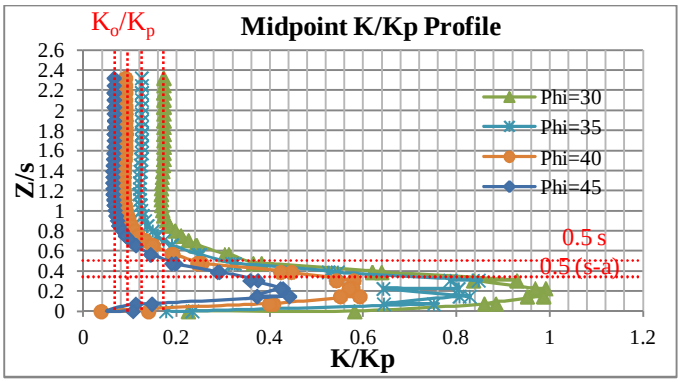
(b) h= 0.7m, Ψ=0° and q= 50 kPa



(c) h= 0.7m, Ψ=0° and q=85KPa



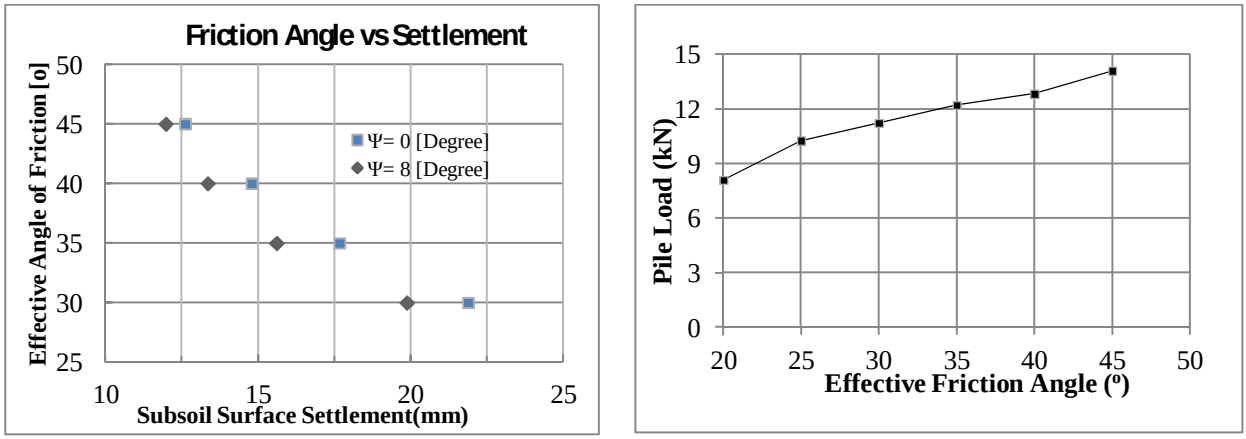
(d) h= 1.0m, Ψ=0° and q= 100KPa



(e) h= 1.3m, Ψ=0° and q= 135KPa

FIG.6. Profiles of normalized earth pressure coefficient (K/Kp) on a vertical profile at the midpoint between piles.

The same results can be observed in FIG.6 (subplots b to e) where the higher φ' the stronger the arching action in the embankment. The higher φ' leads to less K at the same height. The influence of ψ on Subsoil surface settlement is less significant than φ' as shown in FIG. 7(a). However, similar trends to increasing φ' is observed when increasing ψ. The higher subsoil surface settlement is for reduced ψ angle.



(a) (b)

FIG. 7 Shear strength parameters influence

FIG.7. (subplots b and c) demonstrate the effect of external embankment surcharge on piled embankment system. Increasing q value from 50kN to 85kN leads to an increase in K value for φ'= 35° at the same level.

6. CONCLUSION

A parametric finite element study with an advanced soil model was carried out to assess the effect a number of key design variables on the arching of a granular embankment supported by pile caps over a soft soil. The results of a series of hardening soil constitutive relation using axi-symmetric finite element analysis to investigate piled embankment performance. The following conclusions may be drawn, which are based on modelling Zaeske 2001 laboratory model test:

- There is virtually no effect of arching above z/s= 1.0 for h/s= 1.25 embankment and above z/s= 0.9 for h/s= 2.3 embankment therefore embankment height is ine of key parameters when assessing embankment soil arching.

  K value increases with depth reaching Kp below z ≈ 0.5(s-a). Comparing this with a semicircular arch in FIG. 1, the upper limit of the effect of arching is about 1.8 to 2.0 for h/s between 1.25 to 2.3 times higher, but the passive limit is reached for lower angle of friction (FIG.6 (c-e)) below the inner radius of the arch, where the 'infill material is evidently in a plastic state.

- The higher φ' the stronger the arching action in the embankment. The higher φ' leads to less K at the same height.
- The influence of ψ on Subsoil surface settlement is less significant than φ' as shown in FIG. 7(a). However, similar trends to increasing φ' is observed when increasing ψ. The higher subsoil surface settlement is for reduced ψ angle.

It is found the earth pressure coefficient (K= $\frac{\acute{\sigma_h}}{\acute{\sigma_v}}$) normalized by passive earth pressure coefficient plotted on a vertical profile at the midpoint between piles gave a good 'illustration' of arching behaviour and can be used to perform a sensitivity analysis to measure the affect of number of key design variables on the arching of the piled embankment system.

7. REFERENCES

Alphan, I. (1967), "The empirical evaluation of the coefficient K_o and K_{or} . Soils and Foundations; 7: 31-40.

British Standard. (2010). Code of practise for strengthened/ reinforced soils and other fills. BS8006, British Standard Institution, London.

DGGT (2004). EBGEO: Bewehrte erdkörper auf punkt-oder linienföormigen traggliedern, chapter 6.9.

Duncan,J. M. And Chang, C. Y. (1970). "Nonlinear analysis of stress and strain in soil." ASCE Journal of the Soil Mechanics and Geotechnical Engineering.

Handy, R. L. (1987). Closure of discussions of the arch in soil arching. Journal of Geotechnical Engineering, ASCE, 113(3), 275-277.

Han , J. & Gabr, M.A. (2002). Numerical analysis of Geosynthetic reinforced and pile-supported earth platforms over soft soil. Journal of Geotechnical and Geoenvironmental Engineering, January 2002, pp. 44-53.

Hewlett, W.J. & Randolph, M.F. (1988). Analysis of piled embankments. Ground Engineering, April 1988, pp. 12-18.

Kempfert, H.-G., Gobel, C., Alexiew, D. & Heitz, C. (2004). German recommendations for reinforced embankments on pile-similar elements. EuroGeo3: 3rd European Geosynthetics Conference, Geotechnical Engineering with Geosynthetics, Munich, pp. 279-284.

Lamb, T. W. and Whitman, R.V. (1969). "Soil mechanics." John Wiley & sons, New York.

Lee, Y. N. and Jin, B. I. (1979), "Measurment and prediction of K_0." Journal of Korean Society of Civil Engineering, pp. 226-233.

Love, J. & Milligan, G. (2003). Design methods for basally reinforced pile-supported embankments over soft ground. Ground Eng., 36(3), 39-43.

Poulos (2007). Design charts for piles supporting embankments on soft clays. Journal of Geotechnical and Geoenvironmental Engineering, Vol. 133, No 5,pp.493-501.

Satibi, S., Leoni, M., Vermeer, P.A. & Van der Meij, R. (2008). On the numerical analysis of piles embankments. Proceedings of the second international workshop on geotechnics of soft soils. Galsgow, Scotland, September 2008.

Scherzinger, T. (1991). "Materialverhalten von seetonen- Ergebnisse von laboruntersuchungen und ihre bedeutung f*ü*r das Bauen in weichem baugrund; Institut f*ü*r bodenmechanik und felsmechanik der Universität Fridericiana in Karlsruhe, Heft 122.

Sherif, M. A. and Koch, D. E. (1970)."Coefficient of earth pressure at rest as related to soil recompression ratio and liquid limit." Highway research record, Washington, No 323, pp. 39-48.

Terzaghi, K. (1943). Theoretical Soil Mechanics. John Wiley and Sons, New York.

Van Eekelen, S. J. M., Bezuijen, A., & Oung, O. (2003). Arching in piled embankments; Experiments and design calculations. BGA International Conference Foundations: Innovations, Observations, Design and Practice, Dundee, pp.885-894.

Zaeske, D. (2001). Zur Wirkungweise von unbewehrten und bewerhrten mineralischen tragschichten über pfahlartigen Gründungselementen. PhD Thesis, Universität Kassel.Heft 10.

Zhuang, Y. (2009). Numerical Modelling of arching in piled embankments including the effects of reinforcement and subsoil. PhD thesis, The University of Nottingham.

Proceedings of the XVI ECSMGE
Geotechnical Engineering for Infrastructure and Development
ISBN 978-0-7277-6067-8

© The authors and ICE Publishing: All rights reserved, 2015
doi:10.1680/ecsmge.60678

ice Institution of Civil Engineers publishing

Numerical modelling of stone columns in soft soils

Modélisation numérique des colonnes de roches dans les sols mous

W. Al-Ani[1], D. Wanatowski[*2], S. H. Chan[3] and C.J. Serridge[4]

[1] *Faculty of Engineering, The University of Nottingham, Nottingham, UK*
[2]*Department of Civil Engineering, The University of Nottingham, Ningbo, China*
[3]*Department of Civil Engineering, The University of Nottingham Malaysia Campus, Semenyi, Malaysia*
[4]*Balfour Beatty Ground Engineering, Manchester, UK*
[*]*Corresponding Author*

ABSTRACT Great areas all over the world with underlying deep deposits of soft clay have increased the pressure on geotechnical engineers and ground engineering practitioners into looking for various improvement techniques to overcome problems associated with construction on soft soil, due to its low shear strength and high compressibility. For lightly loaded low- rise structures supported by narrow shallow footings, the use of vibro stone columns is gaining acceptance in industry and in construction. In this paper, numerical analysis is used to examine the influence of various parameters such as vibro stone column length, spacing and founding depth on the footing performance. Comparisons are made with the published field trials at the Bothkennar research site in Scotland. It has been found that the upper crust of the Bothkennar profile has a significant impact on settlement performance. In addition, the settlement performance/reduction is more significant once column length to diameter ratio (L/d) exceeds around 8.3. Also, the depth of stone column bulging is between 1.85-2.5 m below ground level which is comparable to the bulging depth suggested by Hughes et al. (1976). Numerical analysis predicts a stress ratio of 2.9 to 3.4 which is comparable with the field measurements.

RÉSUMÉ La présence dans le monde de larges zones avec des dépôts profonds d'argile sous-jacents pousse les ingénieurs géotechniques et autres professionnels en ingénierie des sols à rechercher de nouvelles techniques d'amélioration pour remédier aux problèmes associés à la construction sur sols mous dus à leur faible résistance au cisaillement et haute compressibilité. Pour les structures basses hautement chargées supportées par des appuis réduits et peu profonds, l'utilisation de colonnes de roches compactées par vibration est bien acceptée dans l'industrie et la construction. Dans cet article, une analyse numérique est utilisée pour examiner l'influence de divers paramètres comme la longueur de la colonne de roches compactées par vibration, l'espacement et la profondeur de la fondation sur les performances de l'appui. Des comparaisons avec les essais sur le terrain du site de recherche de Bothkennar en Ecosse sont réalisées. Il a été découvert que la croûte supérieure du profil de Bothkennar a un impact significatif sur les performances de tassement. La réduction du tassement est également plus significative lorsque le rapport de la longueur de la colonne sur son diamètre (L/d) excède approximativement 8.3. La profondeur du renflement de la colonne de roches se trouve entre 1.85 et 2.5 m sous le niveau du sol, ce qui est comparable à la profondeur de renflement suggérée par Hughes et al. (1976). Une analyse numérique prédit un rapport de contrainte de 2.9 à 3.4, ce qui est comparable aux mesures sur le terrain.

1 INTRODUCTION

Great areas all over the world with underlying deep deposits of soft clay have increased the pressure on geotechnical engineers and ground engineering practitioners into looking for various improvement techniques to overcome problems associated with construction on soft soil due to its low shear strength and high compressibility.

The Bothkennar soft clay research site in Scotland is located between Edinburgh and Glasgow on former intertidal mudflats on the south bank of the Forth Estuary and adjacent to the Kincardine Bridge and has been the subject of extensive soft soil research including in situ testing, soil sampling techniques (undisturbed), and also shallow and deep foundations performance on untreated soft clay (Hight et al. 1992, Jardine et al. 1995) together with soft clay reinforced with partial depth vibro stone columns (Watts & Ser-

ridge 2000; Serridge 2013). The soft soil on this site, where comprehensive geotechnical investigation was carried out (e.g. Nash et al. 1992a) was devoid of any peat layers. The soil profile comprises a 1.5m thick desiccated crust underlain by a deep deposit of soft clay. The soft clay strength is relatively small compared to the overlying crust layer. The soft clay becomes soft to firm with depth.

In this paper, numerical analysis is used to examine the influence of various parameters such as vibro stone column length, spacing and founding depth on the footing performance. Comparisons are made with the field trials reported by Watts & Serridge (2000) and Serridge (2013) at the Bothkennar soft clay research site.

2 FIELD TRIAL DESIGN

Stone column design for the Bothkennar field trials (Watts & Serridge 2000; Serridge 2013) was carried out based on the following:

- Step 1: Calculate stone column ultimate load capacity based on the factor of safety against bulging failure (Hughes & Withers 1974).
- Step 2: Calculate stone column length in accordance with Hughes & Withers (1974) observations.
- Step 3: Calculate stress distribution between column and soil as defined by Baumann & Bauer (1974).
- Step 4: Calculate pre-treatment settlement under applied load to demonstrate a requirement for stone column.
- Step 5: Predict settlement with stone columns under the applied load (Priebe 1995).

A design treatment depth was found to be 5.5m below foundation level based on step 2. However, column lengths of 3.7 m and 7.7 m were adopted in the trials to investigate the effect of column length on performance. Table 1 and Figure 1 summarize the Bothkennar field trials footing arrangements and depths following the above design steps.

There were two load increments applied on top of the footings, as given in Table 2.

3 BOTHKENNAR NUMERICAL ANALYSIS

The numerical investigation of the stone column performance in this paper was carried out using PLAXIS 3D (Brinkgreve & Broere, 2008) geotechnical software package.

Table 1. Summary of Bothkennar trial footing arrangements.

Trial footing	Dimension (LxB)	Column length below founding depth	No of columns	Spacing
3	3 x 0.75 m	3.7 m	2	1.5 m
4	3 x 0.75 m	5.7 m	2	1.5 m
5	3 x 0.75 m	7.7 m	2	1.5 m
6	3 x 0.75 m	5.7 m	2	1.5 m
7	1.5 x 1.5 m	5.7 m	2	1.5 m

Table 2. Summary of loading increments to applied to trial footings at Bothkennar.

Trial Footing	Dimension (LxB)	Founding depth	1st Load increment	2nd load increment
3	3 x 0.75 m	0.5 m	33.1 kN/m^2	67.8 kN/m^2
4	3 x 0.75 m	0.5 m	34.9 kN/m^2	71.1 kN/m^2
5	3 x 0.75 m	0.5 m	32.1 kN/m^2	67.0 kN/m^2
6	3 x 0.75 m	1.2 m	34.2 kN/m^2	69.6 kN/m^2
7	1.5 x 1.5 m	0.5 m	32.7 kN/m^2	67.0 kN/m^2

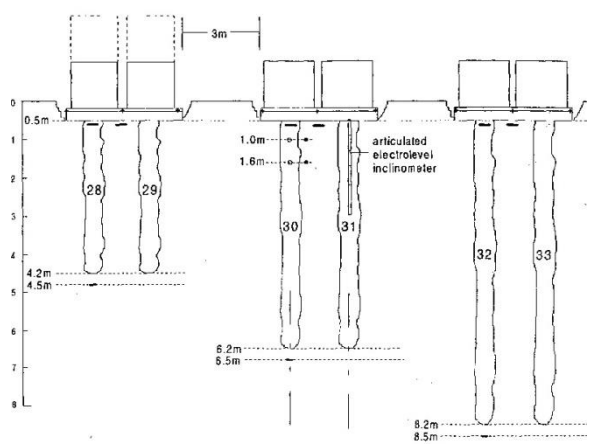


Figure 1. Investigation of vibro stone column length on trial footing performance (footings 3-5) at Bothkennar (Watts & Serridge, 2000; Serridge, 2013).

PLAXIS uses unstructured mesh, which is generated automatically with options for global and local mesh refinement. The meshes were refined around the footing and stone column heads where the stress

gradient was expected to be high. Fifteen-noded wedge elements with six Gaussian integration points were used. Around 6600 elements were used in the finite element analysis as illustrated in Figure 2. An interface element was used at the contact between the stone columns and surrounding weak soil.

For the purposes of building the numerical model in PLAXIS, a detailed soil profile and geotechnical properties are required. For analysis the Bothkennar clay soil stratification has been taken as comprising a thin desiccated crust underlain by a succession of Upper Carse Clay over Lower Carse Clay. Nash et al. (1992b) reported the variation of Carse clay initial void ratio (e_o), compression index (C_c), and swelling index (C_s) with depth. E_{50} and E_{oed} are secant stiffness in standard drained triaxial test and tangent stiffness for primary oedometer loading respectively derived from C_c while the unloading/reloading stiffness is derived from C_s.

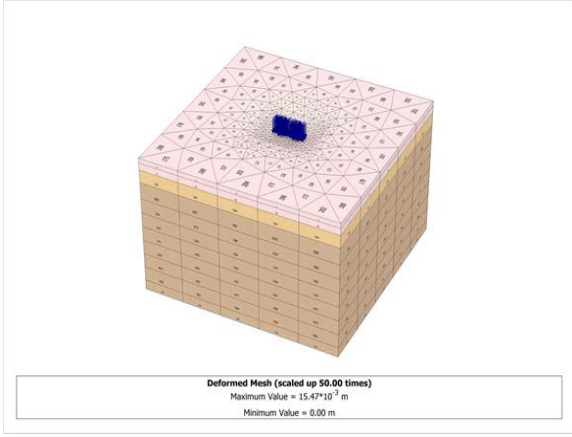


Figure 2. Typical finite element analysis mesh as used for Bothkennar analyses.

Allman & Atkinson (1992) suggested a high critical state friction angle (φ′) of 34° due to the high proportion of angular silt particles in the clay. Also effective cohesion of 1 kPa for the clay was used for numerical stability. However, a slightly higher cohesion (c′) =3 kPa was used for the weathered crust. Soil parameters used in this paper are presented in Table 3. A variation of yield stress has been reported by Nash et al. (1992a) which is equivalent to the over consolidation stress (OCR) measured in an oedometer, and in situ lateral earth pressure coefficient (K_o) with depth, attributable to the influence of erosion, drop in sea level, and fluctuating groundwater levels on stress state.

Table 3. Bothkennar field trials soil parameters (Killeen & McCabe, 2010).

		Crust	Upper Carse Clay	Lower Carse Clay	Stone Backfill
Depth		0-1.5	1.5-2.5	2.5-14	-
φ'	[°]	34	34	34	45
c'	[kPa]	1	1	1	1
Ψ'	[°]	0	0	0	15
γ′	[kN/m^3]	18	16.5	16.5	19
E_{50}^{ref}	[kN/m^2]	1068	506	231	70000
E_{Oed}^{ref}	[kN/m^2]	1068	506	231	70000
E_{ur}^{ref}	[kN/m^2]	5382	3036	1164	210000
OCR	[-]	1	1	1.5	-
POP	[kN/m^2]	15	15	0	-
m	[-]	1	1	1	0.3

In choosing the aggregate for the field trials, guidance published by BRE (2000) was followed. Soil parameters used in this paper including deformation modulus and the angle of shearing resistance of the stone column aggregate are based upon Killeen & McCabe (2010). It is rare for stone column angle of shearing resistance to be measured directly for stone column projects. A value of angle of friction for stone column aggregate of 42° to 45° is recommended for high quality well compacted rounded and angular aggregates. It is conservative to use φ′= 40° as indicated by Killeen & McCabe (2010). Following discussions with Specialist Contractors in the UK a minimum friction angle of the stone backfill, φ′= 45° is suggested for current analysis. This was subject to adequate workmanship combined with the fact that a sample of the backfill material was tested in large triaxial cell apparatus and yielded an angle of shear resistance φ′ in excess 45° (Serridge 2013). The calculation of the angle of dilatancy is based on the relationship ψ = φ′- 30.

A field trial described by Jardine et al. (1995) at Bothkennar has been performed and simulated by PLAXIS 3D foundation software programme in order to substantiate the adoption of the geotechnical parameters detailed in Table 3. The trials were performed for a pad footing at 0.75m depth within the 1.5m thick surface 'crust' and without the support of stone columns. According to Jardine et al. (1995)

2.2m square pad footing (with 0.8m thickness) had been loaded to failure in increments over a period of 3 days using Kentledge blocks. The Plaxis 3-D analysis results were closely aligned with the load-settlement curve for Jardine's trial as reported by Killeen & McCabe (2010) in Figure 3. It is evident from Figure 3 that there is a good agreement affirming the selection of the adopted soil profile and material properties.

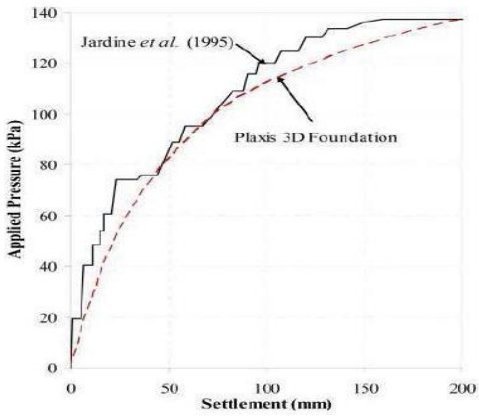


Figure 3. Validation of soil profile and parameters after Killeen & McCabe (2010).

4 RESULTS

The ground response to the load applied on footings placed over different arrangements and depth of stone columns are investigated below for each of the footings. Different footing combinations are used in an attempt to model the key design variables for the vibro stone column field trials described by Watts & Serridge (2000) and Serridge (2013). The depth of the footings is typically 500mm below ground level, whilst footing 6 depth is 1.2 m below ground level (i.e. at the base of the crust), as shown earlier in Table 1. Stone column diameter was measured during the field trials and a 750 mm stone column diameter was adopted in this analysis based upon direct measurements. Vertical stress changes are measured at the top of the stone column and at the same level in the soil between columns. Stress concentration ratio (proportion stress carried by both stone column and soil) was measured and values are summarized in Table 4. The recorded settlements under the load increments are detailed in Table 5.

Table 4 Recorded stress ratios for Bothkennar trial footings (Serridge 2013).

Footing No.	Column length below founding depth	1st load increment	2nd load increment
3	3.7 m	2.29	2.63
4	5.7 m	2.8	3.26
5	7.7 m	2.44	4

Table 5 Recorded vertical settlement (δ) for Bothkennar trial footings (Serridge 2013).

Footing No.	Column length	Founding depth	1st load increment	2nd load increment
3	3.7 m	0.5 m	17.5 mm	37.5 mm
4	5.7 m	0.5 m	20 mm	42.5 mm
5	7.7 m	0.5 m	22 mm	40 mm
6	5.7 m	1.2 m	24 mm	45 mm
7	5.7 m	0.5 m	22 mm	45 mm

4.1 Effect of stone column length

The effect of stone column length on the performance of the partial depth-vibro stone columns has been investigated at the locations of the trial footing 3 (shortest length), footing 4 (intermediate length) and footing 5 (longest length). Settlement data for trial footings 3, 4 and 5 are detailed in Table 6.

Table 6 Calculated vertical settlement for footings 3 to 7.

Footing	1st Load increment		2nd Load increment	
No.	Plaxis 3D	Measured	Plaxis 3D	Measured
3	15.47 mm	17.5 mm	41.66 mm	37.5 mm
4	14.47 mm	20 mm	48.37 mm	42.5 mm
5	11.93 mm	22 mm	40 mm	40 mm
6	14.44 mm	24 mm	43.2 mm	45 mm
7	15.66 mm	22 mm	47.3 mm	45 mm

For the current material data, good agreement with the measured settlement data was achieved for both of the load increments. However, PLAXIS 3D predicted settlement under first load increment was less than measured by up to around 10 mm. It may be due to the influence of foundation 'bedding-in' effects, this would suggest that settlement will occur until an equilibrium condition is reached. In addition, settlement underestimated in the first load increment may

be attributed to increased soil stiffness at low strain which is not accounted for in the current soil model.

Footing 5 over the longer stone column settled the least (around 12 mm under the first load increment and 40 mm under the second load increment) with footing 4 settling marginally less than footing 3 under the first load increment (14.5 mm, compared to 15.5 mm for footing 3). However, footing 4 settled more than footing 3 under the second load increment (48 mm, compared to 42 mm for footing 3).

PLAXIS 3D output suggests that settlement performance is improved with increasing column length as shown from trial footing 5 results. Settlement improvement becomes more significant when column length (L) to diameter ratio (d) exceeds = 8.3.

4.2 Effect of footing shape

Trial footing 7 was used to assess the impact of crust and footing shape on settlement. The dimension of trial footing 7 is 1.5 m x 1.5 m pad with two stone columns. It is important to note that for trial footing 7 area replacement ratio is the same for other trial footings with columns at 1.5 m centres. In order to investigate the effect of footing shape on settlement, footing 7 was compared with trial footing 4 because they are both identical in terms of stone column length and replacement ratio. However, the stress depth influence (stress bulb) is deeper for trial footing 4. It was found that both trial footings 4 and 7 had similar settlement performance under the second load increment as presented in Table 6 which would suggest that the crust has a greater impact than footing shape on footing/foundation performance.

4.3 Stone column bulging

Following completion of numerical analysis of trial footings 3 to 7, it was considered important to investigate stone column deformed shape after load application in order to measure stone column bulging and to compare it with published data. Following observations by Hughes & Withers (1974), a single column bulges under applied load the magnitude of which will be a function of the passive resistance afforded by the surrounding clay soil, which in turn will be a function of its undrained shear strength. Calculated lateral deformations for the stone columns are shown in Table 7. The depth of bulging is between 1.85 m and 2.5 m (2.5 to 3.3 column diameter, D) below ground level (Figure 4). The bulging depth is slightly higher than the 2D that was reported by Hughes et al. (1976) and Serridge (2013) in their field based trials and can be attributed to the influence of the stiffer crust and interface effects at the base of the crust and underlying soft clay.

Table 7 Stone column lateral deformation (trial footings 3 to 7).

Footing No.	1st load increment		2nd load increment	
	Lateral displacement (mm)	Depth (m)	Lateral displacement (mm)	Depth (m)
3	0.5	1.85	3.73	1.85
4	0.9	1.85	5.7	1.85
5	0.5	2.50	4.4	2.50
6	0.7	1.85	5.3	2.50
7	1.3	1.85	6.0	2.50

The greater the applied load, the greater the lateral deformation (bulging) as indicated in Table 7. The bulging is confined to shallow depth immediately below the crust. This is perhaps not surprising given to the influence of a stiffer crust layer over soft clay.

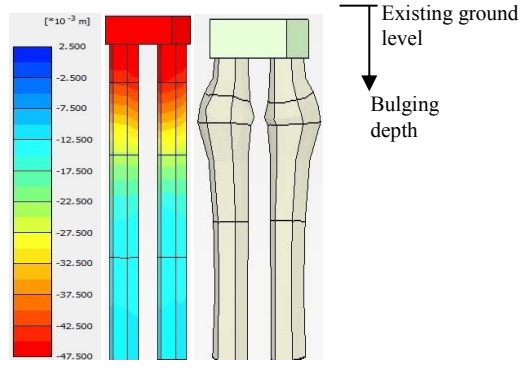


Figure 4. Footing 7- Lateral deformation and bulging.

4.4 Stress ratio

Measured and calculated stresses ratio under the first and second load increment are detailed in Table 8. Under the first load increment, the predicted stress ratio is 3.37 for the short footing (trial footing 3) reducing to 3.07 for the intermediate and long footings (trial footing 4 and 5).

Table 8 Measured and predicted stress ratio.

Footing	1st load increment		2nd load increment	
No.	Plaxis 3D	Measured	Plaxis 3D	Measured
3	3.37	2.29	3.43	2.63
4	3.07	2.8	3.07	3.26
5	3.07	2.44	2.93	4

The values of measured stress ratio are in between 2.3 to 2.8 for all of the three trial footings 3; 4 and 5. Under the second load increment cycle the predicted stress ratio from numerical analysis (Table 8) was 3.4 (L/d= 5.6); 3.1 (L/d=8.3) and 2.9 (L/d= 10.9) respectively for the short (footing 3) intermediate (footing 4) and long (footing 5) stone column lengths compared to 2.6 to 4 stress ratio measured on site and with field trials reported by Goughnour & Bayuk (1979) where recorded stress concentration ratios were between 2.6 to 3.0 on top of the stone column.

It is evident from the results of the numerical analysis that the stress ratio increased with applied load. Also, there is a good agreement between measured and predicted stress ratio. A possible explanation put forward by Hu (1995) was that due to consolidation of intervening soils the confining stress will increase accordingly which leads to the stiffness of the stone soil composite.

5 CONCLUSIONS

Settlement is the most significant parameters in stone column design rather than bearing capacity. In this paper, key variables affecting stone column settlement including column length, footing depth and shape are addressed. These are the main conclusions that may be drawn from this paper:

- PLAXIS 3D output suggests that settlement performance is improved with increasing column length as shown from trial footing 5 results.
- Settlement improvement becomes more significant when column length to diameter ratio exceeds (L/d) =8.3.
- The upper crust layer has a significant impact on settlement performance.
- The depth of stone column bulging is between 1.85-2.5 m below ground level which is comparable to the suggested bulging depth by Hughes et al. (1976).
- PLAXIS outputs suggest stress ratio of 2.9 to 3.4 which is comparable with the site measurements and field trials reported by Goughnour & Bayuk (1979), Watts & Serridge (2000), and Serridge (2013).

REFERENCES

Allman, M. & Atkinson, J. 1992. Mechanical properties of reconstituted Bothkennar soil. *Geotechnique* **42**(2), 289-301.

Baumann, V. & Bauer, G.E.A. 1974. The performance of foundations on various soils stabilized by the vibro-compaction method. *Canadian Geotechnical Journal* **11**(4), 509-530.

Building Research Establishment (BRE). 2000. Specifying vibro stone columns, *BRE Report BR 391*, Garston, UK.

Brinkgreve, R.B.J. & Broere, W. 2008. PLAXIS 3D foundation manual, version 2.0. *Delft University of Technology and PLAXIS*, Netherlands.

Goughnour, R.R. & Bayuk, A.A. 1979. A field study of long-term settlements of loads supported by stone columns in soft ground, International conference on soil reinforcement: *Proceedings, Reinforced earth and other techniques,* Vol.1, 279-285, Paris.

Hight, D.W. Bond, A.J. & Legge, J.D. 1992. Characterization of the Bothkennar clay: an overview, *Geotechnique* **42**(2), 303-347.

Hu, W. 1995. Physical modelling of group behaviour of stone column foundations, *PhD Thesis*, University of Glasgow, UK.

Hughes, J.M.O. & Withers, N.J. 1974. Reinforcing of soft cohesive soils with stone columns, *Ground Engineering* **7**(3), 42-49.

Hughes, J.M.O. Withers, N.J. & Greenwood D.A. 1976. A field trial of the reinforceing effect of a stone column in soil, Ground treatment by deep compaction, *Institution of Civil Engineers*, London.

Jardine, R.J. Lehane, B.M. Smith, P.R. & Gildea, P.A. 1995. Vertical loading experiments on rigid pad foundations at Bothkennar, *Geotechnique* **45**(4), 573-597.

Killeen, M.M. & McCabe, B. 2010. A numerical study of factors affecting the performance of stone columns supporting rigid footings on soft clay. In *Numerical methods in Geotechnical Engineering (Eds: Benz and Nordal)*. Taylor and Francis Group, London.

Nash, D.F.T. Powell, J.J.M. & Lloyd, I.M. 1992a. Initial investigations of the soft clay site at Bothkennar, *Geotechnique* **42**(2), 163-181.

Nash, D.F.T. Sills, G.C. & Davison, L.R. 1992b. One-dimensional consolidation testing of soft clay from Bothkennar, *Geotechnique* **42**(2), 241-256.

Priebe, H.J. 1995. The design of vibro replacement. *Ground Engineering* **28**(10), 31-37.

Serridge, C.J. 2013. An Evaluation of partial depth dry bottom-feed vibro stone columns to support shallow footings in deep soft clay deposits. *PhD Thesis*, Faculty of Science and Technology, Anglia Ruskin University, Chelmsford, UK.

Watts, K.S. & Serridge, C.J. 2000. A trial of vibro bottom-feed stone column treatment in soft clay soil. *Proceedings, 4th International Conference, Grouting, soil improvement geosystems including reinforcement. (Ed.* Rathmayer, H.*),* 594-556. Building Information Limited, Helsinki.

Settlement analysis of floating stone columns

Analyse du tassement de colonnes de pierres flottantes

Wisam Al-Ani
Balfour Beatty Ground Engineering, Derby, DE21 7BG, United Kingdom, wisam.alani@bbge.com

Dariusz Wanatowski
School of Civil Engineering, Faculty of Engineering, University of Leeds, Leeds, LS2 9JT, United Kingdom.

ABSTRACT: In recent years, stone columns have been used to support footings and embankments constructed on soft soils. Several design methods have been developed, including theoretical and numerical solutions to address several design issues. However, more research is needed to develop a simple yet robust design method. A new analytical method is proposed to assess stone column performance under applied external loads. Pile critical length is derived to estimate column length required to resist applied load by a floating stone column only. This method is used together with the numerical analysis to investigate the effectiveness of floating stone columns using relative settlement reduction ratio. The results of numerical parametric study were compared to the derived analytical solutions in order to examine stone column behavior. Despite the simplicity of the analytical approach adopted in this study, the proposed solution enhances the understanding of the stone column performance and can be used for estimating the critical length of the columns.

RÉSUMÉ: Ces dernières années, les colonnes de pierres ont été utilisées pour supporter la base de fondations ou de remblais sur sols meubles. Plusieurs méthodes de design ont été développées, dont des solutions théorique et numérique pour traiter certains problèmes de conception. Cependant plus de travail de recherche est nécessaire pour développer une méthode de conception simple mais robuste. Une nouvelle méthode analytique est proposée pour estimer les performances des colonnes de pierres sous l'application de chargements externes. La longueur critique de pieu est dérivée afin d'estimer la longueur de colonne de pierre flottante requise pour qu'elle résiste à elle seule au chargement appliqué. Cette méthode est utilisée en combinaison avec une analyse numérique pour étudier l'efficacité des colonnes de pierres flottantes en utilisant le rapport de réduction de tassement relatif. Les résultats de l'étude paramétrique ont été comparés aux solutions analytiques dérivées afin d'examiner le comportement des colonnes de pierres. Malgré la simplicité de l'approche adoptée dans cette étude, la solution proposée améliore la compréhension des performances des colonnes de pierres et peut être utilisée pour estimer la longueur critique des colonnes.

KEYWORDS: Stone column, analytical model, floating and design.

1 INTRODUCTION

Piles are often used in the UK and abroad as a foundation for road and rail embankments constructed over soft ground. The main function of the piles is to transfer embankment loads into deeper, more competent strata. It is important to consider the impact of the thickness of a soft soil layer on foundation selection. Generally, end-bearing piles can be an effective solution when the soft soil thickness is relatively small, i.e. up to 25m. However, when the embankment is to be constructed over ground that is soft or compressible to adequately support the embankment, granular columns can be installed in a soft ground as an alternative to piles to provide a foundation with satisfactory performance.

When the installed columns do not reach bearing strata due to the large thickness of the soft soil, the constructed stone columns are called floating columns. Moreover, floating stone columns can be used in lieu of full-length piles to control embankment settlement, satisfy specification performance criteria and to prevent the lateral spreading of the subsoil.

In current practice, the numerical analysis is often used to investigate a stone column settlement performance. A series of analytical and empirical design methods are available to address the settlement improvement associated with stone column installation. In the UK, most designs use Priebe's method to assess settlement improvement (Priebe 1995). In this paper, numerical study of axisymmetric model (an efficient mathematical means of modelling stone column grids) using hard soil model is performed and compared with derived analytical model to understand effectiveness of stone columns. The study is carried out with the intent to provide practicing engineers with a simple tool for assessing the foundation settlement in soft soils.

The focus of this paper is to propose a simplistic analytical model that can predict the settlement improvement in soft soils by the installation of vibro stone columns. The design of stone columns in soft clays is usually governed by performance (settlement) rather than column capacity to support applied load. An analytical approach developed by Satibi (2009) was modified in the current study to assess the performance of an infinite grid of floating stone columns.

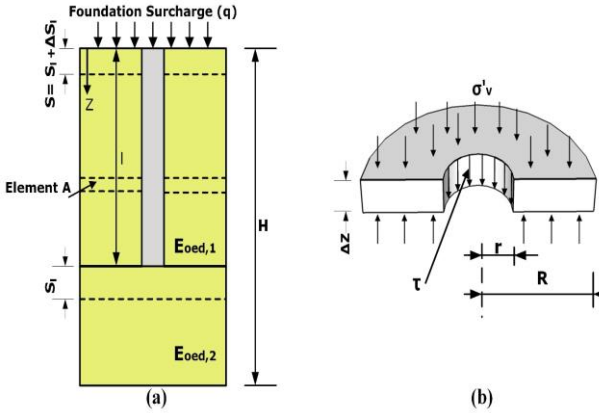


Figure 1. Settlement analysis of one cell of an infinite grid of floating stone columns (a) Vertical cross section (b) Vertical effective force equilibrium of element A (after Satibi 2009).

This approach is used to calculate critical stone column length defined as the minimum required length to resist the applied load solely by a floating stone column (ignoring toe resistance contribution). Although the existence of a critical column length was reported by several researchers (e.g. McKelvey et al. 2004, Wehr 2004), this finding is not supported in this current study because the applied load is at a working level rather than at an ultimate level. The analytical approach is based on the uniformly distributed load applied on top of the stone column following unit cell concept, as shown in Figure 1. Figures 1(a) and 1(b) show the vertical cross section of the axisymmetric cell and an element A illustrating effective vertical forces in equilibrium within the column. The effectiveness of footing or embankment constructed on top of the floating stone columns is then investigated by using a relative settlement reduction ratio (RSR). The relative settlement reduction is defined as:

$$\text{RSR}= \frac{S_0-S}{S_0} \quad (1)$$

where the subscript "0" means no stone column is installed thus S_o is soft soil surface total settlement without ground improvement by stone column installation. S refers to the total settlement at the surface of the soft soil improved by stone columns. It needs to be emphasized that it is necessary to use an advanced method such as the finite element method for detailed design. A program is written by the author in a Visual Basic to model circular cell geometry as illustrated in Figure 1.

2 ANALYTICAL MODEL DERIVATIONS

Stone columns have been increasingly used to support embankments especially when a settlement/differential settlement is involved. Several researchers (e.g. Pulko and Majes 2005 and Sexton and McCabe 2013) have indicated that the settlement of infinite grid of floating stone columns can be considered in a unit cell model. Different types of stone columns have been used, each with different rigidities, and using different installation processes and materials. The analytical model adopted in this research is based on the rigid column theory (Satibi 2009). The soft soil settlement due to the foundation applied load is based on the Hooke's law of elasticity where the soil is idealised as linear elastic, uniform, and isotropic if no stone column is installed. Hence;

$$S_o = S_l + \Delta S_o = (q\ .(H-l))/E_{oed,2} + (q\ .l)/E_{oed,1}) \quad (2)$$

ΔS_0 refers to the partial soft soil settlement up to a depth of *l*. Where *l* is the stone column length if installed. Settlement of the soft soil below the stone column toe level, $S_l.q$, refers to the embankment/foundation surcharge including the external applied load, and H is the soft soil layer thickness. E_{oed} is defined as the oedometer or compression modulus of the soft soil layer. It should be noted that previous investigations (e.g. Balaam et al. 1977) demonstrated that using an elastic analysis will slightly under-predict the settlement performance of stone columns at working loads. Therefore, it is deemed sufficiently accurate to use the elastic approach to investigate the total settlement of stone columns in this paper. If an embankment/foundation is constructed over a soft soil and improved with stone column, then soft soil settlement can be determined by the equilibrium of the effective vertical stress.

Considering floating condition with the ground water at surface, the effective vertical stresses in Figure 1 can be written as follows:

$$[(-\sigma_v' + \sigma_v' + \Delta\sigma_v' - \gamma'.\Delta z)\ .\pi(R^2-r^2)] - 2\pi r.\tau\Delta z = 0 \quad (3)$$

R is the radius of the circular cell, r is the stone column radius, γ' is the effective unit weight of the soil and τ is the stone column shaft friction. In terms of the soil mechanics theory, the ultimate skin friction on the stone column shaft (if it is modelled as rigid column) can be evaluated in soft to firm clays in terms of effective stress using the following equation (Terzaghi et al. 1996).

$$\tau = RF.\acute{\sigma_v} \quad (4)$$

where RF is the lateral reduction factor representing the reduction in the effective angle of friction with increasing depth to the residual value. On the assumption that during rigid column installation surrounding soft clay is in a remoulded state and the cohesion intercept is zero.

$$\text{RF}= K_s\ .\tan\delta \quad (5)$$

where K_s is the coefficient of earth pressure after stone column installation and δ is the average value of the angle of friction between stone column and soil. There are a few methods to simulate stone column installation effects. However, Priebe's approach (Priebe 1995) is the most acceptable method in the industry. It is based on the increase in the coefficient of lateral earth pressure (K_s=1.0) to simulate stone column installation.

Satibi (2009) derived pile critical length and settlement after improvement as follows:

$$l_{crit} = \sqrt{\frac{2\ .\ q}{\beta\ .\ \gamma'}} \quad (6)$$

$$S = S_l + \frac{\left(q+\gamma'\ .l+\frac{\gamma'}{\beta}\right)}{E_{oed,1}\ .\beta}\ .\left(1-\ e^{-\beta l}\ \right) - \frac{\gamma'\ .l}{E_{oed,1}\ .\beta} - \frac{\gamma'\ .l^2}{2\ .\ E_{oed,1}} \quad (7)$$

Critical stone column length l_{crit} is the column length that satisfies the criteria where the entire embankment/foundation load is resisted by the floating stone column and no load is transferred to the soil where β can be calculated as follows:

$$\beta = \left(\frac{2r}{R^2-\ r^2}\right)\ .RF \quad (8)$$

and E_{oed} is the oedometer modulus of the soft soil layers taken as tangent modulus and can be determined by power law relation (Brinkgreve and Broere 2006):

$$E_{oed} = E_{oed}^{ref}\ .\left(\frac{\sigma_v'}{p^{ref}}\right)^m \quad (9)$$

where

E_{oed}^{ref} = Tangent stiffness for primary oedometer loading at the reference pressure p^{ref}=100kPa.

m= Power for stress level dependency of stiffness.

A typical design inputs E_{oed}^{ref} =1.5MPa and m= 1 are used for soft cohesive soils. Therefore, above equation reduces to E_{oed}= 15. σ_v'. The effective stress σ_v' is calculated at the middle of the soft soil layer and includes an additional applied load. Soft soil oedometer modulus can be determined as follows:

$$E_{oed,1} = 15\ .(0.5\ .\ \ l\ .\ \ \gamma' + \ q\ ) \quad (10)$$

$$E_{oed,2} = 15\ .(0.5\ .\ \ (H + l_{crit}).\ \ \gamma' +\ \ q\ ) \qquad (11)$$

Therefore, the effectiveness of the embankments on floating rigid inclusion can be calculated based on the relative settlement reduction (RSR).

3 NUMERICAL PARAMETRIC STUDY AND SETTLEMENT ANALYSIS

The proposed analytical approach has been used to predict the critical length of stone column and to assess the effectiveness of stone columns, with R equal to 0.75m and a stone column radius of 0.3m. In this analysis, the soft soil has an effective unit weight of 6.5 kN/m^3 and an effective angle of internal friction equal to 25°. The coefficient of the lateral earth pressure K_s is equal to 1.0 in order to account for installation effect of stone column, which is consistent with the value proposed by Priebe (1995).

A numerical parametric study has been carried out and compared to the analytical method to examine the impact of various key parameters, such as soft layer thickness and stone column spacing, on the column-foundation system behaviour. The Finite element (FE) program Plaxis 2D was used to model the stone column behaviour. The stone column reinforced foundation has been analyzed by the axisymmetric soil model similar to that used in the analytical approach. The geometry and mesh used in the FE analysis are shown in Figure 2. The mesh has a radius of 0.75m to 1m to simulate a typical column spacing of 1.5m to 2m and the stone column radius is equal to 0.3m.

In the subsequent FE and analytical analyses, the settlement behaviour of various configurations of soft soil thickness and stone column spacing is examined for loads up to 50kPa. Boundary conditions are applied by preventing horizontal displacement at the vertical side of the mesh and preventing both vertical and horizontal movement at the bottom. The ground water level is set to be at the ground level. The hardening soil constitutive model is used for the soft soil and stone column materials. The soft soil and column backfill properties used in FE calculations are listed below in Table 1.

Table 1 Material property as used in FE- Analysis

Properties		Soft Soil	Stone
φ'	[°]	25	45
c'	kPa	0.1	0.1
ψ	[°]	0	15
γ	kN/m^3	16.5	19
$E_{50}^{ref} = E_{oed}^{ref}$	MPa	1.5	70
E_{ur}^{ref}	MPa	4.5	210
υ_{ur}	[-]	0.2	0.2
m	[-]	1	0.5

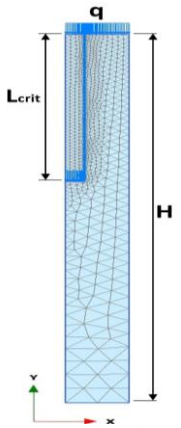


Figure 2. FE mesh and geometry

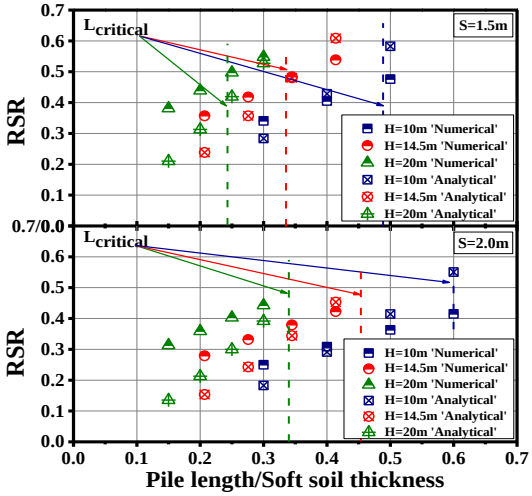


Figure 3. RSR improvement with pile length

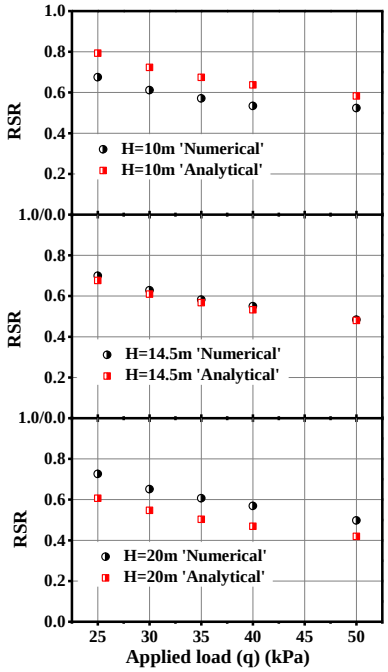


Figure 4. Effectiveness of floating stone columns upon the variation of foundation surcharge for a soft soil thickness of 10m, 14.5m and 20m with column spacing of 1.5m at critical column length.

4 RESULTS

The influence of column length and soft soil thickness upon the performance of a unit cell model is shown in Figure 3. The relative settlement reduction against stone column length with different soft soil thicknesses is shown for the applied load of 40kPa on top of the stone column which is a typical working load for foundations constructed over the stone columns.

The effectiveness of the stone column as ground improvement technique is represented by the relative settlement ratio. The relative settlement ratio increases with the increasing of the stone column length. In general, the effectiveness is between 50 and 60% at a critical stone column length for columns installed at the spacing of 1.5m. The effectiveness of stone columns is slightly decreased where the RSR deceases to around 45 to 55% at critical column length if the column spacing increases to 2m centre to centre . The effectiveness is reduced because the more widley spaced stone columns attract a higher proportion of the load. It is also shown in Figure 3 that the improvement in settlement due to

stone column installation is relatively more pronounced with reducing soft soil layer thickness.

Based on the analysis performed on the unit cell model, it was observed that there is a good agreement between numerical and analytical solutions (Figures 3, 4 and 5). It can also be seen from Figures 4 and 5 that convergence is more pronounced at higher loads (around 50kPa).

Generally, both the numerical and analytical methods predict similar reduction in the settlement at a critical stone column length. However, there is a slight difference in the RSR between the numerical and analytical solutions for soft layer thickness of 10m and 20m (maximum difference of about 12%). The difference may be attributed to the assumption of constant oedometer stiffness in the analytical model, whereas in the FE modeling, stress dependent oedometer stiffness values are applied.

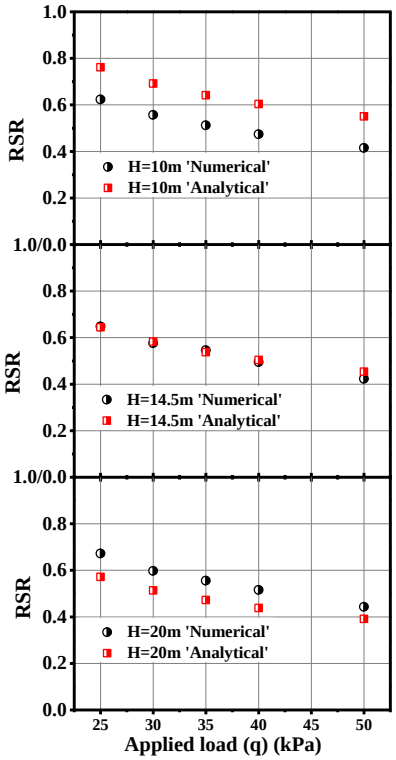


Figure 5. Effectiveness of floating stone columns upon the variation of foundation surcharge for a soft soil thickness of 10m, 14.5m and 20m with column spacing of 2.0m at critical column length.

The variations of the RSR with the applied load are compared in Figures 4 and 5. As the thickness of the soft clay layer at the bottom of the column increases, the RSR decreases irrespective of the column spacing as predicted in the analytical model. At lower loading, the settlement improvement is marginally higher than that at higher loads as presented in Figures 4 and 5. The marginal improvement in the RSR at lower loads is due to the initial readjustment of the stone particles. However, as the load increases, the improvement in settlement decreases rapidly.

5 CONCLUSIONS

In this paper, the settlement performance of stone columns was studied. An analytical method was proposed to predict the improvement in settlement due to stone column installation at any depth up to the critical column length predicted by the analytical model.

Based on the results obtained from the derived analytical model and the parametric study through the FE analysis, the following conclusions may be drawn:

1. Stone columns improve the foundation settlement behaviour. As the length of stone column increases, there is an increase in the RSR (Relative Settlement Reduction) ratio.
2. The parametric study shows that the RSR ratio is about 45 to 60% at the critical stone column length.
3. The column spacing has an impact on the settlement reduction. Increasing the column spacing and thereby reducing the ratio between the area of cross-section of stone column and the area of surrounding soil, leads to a slight reduction in the RSR.
4. The analytical model predicts that the RSR ratio decreases as the thickness of soft layer increases irrespective of the column spacing.
5. At lower loading levels, the settlement improvement is marginally higher than that at higher load levels. The marginal improvement in the RSR at lower loads is due to the initial realignment of the stone particles until an equilibrium condition is met.

It should be noted that these conclusions are based on the numerical and analytical analyses of a single column under an applied vertical load. The behaviour of a stone column in groups such as stone column suppporting an embankment, is typically different from the case of a single stone column analysis.

It should be pointed out that the proposed analytical model is based on the Hooke elastic theory and the rigid column theory. Therefore, the settlement performance of stone columns at working loads is slightly underestimated. Despite the simplicity of the analytical approach adopted in this study, the proposed solution enhances the understanding of stone column performance and may be used for estimating the critical length of stone columns.

6 ACKNOWLEDGEMENTS

This material presented in this paper is based on a research work supported in part by the University of Nottingham and Balfour Beatty Ground Engineering.

7 REFERENCES

Balaam N.P., Brown P.T. and Poulos H.G. 1977. Settlement analysis of soft clays reinforced with granular piles. *Proc. 5th Southeast Asian Conf. on Soil Engineering*, Bangkok, Thailand, pp.81-92.

Brinkgreve R.B.J., and Broere, W. 2006. *PLAXIS 3D Foundation Manual Version 2*. PLAXIS BV.

McKelvey D., Sivakumar V., Bell A. and Graham J. 2004. Modelling vibrated stone columns in soft clay. *Proc. Institution of Civil Engineers – Geotechnical Engineering* 157 (3), 137-149.

Priebe H.J. 1995. The design of vibro replacement. *J. Ground. Eng.* 28, 31-37.

Pulko B. and Majes B. 2005. Simple and accurate prediction of settlements of stone column reinforced soil. *Proc. 16th Int. Conf. on Soil Mechanics and Geotechnical Engineering*, Osaka, Japan, pp. 1401–1404.

Satibi S. 2009. *Numerical analysis and design criteria of embankments on floating piles.* PhD thesis, University of Stuttgart, Germany.

Sexton B.G. and McCabe B.A. 2013. Numerical modelling of the improvements to primary and creep settlements offered by granular columns. *Acta Geotechnica* 8 (4), 447-464.

Terzaghi K., Peck R.B. and Mesri G. 1996. *Soil Mechanics in Engineering Practice. 3rd ed.*, Wiley, New York.

Wehr W. 2004. Stone columns – single columns and group behavior. *Proc. 5th Int. Conf. on Ground Improvement Techniques*, Malaysia, pp. 329-340.